

University of New Hampshire

## University of New Hampshire Scholars' Repository

---

Doctoral Dissertations

Student Scholarship

---

Fall 2020

### Evaluation and Identification of Cracking Susceptibility of Asphalt Binders and Mixtures by Incorporation of Effects of Aging on Performance

Runhua Zhang

*University of New Hampshire, Durham*

Follow this and additional works at: <https://scholars.unh.edu/dissertation>

---

#### Recommended Citation

Zhang, Runhua, "Evaluation and Identification of Cracking Susceptibility of Asphalt Binders and Mixtures by Incorporation of Effects of Aging on Performance" (2020). *Doctoral Dissertations*. 2537.  
<https://scholars.unh.edu/dissertation/2537>

This Dissertation is brought to you for free and open access by the Student Scholarship at University of New Hampshire Scholars' Repository. It has been accepted for inclusion in Doctoral Dissertations by an authorized administrator of University of New Hampshire Scholars' Repository. For more information, please contact [nicole.hentz@unh.edu](mailto:nicole.hentz@unh.edu).

**Evaluation and Identification of Cracking Susceptibility of Asphalt Binders  
and Mixtures by Incorporation of Effects of Aging on Performance**

BY

**RUNHUA ZHANG**

B.S. Transportation Engineering, Henan University of Urban Construction

M.S. Civil Engineering, Chongqing Jiaotong University

DISSERTATION

Submitted to the University of New Hampshire

in Partial Fulfillment of

the Requirements for the Degree of

**Doctor of Philosophy**

in

**Civil and Environmental Engineering**

September 2020

This dissertation was examined and approved in partial fulfillment of requirements for the degree of Doctor of Philosophy in Civil and Environmental Engineering by:

Dissertation Director, Jo E. Sias  
Professor, Civil and Environmental Engineering,  
University of New Hampshire

Eshan V. Dave  
Associate Professor, Civil and Environmental Engineering,  
University of New Hampshire

Majid Ghayoomi  
Associate Professor, Civil and Environmental Engineering,  
University of New Hampshire

David J. Mensching  
Asphalt Materials Research Program Manager,  
Federal Highway Administration

Michael D. Elwardany  
Program Manager for Paving Asphalts, Asphalt & Petroleum Technologies  
Western Research Institute

On April 16, 2020

Approval signatures are on file with the University of New Hampshire Graduate School.

## **ACKNOWLEDGEMENT**

First and foremost, I would like to acknowledge my advisers Dr. Jo E. Sias and Dr. Eshan Dave for all of their endless support, patience, motivation and immense knowledge. This Ph.D. would have never been accomplished without your trust in me and providing excellent guidance to my research. I am grateful that I had the chance of working with and learning from you as your student.

I would like to also thank my committee members, Dr. Majid Ghayoomi, Dr. David J. Mensching and Dr. Michael D. Elwardany for their invaluable input to me thesis.

Many thanks to all my colleagues in the asphalt research group at UNH: Dr. Reyhaneh Rahbar-Rastegar, Dr. Mirkat Oshone, Dr. Rasool Nemati, Dr. Yaning Qiao, Chris Decarlo, Katie Haslett, Francesco Preti, Chibuike Ogbo and Danial Mirzaiyanrajeh. We have always had a friendly environment and you mean more than friends to me.

Last but not least, I would like to thank my parents for all the endless love and support.

## Table of Contents

1	Introduction.....	1
1.1	Background and Motivation .....	1
1.2	Objectives.....	2
1.3	Overall Research Approach .....	2
1.3.1	Selection of Laboratory Conditioning Methods .....	3
1.3.2	Evaluation of Aging Effect on Asphalt Mixtures .....	4
1.3.3	Evaluation of Aging Effect on Asphalt Binders .....	4
1.3.4	Comparison and Correlation between the Mixture and Binder Cracking Parameters .....	5
1.4	Organization of the Dissertation .....	5
2	Literature Review.....	9
2.1	Asphalt Chemistry and Aging Mechanism .....	9
2.1.1	Volatilization.....	10
2.1.2	Oxidation.....	10
2.2	Laboratory Conditioning Methods.....	11
2.2.1	Aging of Asphalt Binder.....	12
2.2.1.1	Short Term Aging .....	12
2.2.1.2	Long Term Aging.....	13
2.2.2	Aging of Asphalt Mixture.....	13
2.2.2.1	Short Term Aging .....	13
2.2.2.2	Long Term Aging.....	14
2.3	Models to Track Changes of Binder/Mixture Properties .....	18
3	Materials and Methodology .....	22
3.1	Materials.....	22
3.1.1	Asphalt Mixtures.....	22
3.1.2	Asphalt Binders.....	23
3.2	Aging and Specimen of Fabrication Methods .....	24
3.3	Testing and Analysis Methods.....	25
3.3.1	Mixture Testing.....	25
3.3.1.1	Complex Modulus Testing.....	25
3.3.1.2	Semi-Circular Bend (SCB) Test .....	28
3.3.1.3	Direct Tension Cyclic Fatigue Test .....	29
3.3.1.4	Disk-Shaped Compact Tension Test (DCT) .....	30
3.3.2	Binder Testing.....	31
3.3.2.1	DSR Test.....	31
3.3.2.2	Linear Amplitude Sweep (LAS) test.....	34
3.4	Cracking Performance Simulation and Prediction: FlexPAVE™ and IlliTC.....	36
3.4.1	Fatigue Performance Simulation using FlexPAVE™ .....	36
3.4.2	Thermal Cracking Performance Simulation using IlliTC .....	36
4	Impact of Aging on the Viscoelastic Properties and Cracking Behavior of Asphalt Mixtures (Paper 1, Appendix A).....	38
4.1	Significance of the Study.....	38

4.2	Abstract .....	38
5	Development of a Rheology-based Mixture Aging Model to Evaluate the Cracking Performance of Asphalt Material over Time (Paper 2, Appendix B) .....	40
5.1	Significance of the Study .....	40
5.2	Abstract .....	40
6	Correlating Laboratory Conditioning with Field Aging for Asphalt Using Rheological Parameters (Paper 3, Appendix C).....	42
6.1	Significance of the Study .....	42
6.2	Abstract .....	42
7	Development of New Performance Indices to Evaluate the Fatigue Properties of Asphalt Binders with Aging (Paper 4, Appendix D).....	44
7.1	Significance of the Study .....	44
7.2	Abstract .....	44
8	Comparison and Correlation of Asphalt Binder and Mixture Cracking Parameters Incorporating the Aging Effect (Paper 5, Appendix E) .....	46
8.1	Significance of the Study .....	46
8.2	Abstract .....	46
9	Summary and Conclusions .....	48
9.1	Summary .....	48
9.2	Conclusions .....	50
9.3	Future Extension .....	52
10	References.....	54
	Appendix A.....	A-1
	Appendix B.....	B-1
	Appendix C.....	C-1
	Appendix D.....	D-1
	Appendix E.....	E-1

## List of Figures

Figure 1-1 Overall Research Approach and Dissertation Structure.....	3
Figure 2-1 Typical Asphalt Components [11] .....	9
Figure 2-2 Kinetic Oxidation of Asphalt Binder [reproduced from 37].....	11
Figure 3-1 Schematic of Cutting of the Field Cores (surface layer) for Binder Extraction and Recovery .....	23
Figure 3-2 Complex Modulus Test Result and Setup [99] .....	26
Figure 3-3 Shape Parameters from Dynamic Modulus Master Curve.....	27
Figure 3-4 Shape Parameters from Phase Angle Master Curve .....	27
Figure 3-5 Semi-circular Bend Test Result and Setup [99].....	29
Figure 3-6 Damage Characteristic Curve and Direct Tension Cyclic Fatigue Test Setup [99] .....	30
Figure 3-7 Disk-shaped Compact Tension Test Result, Setup and Specimen Geometry [99] .....	31
Figure 3-8 4mm DSR Test Result and Setup [2] .....	32
Figure 3-9 $T_g$ , $T_t$ and $T_{IR}$ in $G'$ and $G''$ Master Curve (Temperature Domain) .....	34
Figure 3-10 Typical Damage Characteristic Curve (DCC) from LAS Test .....	35
Figure 3-11 Typical Fatigue Characterization ( $N_f$ -strain) Plot from LAS Test.....	36

**List of Tables**

Table 1-1 Status of the Technical Papers Culminating from This Doctorate Research. ....8

Table 2-1 Studies on Accelerated Laboratory Aging Procedures Developed for Compacted  
Asphalt Specimens ..... 15

Table 2-2 Studies on Accelerated Laboratory Aging Procedures Developed for Loose Asphalt  
Specimens ..... 16

Table 3-1 Mixtures Properties and Information.....22

Table 3-2 Summary Information for Binder Samples .....23

Table 3-3 Air Voids for Samples from Field Cores.....24



## Abstract

An important aspect which causes a significant effect on performance of asphalt materials is aging. With increase of aging, asphalt materials lose their relaxation capabilities and becomes more susceptible to cracking. Thus, an improved understanding of how aging impacts the cracking behavior of asphalt materials will allow for design of more reliable and durable asphalt pavements. In this study, different laboratory aging levels were performed to simulate different periods of pavement service life. Various performance tests (including Complex Modulus ( $E^*$ ), Simplified Viscoelastic Continuum Damage (S-VECD), Semi Circular Bending (SCB) and Disk Shaped Compact Tension (DCT) tests for asphalt mixtures; Frequency and Temperature Sweep test using a Dynamic Shear Rheometer (DSR) with 4mm plate and Linear Amplitude Sweep (LAS) test for asphalt binders) were conducted to evaluate the changes of material's properties (including fundamental viscoelastic/rheological property, fatigue characterization, and fracture behavior) over time. The advanced Mechanistic-Empirical (ME) Models (FlexPAVE and IlliTC) were also employed to simulate the aging effects using the predicted fatigue and thermal cracking performance of asphalt mixtures in context of pavement structure, traffic and climatic conditions. The performance tests and simulation models provided a way to quantify the effects of aging on cracking behavior of asphalt materials and they can estimate the roles of various mixture variables on the cracking performance. Based on the testing and simulation results, this study also (1) developed new performance indices to evaluate the fatigue performance of asphalt binders with aging; (2) developed a rheological-based mixture aging model to evaluate cracking and aging susceptibility of asphalt mixtures over time; (3) provided insights on the relationships between binder and mixture cracking

behaviors. This dissertation makes a contribution in improvement of the approaches for evaluation of cracking potential of asphalt pavements and allows for assessment of different mixtures at early stage of material selection and mixture design.

# 1 Introduction

## 1.1 Background and Motivation

Cracking is a primary concern for asphalt pavements since it affects ride quality and allows water to penetrate from the surface to underlying base and soil layers, decreasing the serviceability of the pavement, elevating the chance of road accidents and requiring considerable amount of taxpayers' money on the frequent maintenance or rehabilitation. The American Society of Civil Engineers estimates that deteriorating roads are costing taxpayers \$67 billion per year [1]. It has also been well recognized in the literature and through field observations that asphalt materials' resistance to cracking decreases with time as it ages in the field, due to the decrease of the relaxation capability and increase of brittleness of the asphalt binders and mixtures. Since the asphalt mixtures, which is made up with different variables, (e.g. aggregates, asphalt binders, and recycled materials from existing roadways) will have very different cracking behaviors with increase of aging, it is important to have an understanding of how the cracking resistance of the binders and mixtures will change over time at the time materials are selected and pavements are constructed. This can help the agencies and contractors to adjust mix variables and improve cracking performance of designed pavements, addressing four of the six FHWA high-priority highway challenges [2]: enhancing performance; promoting sustainability; maintaining infrastructure integrity; preparing for future.

Asphalt pavements undergo aging during construction (short term aging, mostly evaporation of lighter weight molecules at the high production temperatures), and also over the pavement service life (long term aging due to oxidation and continued loss of lighter weight hydrocarbons), which increases the brittleness and cracking susceptibility of asphalt material. During design phase of pavement, it is imperative to know beforehand what the properties of the pavement will be after field aging. This will help to minimize maintenance cost due to premature failure and to increase the reliability of the pavement design. It is evident; therefore, that there is a need for accelerated laboratory conditioning (aging) method that can simulate binder properties similar to that of field aged binder.

At present, many agencies' material specifications rely primarily on volumetric properties and their empirical relationship to performance. The current asphalt material specifications do not put emphasis on need for mechanical testing of asphalt materials. Research and experimental construction projects [3,4] have shown that the Superpave volumetric mixture design method alone is not enough to ensure reliable mixture performance over a wide range of materials, traffic and climatic conditions. There have been considerable amounts of research efforts to

develop so called “Asphalt Performance Tests” that can link laboratory measured parameters to actual pavement performance [3]. Some research is also undertaken to refine the asphalt mix design method so that laboratory tests and procedures can be incorporated as part of material specification [5]. Research efforts are needed to explore availability of such “asphalt performance tests”, their suitability and their use for evaluation of the local and regional mixtures and projects.

Motivated by these aspects, this doctorate dissertation evaluates different laboratory conditioning procedures which are able to reliably simulate the aging of asphalt materials in field and further proposes models for prediction of mechanical properties over pavement life based on the laboratory testing on the study binders/mixtures.

In addition to investigating and exploring different laboratory conditioning methods and performance tests, the advanced pavement performance simulation and prediction tools, such as IlliTC and FlexPAVE™, are also evaluated and utilized in this dissertation work. These programs typically use the fundamental properties measured from the laboratory performance tests to determine the structural pavement response due to traffic and environmental loading. Then, the pavement distresses can be quantitatively simulated and calculated, such as the percent damage of the road cross section, amount of cracking and rutting depth on pavement. Using of the performance simulation and prediction programs can close the gap of how well we can test and evaluate the mixtures to quantify the expected or future performance of the asphalt mixtures in context of pavement structure, local climate and traffic conditions.

## **1.2 Objectives**

The principal objectives of this research are to:

1. Quantitatively evaluate how the cracking performance of both asphalt mixture and binder changes over pavement service life;
2. Correlate the laboratory conditioning (aging) methods with actual field aging duration; and,
3. Provide recommendations and guidelines on how to identify crack and aging susceptible binders/mixtures during material selection and mix design.

## **1.3 Overall Research Approach**

In order to fulfill the dissertation objectives a number of research efforts are undertaken to evaluate the cracking performance of asphalt mixtures and binders that are included in this dissertation work. The research approach used in this study generally includes:

- a) Selection of Laboratory Conditioning Methods

- b) Evaluation of Aging Effect on Asphalt Mixtures
- c) Evaluation of Aging Effect on Asphalt Binders
- d) Comparisons and Correlations between the Mixture and Binder Cracking Parameters (in context of their evolution with aging)

Figure 1-1 presents a simplified process diagram of the overall research approach. The overview and brief discussion of each facet will be presented next.

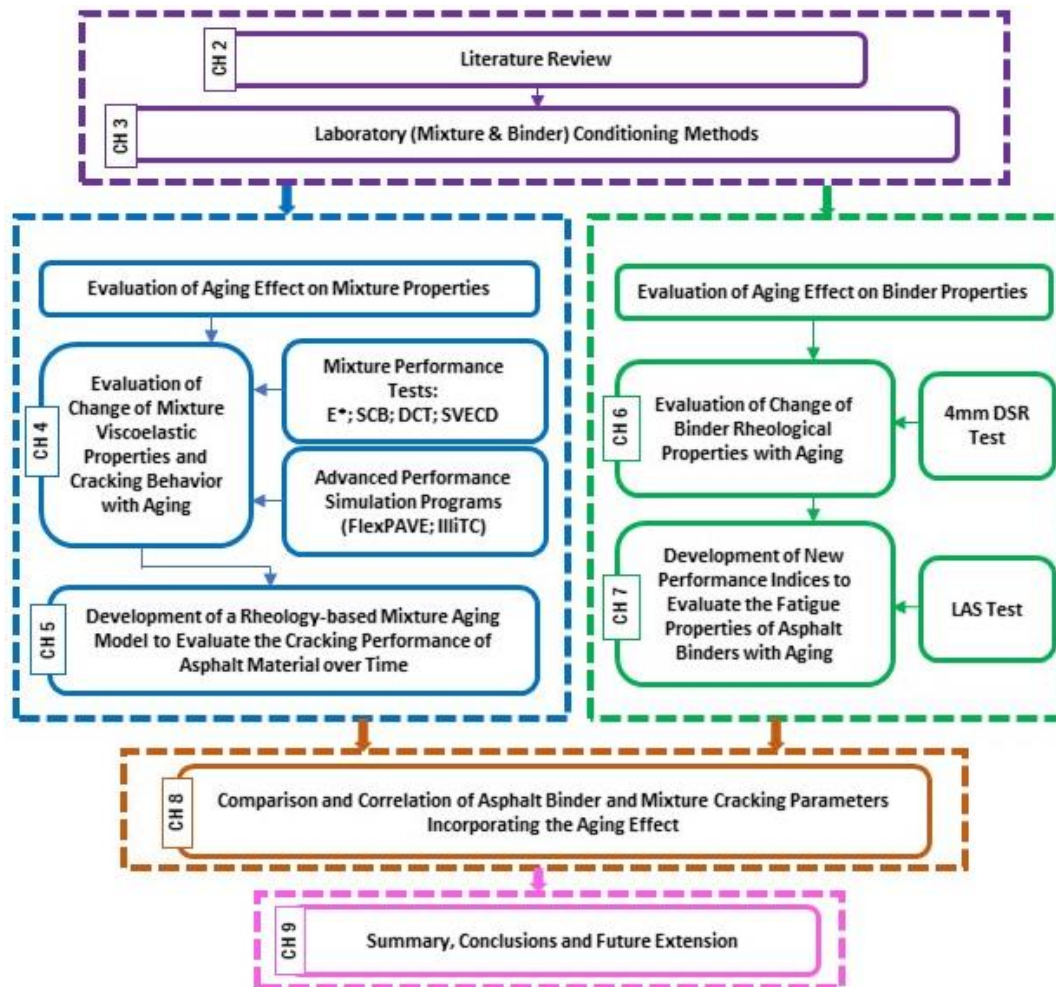


**Figure 1-1 Overall Research Approach and Dissertation Structure**

### 1.3.1 Selection of Laboratory Conditioning Methods

In order to capture the long-term performance of the asphalt mixtures and binders and, simulate the physical and chemical changes of asphalt material in field, the appropriate laboratory conditioning (aging) methods are needed. In this dissertation work, the traditional binder conditioning methods documented in the Superpave binder specification including the rolling thin film oven (RTFO) procedure and the typical 20 hours pressure aging vessel (PAV) method are included. Several long-term mixture conditioning protocols including the Asphalt Institute

procedure (24 hr. at 135°C on loose mix) and the NCHRP 09-54 project recommendations (1-12 days at 95°C on loose mix) are included and performed on the plant-produced mixtures.

### ***1.3.2 Evaluation of Aging Effect on Asphalt Mixtures***

To evaluate the impact of aging on mixture properties, a set of 11 different mixtures from New Hampshire Department of Transportation (NH DOT) are subject to the various mixture conditioning protocols and then tested using the mixture performance tests. Mixture (including the field cores) characterization is done using Complex Modulus, Simplified Viscoelastic Continuum Damage (SVECD) fatigue, Semi Circular Bending (SCB) and Disc-Shaped Compact Tension (DCT) tests to measure the linear viscoelastic (LVE) properties, fatigue behavior, and fracture performance, respectively. Various mixture performance indices calculated from the test measurements are used to quantitatively evaluate and investigate the aging and cracking susceptibility of the mixtures with different mix variables. In addition to the laboratory performance tests, the advanced pavement performance simulation and prediction programs including FlexPAVE™ and IlliTC are also used to predict and compare the fatigue and thermal cracking performance of different mixtures with various aging conditions in context of pavement structure, climatic and traffic conditions. The climatic aging index (CAI) model developed by NCHRP 09-54 project is also utilized to calculate the appropriate field aging duration corresponding with the different laboratory mixture conditioning protocols.

Based on the mixture testing results, the mixture Glover-Rowe (G-Rm) parameter, that incorporates both stiffness and relaxation capacity, is selected and used as the Aging Index Property (AIP) to model the evolution of mixture cracking performance with aging. The simplified and experimental mixture aging model developed from this study along with the CAI model are used to evaluate and predict the aging and cracking susceptibility of the asphalt mixtures over their service lives.

### ***1.3.3 Evaluation of Aging Effect on Asphalt Binders***

To evaluate the impact of aging on the binder properties in this dissertation work, binder samples extracted and recovered from the aged mixtures and field cores (three layers with 0.5in per each) are tested. Rheological characterization of the binder samples is performed by a typical Frequency and Temperature Sweep test using the Dynamic Shear Rheometer (DSR) with a 4mm plate. Various rheological indices (e.g. binder Glover-Rowe parameter, R-value) measured from the 4mm DSR test are employed to evaluate the aging and cracking susceptibility of the different asphalt binders. The field aging gradient is evaluated and the laboratory conditioning durations corresponding with the field aging durations at different

pavement depths are calculated. In addition, the comparison between the laboratory mixture conditioning protocols with the binder aging methods is evaluated and investigated.

The fatigue behavior of the binders with various aging levels are measured by the Linear Amplitude Sweep (LAS) test with an 8mm plate. In addition to the traditional parameters (A, B parameter and the  $N_f$ -strain plot), several new indices that can be used to better evaluate the change of asphalt binder's fatigue performance with aging are developed based on the viscoelastic continuum damage (VECD) theory and failure energy. Comparing with the traditional parameters measured from the LAS test, these developed indices can capture the actual failure point of the binder samples and show a consistent decrease in the fatigue performance of the binder samples with aging. These new parameters also have the potential to be used to evaluate the mixture fatigue performance by incorporating the aging effect.

#### ***1.3.4 Comparison and Correlation between the Mixture and Binder Cracking Parameters***

The different mixture and binder performance tests and the corresponding performance indices described above provide researchers a valuable way to quantitatively evaluate the cracking and aging susceptibility of different asphalt binders and mixtures. However, the relationship between binder cracking performance and mixture cracking behavior is still not completely understood, and there is still a question of how mixture properties change with changes in binder characteristics and how the binder and mixture testing methods and parameters may differentially evaluate expected performance of asphalt materials with respect to cracking. To fill the existing gap, a comprehensive comparison and correlation between the mixture and binder cracking performance is conducted, while also taking aging effect into account.

### **1.4 Organization of the Dissertation**

This doctorate dissertation is organized in 9 chapters as indicated in Figure 1-1. A short summary of each chapter is provided in this section and full manuscripts are either attached as appendices to this document or have been discussed within the thesis under designated chapter number and title.

Chapter 1 is dedicated to the introduction and motivation for this research, as well as the study objectives. An overview of the research approach that is used in this dissertation work to fulfill the study objectives is also included in this chapter.

Chapter 2 includes the background and literature review on the topics of aging mechanism and the different laboratory conditioning methods to simulate the aging in field, as well as the various models in the literature that have been developed and used to track changes of binder/mixture properties over time.

Chapter 3 discusses the breadth of materials that are examined in this study, followed by a description of the different laboratory conditioning (aging) methods used to simulate the aging in field, various mechanistic and performance-based laboratory tests, as well as the advanced programs that are employed to characterize the asphalt mixtures' performance within the structure, climate and traffic conditions.

Chapters 4 evaluates the effect of aging on mixture properties including the viscoelastic characteristics and the cracking performance (cracking initiation and fracture behavior) through use of various mechanic tests and advanced performance simulation and prediction programs. Also, the correlations between the different laboratory mixture conditioning methods and the actual field aging durations are also investigated.

A mixture rheology-based aging model is developed and discussed in Chapter 5. This developed aging model can be used to not only capture the two aging reaction periods of asphalt material, but also track and predict the change of mixture cracking performance over time (pavement service life) and identify the aging susceptibility of the mixtures with different mix variables.

Chapters 6 evaluates the effect of aging on binder rheological property through testing on the binder samples extracted and recovered from the laboratory conditioned mixtures and the cores taken from the field sections. The comparison between the laboratory mixture aging protocols with the binder aging methods is investigated, and the aging gradient within the pavement structure is also evaluated in this chapter.

Chapter 7 discusses the development of the new performance indices that are used to evaluate the fatigue performance of asphalt binders by incorporating aging effect. These parameters are developed based on the viscoelastic continuum damage (VECD) theory and failure energy and, they are shown to capture the actual failure point of the binder samples during the test.

Chapter 8 combines the findings from previous chapters where the correlations and comparisons between the mixture and binder cracking performance are investigated and evaluated.

Chapter 9 summarizes the findings of the research and contribution of the thesis, which provides the recommendations and guidelines for selection of more appropriate asphalt material and design of more durable asphalt pavement. The limitations of the dissertation study and recommended future work are also briefly described.

Details of research efforts and corresponding results and discussion from Chapters 4 thru 8 of this dissertation are in form of peer-reviewed journal manuscripts. A brief synopsis of the work



from these manuscripts are provided as body of these chapters. The current status of these five papers is indicated in Table 1-1.

**Table 1-1 Status of the Technical Papers Culminating from This Doctorate Research.**

<b>Chapter</b>	<b>Paper</b>	<b>Journal</b>	<b>Status</b>	<b>Contribution to the Objectives</b>
<b>4</b>	<b>Evaluation the Impact of Aging on the Viscoelastic Properties and Cracking Behavior of Asphalt Mixtures</b>	<b>Transportation Research Record</b>	<b>Published</b>	<b>Direct contributions to objective 1,2</b>
<b>5</b>	<b>Development of a Mixture Aging Model to Evaluate the Cracking Performance of Asphalt Material over Time</b>	<b>Materials and Structures</b>	<b>Submitted, under review</b>	<b>Direct contributions to objective 1,3</b>
<b>6</b>	<b>Correlating Laboratory Conditioning with Field Aging for Asphalt Using Rheological Parameters</b>	<b>Transportation Research Record</b>	<b>Accepted, will be published online soon</b>	<b>Direct contributions to objective 1,2</b>
<b>7</b>	<b>Development of New Performance Indices to Evaluate the Fatigue Performance of Asphalt Binders with Aging</b>	<b>Road Materials and Pavement Design</b>	<b>Submitted, under review</b>	<b>Direct contributions to objective 1,3</b>
<b>8</b>	<b>Comparison and Correlation of Asphalt Binder and Mixture Cracking Parameters Incorporating the Aging Effect</b>	<b>Construction and Building Materials</b>	<b>Submission planned by April</b>	<b>Direct contributions to objective 1,3</b>

## 2 Literature Review

### 2.1 Asphalt Chemistry and Aging Mechanism

Asphalt is either derived from natural deposits or obtained as a residue of crude petroleum or a product of solvent extraction of petroleum. Asphalt binder is a complex material consists of high molecular weight hydrocarbon molecules (composed of carbon (typically 80–88%) and hydrogen atoms (10–12%)), and naturally occurring heteroatoms (include nitrogen (0–2%), oxygen (0–2%), and sulphur (0–9%)), as well as small amount (typically far less than 1%) of trace metals (e.g., vanadium and nickel) that contribute to the polarity within the asphalt molecules [6-8]. The hydrocarbons constitute the basic structure of asphalt binders while the metal atoms provide indication or characteristic of asphalt crude source. Heteroatoms contribute to many of asphalt's unique chemical and physical properties by interacting with molecules.

Based on Corbett's method [9], Asphalt binder can be described as a colloid which consists of a dispersion of asphaltenes with large molecular weight in an oily matrix constituted by saturates, aromatics, and resins (as illustrated in **Figure 2-1**). Asphaltenes and saturates are normally incompatible compounds and are brought together by aromatics. Asphaltenes are mainly responsible for viscosity/stiffness while abundance of aromatics and saturates increases the ductility of asphalt materials. Studies regarding changes of chemical composition of asphalt through aging indicate that the asphaltenes content generally increases, while the resins and aromatics contents decrease [10]. Details of how the aging changes the chemical components of asphalt binder will be discussed in section 2.1.1 and 2.1.2 below.

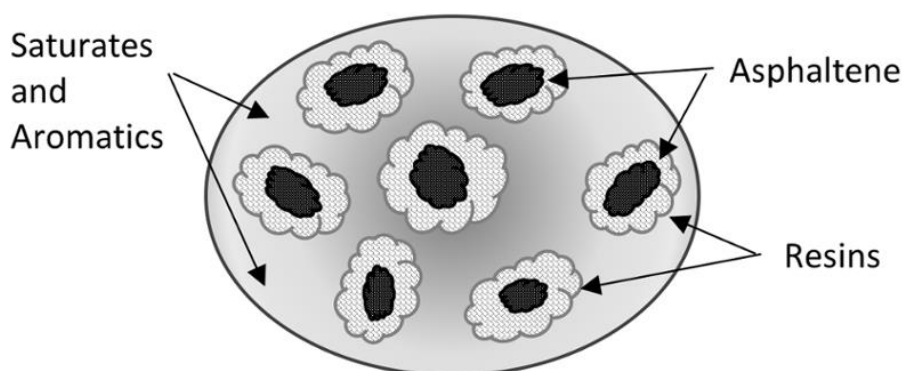


**Figure 2-1 Typical Asphalt Components [11]**

Since aging can significantly impact the composites and properties of asphalt material, numerous researchers have continued to develop an understanding of the mechanisms causing of aging [12]. Mechanisms causing binder aging include volatilization, oxidation, thixotropy

(or steric hardening), polymerization due to actinic light, and condensation polymerization due to heat [13-17]. Among them, volatilization and oxidation are considered as the two leading mechanisms for the aging of asphalt materials [18]. During production and construction (laydown and compaction), stages that are commonly referred to as short-term aging (STA), asphalt binders/mixtures are exposed to higher temperatures which results in loss of volatile compounds. On the contrary, long-term aging (LTA) during pavement service life takes place at ambient temperature, the mechanism for LTA is primarily due to oxidation of organic compounds [19].

### **2.1.1 Volatilization.**

Volatilization is one of the important aging mechanisms for asphalt material. Volatilization mainly occurs during the production and construction stages due to the evaporation of the lighter fractions (hydrocarbons) under the high temperatures of mixing and compaction [20,21]. When the asphalt binder is heated up or the thin asphalt film comes into contact with hot aggregates in the plant, aromatic fractions rapidly evaporate, resulting in the increase of asphaltene fractions between 1 and 4% [22]. As a result of these changes in the components of asphalt binder, the properties are significantly affected. Researchers [13, 23] have found viscosity increases between 150 to 400% and significant increase of modulus and decrease of phase angle because of volatilization process [24]. Anderson and Bonaquist [19] suggested that quantifying the amount of volatile compound loss is essential for better understanding of the asphalt properties after STA.

### **2.1.2 Oxidation.**

Oxidative aging is another important aging mechanism for asphalt material. Significant research efforts have been dedicated to address binder oxidation chemistry [25-29]. Oxidation is generally known as the irreversible chemical reaction process resulting in significant alterations to the chemical, physical and/or mechanical properties of asphalt materials. Oxidative aging of asphalt is typically caused by the generation of oxygen-containing polar chemical functionalities on asphalt molecules that further leads to the agglomeration among molecules caused by the increased chemo-physical associations such as hydrogen bonding, van der Waals force, and Coulomb force [30-32].

Asphalt oxidation significantly changes the chemical composition of asphalt. During the oxidation process, saturates typically remain unchanged because of their low chemical reactivity while other three fractions exhibit significant variations [33,34]. Due to oxidative aging, chemical and functional groups (i.e., carbonyl and sulfoxide groups) are formed, leading to decrease in aromatic fractions and increase of asphaltenes fractions [35]. Many researches and studies have quantified oxidation effects by measuring and characterizing these functional

elements/groups. Liu et al. [36] indicated that the area of carbonyl region (CA) measured from Fourier transform infrared spectroscopy (FTIR) can be used to assess the binder composition changes due to oxidative aging and be an effective measurement of binder oxidation effect [25].

Research conducted by Petersen et al. [32] indicated that oxidation reaction kinetics between binder and oxygen exhibits the “Dual, Sequential Reaction Kinetics”, which consists an initial high reactivity rate (also known as “spurt”) followed by a slower relatively constant reaction rate. The observation is typically caused by the different chemical products formed during the oxidation reaction period. Petersen et al. [37] proposed that during the binder oxidation process, Ketones and Sulfoxides are the two main reaction products, while only a minor amount of dicarboxylic anhydrides and carboxylic acids are formed during oxidation stage. During the spurt stage, sulfoxides are the major oxidation product and cause an increase in viscosity. During the slower (constant) reaction period, ketones are the major product and drive the increase in viscosity [37]. **Figure 2-2** illustrates the two oxidation reaction periods with the corresponding chemical reaction products.

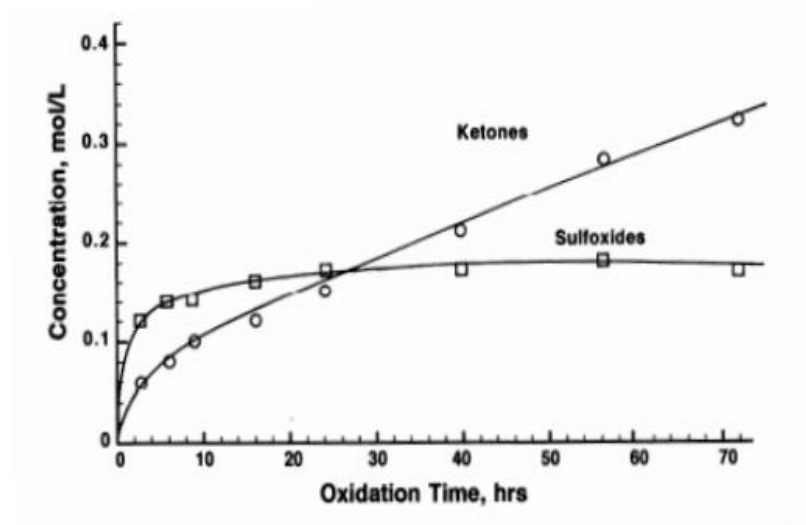


**Figure 2-2 Kinetic Oxidation of Asphalt Binder [reproduced from 37]**

## 2.2 Laboratory Conditioning Methods

Aging can significantly impact the performance of asphalt materials and can drastically alter the serviceable life of asphalt pavements. Considering the performance prediction of asphalt materials with aging and the importance of performance-based design methodologies, there is a need for accelerated laboratory aging methods that can simulate and predict the change of binder and mixture properties over the whole pavement service life. This will help to minimize

maintenance and rehabilitation costs due to the different pavement distresses and to increase the confidence level of the pavement designs. Significant research efforts have been dedicated to developing and establishing the appropriate laboratory conditioning methods to simulate the corresponding field aging periods. These procedures can be generally classified based on the type of material during aging: binders, and asphalt mixtures.

### ***2.2.1 Aging of Asphalt Binder***

Different accelerated conditioning methods have been developed to age the asphalt binders in the laboratory. By increasing temperature, decreasing binder film thickness, increasing more contact with air (greater flow), and increasing pressure, the aging process of asphalt material can be dramatically accelerated, providing a way to simulate the long-term aging of asphalt pavement in the lab. After aging acceleration treatment, samples are usually studied and investigated to evaluate the changes in the asphalt binder properties, e.g. weight loss, viscosity, penetration, functional groups and stiffness modulus (commonly known as AIP) to quantify the aging effect.

#### ***2.2.1.1 Short Term Aging***

The Thin-Film Oven test ((TFOT) ASTM D1754/AASHTO T179) was first introduced [38] to simulate STA by conditioning the binder samples at a temperature of 163°C with a binder film thickness of 3.2 mm for 5 hours' duration. However, it has been received many criticisms due to the thicker film thickness than that is commonly observed in the field [17]. Later, many studies have been attempted to improve the conditioning methods to better simulate the STA, including the Modified Thin Film Oven test [39], Shell Micro Film test [40], Rolling Micro Film Oven test [41], Tilt Oven Durability test [42], and Thin Film Accelerated Aging test [43].

Among these methods, the most significant modification of the TFOT was the Rolling Thin-Film Oven test (RTFOT), developed by the California Division of Highway [44], where the asphalt samples are exposed to air flow and heat at the temperature of 325°F (163°C) for 85 minutes with a thin film of 1.25 mm. This method ensures uniform aging of asphalt [45], and has been proved to be a reasonable and effective way of simulating the STA of unmodified binders not only with respect to physical property changes but also with respect to volatilization, as measured by changes in the infrared absorption spectrum [46]. However, several researchers [47-49] identified a number of deficiencies (e.g., spilling out from RTFOT bottles, surface skin formation and poor flow in the bottles) in RTFOT especially for conditioning of the modified asphalt binders. To overcome these limitations, researchers developed improved testing methods such as Modified Rolling Thin Film Oven Test (RTFOTM) [50], Modified German Rotating Flask (MGRF) [51], and Stirred Air Flow Test (SAFT) [52] to evaluate STA of both neat and modified asphalt binder.

### *2.2.1.2 Long Term Aging*

A number of studies have been conducted by combining thin film oven tests with the oxidative aging methods such as Pressure Aging Vessel (PAV) [23, 53], Iowa Durability test [54], Pressure Oxidation Bomb [39], and High Pressure Aging test [55] and Accelerated Aging Test device [56] to simulate and capture the long-term aging effect. Among those different conditioning methods, PAV treatment is generally believed and widely accepted for simulation of long-term aging in field. Standard PAV method typically conditions the binder samples under pressure of 300 psi (2070 kPa) with a temperature of 194°, 212°, 230°F (90°, 100°, or 110°C) for 20 hours. Different temperatures are typically used to simulate the LTA of asphalt pavement under different climate conditions. RTFO together with PAV method is expected to simulate 7–10 years oxidation of asphalt in service based on AASHTO R 28 [57]. However, 20 hours conditioning in PAV may not be sufficient for simulation of LTA under the severe weather conditions like in the Middle East where up to 70 hours of conditioning may be needed to simulate the 5 years field aging of asphalt pavement. Many researchers already started to use the extended PAV aging methods, such as the PAV conditioning with 40, 60 and 80 hours' duration to capture the aging effect throughout the pavement life.

## *2.2.2 Aging of Asphalt Mixture*

The different binder conditioning methods provide researchers and agencies the valuable ways to simulate the field aging in laboratory, however, the main drawback of the binder conditioning methods is that the binder aging kinetics in field also depend on the mixture parameters (such as air voids and binder content) [25]. Therefore, researchers [58-62] recommend aging the asphalt mixture in the oven to capture the effect of mixture parameters on the asphalt binder oxidation process, such as the air voids, binder content, and the interactions between recycled and virgin binder.

### *2.2.2.1 Short Term Aging*

AASHTO R 30 is the current standard laboratory conditioning procedure that has been widely adopted by states to simulate both short-term and long-term aging conditions. For STA, it suggested to place the pans of loose mix asphalt in a forced-draft oven for 4 hours at a temperature of 275°F (135°C). The loose mix asphalt should be stirred after 1 hour to obtain uniform conditioning. This procedure has been proved by many researches with respect to its effectiveness to capture the STA effect [16,63].

Many other researchers have also tried to simulate STA by applying different temperatures with different conditioning durations. Aschenbrener and Far [64] suggested conditioning the laboratory-produced mixtures for 2 hours at the field compaction temperature in order to simulate asphalt aging and absorption during plant production. Epps Martin et al. [65]

evaluated different short-term aging protocols, and the finally recommended to condition loose mixture at 135°C for 2 hours before compaction. Brown and Scholz [66] also tried to condition the compacted specimens at 135°C for 2-5 hours to simulate the STA of asphalt material.

Many recent studies have also been undergone to develop the appropriate STA conditioning method for warm mix asphalt (WMA). Research conducted by Estakhri et al. [67] performed the HWTT on the WMA and HMA mixtures with different conditioning levels. They finally recommended a 4 hours' oven aging (at 135°C) as the optimum conditioning method for WMA mixtures. The NCHRP project 9-43 [68] and Project 9-49 [34] also investigated the appropriate aging time and temperature on WMA mixtures. NCHRP 9-43 study recommended 2-hours oven aging for WMA at the compaction temperature, whereas NCHRP 9-49 suggested conditioning WMA for 2 hours at 240°F (116°C), and 2 hours at 275°F (135°C) for HMA to simulate the STA.

#### *2.2.2.2 Long Term Aging*

Several asphalt mixture laboratory conditioning procedures to simulate the long-term aging of asphalt pavement in the field are documented in the literature. These procedures can be further classified based on state of mixture during aging: (a) compacted specimen (b) loose mix.

##### *2.2.2.2.1 Aging of compacted specimen*

Experimental results from Bell et al. [13,58] recommended to condition the compacted specimen at 85°C for 2 days or 100°C for 1 day duration to simulate around 1 to 3 years' field aging condition. A longer conditioning time (4 to 8 days for 85°C or 2 to 4 days for 100°C) was needed to simulate 9-10 years' field aging. The higher conditioning temperature (100°C) was suggested to be avoided by the authors since conditioning the mixtures at this temperature could cause damage to the specimens. The outcome of these studies (part of the SHRP project) was standardized as AASHTO R30 for the long-term aging of compacted asphalt specimens in the laboratory, which can approximately represent five to ten years of aging in the field [59]. Houston et al. [69] conditioned the compacted asphalt specimens at 5 days at multiple temperatures (80°C, 85°C, and 90°C) to simulate the LTA for different sites across the United States with the different aggregates and binders. High variability was observed from the data, and due to this variability and inability to account for various variables including the environmental conditions and mix properties, the researchers were not able to scandalize a new long-term conditioning procedure for asphalt mixtures. It was concluded that the current standard procedure is not sufficient to truly simulate and predict the long-term aging of asphalt mixtures in the field. A new laboratory conditioning procedure that accounts for different environmental conditions and mix properties is highly desirable.



Several other procedures for conditioning of the compacted mixture specimens have also been proposed in the literature. A summary of these methods is provided in **Table 2-1**.

**Table 2-1 Studies on Accelerated Laboratory Aging Procedures Developed for Compacted Asphalt Specimens**

<b>References</b>	<b>Laboratory Conditioning Method</b>	<b>Key Findings</b>
<b>Brown and Scholz [66]</b>	4 and 5 days at 85°C	1. 5 days at 85°C can simulate long-term aging of asphalt pavements in UK; 2. 4 days at 85°C simulates 15 years old pavement in the US
<b>Harrigan [60]; Houston et al. [69]</b>	5 days at 80, 85, and 90°C	5 days at 85°C simulates 7–10 years of field aging
<b>Epps Martin et al. [65]</b>	1 to 16 weeks at 60°C	4–8 weeks at 60°C simulates first year of field aging
<b>Sirin et al. [70]</b>	0, 3, 7, 15, 30, 45, 60, 90, and 120 days at 85°C	45 and 75 days at 85°C simulate 5 years field aging in Middle East condition for wearing and base course, respectively
<b>Nicholls [71]</b>	2 days at 60°C	Simulates around 1 year aging in the field
<b>Van den Bergh [72]</b>	16 hours at 110-120°C	The method can simulate around 20 years of aging in field

However, research [73-76] has shown that aging on the compacted specimen leads to a change in air void distribution [77] and the development of an aging gradient from the specimen's center to its periphery and can result in different aging extents for different specimen geometries. This variability complicates the interpretation of results from different performance testing on the aged mixtures.

#### 2.2.2.2.2 Aging of loose mix

Some studies recommend aging loose mixtures in the laboratory to simulate the aging of asphalt pavements instead of aging compacted specimens [72, 78]. The primary advantages of loose mixture aging over compacted specimen aging are: (1) problems associated with the conditioning of compacted specimen (e.g., change in air void distribution and aging gradient) during laboratory aging may be reduced; (2) air and heat can easily circulate inside the loose asphalt mixture, which not only allows for uniform aging throughout the mix but also significantly shortens the conditioning time needed due to a larger area of the binder surface being exposed to oxygen.

Several aging procedures for loose mixture conditioning have been proposed in the literature. A summary of these methods is provided in **Table 2-2**.

**Table 2-2 Studies on Accelerated Laboratory Aging Procedures Developed for Loose Asphalt Specimens**

<b>References</b>	<b>Laboratory Aging Condition</b>	<b>Key Findings</b>
<b>Asphalt Institute [79]</b>	24 hours at 135°C	This method can simulate 7 to 10 years of aging in the field
<b>Von Quintus [80]; Van den Bergh [72,81]</b>	8, 16, 24, and 36 hours at 135°C	<ol style="list-style-type: none"> <li>1. STA at 130°C for 3 hours following LTA at 90°C for 168 hours;</li> <li>2. STA at 134°C for 4 hours following LTA at 85°C for 168 hours</li> <li>3. Two methods can be used to simulate 7 to 10 years field aging</li> </ol>
<b>Yin et al. [82]</b>	2 weeks at 60°C; 3 days at 85°C; and 5 days at 85°C	<ol style="list-style-type: none"> <li>1. 2 weeks at 60°C simulates 7 to 12 months field aging;</li> <li>2. 5 days at 60°C simulates 12 to 23 months field aging</li> </ol>
<b>Sirin et al. [72]</b>	0, 1, 2, and 3 days at 135°C on loose mixtures	2-3 and 1-2 days at 135°C can simulate 5 years field aging in Middle East condition for wearing and base course, respectively
<b>Islam et al. [83]</b>	1, 5, 10, 15, 20, and 25 days of oven aging at 85°C	1 day laboratory aging is close to 1-year of field aging

<b>RILEM TG5 [84]</b>	7-9 days at 85°C	<ol style="list-style-type: none"> <li>1. Laboratory aging of loose mix provides an appropriate way to produce RAP material;</li> <li>2. A more homogenous aged mix obtained from aging of loose mix</li> </ol>
<b>Mollenhauer and Mouillet [78]</b>	90°C with 2.1 MPa pressure for 20 hours; 85°C for nine days	Both can simulate 11 to 12 years field aging
<b>Reed [77]</b>	Loose mix at 85°C for 5 days; Compacted sample at 85°C for 14 days	<ol style="list-style-type: none"> <li>1. Uniform aging of the asphalt around each aggregate particle in the laboratory-aged loose mix;</li> <li>2. Significant changes in air void content during the long-term aging of the compacted specimens</li> </ol>
<b>Yousefi et al. [61]</b>	Loose mix at 70°C, 85°C and 95°C for different durations; Loose mix at 135°C with different durations	<p>Aging asphalt at temperatures above 100°C may</p> <ol style="list-style-type: none"> <li>1. disrupt polar molecular associations, which leads to the thermal decomposition of sulfoxides in asphalt binders;</li> <li>2. lead to significantly different cracking performance results compared to the material testing and pavement simulations for aging below 95°C</li> </ol>

In addition, the recent findings of the National Cooperative Highway Research Program (NCHRP) 09-54 project on long term aging of asphalt mixtures suggests 95°C as an optimal temperature for aging loose mix [62]. The aging time varies with the geographical location of the pavement and should be adjusted based on climate conditions and pavement depth. Also, a climatic aging index (CAI), based on a simplification of the aging kinetics model, was developed from NCHRP 09-54 project to determine laboratory aging durations at 95°C for asphalt mixtures that best reflect the time, climate, and pavement depth for a given pavement location in the United States using Enhanced Integrated Climatic Model (EICM) hourly pavement temperature data [62].

### 2.3 Models to Track Changes of Binder/Mixture Properties

As mentioned above, aging has a significant impact on the chemical, microstructural, and physical and engineering properties of asphalt material. Thus, fundamental modeling of asphalt aging and the accurate prediction of asphalt mixture properties in terms of pavement service life is of pragmatic importance as more powerful pavement design and performance prediction methods are implemented.

A number of valuable aging models are proposed in the literature. Generally, temperature and pressure dependency of the oxidation reaction rate can be described using the Arrhenius equation [85], as shown in the general form given in **Eq. 2-1**.

$$k = AP^\alpha \exp\left(\frac{-E_a}{RT}\right) \quad \text{Equation 2-1}$$

Where,

$k$  is rate of reaction;

$A$  is reaction frequency factor;

$P$  is absolute oxygen pressure;

$E_a$  is reaction activation energy (KJ/mol);

$R$  is universal gas constant;

$T$  is reaction temperature (K).

Herrington et al. [86] proposed a kinetics expression, shown in **Eq. 2-2**, using binder viscosity as an Aging Index Properties (AIP) where the fast reaction rate ( $k_f$ ) and constant reaction rate ( $k_c$ ) can be expressed using **Eq. 2-3** and **2-4**, neglecting the pressure dependency term.

$$\log \eta = \log \eta_0 + M(1 - \exp(-k_f t)) + k_c t \quad \text{Equation 2-2}$$

$$k_f = A_f \left( \exp \frac{-E_{af}}{RT} \right) \quad \text{Equation 2-3}$$

$$k_c = A_c \left( \exp \frac{-E_{ac}}{RT} \right) \quad \text{Equation 2-4}$$

Where,

$\eta$  is long-term aged binder viscosity;

$\eta_0$  is short-term aged binder viscosity;

$M$  is fitting parameter related to fast reaction reactive material;

$t$  is reaction time (s);

$k_f$  is rate of fast reaction;

$k_c$  is rate of constant reaction;

$A_f$  is fast reaction frequency factor;

$A_c$  is constant reaction frequency factor;

$E_{af}$  is fast reaction activation energy (KJ/mol);

$E_{ac}$  is constant reaction activation energy (KJ/mol).

Several extensive studies to model the kinetics of asphalt binder oxidative aging using carbonyl area as an AIP have been conducted [87-91]. Lau et al. [87] presented a comprehensive study using results from 10 asphalt binders and determined the values of activation energy  $E$  and frequency (pre-exponential) factor  $A$ . Eq. 2-5 is the kinetics model developed by Glover and his research team [25]. Glover et al. [25] presented an interrelation among kinetics parameters of fast and constant reactions as shown in Eq. 2-6 – 2-8.

$$CA = CA_0 + M(1 - \exp(-k_f t)) + K_c t \quad \text{Equation 2-5}$$

$$E_{af} = 0.85E_{ac} - 10.4 \quad \text{Equation 2-6}$$

$$A_f = 0.52 \exp(0.3328E_{af}) \quad \text{Equation 2-7}$$

$$A_c = 0.0266 \exp(0.3347E_{ac}) \quad \text{Equation 2-8}$$

Where,

$CA$  is long-term aged binder carbonyl area;

$CA_0$  is short-term aged binder carbonyl area.

Glaser et al. [91] used cumulation of carbonyl and sulfoxide absorbance peaks as an AIP to fit the oxidation of 12 asphalt binders that originated from a wide variety of sources. The fitting used the same Arrhenius parameters for all 12 binders studied, with only one adjustable parameter, which corresponded to the amount of the fast reaction reactive material ( $M$ ). Eq. 2-9 shows the integral form of the model that was used to fit the isothermal data to determine the adjustable parameters ( $M$ ). Eq. 2-10 shows the form of the model taking into account pressure dependency terms for fast and slow reactions. If the Arrhenius parameters can be applied

universally as Glaser et al.'s results suggest, a single aging trial at a single temperature is all that is needed to derive a kinetics model for unmodified binders [91,92].

$$(C + S) = (C + S)_0 + M \left(1 - \frac{k_c}{k_f}\right) (1 - \exp(-k_f t)) + k_c M t \quad \text{Equation 2-9}$$

$$(C + S) = (C + S)_0 + M \left(1 - \frac{k_c * P^n}{k_f * P^m}\right) (1 - \exp(-k_f P^m t)) + k_c M P^n t \quad \text{Equation 2-10}$$

Where,

$(C+S)$  is long-term aged binder carbonyl + sulfoxide absorbance peaks;

$(C+S)_0$  is short-term aged binder carbonyl + sulfoxide absorbance peaks;

$m$  is the reaction order of fast reaction;

$n$  is the reaction order of constant reaction.

All of the models presented above are based on experimental data obtained by studying the AIPs of asphalt binders aged in thin films at elevated temperatures and/or under pressure. Elwardany et al. [75] recommended aging of loose mix in the oven after evaluating different laboratory methods for asphalt mixture to simulate oxidative aging for performance testing. Aging of loose mixture in the oven allows for capturing the physicochemical effects of mineral fillers and aggregate on asphalt binder oxidation rates. Thus, it is assumed to provide better representation of field aging. Based on Glaser et al's [91] kinetics model framework, Elwardany et al. [93] proposed a binder aging model using  $\log G^*$  at 64°C and 10 rad/s frequency as the AIP to track the change of binder properties with aging, as shown in **Eq. 2-11** below:

$$\log G^* = \log G_0^* + M \left(1 - \frac{k_c}{k_f}\right) (1 - \exp(-k_f t)) + k_c M t \quad \text{Equation 2-11}$$

Where,

$G^*$  is long-term aged binder shear modulus at 64°C and 10 rad/s (kPa);

$G_0^*$  is short-term aged binder shear modulus at 64°C and 10 rad/s (kPa).

In addition to the models described above, Mirza and Witczak [94] developed an empirical model (global aging system (GAS) model) that allows for the prediction of the change in binder viscosity as a function of time, given the mean annual air temperature (MAAT), and also considers the aging gradient with pavement depth. The model assumes a hyperbolic aging function that predicts a decreasing rate of viscosity with an increase in age (generally consistent with the observations made for the two-stage oxidation kinetics model discussed previously),

under the assumption that most age hardening occurs within the first ten years of a pavement's service life. The GAS model has been adopted in the MEPDG design and in other research studies. The GAS model is summarized in **Eq. 2-12** and **2-13**.

$$\log \log(\eta_{aged}) = \frac{\log \log(\eta_{t=0}) + At}{1+Bt} F_v \quad \text{Equation 2-12}$$

$$\log \log(\eta_{aged,z}) = \frac{\eta_{aged}^{(4+E)} - E * \eta_{t=0}^{(1-4z)}}{4(1+E*z)} F_v \quad \text{Equation 2-13}$$

Where,

$\eta_{aged}$  is the binder viscosity after aging (centipoise);

$\eta_{t=0}$  is the binder viscosity at mix/placement (centipoise);

A and B are functions of temperature and MAAT for the location of interest;

$F_v$  is the optional air void content adjustment factor;

T is time in months;

Z is pavement depth;

E function of MAAT.

Although significant research efforts have been dedicated to model the kinetics of asphalt binder aging, as discussed above, relatively little attention has been devoted to modeling the aging of asphalt mixtures. The lack of major studies in this area reflects the complexities involved in studying mixture aging. Oxidative reaction rate and mechanism are affected by the physicochemical interaction between the asphalt binder and the aggregate, as well as the mixture variables [95-98]. Also, most aging models as discussed above focus only on the modelling and prediction of the stiffness over time, ignoring the relaxation capability (phase angle) of the asphalt (viscoelastic) material. However, researchers [61,62,76] have shown that phase angle plays the significant role in the performance of both asphalt binder and mixture.

### 3 Materials and Methodology

#### 3.1 Materials

##### 3.1.1 Asphalt Mixtures

This dissertation work includes laboratory testing on totally eleven plant mixed, lab compacted surface mixtures. **Table 3-1** summarizes the mixture information (Recycled binder content is the ratio of the weight of recycled binder to the total binder weight). The different aging conditioning methods applied on these mixtures will be described in **section 3.2** below. Letters in the cells indicate the testing conducted at each of the mixture-aging combinations. The mix ID has the specific meaning: the first four-digit numbers indicate binder PG grade, the following letters “S” and “L” mean the nominal maximum aggregate size (NMAS) of 9.5mm and 12.5mm, respectively. The last letter represents the recycled binder content: “V” means no recycled binder, “M” means 14.8-18.9% recycled binder content, “L” means 28.3% recycled binder content. Field cores for four mixtures (5234LM, 5234LL, 5828LM and 5828LL); taken after 4 years in service) are also available in this study.

**Table 3-1 Mixtures Properties and Information**

Mixture ID	Virgin Binder Grade	Design Gyration	NMAS (mm)	Total Binder Content (%)	Recycled Binder Content (%)	STA	LTOA			Field Cores
		Levels					5 days 95°C	12 days 95°C	24 hours 135°C	
5234LM	PG 52-34	50	12.5	5.3	18.9	A	ABCD	ABCD	ABCD	ABC
5234LL	PG 52-34	50	12.5	5.3	28.3	A	ABCD	ABCD	ABCD	ABC
5834LM	PG 58-34	50	12.5	5.4	18.5	CD	CD	CD	CD	NA
5828SM	PG 58-28	50	9.5	5.9	16.9	ABCD	ABCD	ABCD	ABCD	NA
5828LM	PG 58-28	50	12.5	5.3	18.9	A	D	ABCD	ABCD	ABC
5828LL	PG 58-28	75	12.5	5.3	28.3	A	D	ABCD	ABCD	ABC
6428SV	PG 64-28	75	9.5	6.4	0	ABCD	ABCD	ABCD	ABCD	NA
6428SM	PG 64-28	75	9.5	6.3	18.5	ABCD	ABCD	ABCD	ABCD	NA
6428LM	PG 64-28	75	12.5	5.8	18.5	ABCD	ABCD	ABCD	ABCD	NA
7034LV	PG 70-34	75	12.5	5.8	0	ABCD	ABCD	ABCD	ABCD	NA
7628SM	PG 76-28	75	9.5	6.1	14.8	ABCD	ABCD	ABCD	ABCD	NA

**A: Complex Modulus Testing; B: S-VECD Fatigue Testing; C: SCB Testing; D: DCT Testing;**



### 3.1.2 Asphalt Binders

Table 3-2 below shows the summary information for binder samples extracted and recovered from the eleven study mixtures with different aging conditions. The field cores were cut into three layers (0.5";0.5";0.5", as shown in Figure 3-1) and then subjected to the extraction and recovery process. The binder extraction was performed by NHDOT in accordance with AASHTO T 164, procedure 12, using a centrifuge extractor and toluene solvent in order to determine the asphalt binder content. The asphalt binder was recovered based on ASTM D7906-14 using a rotary evaporator. Additionally, seven binder samples (virgin tank samples with 20hr. PAV aging) were received and tested at UNH.

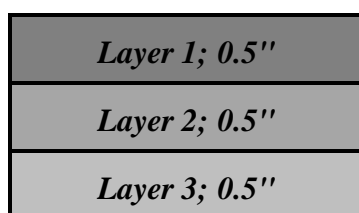


**Figure 3-1 Schematic of Cutting of the Field Cores (surface layer) for Binder Extraction and Recovery**

**Table 3-2 Summary Information for Binder Samples**

Binder Type	Mixture ID	Total Binder Content (%)	Recycled Binder Content (%)	Testing/Analysis					
				STA	95°C@5d	95°C@12d	135°C@24hr.	Field Cores	Original Binder (20 hr. PAV)
PG 52-34	5234LM	5.3	18.9	A	A	A	A	AB	NA
PG 52-34	5234LL	5.3	28.3	A	A	A	A	A	NA
PG 58-34	5834LM	5.4	18.5	AB	AB	AB	NA	NA	✓
PG 58-28	5828SM	5.9	16.9	NA	NA	NA	NA	NA	✓
PG 58-28	5828LM	5.3	18.9	A	NA	A	A	A	NA
PG 58-28	5828LL	5.3	28.3	A	NA	A	A	AB	NA
PG 64-28	6428SV	6.4	0	AB	AB	AB	NA	NA	✓
PG 64-28	6428SM	6.3	18.5	AB	AB	AB	NA	NA	✓
PG 64-28	6428LM	5.8	18.5	NA	NA	NA	NA	NA	✓
PG 70-34	7034LV	5.8	0	AB	AB	AB	NA	NA	✓
PG 76-28	7628SM	6.1	14.8	AB	AB	AB	NA	NA	✓

**A: 4mm DSR; B: LAS.**

### 3.2 Aging and Specimen of Fabrication Methods

The Superpave RTFO+PAV (20hr.) on original binders, the Asphalt Institute procedure (24 hours at 135°C) and NCHRP recommended 95°C for 5 and 12 days on the plant produced mixtures which have already undergone Short Term Aging (STA) during production are the laboratory conditioning protocols included in this study. After aging, the mixtures were cooled and then reheated at 135°C for 2 hours and compacted to achieve final test specimens with air void contents of  $6 \pm 0.5\%$ .

Field cores were further processed by coring (complex modulus and fatigue test) horizontally to obtain the test specimen(s) from the surface layer, the average air void contents of those samples are documented in Table 3-3. The air voids of the samples for complex modulus tests cored from the field cores are generally lower than the laboratory aged and fabricated samples.

**Table 3-3 Air Voids for Samples from Field Cores**

MIX ID (Field Cores)	Replicates	5234LM	5234LL	5828LM	5828LL
Complex Modulus	Replicate 1	4.83%	4.43%	5.26%	6.65%
	Replicate 2	4.37%	5.01%	2.56%	7.57%
	Replicate 3	6.85%	7.48%	4.59%	2.14%
	Replicate 4	5.69%	6.03%	3.49%	3.74%
	<b>Average</b>	<b>5.41%</b>	<b>5.74%</b>	<b>3.91%</b>	<b>5.03%</b>

The climatic aging index (CAI) was also developed from NCHRP 09-54 to determine laboratory aging durations at 95°C for asphalt mixtures that best reflect the time, climate, and pavement depth for a given pavement location in the United States using Enhanced Integrated Climatic Model (EICM) hourly pavement temperature data [62]. The detailed calculation of CAI is shown below:

$$t_{oven} = CAI = \sum_{i=1}^N DA \exp(-E_a / RT_i) / 24 \quad \text{Equation 3-1}$$

$$D = \begin{cases} 3.4311 * d^{-0.683}, & 6mm \leq d \leq 35mm \\ 0.3056, & d \geq 35mm \end{cases} \quad \text{Equation 3-2}$$

Where,

$t_{oven}$  is the required oven aging duration at 95°C to reflect field aging;

$CAI$  is climatic aging index;

$D$  is the depth correction factor;

$A$  is the reaction frequency factor;

$E_a$  is the reaction activation energy;

$R$  is the universal gas constant;

$T_i$  is the pavement temperature obtained from Enhanced Integrated Climatic Model (EICM) at the depth of interest at the hour of interest;

$B$  is the depth dependent fitting parameter;

$d$  is depth of interest.

### 3.3 Testing and Analysis Methods

#### 3.3.1 Mixture Testing

##### 3.3.1.1 Complex Modulus Testing

To capture the linear viscoelastic properties of asphalt mixtures at different aging levels, the complex modulus ( $E^*$ ) test is performed in accordance with AASHTO T342 standard using an Asphalt Mixture Performance Tester (AMPT) machine on 150×100 mm cylindrical specimens (110×38 mm for field cores). The test is conducted on three replicate specimens at different temperatures (4.4, 21.1 and 37.8°C; 2.9, 18.0, 30.0°C for field cores) and loading frequencies (25, 10, 5, 1, 0.5, 0.1 Hz), using a sinusoidal loading protocol and three Linear Variable Differential Transformers (LVDT) for measurement of the on-specimen strains. From the  $E^*$  tests, the dynamic modulus and phase angle master-curves are constructed at a reference temperature of 21.1°C using Abatech RHEA® software. **Eq. 3-3 and 3-4** indicate the dynamic modulus and phase angle calculations. Figure 3-2 shows the test setup and one typical cycle of test data.

$$|E^*| = \frac{\sigma_{amp}}{\varepsilon_{amp}} \quad \text{Equation 3-3}$$

$$\delta = 2\pi f \Delta t \quad \text{Equation 3-4}$$

$|E^*|$  : Dynamic modulus (psi),

$\sigma_{amp}$  : Amplitude of applied stress (psi),

$\varepsilon_{amp}$  : Amplitude of strain response (in/in),

$\delta$ : Phase angle (degrees),

$f$ : Load frequency (Hz),

$\Delta t$ : The time lag between stress and strain peak to peak.

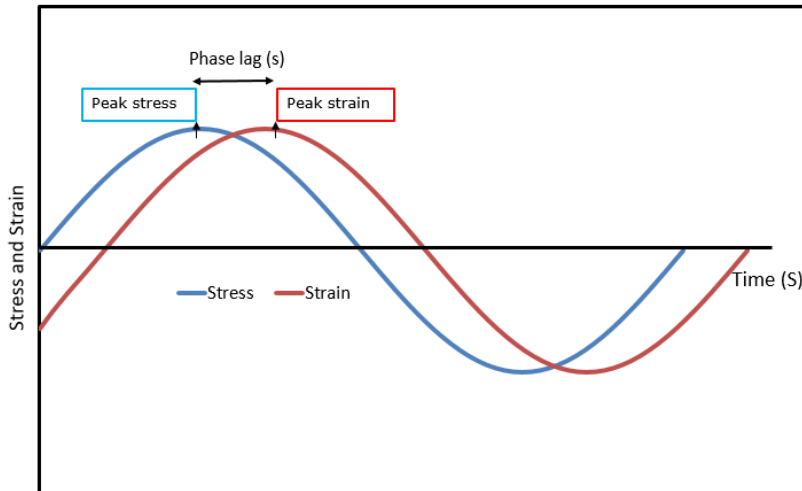


**Figure 3-2 Complex Modulus Test Result and Setup [99]**

A generalized sigmoidal equation with five parameters is generally used to fit the  $|E^*|$  master curves:

$$\log|E^*| = \delta + \frac{\alpha}{1 + e^{\beta + \gamma \log(\omega)}} \quad \text{Equation 3-5}$$

where  $|E^*|$  is dynamic modulus,  $\omega$  is frequency, and  $\delta$ ,  $\alpha$ ,  $\beta$ , and  $\gamma$  are the fit coefficients that describe the shape of the dynamic modulus master curve. The  $\alpha$  and  $\delta$  parameters are related to the glassy modulus (upper asymptote) and the equilibrium modulus (lower asymptote) of the master curve, respectively. The  $\gamma$  value controls the width of relaxation spectra, and the frequency of the inflection point can be calculated from  $10^{-\beta/\gamma}$ , which describes the elastic-viscous transition exhibited as a result of a shift between behavior dominated by the aggregate structure and the binder. These shape parameters from dynamic modulus master curves are described and illustrated in Figure 3-3. Generally,  $\gamma$  increases when aging level increases, while  $-\beta/\gamma$  decreases as aging level increases, which means the asphalt mixtures will become more elastic as the elastic-viscous transition point moves to a lower frequency, resulting in a flatter dynamic modulus curve.

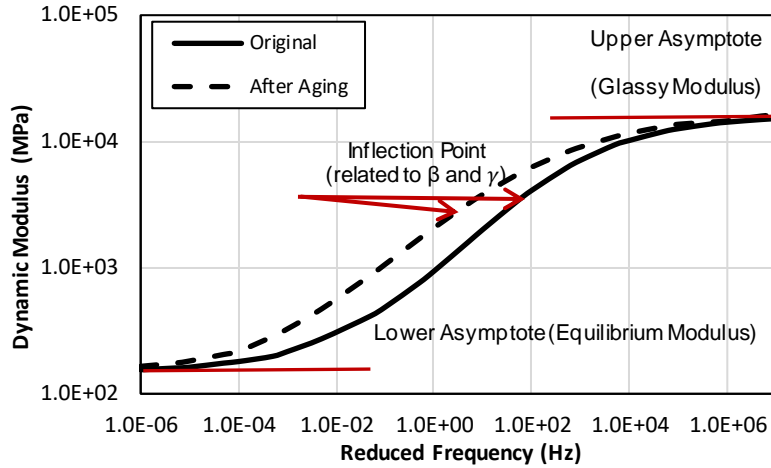


**Figure 3-3 Shape Parameters from Dynamic Modulus Master Curve**

A generalized Lorentzian model (Eq. 2.6) with three parameters is used to fit the  $\delta$  master curves:

$$\delta = \frac{a \cdot b^2}{[(\log(\omega) - c)^2 + b^2]} \quad \text{Equation 3-6}$$

where  $\delta$  is phase angle (degree),  $\omega$  is frequency (Hz), and a, b, and c are the fit coefficients as follows: “a” shows the peak value of phase angle, b controls the slope of the curve, and c is related to the horizontal position of the peak point (the frequency of the peak point can be calculated from  $10^c$ ). The “a” and c values typically decrease as aging level increases, moving the curve to the bottom left of the plot. The shape parameters from phase angle master curves are also described and illustrated in Figure 3-4.

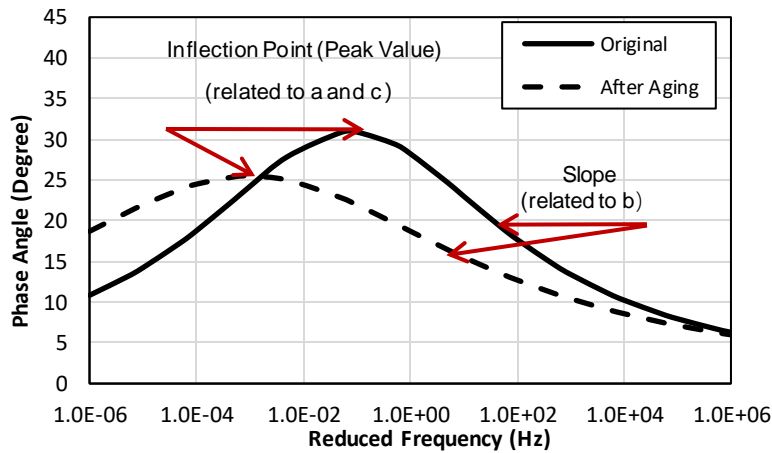


**Figure 3-4 Shape Parameters from Phase Angle Master Curve**

The mixture Glover-Rowe ( $G-R_m$ ) parameter can be also calculated from the master curves. The Glover-Rowe parameter was initially proposed to assess the cracking resistance of asphalt

binders. The basis of this approach was originally proposed by [100]. It suggested a correlation between a new DSR function with ductility using a temperature-frequency combination of 15°C and 1 rad/s. Rowe et al. [101] rearranged Glover's criterion and using some simplifications, suggested a new expression to evaluate the cracking performance of binders. The Glover-Rowe (G-R) parameter captures the complex shear modulus ( $|G^*|$ ) and binder phase angle ( $\delta$ ) at a temperature-frequency combination of 15°C-0.005 rad/s. Later, Mensching et al. [102] developed a parameter to evaluate the cracking performance of asphalt mixture in the format of the binder Glover-Rowe parameter, but employing stiffness and phase angle measured on the mixture ( $|E^*|$  and  $\delta$ ), as shown in **Eq. 3-7**:

$$G - R_m = \frac{|E^*|(\cos\delta)^2}{\sin\delta} \quad \text{Equation 3-7}$$

where  $|E^*|$  is dynamic modulus and  $\delta$  is phase angle of the mixture. In this study, the parameter is calculated at the temperature-frequency combination of 20°C-5Hz, following additional development of the G- $R_m$  parameter to use a typically measured point to evaluate the cracking performance of asphalt mixtures in the NCHRP 09-58 project [103,104]. A threshold value of 19000 MPa generally is suggested to minimize the material cracking potential.

### 3.3.1.2 Semi-Circular Bend (SCB) Test

The Semi-Circular Bend test is conducted to characterize fracture properties of asphalt mixtures at the intermediate temperature in accordance with AASHTO TP 124 standard. The test is performed in monotonic loading conditions, using a line-load displacement rate of 50mm/min at 25°C for 4 replicates. Two performance parameters Fracture energy ( $G_f$ ), defined as the amount of energy required to create unit fracture surface, and Illinois Flexibility Index (FI) which normalizes the fracture energy by the post peak slope at the inflection point are calculated using **Eq. 3-8** and **3-9** respectively [105]. While the fracture energy of different mixtures can be the same, the inclusion of the post peak slope has been shown to better discriminate the fracture resistance of mixtures. Generally, an FI value greater than or equal to 8 has been found to be an adequate threshold for distinguishing good performing from poor performing mixtures [106]. Figure 3-5 shows the test setup and one typical result for semi-circular bend test.

$$G_f = \frac{\text{Area under load-displacement curve (Fracture work)}}{\text{Fracture Area}} \quad \text{Equation 3-8}$$

$$FI = \frac{G_f}{\text{Slope at post peak inflection point}} \quad \text{Equation 3-9}$$

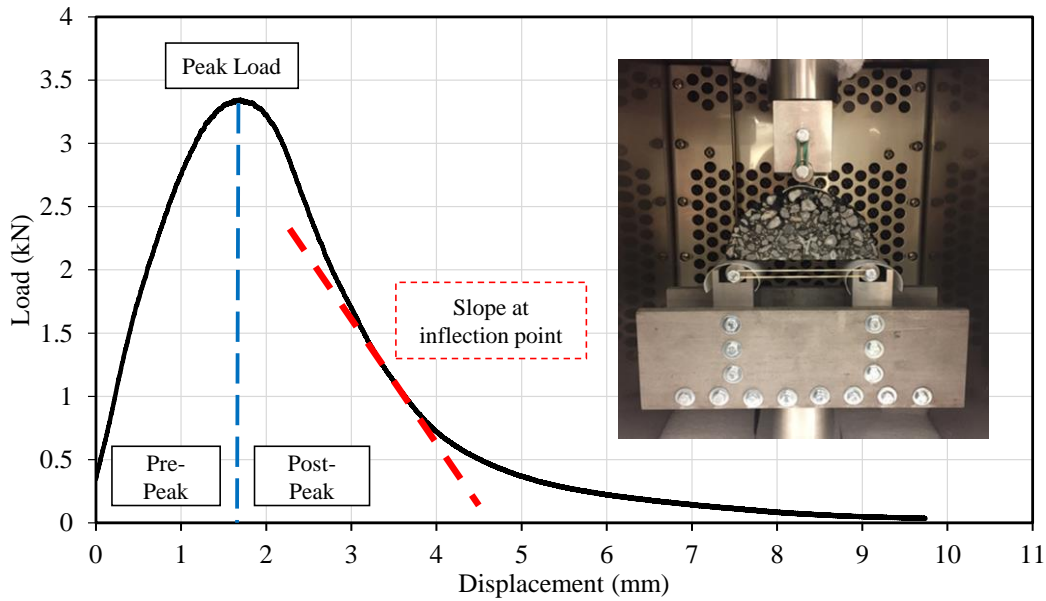


**Figure 3-5 Semi-circular Bend Test Result and Setup [99]**

In addition to the fracture energy ( $G_f$ ) and flexibility index (FI), Nemati et al. [107] develop the rate-dependent cracking index (RDCI) to better discriminate the asphalt mixtures with various mix variables. The calculation of RDCI is shown below:

$$RDCI = \frac{\int_{t_{peak}}^{t_{0.1peak}} W_C dt}{P_{t_{peak}} \times \text{ligament area}} \times C \quad \text{Equation 3-10}$$

where RDCI is the rate-dependent cracking index,  $\int_{t_{peak}}^{t_{0.1peak}} W_C dt$  is the post-peak area under the cumulative work versus time curve,  $P_{t_{peak}}$  is the instantaneous power at peak force,  $C$  is the unit correction factor set to 0.01 to lower the order of magnitude of the RDCI and for simplicity of plotting and ligament area is the specimen thickness times the ligament length.

### 3.3.1.3 Direct Tension Cyclic Fatigue Test

The uniaxial fatigue test is conducted in a direct cyclic tension mode in accordance with AASHTO TP 107 and the analysis is performed using Simplified Viscoelastic Continuum Damage (S-VECD) theory. The test specimens (130×100 mm) are preconditioned with respect to binder performance grade at temperature equal to  $(\frac{PGHT - PGLT}{2} - 3^\circ C)$ . The test is conducted on four replicates each at a different strain level under cyclic tension and constant crosshead testing mode. The main output of this test and analysis is the Damage Characteristic Curve (DCC) which is a mixture property that is independent of loading mode and temperature and indicates the trend of reduction of sample integrity with increase of accumulative damage. As

the cyclic load is applied, damage in the form of micro-cracks is induced in the whole body of the specimen. This results in reduction in material's capacity until micro-cracks are localized and form macro-cracks and specimen failure happens. Figure 3-6 indicates a typical DCC curve and the test setup.

The performance parameter  $D^R$  which is the average reduction in pseudo stiffness per loading cycle is used as the output to estimate the ability of the mixtures to resist fatigue cracking [108]. The calculation of  $D^R$  parameter is shown below:

$$D^R = \frac{\int_0^{N_f} (1-C) dN}{N_f} \quad \text{Equation 3-11}$$

Where:  $C$ : Pseudo stiffness,  $N_f$ : number of loading cycles to failure.

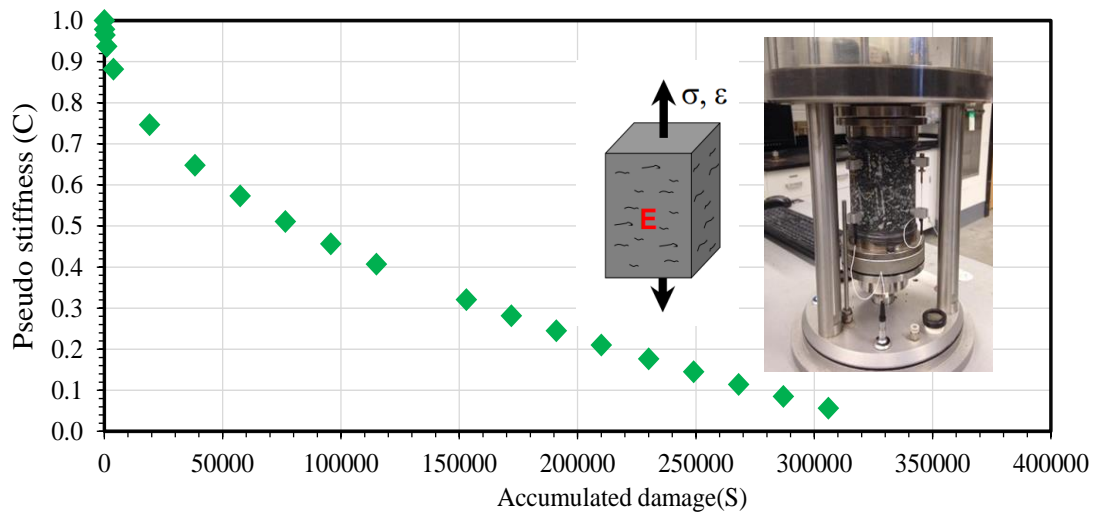


**Figure 3-6 Damage Characteristic Curve and Direct Tension Cyclic Fatigue Test Setup [99]**

#### 3.3.1.4 Disk-Shaped Compact Tension Test (DCT)

The disk-shaped compact tension (DCT) test is conducted to measure the low temperature fracture properties of the asphalt mixtures in accordance with the ASTM D7313 standard. The test is performed in monotonic loading conditions with three replicates. The displacement on the specimen is usually measured by the crack mouth opening displacement (CMOD) setup which is perpendicular to the crack path. The DCT testing temperature is calculated at 98% reliability +10°C from the LTPPBind database for the nearest weather station to the actual project site. The two index parameters calculated are the Fracture Energy ( $G_f$ ) and the Fracture Strain Tolerance (FST) [109]. Figure 3-7 indicates a typical DCT test result and setup as well as the specimen geometry. Eq. 3-12 and 3-13 show the calculation of the FST.



$$S_f = \frac{2P(2W+a)}{t(w-a)^2} \quad \text{Equation 3-12}$$

$$FST = \frac{G_f}{S_f} \quad \text{Equation 3-13}$$

$S_f$  : Fracture strength

$P$ : Maximum load sustained by specimen

$w$  and  $a$  are indicated in

$t$ : Specimen thickness

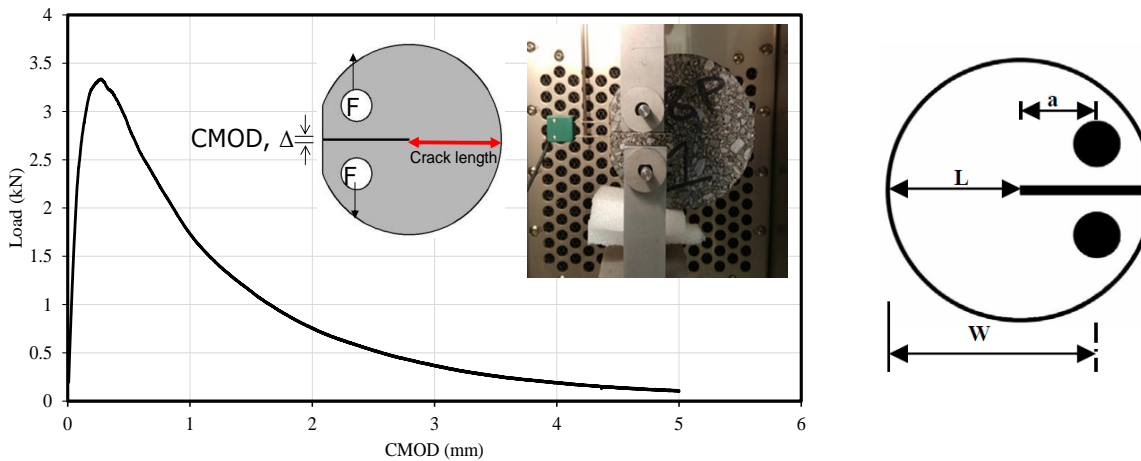


**Figure 3-7 Disk-shaped Compact Tension Test Result, Setup and Specimen Geometry [99]**

### 3.3.2 Binder Testing

#### 3.3.2.1 DSR Test

The thermo-rheological properties of asphalt binders were measured using a Dynamic Shear Rheometer (DSR) with a 4mm plate [91] (Glaser et al., 2015). This test covers a wide range of temperatures (-36°C to 40°C, usually in 3 degree increments), and frequencies (15 frequencies from 100 rad/sec to 0.2 rad/sec), by using the appropriate strain level at each combination of test temperature and frequency. The isotherm tests are conducted from the coldest to the warmest temperature and from the highest to the lowest frequencies.

The complex shear modulus master curve is constructed at certain reference temperature and converted to the relaxation modulus master curve using Christensen's equation. **Eq. 3-14** and **3-15** below indicate the complex shear modulus and phase angle calculations. Figure 3-8 shows the test setup and one typical cycle of test data.

$$|G^*| = \frac{\sigma_{amp}}{\varepsilon_{amp}} \quad \text{Equation 3-14}$$

$$\delta = 2\pi f \Delta t \quad \text{Equation 3-15}$$

$|G^*|$  : Complex shear modulus (pa),

$\sigma_{amp}$  : Amplitude of applied stress (pa),

$\varepsilon_{amp}$  : Amplitude of strain response (mm/mm),

$\delta$ : phase angle (degrees),

$f$ : load frequency (Hz),

$\Delta t$ : The time lag between stress and strain peak to peak.

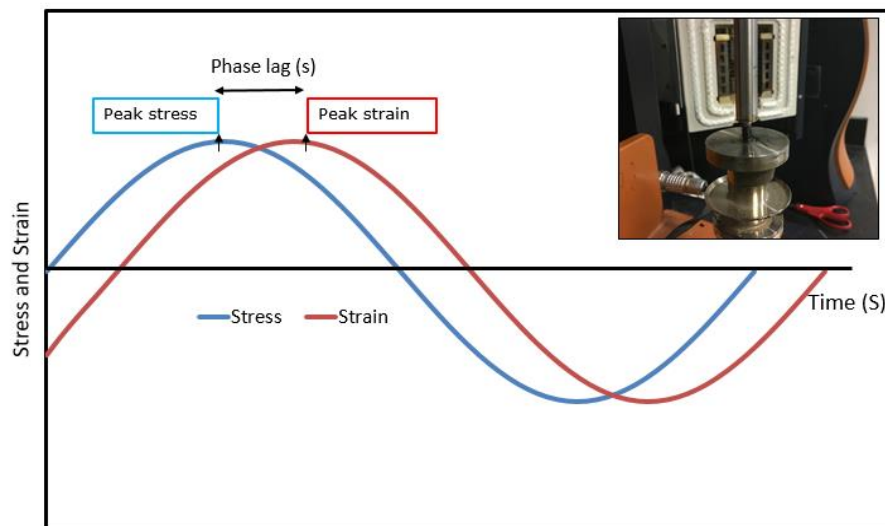


**Figure 3-8 4mm DSR Test Result and Setup [2]**

**Sui et al. [110]** developed a method to calculate the slope and magnitude of the shear stress relaxation modulus  $G(t)$  from the relaxation modulus master curve constructed from the 4mm DSR test at 60 seconds and  $10^{\circ}\text{C}$  warmer than the PG grading temperature, which are correlated with the corresponding  $S(t)$  and  $m$ -values at 60 seconds and  $10^{\circ}\text{C}$  above the true low PG grading temperature from BBR measurements. The  $\Delta T_c$  parameter can be then calculated from the critical temperatures determined by the  $S(t)$  and  $m$ -value.  $\Delta T_c$  is defined as the difference between the temperature at which the creep stiffness,  $S(t)$ , and  $m$ -value criteria from the BBR testing are met, as shown in **Eq. 3-16**.

$$\Delta T_c = T_{(stiffness)} - T_{(m-slope)}$$

Equation 3-16

$T_{(stiffness)}$  is the critical low temperature where  $S(60) = 300$  MPa, and  $T_{(m-slope)}$  is the critical low temperature where  $m(60) = 0.300$ . When the  $\Delta T_c$  value is higher than 0, the binder grade is controlled by the stiffness (S-controlled); when the  $\Delta T_c$  value is lower than 0 the binder grade becomes m-controlled. S-controlled binders have “extra” relaxation capability and are therefore typically less prone to cracking. Asphalt Institute [101,111] suggests using  $\Delta T_c = -2.5^\circ\text{C}$  as a crack warning limit and  $\Delta T_c = -5.0^\circ\text{C}$  as the cracking limit.

The complex modulus master curve from 4mm DSR test is also used to calculate the R-value and binder Glover-Rowe parameter. R-value is the difference between the logarithmic glassy modulus and the logarithmic equilibrium modulus of the binder, simplified as  $\text{Log } |G^*|$  at glassy asymptote minus  $\text{Log } |G^*|$  at the crossover frequency. Rowe et al. [102] developed the binder Glover-Rowe parameter to evaluate the cracking susceptibility of asphalt binders, as shown in **Eq. 3-17**. A lower G-R parameter indicates better capability to resist durability cracking. A limiting value of 180kPa is proposed as a crack warning limit, a second value of 600kPa is suggested for the development of significant cracking (block cracking).

$$G - R = \frac{|G^*|(\cos\delta)^2}{\sin\delta}$$

Equation 3-17

where  $|G^*|$  is the complex shear modulus and  $\delta$  is phase angle of the binder. The binder G-R parameter is generally calculated at the temperature and frequency combination of  $15^\circ\text{C}$  and  $0.005\text{rad/sec}$ .

In addition to these rheological parameters, the transition temperatures (glassy transition temperature ( $T_g$ ); viscoelastic (crossover) transition temperature ( $T_t$ ); and the intermediate region temperature range ( $\Delta T_{IR}$ )) can also be measured from the 4mm DSR test [112]. These three temperatures are typically calculated from the storage and loss modulus master curves in the temperature domain with a frequency of 10 rad/s or 1.59 Hz (as shown in **Figure 3-9**). Glass transition temperature ( $T_g$ ) is the temperature where the loss modulus starts to drop near the glassy transition region, while viscoelastic transition temperature ( $T_t$ ) is the temperature where loss modulus is equal to storage modulus in between of the intermediate and terminal region. The Intermediate Region Temperature ( $\Delta T_{IR}$ ) is the difference between the viscoelastic temperature and the glassy transition temperature, indicating the “length” of the intermediate “transition” region.

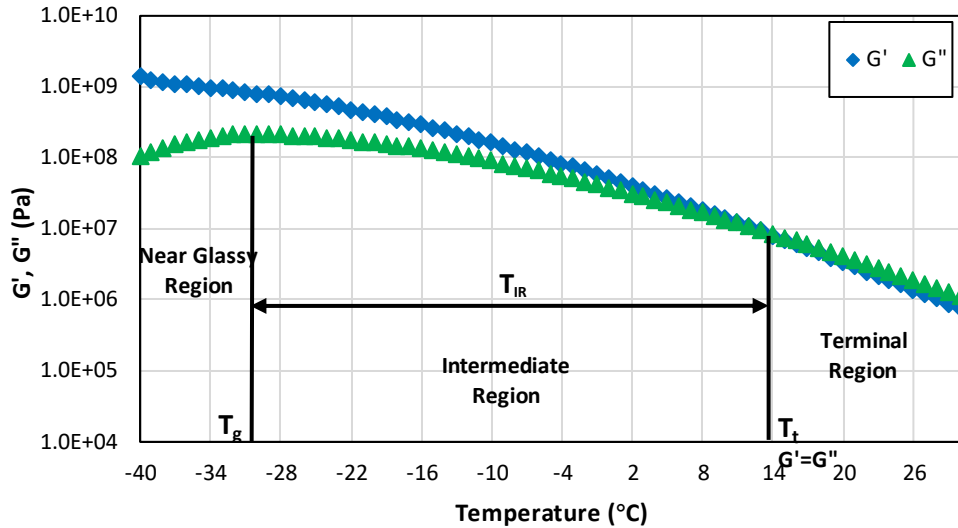


**Figure 3-9  $T_g$ ,  $T_t$  and  $T_{IR}$  in  $G'$  and  $G''$  Master Curve (Temperature Domain)**

### 3.3.2.2 Linear Amplitude Sweep (LAS) test

The LAS test evaluates the ability of asphalt binder to resist fatigue damage. This test is an oscillatory strain sweep test that generates damage to the binder by applying linearly increasing load amplitudes. The LAS test consists of two steps: first, a frequency sweep is performed in order to get information about undamaged material properties and evaluate the rheological characteristics of the binder. Second, the damage characteristics of the binder are measured employing a linear amplitude strain sweep test. In this study, frequency sweeps are conducted at a strain amplitude of 0.1% with a range of frequencies from 0.2 to 30 Hz according to AASHTO TP101. Amplitude sweep test is performed at a constant frequency of 10 Hz. The testing protocol consisted of applying a linearly increasing strain from zero to 30% over 3100 cycles of loading. All tests are conducted using DSR device with an 8 mm diameter parallel plate and a 2 mm gap. Three replicates are run for each binder. The integrity  $C(t)$  and damage accumulation  $D(t)$  curve (fatigue law, also referred to as damage characteristic curve (DCC)) of the binder sample during the test is calculated by **Eq. 3-18-20**. The relationship between  $C(t)$  and  $D(t)$  can be fit to the power law, as **Eq. 3-20** shown.

$$C(t) = \frac{G^* \sin \delta(t)}{G^* \sin \delta_{initial}} \quad \text{Equation 3-18}$$

$$D(t) = \sum_{i=1}^N [\pi \gamma_0^2 (C_{i-1} - C_i)]^{\frac{\alpha}{1+\alpha}} (t_i - t_{i-1})^{\frac{1}{1+\alpha}} \quad \text{Equation 3-19}$$

$$C_{(t)} = C_0 - C_1 (D)^{C_2} \quad \text{Equation 3-20}$$

where  $G^*$  is the complex modulus;  $\delta$  is the phase angle;  $\gamma_0$  is the applied strain;  $\alpha$  is calculated from the frequency sweep test;  $t$  is test time. **Figure 3-10** below shows the typical C-D plot determined from the LAS test.

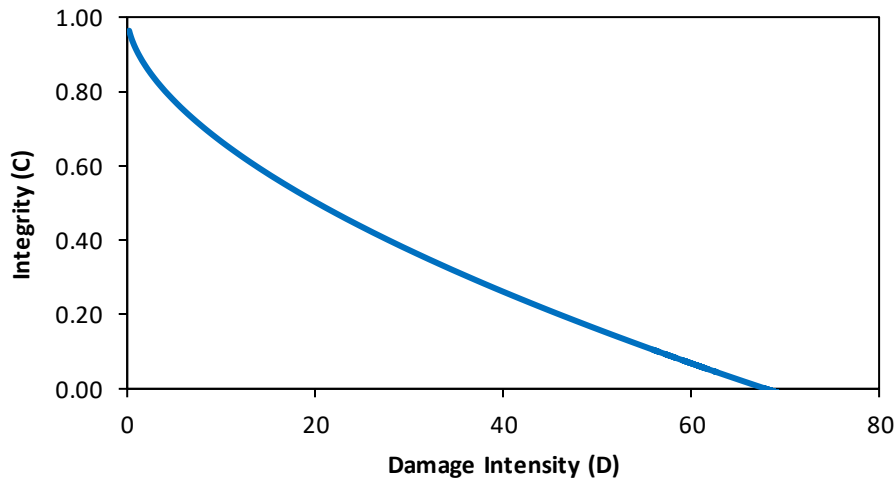


**Figure 3-10 Typical Damage Characteristic Curve (DCC) from LAS Test**

The number of cycles to failure is calculated using **Eq. 3-21-24**. The failure definition in LAS test is defined as 35% reduction in the initial modulus [113].

$$N_f = A(r_{max})^B \quad \text{Equation 3-21}$$

$$A = \frac{f(D_f)^k}{k(\pi I_D c_1 c_2)^\alpha} \quad \text{Equation 3-22}$$

$$B = 2\alpha \quad \text{Equation 3-23}$$

$$D_f = 0.35 \left( \frac{c_0}{c_1} \right)^{\left( \frac{1}{c_2} \right)} \quad \text{Equation 3-24}$$

where  $A$  and  $B$  are VECD model coefficients that depend on the material characteristics,  $r_{max}$  is the applied strain,  $D_f$  is defined as damage at failure, which corresponds to a 35% reduction in  $G^* \sin \delta$ ;  $f$  is loading frequency (10Hz). With the measured  $A$  and  $B$  parameter from the LAS test,  $N_f$  vs. strain curve can be calculated following **Eq. 3-21**, and plotted in **Figure 3-11**. Generally, “ $A$ ” parameter represents the material’s ability to keep its integrity during loading cycles and accumulated damage. This parameter is directly related to the storage modulus. In other words, as the storage modulus decreases through loading cycles, the  $A$  parameter decreases, which indicates the decreasing ability of the binder to maintain its integrity. The sensitivity of the asphalt binder to strain level is described by the  $B$  parameter.

Higher absolute values of B indicate that the fatigue life decreases at a higher rate (steeper (negative) slope of the  $N_f$ -strain curve as shown in **Figure 3-11**) when strain level increases. In general, more fatigue resistant binders tend to have higher A values and lower absolute B values [113].

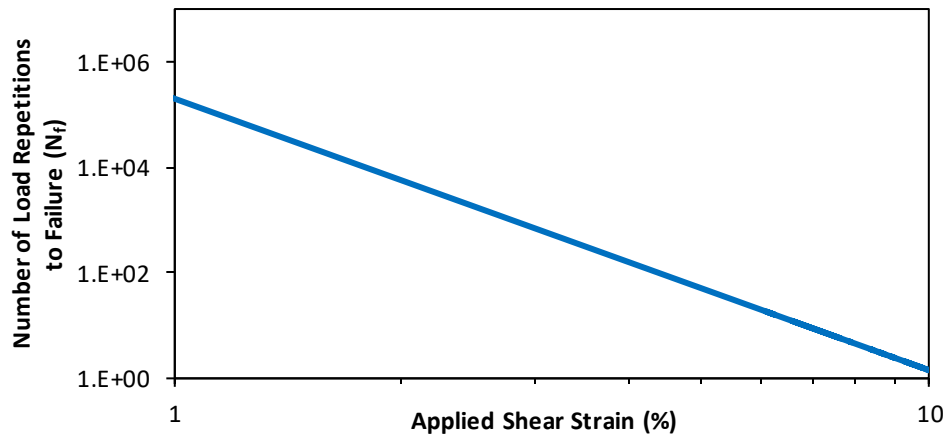


**Figure 3-11 Typical Fatigue Characterization ( $N_f$ -strain) Plot from LAS Test**

### **3.4 Cracking Performance Simulation and Prediction: FlexPAVE™ and IlliTC**

Use of prediction models are essential in predicting the performance of asphalt mixtures during, and at the end of service life. In this dissertation work, the FlexPAVE™ (formerly known as the LVECD program) developed by North Carolina State University (NCSU) is used to predict and compare the fatigue performance of the mixtures with different aging levels. The IlliTC thermal cracking prediction system is used for thermal cracking simulations and predictions.

#### **3.4.1 Fatigue Performance Simulation using FlexPAVE™**

FlexPAVE™ predicts pavement responses and damage evolution (fatigue and rutting) in both spatial distribution and time history modes. One of the outputs of this program is percent damage which is calculated on the basis of cumulative damage model and Miner's rule. To simulate and predict the fatigue performance, the material properties including the viscoelastic property measured from the  $E^*$  test and the fatigue properties measured from the DTCF fatigue test, associated with the pavement structure and local and regional climatic and traffic conditions are the required inputs for the FlexPAVE™ simulations and predictions.

#### **3.4.2 Thermal Cracking Performance Simulation using IlliTC**

IlliTC thermal cracking prediction system utilizes a two steps analysis approach for maintaining practical analysis times for various cases. The system is designed to use critical

cracking conditions approach; whereby thermo-viscoelastic stress analysis identifies the time period when thermal stresses exceed 80% of mixture tensile strength. These critical conditions are evaluated using finite element analysis with cohesive zone fracture model to simulate quasi-brittle cracking in asphalt concrete. A number of researchers have shown that cohesive zone fracture approach is well suited for simulation of discrete cracking in asphalt mixtures [76, 99, 107].

## **4 Impact of Aging on the Viscoelastic Properties and Cracking Behavior of Asphalt Mixtures (Paper 1, Appendix A)**

The content of this chapter of dissertation is in form of a peer-reviewed journal article. Manuscript for the article is provided in the appendix to this dissertation. Significance of this article within the overall scope of this dissertation and the abstract of the study are described next.

### **4.1 Significance of the Study**

Aged mixtures have increased cracking susceptibility with potentially shorter pavement service lives and lower serviceability of the pavement. Considering the prediction of the performance of the asphalt mixtures with aging and the importance of performance-based design methodologies, the evaluation of performance of aged asphalt mixtures is desired during the mix design stage. Therefore, the main objective of work presented in this chapter (paper-1) is to evaluate how the viscoelastic, fatigue, and fracture properties and cracking performance of typical NH asphalt mixtures evolve with different aging protocols and the corresponding field aging durations, and identify how the mixture properties may influence the magnitude in change of properties with aging. The research conducted in this portion of thesis provides a comprehensive evaluation of how the aging impacts the different properties of asphalt mixtures that generally used in NH and identifies the aging and cracking susceptible mixtures for material selection and mixture design. The field aging periods corresponding with the different laboratory conditioning protocols included in this study are also calculated, bridging the current gap between the research methods with the practices in the real world. This chapter directly contributes to the thesis objectives 1 and 2.

### **4.2 Abstract**

Aging can significantly affect the viscoelastic properties and cracking behavior of asphalt mixtures, causing increase in stiffness, reduction in relaxation capability and increase in brittleness. Eleven mixtures are evaluated using different laboratory conditioning protocols to evaluate how the properties of asphalt mixtures, including viscoelastic properties, fatigue, and fracture behavior will change over time. Comparisons between different aging levels and mixtures are conducted by using complex modulus ( $E^*$ ) (field cores are included), Simplified Viscoelastic Continuum Damage (S-VECD) approach, Semi Circular Bending (SCB) and Disk-shaped Compact Tension (DCT) fracture tests. The climatic aging index developed by the NCHRP 09-54 project is utilized in this study to calculate the appropriate field aging duration corresponding to the different laboratory aging protocols. Pavement evaluation tools



FlexPAVE™ and IlliTC are also used to predict and compare the fatigue and thermal cracking performance of these mixtures. The results of E\* and S-VECD tests indicate that the mixtures are more prone to fatigue cracking with aging, and the two long term conditioning protocols induce statistically similar changes in linear viscoelastic and fatigue properties. However, prediction of fatigue performance from FlexPAVE™ does not show a consistent trend once pavement structure and traffic are considered. Fracture tests and IlliTC predictions show the virgin mixtures and those with soft base binders will have better capability to resist cracking after long term aging. In this study, the two mixtures with the largest difference between PG high and low temperatures show the largest change in fracture and fatigue properties with aging.

## **5 Development of a Rheology-based Mixture Aging Model to Evaluate the Cracking Performance of Asphalt Material over Time (Paper 2, Appendix B)**

The content of this chapter of dissertation is in form of a peer-reviewed journal article. Manuscript for the article is provided in the appendix (Paper-3) to this dissertation. Significance of this article within the overall scope of this dissertation and the abstract of the study are described next.

### **5.1 Significance of the Study**

Aging has a significant impact on the chemical, microstructural, and different physical and engineering properties of asphalt material. Fundamental modeling of asphalt aging and the accurate prediction of asphalt mixture properties in terms of pavement service life is of pragmatic importance as more powerful pavement design and performance prediction methods are implemented. Significant research efforts have been dedicated to model the kinetics of asphalt binder aging; however, relatively little attention has been devoted to modeling the aging of asphalt mixtures. In addition, most aging models developed focus only on the modelling and prediction of the stiffness over time, ignoring the relaxation capability (phase angle) of the asphalt (viscoelastic) material. Researchers have shown that phase angle plays the significant role in the performance of both asphalt binder and mixture. In order to address the problems mentioned above, a simplified and experimental mixture aging model is developed and validated in the research presented in this chapter (paper-3), taking into account mixture variables such as performance grade (PG), RAP and binder content. The proposed model uses mixture Glover-Rowe (G-Rm) parameter as the AIP to modelling the change of mixture properties with aging, which incorporates both stiffness and relaxation capacity (phase angle) to evaluate the cracking performance of asphalt mixtures. The research conducted in this portion of thesis provides a simplified and experimental mixture aging model for accurate prediction of asphalt mixture properties in terms of pavement service life, culminating in a more effective, simple, and convenient material selection and pavement design approach. This chapter directly contributes to the thesis objectives 1 and 3.

### **5.2 Abstract**

Aging has a significant effect on the performance of asphalt material. Reliable modelling of the change of asphalt mixtures' properties over time is crucial to evaluating and predicting the performance of the designed pavement. The objective of this study is to develop an aging model to accurately predict the cracking performance of asphalt mixtures with different variables (e.g.

binder performance grades and recycled binder content) over the pavement service life, as well as evaluate the aging susceptibility of mixtures over time. In this study, nine loose mixtures were conditioned in an oven at 95°C for multiple durations to simulate different field aging times. The climatic aging index (CAI) developed by the National Cooperative Highway Research Program (NCHRP) 09-54 project was utilized to calculate the appropriate field aging durations corresponding to the different laboratory aging conditions. Complex modulus tests ( $E^*$ ) were conducted to measure the rheological properties of the conditioned mixtures and further construct the complex modulus and phase angle mastercurves. The mixture Glover-Rowe (G-Rm) parameter, incorporating both stiffness and relaxation capacity, was selected and used as the Aging Index Properties (AIP) to modelling the change of mixture cracking performance with aging. The results of this study indicate that the developed mixture aging model can effectively capture the two aging reaction periods (fast and constant) of asphalt materials. The developed model can not only be used to evaluate the change of cracking performance over pavement service life, but also detect the aging susceptibility of asphalt mixtures.

## **6 Correlating Laboratory Conditioning with Field Aging for Asphalt Using Rheological Parameters (Paper 3, Appendix C)**

The content of this chapter of dissertation is in form of a peer-reviewed journal article. Manuscript for the article is provided in the appendix (Paper 2) to this dissertation. Significance of this article within the overall scope of this dissertation and the abstract of the study are described next.

### **6.1 Significance of the Study**

Even though there are many research efforts that have been dedicated to develop the appropriate laboratory conditioning methods to simulate aging of asphalt material and evaluate the aging effect on binder/mixture properties, apparent gaps still exist between published research and precise description of aging behavior of asphalt materials in the field. One of the biggest concerns of field aging is the aging gradient within the pavement structure due to different factors such as the temperature gradient, oxygen availability and air void distribution. Overlooking aging gradient leads to inappropriate characterization of the aging behavior of asphalt mixtures. The main objective of this study (chapter) is to correlate the asphalt binder and mixture laboratory conditioning methods with field aging by exploring evolution of rheological parameters of asphalt binders over time, as well as evaluating changes in the aging kinetics with pavement depth. The rheological indices of binder samples with different aging conditions are measured to evaluate how the properties of asphalt binders change with time. The field aging gradient is evaluated and investigated by testing binder samples extracted and recovered from different layers of field cores. The laboratory aging durations corresponding with the field aging durations of the different layers from field cores are also determined based on New Hampshire climate conditions. The research conducted in this portion of thesis not only evaluates how the aging impacts the binder rheological behaviors, but also provides a way to optimize the laboratory conditioning durations and evaluate the performance of asphalt material with respect to pavement life (time) and depth (location) within the pavement structure. This chapter directly contributes to the thesis objectives 1 and 2.

### **6.2 Abstract**

Aging has a significant effect on performance of asphalt materials. Reliable characterization of asphalt binder properties with aging is crucial to improving asphalt binder specifications as well as modification and formulation methods. The objective of this study is to correlate the laboratory conditioning methods with field aging using evolution of binder rheological parameters with time and pavement depth. Loose mixtures are aged in the lab (5 and 12 days

aging at 95°C, and 24 hours at 135°C) and recovered binder rheological properties are compared with those from different layers of field cores. The virgin binder results with 20 hours PAV aging are also included. Binder testing is conducted using a dynamic shear rheometer (DSR) with a 4mm plate over a wide range of frequencies and temperatures. Rheological parameters calculated from the master curves, performance grade (PG) system, and binder Christensen-Anderson-Marasteanu (CAM) model are used to evaluate changes with aging. The field aging gradient is evaluated and the laboratory conditioning durations corresponding with the field aging durations at different pavement depths are calculated. The results show that 5 days aging can simulate around 8 years field aging (in New Hampshire) for the top 12.5mm pavement, while 12 days aging can simulate approximately 20 years; 20 hours PAV binder aging is not adequate to capture the long-term performance of the pavement. This study provides a way to optimize the laboratory conditioning durations and evaluate the performance of asphalt material with respect to pavement life (time) and depth (location) within the pavement structure.

## **7 Development of New Performance Indices to Evaluate the Fatigue Properties of Asphalt Binders with Aging (Paper 4, Appendix D)**

The content of this chapter of dissertation is in form of a peer-reviewed journal article that has been submitted for review. Manuscript for the article is provided in the appendix (Paper-4) to this dissertation. Significance of this article within the overall scope of this dissertation and the abstract of the study are described next.

### **7.1 Significance of the Study**

It is reported that among the mixture components, binder plays the most important role in fatigue behavior of asphalt mixtures. Hence, it is important to find a valid test method and the corresponding parameters to efficiently and effectively capture the fatigue properties of asphalt binders. The recent developed Linear Amplitude Sweep (LAS) test and its current performance parameters have been used by many studies to investigate the fatigue performance of asphalt material, however, researchers recently have found some challenges with using the current performance parameters measured from the LAS test to investigate the effect of asphalt modifiers on binder fatigue behavior and the aging effect on binder's long-term performance. Aiming to solve these challenges, the primary objective of this study is to explore and develop the new performance parameters to better understand and evaluate the fatigue properties of asphalt binders by incorporating the aging effects. In addition, the effect of asphalt modifiers is also evaluated in this study on limited basis. The research conducted in this portion of thesis allows for more appropriate evaluation of the long-term fatigue properties of asphalt materials. This chapter directly contributes to the thesis objectives 1 and 3.

### **7.2 Abstract**

This work presents the development of new fatigue performance indices for asphalt binders based on viscoelastic continuum damage (VECD) theory and failure energy. Five plant-produced asphalt mixtures were subjected to three different conditioning levels (short term aging during production and loose mix aging for 5 and 12 days at 95°C in the laboratory) and the corresponding binders were extracted and recovered. Direct Tension Cyclic Fatigue (DTCF) tests were performed on the mixtures to characterize the mixture fatigue properties using the simplified viscoelastic continuum damage (S-VECD) analysis approach. Frequency and temperature sweep tests using a Dynamic Shear Rheometer (DSR) with a 4 mm parallel plate and the Linear Amplitude Sweep (LAS) test were conducted on the recovered binders to evaluate the binder rheological and fatigue properties. Three new performance indices are

explored from the LAS test: Strain Tolerance ( $\epsilon_T$ ), Strain Energy Tolerance ( $E_f$ ), and Average Reduction in Integrity to Failure ( $I^R$ ). These indices were used to track the evolution of binder fatigue properties with aging. A unique aspect of these indices is that they capture the failure point of the binder during the LAS test and combine the stress and strain histories of the material. Compared with the traditional A and B parameters from the LAS test, the new indices show a consistent decrease in the fatigue properties of the binders with aging. The newly proposed parameters show improved correlations with mixture fatigue performance index ( $D^R$ ) from the DTCF test, indicating their potential for evaluation of asphalt mixture's fatigue properties. In addition, the new indices developed from this study have been shown to effectively capture the aging gradient within the pavement structure and can also be used together with the binder rheological indices (e.g. G-R parameter and  $\Delta T_c$ ) to evaluate both environmental and fatigue cracking of asphalt pavements at the same time.

## **8 Comparison and Correlation of Asphalt Binder and Mixture Cracking Parameters Incorporating the Aging Effect (Paper 5, Appendix E)**

The content of this chapter of dissertation is in form of a peer-reviewed journal article that is under preparation. Manuscript for the article is provided in the appendix (Paper-5) to this dissertation. Significance of this article within the overall scope of this dissertation and the abstract of the study are described next.

### **8.1 Significance of the Study**

In order to efficiently and effectively evaluate and control the cracking performance of asphalt pavement, significant research efforts have been dedicated to developing and promoting the different laboratory engineering tests and the corresponding performance parameters, which provide agencies and researchers a valuable way to qualitatively and quantitatively evaluate the cracking susceptibility for both asphalt binders and mixtures. However, there is still a question of how the mixture properties change with changes in binder characteristics and how the binder and mixture testing methods may differentially evaluate expected performance of asphalt materials with respect to cracking. Also, the relationship between binder cracking performance and mixture cracking behavior is still not completely understood. A few preliminary studies have recently been conducted to explore this relationship, but these studies are performed using limited testing and analysis methods to evaluate the specific cracking behavior (e.g. fatigue or thermal) of asphalt material. In addition, relatively little attention has been devoted to evaluating this relationship while also incorporate the effects of aging, since aging significantly impacts the cracking performance for both binders and mixtures. With this current research gap, the primary objective of this portion of the dissertation research (paper 5) is to comprehensively compare and correlate the asphalt mixture and binder cracking properties by conducting the different advanced performance tests and employing the various statistical methods, while also considering the aging effects by laboratory conditioning to simulate the different field aging periods. The research conducted in this portion of thesis provides agencies and researchers a better understanding and more systematic insight on the relationships between binder and mixture cracking behaviors. This chapter directly contributes to the thesis objectives 1 and 3.

### **8.2 Abstract**

Cracking is one of the primary distresses in asphalt pavements, and aging can significantly affect the cracking performance of asphalt material. The primary objective of this study is to



investigate the comparisons and correlations between the current binder and mixture cracking performance parameters by incorporating the aging effect. Nine plant produced mixtures are subjected to various conditioning protocols (5 and 12 days aging at 95°C, and 24 hours at 135°C on loose mixtures), and the corresponding binders are extracted and recovered from those mixtures. Mixture performance are measured from Complex Modulus ( $E^*$ ), Direct Tension Cyclic Fatigue (DTCF), Semi Circular Bending (SCB) and Disk-shaped Compact Tension (DCT) fracture tests. Binder tests include the typical Frequency and Temperature Sweep test on the Dynamic Shear Rheometer (DSR) and the Linear Amplitude Sweep (LAS) test. Different statistical analysis methods including the Pearson, Kendall and Hoeffding's D analysis are then applied to investigate the comparisons and correlations between the parameters measured from the different tests. The results from this study indicate that mixture Glover-Rowe (G-Rm) and Flexibility Index (FI) parameter generally show the moderate to strong correlations with many of the mixture cracking parameters, binder rheological index  $\Delta T_c$  and G-R, transition temperature  $\Delta T_{IR}$  and fatigue parameter  $I^R$  generally show the good correlations with other binder cracking parameters. Comparing the binder parameters with mixture indices, mixture G-Rm, FI and two master curve parameters  $-\beta/\gamma$  and  $c$  show the moderate to strong correlations with all the binder parameters. Binder fatigue parameters typically show the strong correlation with mixture fatigue index  $D^R$ , indicating the possibility of using binder fatigue parameters for evaluation of mixtures' fatigue properties. Overall, the good correlations between binder and mixture cracking parameters observed from this study indicate that binders play the most important role in the cracking performance of asphalt mixtures.

## 9 Summary and Conclusions

### 9.1 Summary

Cracking is a primary concern for asphalt pavements, and aging can significantly impact the cracking performance of asphalt material over the pavement service life. Since the asphalt mixtures made up with different variables will have very different cracking behaviors with increase of aging, thus, this doctoral thesis is designed and aims to provide a better understanding of how the cracking resistance of different binders and mixtures changes over time and propose the recommendations and guidelines for selection of more appropriate materials and design of more durable and sustainable asphalt pavements. A brief summary and discussion of how the overall objectives in this dissertation work are achieved by the different technical chapters (papers) are provided in this section:

1. Quantitatively evaluate how the cracking performance of both asphalt mixture and binder changes over time;

In chapter 4, the effect of aging on mixture properties, including the viscoelastic properties, fatigue, and fracture behavior were evaluated by conducting the various performance tests, including  $E^*$ , DTCF fatigue, SCB and DCT fracture tests on the study mixtures with various laboratory condition methods. Pavement evaluation tools FlexPAVE™ and IlliTC were also employed to predict and compare the fatigue and thermal cracking performance of mixtures with different aging levels, in context of pavement structure, traffic and climatic conditions.

Chapter 5 directly evaluated the effect of aging on binder rheological properties through testing on the binder samples extracted and recovered from the laboratory conditioned mixtures and the cores taken from the field sections. Various rheological parameters were calculated and evaluated, including the binder complex shear modulus and phase angle master curves, performance grade low temperature, binder R-value and Glover-Rowe parameter, critical temperatures determined by creep stiffness ( $T_c(S)$ ) and the relaxation rate ( $T_c(m)$ ), and the difference between those two ( $\Delta T_c$ ). The fatigue properties of the binder samples were investigated using the new performance indices developed in chapter 7. Compared with the traditional parameters, the new indices showed a consistent decrease in the fatigue properties of asphalt binders with aging. The newly proposed parameters were also found to have the potential for evaluation of asphalt mixture's fatigue properties and can be used to effectively capture the aging gradient within the pavement structure.

Chapter 8 summarized the testing and analysis results from this dissertation work, and further evaluated and investigated the correlations and comparisons between the mixtures' and binders'

cracking performance. Different statistical methods (Pearson correlation coefficient, Kendall rank correlation coefficient and the Hoeffding's D correlation) were used to evaluate both linear and non-linear, monotonic and non-monotonic correlations among the parameters in terms of both values and ranking of mixtures. The frequency (density) curve was employed to evaluate the distribution of each parameter with change of aging conditions. The overall good correlations between binder and mixture cracking parameters observed in chapter 8 indicate that binders play the most important role in the cracking performance of asphalt mixtures.

2. Correlate the laboratory conditioning (aging) methods with actual field aging duration;

The climatic aging index (CAI) model was utilized together with the performance testing on the field cores to calculate the appropriate field aging periods corresponding to the different laboratory conditioning protocols in chapter 5. The results showed that 5 days at 95°C laboratory aging condition appears to simulate approximately four years of field aging for the surface mixtures in NH, while 12 days at 95°C laboratory aging can simulate approximately 10 years of field aging.

Chapter 6 correlated the different laboratory conditioning methods with field aging periods using evolution of binder rheological parameters with time and pavement depth. The results showed that 5 days aging can simulate around 8 years field aging in NH for the top 12.5mm pavement, while 12 days aging can simulate approximately 20 years; 20 hours PAV binder aging is not adequate to capture the long-term performance of the pavement. The general method described in this chapter provided agencies and researchers a way to optimize the laboratory conditioning durations and evaluate the performance of asphalt material with respect to pavement life (time), and depth (location) within the pavement structure.

As the results shown above, same laboratory conditioning method (5 or 12 days at 95°C) appears to simulate different field aging periods in NH based on the mixture evaluation and binder evaluation. There are some potential reasons to explain the difference: the extraction process may change the binder characteristics because of the remaining solvent, the Fourier-transform Infrared Spectroscopy (FTIR) test can be used to further detect the chemical composition of the extracted binders; the binder test does not take account the differences in air void of the field cores or damage from traffic that may have occurred. Finally, extracted binders represent fully blended conditions between virgin and recycled binders.

3. Provide recommendations and guidelines on how to identify crack and aging susceptible binders/mixtures during material selection and mix design.

The different performance tests, as well as the advanced performance simulation and prediction programs included in this dissertation work have shown the capability to track the change of asphalt binders' and mixtures' cracking performance and identify the cracking susceptible

asphalt material as discussed in chapter 4, 5 and 7. These methods together with the findings overserved from this study can be directly used as the suggestions and guidelines for agencies and contractors during material selection and mixture design procedures.

In addition, the mixture rheology-based aging model developed and discussed in Chapter 6 has been shown to not only be able to effectively capture the two aging reaction periods of asphalt material, but also track and predict the change of mixture cracking performance over pavement service life and identify the aging susceptible mixtures with different variables. This mixture aging model can be directly used as an effective, simple and convenient material selection approach and be incorporated into the mix design procedure for design and construction of more reliable and durable asphalt pavement.

## 9.2 Conclusions

The primary objective of this dissertation work is to evaluate how the aging impacts the cracking performance of asphalt material (both binder and mixture). Based on the testing and evaluation conducted in this study, the following conclusion remarks can be drawn from this research:

### 1. Asphalt Binder Evaluation

- The linear viscoelastic properties of binders with 24 hr. at 135°C and 12 days at 95°C aging are statistically similar.
- Binders with the softer PGLT and with the largest difference between PGHT and PGLT generally show the most impact from aging. The binders extracted and recovered from virgin mixtures generally show the good cracking performance at each aging condition.
- Based on evaluation of the rheological behaviors of study binders, the 20 hours PAV binder conditioning protocol generally produces less aging of the asphalt material than 5 days at 95°C mixture conditioning method.
- The binder samples extracted from the field cores illustrate the aging gradient in field, with the top layers (1 inch) aged the most.
- The developed three new binder fatigue parameters (Strain Tolerance( $\epsilon_T$ ), Energy to Failure ( $E_f$ ), and Average Reduction in Integrity to Cracking Initiation ( $I^R$ )) can effectively capture the failure point of the binder samples during LAS test, the  $\epsilon_T$  and  $E_f$  can also evaluate the cracking development after damage is initiated. The new parameters show a consistent decrease in the fatigue performance of the binder samples with aging.

- The new fatigue parameters show the good correlations with mixture fatigue performance index  $D^R$  value, indicating the new parameters have the potential to be used for evaluation of the fatigue properties of asphalt mixtures while also taking aging into account.

## 2. Asphalt Mixture Evaluation

- The linear viscoelastic properties of mixtures with 24 hr. at 135°C and 12 days at 95°C aging are statistically similar. However, mixtures after 24hr. at 135°C condition typically show the worst fracture properties.
- The two mixtures with the softer binders and the binder with the largest difference between PGHT and PGLT generally show the most impact from aging based on the fracture and fatigue testing results. However, the virgin mixture still has good fracture and fatigue performance after aging.
- Combining the results of the complex modulus testing with the CAI calculation, 5 days at 95°C laboratory aging condition appears to simulate approximately four years of field aging for the surface mixtures in NH, while 12 days at 95°C laboratory aging simulates 9.6 years of field aging.
- The developed mixture aging model can not only effectively capture the two aging reaction periods of asphalt material, but also track and predict the change of mixture cracking performance over pavement service life and identify the aging susceptibility of the mixtures with different mix variables.

## 3. Comparison and Correlation the Cracking Performance between Asphalt Binders and Mixtures

- The mixture  $G-R_m$  parameter has moderate to strong correlations with many of the mixture and binder parameters indicating that it has the potential to be used as a simplified index to evaluate and differentiate the cracking performance of asphalt material in general. In addition, the two inflection point parameters  $-\beta/\gamma$  and  $c$  also show the moderate and strong correlations with most of the mixture and binder cracking parameters.
- Most of the mixture and binder cracking parameters dramatically decrease in their values with increase of aging condition from STA to intermediate aging condition, and then gradually drop from intermediate aging to the two long-term aging conditions. These changes match up with the trends observed for change of binder chemical composite with aging, indicating the fundamental relationships between the asphalt chemistry and its physical and engineering properties.

- The good correlations between binder and mixture cracking parameters in context of aging effect indicate that binders play the significant role in the cracking performance of asphalt mixtures.

In closing, evaluation of the impact of aging on the cracking behaviors for both asphalt binder and mixture realized from this study will culminate in a more effective and efficient material selection and pavement design, enhancing performance and promoting sustainability of designed pavement. This dissertation work will benefit both owner agencies and contractors: owner agencies can set their own performance limits and obtain confidence that the pavement can avoid significant cracking for a given period of time based on accurately predicted performance, while the contractors with the knowledge of the key parameters for improving the cracking resistance of pavements, will be driven to adjust their mix accordingly. The results of this study will help to improve the service life and ride quality of pavement, benefitting both asphalt industry and travelling public. This dissertation makes a good contribution in asphalt industry to improve the cracking evaluation and prediction approaches.

### **9.3 Future Extension**

This section summarizes recommendations for future work to further develop and refine the conclusions presented above based on the testing and analysis conducted in this dissertation work.

#### **1. Asphalt Binder Evaluation**

- Appropriate binder aging/conditioning protocols to simulate long term field performance and allow for screening of binders need to be further explored. In particular, longer PAV times and the Extended Bending Beam Rheometer (EBBR) protocols should be explored to quantify the equivalent field aging levels.
- Threshold values for the various thermo-rheological parameters need to be developed/improved based on the field performance that are collected over time.
- Chemical analytical test (e.g. Fourier Transform Infrared (FTIR) test) should be investigated for inclusion in comprehensive evaluation of the change of asphalt binders' properties with aging.

#### **2. Asphalt Mixture Evaluation**

- Continued collection of field performance data for the study mixtures to allow for further development, calibration, and verification of threshold values for laboratory measured performance indices.

- Periodic sampling of field cores for study mixtures and additional projects to refine the aging model with time and better define the aging gradient with depth.
- Research on air void adjustments for measured properties to better evaluate and compare the properties between field cores with lab aged and fabricated samples.
- Statistical analysis should be applied on the database generated from the binder/mixture tests to evaluate the volumetrics-performance relationship, which can provide agencies and contractors the valuable suggestions for improving their material selection and mix design procedures.

## 10 References

1. American Society of Civil Engineers. “2013 Report Card for America’s Infrastructure”,2013 <<http://www.infrastructurereportcard.org/a/documents/Roads.pdf>>.
2. Trentacoste, M.F. “Research and Innovative Solutions for the Nation’s Highway Challenges”. Federal Highway Administration. 2015.
3. Dave, E.V. “Synthesis of Performance Testing of Asphalt Concrete (Final Report)”. University of Minnesota Duluth. 2011.
4. Cominsky, R.J., Killingsworth, B.M., Anderson, D.A., Crockford W.W. “Quality Control and Acceptance of Superpave-Designed Hot Mix Asphalt”. Transportation Research Board, 1998.
5. Brown, E.R., Kandhal, P.S., Zhang, J. “Performance Testing for Hot Mix Asphalt (Executive Summary).” NCAT at Auburn University, National Asphalt Pavement Association, AL, 2001
6. Branthaver F., Petersen J. C., Robertson R. E. “Binder characterization and evaluation: chemistry,” Report No SHRP-A-368, vol. 2, SHRP, National Research Council, Washington, DC, USA, 1993.
7. Mortazavi M. and Moulthrop J. S., “SHRP materials reference library,” SHRP Report A-646, National Research Council, Washington, DC, USA, 1993.
8. Read J. and Whiteoak D., The Shell Bitumen Handbook, Thomas Telford Publishing, London, UK, 5th edition, 2003.
9. Corbett L. W., “Composition of asphalt based on generic fractionation using solvent deasphalteneing, elution adsorption chromatography and densiometric characterization,” Analytical Chemistry, vol. 41, no. 4, pp. 576–579, 1969.
10. Heneash U., Effect of the Repeated Recycling on Hot Mix Asphalt Properties, Ph.D. thesis, University of Nottingham, Nottingham, UK, 2013.
11. Notional Center for Asphalt Technology (NCAT).  
<http://www.eng.auburn.edu/research/centers/ncat/newsroom/2018-spring/aging.html>
12. Welborn J. Y., Relationship of Asphalt Cement Properties to Pavement Durability, National Cooperative Highway Research Program, Synthesis 59, Transportation Research Board, Washington, DC, USA, 1979.



13. Bell C. A., "Summary report on aging of asphalt-aggregate systems," Research Report No. SR-OCU-A-003A-89-2, SHRP-A-305, Strategic Highway Research Program, National Research Council, Washington, DC, USA, 1989.
14. Traxler R. N., "Relation between asphalt composition and hardening by volatilization and oxidation," *Proceedings of Association of Asphalt Paving Technologists*, vol. 30, pp. 359-377, 1961.
15. Petersen J. C., "Chemical composition of asphalt as related to asphalt durability: state of the art," *Transportation Research Record*, vol. 999, pp. 13-30, 1984.
16. Bell C. A., Wieder A. J., and Fellin M. J., "Laboratory aging of asphalt-aggregate mixtures: field validation," Research Report SHRP-A-390, Oregon State University, Corvallis, OR, USA, 1994.
17. Airey G., "State of the art report on ageing test methods for bituminous pavement materials," *International Journal of Pavement Engineering*, vol. 4, no. 3, pp. 165-176, 2003.
18. Apeageyi A. K., "Laboratory evaluation of antioxidants for asphalt binders," *Construction and Building Materials*, vol. 25, no. 1, pp. 47-53, 2011.
19. Anderson D. A. and Bonaquist R., "Investigation of shortterm laboratory aging of neat and modified asphalt binders," Research Report NCHRP-709, Transportation Research Board, Washington, DC, USA, 2012.
20. Lesueur D., "The colloidal structure of bitumen: consequences on the rheology and on the mechanisms of bitumen modification," *Advances in Colloid and Interface Science*, vol. 145, no. 1-2, pp. 42-82, 2009.
21. Traxler R. N., "Relation between asphalt composition and hardening by volatilization and oxidation," *Proceedings of Association of Asphalt Paving Technologists*, vol. 30, pp. 359-377, 1961.
22. Farcas F., "Etude d'une methode de simulation du vieillissement sur route des bitumes," Ph.D. thesis, Pierre and Marie Cury University, Paris, France, 1996, in French.
23. Christensen D. W. and Anderson D. A., "Interpretation of dynamic mechanical test data for paving grade asphalt cements," *Journal of the Association of Asphalt Paving Technologists*, vol. 61, pp. 67-116, 1992.
24. Cui P. C., Wu S., Xiao Y., and Zhang H., "Study on the deteriorations of bituminous binder resulted from volatile," *Construction and Building Materials*, vol. 68, pp. 644-

649, 2014.

25. Glover C. J., Martin E., Chowdhury A., “Evaluation of binder aging and its influence in aging of hot mix asphalt concrete: literature review and experimental design,” Research Report No. FHWA/TX-08/0-6009-1, Texas Transportation Institute, College Station, TX, USA, 2009.
26. Pan T., Sun L., and Yu Q., “An atomistic-based chemophysical environment for evaluating asphalt oxidation and antioxidants,” *Journal of Molecular Modeling*, vol. 18, no. 12, pp. 5113–5126, 2012.
27. Lee D. Y. and Huang R. J., “Weathering of asphalts as characterized by infrared multiple internal reflection spectra,” *Applied Spectroscopy*, vol. 27, no. 6, pp. 435–440, 1973.
28. Lau C. K., Lunsford K. M., Glover C. J., Davison R. R., and Bullin J. A., “Reaction rates and hardening susceptibilities as determined from pressure oxygen vessel aging of asphalts,” *Transportation Research Record*, vol. 1342, pp. 50–57, 1992.
29. Petersen J. C., Branthaver J. F., Robertson R. E., Harnsberger P. M., Duvall J. J., and Ensley E. K., “Effects of physicochemical factors on asphalt oxidation kinetics,” *Transportation Research Record*, vol. 1391, pp. 1–10, 1993.
30. Branthaver J. F., Petersen J. C., Robertson R. E., “Binder characterization and evaluation: chemistry,” Report No SHRP-A-368, vol. 2, SHRP, National Research Council, Washington, DC, USA, 1993.
31. Davis T. C. and Petersen J. C., “An inverse GLC study of asphalts used in the Zaca-Wigmore experimental test road,” *Proceedings of Association of Asphalt Paving Technologists*, vol. 36, pp. 1–15, 1967.25
32. Petersen J. C., “Asphalt aging: a dual oxidation mechanism and its inter-relationships with asphalt composition and oxidative age hardening,” *Transportation Research Record*, vol. 1638, pp. 47–55, 1998.
33. Wright J. R., “Weathering: theoretical and practical aspects of asphalt durability,” in *Bituminous Materials: Asphalts, Tars and Pitches*, A. J. Hoiberg, Ed., vol. 2, no. 1, pp. 249–306, Interscience Publishers, New York, NY, USA, 1965.
34. Corbett L. W. and Merz R. E., “Asphalt binder hardening in the Michigan test road after 18 years of service,” *Transportation Research Record*, vol. 544, pp. 27–34, 1975.
35. Lesueur D., “The colloidal structure of bitumen: consequences on the rheology and on the mechanisms of bitumen modification,” *Advances in Colloid and Interface Science*,

- vol. 145, no. 1-2, pp. 42–82, 2009.
36. Liu M., Ferry M. A., Davison R. R., Glover C. J., and Bullin J. A., “Oxygen uptake as correlated to carbonyl growth in aged asphalts and asphalt corbett fractions,” *Journal of the Industrial and Engineering Chemistry Research*, vol. 37, no. 12, pp. 4669–4674, 1998.
  37. Petersen, J. C., P. M. Harnsberger, and R. E. Robertson. Factors Affecting the Kinetics and Mechanisms of Asphalt Oxidation and the Relative Effects of Oxidation Products on Age Hardening. Preprints of Papers, American Chemical Society, Division of Fuel Chemistry, Vol. 41, No. CONF-960807, 1996.
  38. Lewis and Welborn J. Y., “Report on the properties of the residues of 50-60 and 85-100 penetration asphalts from oven tests and exposure,” *Proceedings of Association of Asphalt Paving Technologists*, vol. 11, pp. 86–157, 1940.
  39. Edler A. C., Hattingh M. M., Servas V. P., and Marais C. P., “Use of ageing tests to determine the efficacy of hydrated lime additions to asphalt in retarding its oxidative hardening,” *Proceedings of Association of Asphalt Paving Technologists*, vol. 54, pp. 118–139, 1985.
  40. Griffin R. L., Miles T. K., and Penther C. J., “Microfilm durability test for asphalt,” *Proceedings of Association of Asphalt Paving Technologists*, vol. 24, pp. 31–62, 1955.
  41. Schmidt R. J. and Santucci L. E., “The effects of asphalt properties on the fatigue cracking of asphalt concrete on the Zaca-Wigmore test project,” *Proceedings of Association of Asphalt Paving Technologists*, vol. 38, pp. 39–64, 1969.
  42. Kemp G. R. and Prodoehl N. H., “A comparison of field and laboratory environments on asphalt durability,” *Proceedings of Association of Asphalt Paving Technologists*, vol. 50, pp. 492–537, 1981.
  43. Petersen J. C., “A thin-film accelerated aging test for evaluating asphalt oxidative aging,” *Proceedings of Association of Asphalt Paving Technologists*, vol. 58, pp. 220–237, 1989.
  44. Hveem F. N., Zube E., and Skog J., “Proposed new tests and specifications for paving grade asphalts,” *Proceedings of Association of Asphalt Paving Technologists*, vol. 32, pp. 247–327, 1963.
  45. Whiteoak C. D., *Shell Bitumen Handbook*, \*omas Telford, Surrey, UK, 1990.
  46. Jemison, H. B., Davison R. R., Glover C. J., and Bullin J. A.. "Evaluation of Standard Oven Tests for Hot-Mix Plant Aging". Transportation Research Record 1323, TRB,

- National Research Council, Washington, D.C., 1991, pp. 77–84.
47. Sirin O., Shih C.-T., Tia M., and Ruth B. E., “Development of a modified rotavapor apparatus and method for short-term aging of modified asphalts,” *Transportation Research Record*, vol. 1638, pp. 72–81, 1998.
  48. Vassilev N. Y., Davison R. R., and Glover C. J., “Development of a stirred airflow test procedure for short-term aging of asphaltic concrete,” *Transportation Research Record*, vol. 1810, pp. 25–32, 2007.
  49. Lee S.-J., Amirkhanian S. N., Shatanawi K., and Kim K. W., “Short-term aging characterization of asphalt binders using gel permeation chromatography and selected Superpave binder tests,” *Construction and Building Materials*, vol. 22 pp. 2220–2227, 2007.
  50. Bahia H. U., Hislop W. P., Zhai H., and Rangel A., “Classification of asphalt binders into simple and complex binders,” *Journal of the Association of Asphalt Paving Technologists*, vol. 67, pp. 1–41, 1998.
  51. Robertson R. E., Branthaver J. F., Harnsberger P. M., “Fundamental properties of asphalts and modified asphalts,” Interpretive Report, FHWA-RD-99–212, vol. 1, U. S. Department of Transportation, Federal Highway Administration, McLean, VA, USA, 2001.
  52. Glover C. J., Davison R. R., and Vassiliev N., “Development of stirred air flow test (SAFT) for Improved HMA plant binder aging simulation and studies of asphalt air blowing,” Report Number FHWA/TX-02/1742–4, Texas Department of Transportation, 2001.
  53. Petersen J. C., Robertson R. E., Anderson D. A., Christensen D. W., Button J. W., and Glover C. J., “Binder characterization and evaluation volume 4: test methods, SHRP-A-403,” Strategic Highway Research Program (National Research Council), Washington, DC, USA, 1994.
  54. Lee D. Y., “Asphalt durability correlation in Iowa,” *Transportation Research Record*, vol. 468, pp. 43–60, 1973.
  55. Hayton B., Elliott R. C., Airey G. D., and Raynor C. S., “Long term ageing of bituminous binders,” in Proceedings of Eurobitume Workshop 99, Paper No. 126, Luxembourg, 1999.
  56. Verhasselt A. F. and Choquet F. S., “A new approach to studying the kinetics of bitumen

- ageing,” in *Proceedings of Chemistry of Bitumens: International Symposium*, vol. 2, pp. 686–705, Rome, Italy, 1991.
57. Fern'andez-G'omez W. D., Rond'on Quintana H., and Reyes Lizcano F., “A review of asphalt and asphalt mixture aging,” *Ingenier'ia e Investigaci'on*, vol. 33, no. 1, pp. 5–12, 2013.
  58. Bell, C. A., Y. AbWahab, R. E. Cristi, and D. Sognovske. "Selection of Laboratory Aging Procedures for Asphalt-Aggregate Mixtures." Washington, DC: Strategic Highway Research Program, National Research Council, 1994.
  59. Harrigan, E. T. "Simulating the Effects of Hot Mix Asphalt Aging for Performance Testing and Pavement Structural Design". Final Report, National Cooperative Highway Research Program, Research Results Digest 324, National Research Council, Washington, D.C., 2007.
  60. Arega, Z. A., A. Bhasin, and T. De Kesel. “Influence of Extended Aging on the Properties of Asphalt Composites Produced Using Hot and Warm Mix Methods,” *Construction and Building Materials*, Vol. 44, pp. 168-174, 2013.
  61. Yousefi Rad, F., M. D. Elwardany, C. Castorena, and Y. R. Kim, “Investigation of Proper Long-Term Laboratory Aging Temperature for Performance Testing of Asphalt Concrete,” *Construction and Building Materials*, Vol. 147, pp. 616-629, 2017.
  62. Kim, R. Y., Castorena, C., Elwardany, M., Yousefi Rad, F., Underwood, S., Gundha, A., Gudipudi, P., Farrer, M. J., Glaser, R., R. "Long-term Aging of Asphalt Mixtures for Performance Testing and Prediction", Final Report, NCHRP 09-54. 2018.
  63. Von Quintus H., Scherocman J., Kennedy T., and Hughes C. S., “Asphalt aggregate mixture analysis system,” Final Report to NCHRP 09–06(1), National Research Council, Washington, DC, USA, 1988.
  64. Aschenbrener T. and Far N., “Short-term aging of hot mix asphalt,” Report No. CDOT-DTD-R-94-11, Colorado Department of Transportation Public, Denver, CO, USA, 1994.
  65. Epps Martin A., Arambula E., Yin., “Evaluation of the moisture susceptibility of WMA technologies,” NCHRP Report 763, Transportation Research Board, Washington, DC, USA, 2014.
  66. Brown S. F. and Scholz T. V., “Development of laboratory protocols for the aging of asphalt mixtures,” in *Proceedings of 2nd Eurasphalt and Eurobitume Congress*, vol. 1, pp. 83–90, Barcelona, Spain, September 2000.

67. Eslaminia, M., Thirunavukkarasu, S., Guddati, M. N., & Kim, Y. R. Accelerated pavement performance modeling using layered viscoelastic analysis. Proceedings of the 7<sup>th</sup> international RILEM conference on cracking in pavements, Delft, The Netherlands, 2012
68. Bonaquist R. Mix Design Practices for Warm Mix Asphalt. Technical Report. 2011.
69. Houston W. N., Mirza M. W., Zapata C. E., and Raghavendra S., “Environmental effects in pavement mix and structural design systems,” Part 1 of Contractor’s Final Report for NCHRP Project 9-23, Arizona State University, Phoenix, AZ, USA, 2005.
70. Sirin O. Kassem M., and Paul D. K., (Under review). Comprehensive Evaluation of Long-Term Aging of Asphalt Mixtures in Hot Climatic Condition Submitted for Publication to Journal of Road Materials and Pavement Design (Manuscript ID RMPD-17-09-17).
71. Nicholls, C. Analysis of Available Data for Validation of Bitumen Tests. Forum of European National Highway Research Laboratories, ed. Cliff Nicholls, TRL. UK: Report on Phase 1 of the BiTVaI Project, Forum of European National Highway Research Laboratories, 2006.
72. Van den Bergh, W. The Effect of Aging on Fatigue and Healing Properties of Bituminous Mortars. Ph.D Thesis, Delft University of Technology, Delft University, 2011.
73. Collop, A., Choi, Y., Airey, G., and Elliott, R. Development of a Combined Aging/Moisture Sensitivity Laboratory Test. Vienna: 4th Euroasphalt and Eurobitume Congress, 2004.
74. Kim, R. Y., Hintz, C., Yousefi Rad, F., Underwood, S., Farrer, M. J., Glaser, R., R., “Long-term Aging of Asphalt Mixtures for Performance Testing and Prediction” Interim Report, NCHRP 09-54, 2013.
75. Elwardany, M. D., F. Yousefi Rad, C. Castorena, and Y. R. Kim. “Evaluation of Asphalt Mixture Laboratory Long-Term Ageing Methods for Performance Testing and Prediction,” Road Materials and Pavement Design, Vol. 18, No. 1, , pp. 28-61, 2017(b).
76. Zhang, R., Sias, J. E., Dave, E. V., & Rahbar-Rastegar, R. "Impact of Aging on the Viscoelastic Properties and Cracking Behavior of Asphalt Mixtures". Transportation Research Record. 2019. <https://doi.org/10.1177/0361198119846473>
77. Reed, J. Evaluation of the Effects of Aging on Asphalt Rubber Pavements. Masters

- Thesis, PhD Dissertation., Arizona State University, 2010.
78. Mollenhauer, K., and Mouillet, V. Re-road – End of Life Strategies of Asphalt Pavements. European Commission DG Research, 2011.
  79. Blankenship, P.B., Anderson, M. A., King, G. N., and Hanson, D. I. “A Laboratory and Field Investigation to Develop Test Procedures for Predicting Non-Load Associated Cracking of Airfield HMA Pavements, Airfield Asphalt pavement technology Program, 2010.
  80. Van Gooswilligen, G., De Bats, F., and Harrison, T. Quality of Paving Grade Bitumen - A Practical Approach in Terms of Functional Tests. Proc. 4th Eurobitume Symp., pp. 290-297, 1989.
  81. Van den Bergh, W. The Development of an Artificially Aged Asphalt Mixture (in Dutch): Artificial Aged Asphalt mixture. Gent, Belgium: In: Belgian Road Congress, 2009.
  82. Yin F., Arambula-Mercado E., Epps Martin E., David ' Newcomb D., and Tran N., “Long-term aging of asphalt mixtures,” Road Materials and Pavement Design, vol. 18, no. 1, pp. 2–27, 2017.
  83. Islam M. R., Hossain M. I., and Tarefder R. A., “A study of asphalt aging using indirect tensile strength test,” Construction and Building Materials, vol. 95, pp. 218–223, 2015.
  84. De la Roche, C., Van de Ven, M., Van den Bergh, W., Gabet, T., Dubois, V., Grenel, J., and Porot, L. Development of a Laboratory Bituminous Mixtures Aging Protocol. Advanced Testing and Characterization of Bituminous Materials 331, 2009.
  85. Laidler K J. Chemical Kinetics. Third Edition, Harper & Row, New York, pp 42, 1987.
  86. Herrington P.R., Patrick J.E., and Ball G.F. Oxidation of roading asphalts. Industrial and Engineering Chemistry Research, Vol. 33 (11), pp. 2801-2809, 1994.
  87. Lau C.K., Lunsford K.M., Glover C.J., Davison R.R., and Bullin J.A. Reaction rates and hardening susceptibilities as determined from pressure oxygen vessel aging of asphalts. Transportation Research Record 1342, pp.50-56, 1992.
  88. Davison R.R., Bullin J.A., Glover C.J., Chaffin J.M., Peterson G.D., Lunsford K.M., Lin M.S., Liu M., and Ferry M.A. Verification of an asphalt aging test and development of superior recycling agent and asphalts. 1994.  
<https://static.tti.tamu.edu/tti.tamu.edu/documents/1314-1F.pdf>.

89. Liu M., Lunsford K.M., Davison R.R., Glover C.J., and Bullin J.A. The kinetics of carbonyl formation in asphalt. *American Institute of Chemical Engineers Journal*, Vol. 42 (4), pp. 1069-1076, 1996.
90. Domke C.H., Davison R.R., and Glover C.J. Effect of oxygen pressure on asphalt oxidation kinetics. *Industrial and Engineering Chemistry Research*, no. 3: pp. 592-598, 2000.
91. Glaser R., Turner T.F., Loveridge J.L., Salmans S.L., and Planche J.P. Fundamental properties of asphalts and modified asphalts, Volume III. Quarterly Technical Report, Federal Highway Administration (FHWA), Washington D.C, USA, 2013.
92. Glaser R., Turner T.F., Loveridge J.L., Salmans S.L., and Planche J.P. Fundamental properties of asphalts and modified asphalt, Volume III. Aging Master Curve (FP 10) and Aging Rate Model (FP 11). Technical White Paper, Western Research Institute, Laramie, Wyoming, USA, 2015.
93. Elwardany, M.D., Yousefi Rad F., Castorena C., Kim Y.R. Climate-, depth-, and time-based laboratory aging procedure for asphalt mixtures. *Journal of the Association of Asphalt Paving Technologists*, 87(0270-2932):pp. 467-512, 2018.
94. Mirza, M. W. and M. W. Witczak, "Development of Global Aging System for Short- and Long-Term Aging of Asphalt Cements." *Journal of the Association of Asphalt Paving Technologists*, Vol. 64, pp. 393-430, 1995.
95. Moraes R., Bahia H.U.. Effect of mineral filler on changes in molecular size distribution of asphalt during oxidative ageing. *Road Materials and Pavement Design*, Vol. 16, pp. 55-72, 2015.
96. Wu J.T., Han W.P., Airey G., and Yusoff N.I.M. The influence of mineral aggregates on bitumen ageing. *International Journal of Pavement Research and Technology*, Vol. 7(2), pp. 115-123, 2014.
97. Petersen J.C. A review of the fundamentals of asphalt oxidation: chemical, physicochemical, physical property, and durability relationships. *Transportation Research E-Circular (E-C140)*, Transportation Research Board, Washington, D.C., 2009.
98. Little D.N., Epps J.A., and Sebaaly P.E. Hydrated lime in hot mix asphalt. *National Lime Association*. 2006. <https://www.lime.org/lime-basics/uses-of-lime/construction/asphalt/>



99. Sias J.E., Dave E.V., Zhang R., Rahbar-Rastegar M R. Incorporating Impact of Aging on Cracking Performance of Mixtures during Design. Technical Report, No. FHWA-NH-RD-269620, 2019.
100. Glover, C.J., Davison, R.R., Domke, C.H., Ruan, Y., Juristyarini, P., Knorr, D.B., Jung, S.H. Development of A New Method for Assessing Asphalt Binder Durability with Field Validation. Final Report, 2005.
101. Rowe, G. M. Prepared Discussion for the AAPT paper by Anderson et al.: Evaluation of the Relationship between Asphalt Binder Properties and Non-Load Related Cracking, Journal of the Association of Asphalt Paving Technologists, Vol. 80, pp. 649-662, 2011.
102. Mensching, D. J., Rowe G.M., and Daniel J.S. A mixture-based Black Space parameter for low-temperature performance of hot mixture asphalt. Road Materials and Pavement Design, 404-425, 2017.
103. Martin, A.E., Zhou, f., Arambula, E., Park, E.S., Chowdhury, A., Kaseer, F., Carvajal, J., Hajj, E., Daniel, J.S., Glover, C. The Effects of Recycling Agents on Asphalt Mixtures with High RAS and RAP Binder Ratios. Interim Report. NCHRP 09-58 Project, 2015.
104. Martin, A.E., Kaseer, F., Arambula, E., Bajaj, A., Daniel, J.S., Hajj, E., Morian N., Ogbo, C. Component Materials Selection Guidelines and Evaluation Tools for Binder Blends and Mixtures with High Recycled Materials Content and Recycling Agents. Submitted to AAPT conference, 2018.
105. Ozer, H., Al-Qadi, I. L., Lambros, J., El-Khatib, A., Singhvi, P., & Doll, B. Development of the fracture-based flexibility index for asphalt concrete cracking potential using modified semi-circle bending test parameters. Construction and Building Materials, 115, 390-401, 2016.
106. Al-Qadi, I. L., S. Wu, D. L. Lippert, H. Ozer, M. K. Barry, and F. R. Safi. Impact of high recycled mixed on HMA overlay crack development rate. Road Materials and Pavement Design, Vol. 18, No. sup4, pp. 311–327, 2017.
107. Nemati, R., Haslett, K., Dave, E.V., Sias, J.E. Development of a rate-dependent cumulative work and instantaneous power-based asphalt cracking performance index, Road Materials and Pavement Design, 20:sup1, S315-S331, 2019. DOI: 10.1080/14680629.2019.1586753
108. Wang, Y., and Kim Y.R. Development of a pseudo strain energy-based fatigue failure criterion for asphalt mixtures. International Journal of Pavement Engineering: 1-11, 2017.

109. Zhu, Y., Dave, E. V., Rahbar-Rastegar, R., Daniel, J. S., and Zofka, A. Comprehensive Evaluation of Low Temperature Cracking Fracture Indices for Asphalt Mixtures, Road Materials and Pavement Design, 2017.
110. Sui, C., Farrar, M. J., Harnsberger, P. M., Tuminello, W. H., & Turner, T. F. "New Low-Temperature Performance-Grading Method: Using 4-mm Parallel Plates on a Dynamic Shear Rheometer". Transportation Research Record, 2207(1), 43–48, 2011.  
<https://doi.org/10.3141/2207-06> stration (FHWA) Contract No. DTFH61-07-D-00005, October 2013.
111. Anderson, M., G. King, D. Hanson, and P. Blankenship, "Evaluation of the Relationship Between Asphalt Binder Properties and Non-Load Related Cracking" Journal of the Association of Asphalt Paving Technologists, Vol. 80, pp. 615-661, 2011.
112. Elwardany, M.D., Planche, J.P., Adams, J.J. Determination of Binder Glass Transition and Crossover Temperatures using 4-mm Plates on a Dynamic Shear Rheometer. Transportation Research Record, 2019. <https://doi.org/10.1177/0361198119849571>
113. Hintz C., Velasquez R., Johnson C., Bahia H., Modification and validation of linear amplitude sweep test for binder fatigue specification, Transp. Res. Rec.: J. Transp. Res. Board 2207 99–106, 2011.

## **Appendix A Paper 1 (Chapter 4)**

### **Impact of Aging on the Viscoelastic Properties and Cracking Behaviour of Asphalt Mixtures**

#### **Runhua Zhang**

University of New Hampshire  
W161 Kingsbury Hall, 33 Academic Way, Durham, NH 03824  
Tel: 603-285-8739; Email: [rz1015@wildcats.unh.edu](mailto:rz1015@wildcats.unh.edu)

#### **Jo E. Sias , Ph.D., P.E.**

University of New Hampshire  
W183B Kingsbury Hall, 33 Academic Way, Durham, NH 03824  
Tel: 603-862-3277; Email: [jo.sias@unh.edu](mailto:jo.sias@unh.edu)

#### **Eshan V. Dave, Ph.D.**

University of New Hampshire  
W173 Kingsbury Hall, 33 Academic Way, Durham, NH 03824  
Tel: 603-862-5268; Email: [eshan.dave@unh.edu](mailto:eshan.dave@unh.edu)

#### **Reyhaneh Rahbar-Rastegar, Ph.D.**

Purdue University  
HAMP 4105, 550 W Stadium Ave., West Lafayette, IN 47907  
Tel: 765-494-7289; Email: [rrahbar@purdue.edu](mailto:rrahbar@purdue.edu)

Word count: 5,885 words text + 2 tables × 250 words (each) = 6,385 words

Submission Date: August 1, 2018

## INTRODUCTION

One important aspect which can significantly affect the performance of asphalt mixtures is aging. Aging of the asphalt mixture consists of two primary processes: volatilization and oxidation. Volatilization mainly occurs during the early production and construction stages where evaporation of the lighter fractions (hydrocarbons) occurs under the high temperatures of mixing and compaction. Oxidation occurs mainly over its service life as the hydrocarbons in asphalt chemically react with oxygen. Oxidation causes an imbalance in electrochemical forces and polarity increases in the binder molecules, which in turn increases the stiffness and brittleness of the asphalt mixture and decreases the stress relaxation capability at the same time. Consequently, aged mixtures have increased cracking susceptibility with potentially shorter pavement service lives and lower serviceability of the pavement. Considering the prediction of the performance of the asphalt mixtures with aging and the importance of performance-based design methodologies, the evaluation of viscoelastic properties and cracking behaviour of aged asphalt mixtures is desired during the mix design stage.

Several methods for laboratory conditioning of asphalt mixtures to simulate field aging are documented in the literature. In the AASHTO R30 procedure, the loose hot asphalt mixture is subjected to short-term aging at  $135 \pm 3^\circ\text{C}$  ( $275 \pm 5^\circ\text{F}$ ) for 4 hr.  $\pm$  5 min in a forced-draft oven (1,2). For long term aging, short term aged mixtures are compacted (following AASHTO T 312) into a specimen that is then conditioned in a forced-draft oven for  $120 \pm 0.5$  hours at  $85 \pm 3^\circ\text{C}$  to represent five to ten years of aging in the field (3). The major drawback of this aging method is that only one single conditioning time and temperature is considered to match field aging at any location, regardless of the temperature history and climatic region of the pavement of interest (4). Also, the conditioning of the compacted specimens in an oven at  $85^\circ\text{C}$  leads to the development of an oxidation gradient from the specimen's center to its periphery, which violates the representative volume element requirement for performance testing, and results in different aging extents for different geometry specimens (5).

Recently, several researchers have proposed that asphalt mixtures should be subjected to long-term aging in the loose state (6,7). Loose mixture aging produces uniform aging and reduces the aging time significantly as compared to compacted specimen aging (5). Asphalt Institute recommends loose mix asphalt conditioning for 24 hr. at  $135^\circ\text{C}$  to simulate long term aging in the field. This level of conditioning is expected to simulate 7 to 10 years of aging in the field (8). However, Yousefi et al. (9) proposed that aging at  $135^\circ\text{C}$  causes changes in the chemistry of the binder that do not occur at temperatures at or below  $95^\circ\text{C}$  and thus do not adequately reflect field aging. These chemical changes of the binder under higher temperature can lead to significantly different cracking performance results compared to the material testing and pavement simulations for aging at  $95^\circ\text{C}$  (9).

The recent findings of the National Cooperative Highway Research Program (NCHRP) 09-54 project on long term aging of asphalt mixtures suggests  $95^\circ\text{C}$  as an optimal temperature for aging loose mix (10). The aging time varies with the geographical location of the pavement and should be adjusted based on climate conditions and pavement depth. Also, a climatic aging index (CAI), based on a simplification of the aging kinetics model, was developed to determine laboratory aging durations at  $95^\circ\text{C}$  for asphalt mixtures that best reflect the time, climate, and pavement depth for a given pavement location in the United States using Enhanced Integrated Climatic Model (EICM) hourly pavement temperature data (11).

In this study, the Asphalt Institute procedure (24 hr. at 135°C on loose mix) and NCHRP recommended 95°C for 5 and 12 days corresponding to preliminary recommendations of NCHRP 09-54 study (12), are used as the long term oven aging (LTOA) conditions on the eleven plant produced mixtures which have already undergone short term aging (STA) during production. The field aging duration is calculated and extrapolated to match up with the 5 days and 12 days (95°C) laboratory aging condition from the CAI calculation based on the climatic condition of New Hampshire. Finally, the tested properties of the aged mixtures are used in FlexPAVE™ and IlliTC to predict and compare the fatigue and thermal cracking performances of these mixtures.

The main objective of this study is to evaluate how the viscoelastic, fatigue, and fracture properties and cracking performance of typical NH asphalt mixtures evolve with different aging protocols and the corresponding field aging durations, and identify how the mixture properties may influence the magnitude in change of properties with aging.

### Materials and Testing

This study includes laboratory testing on eleven plant mixed, lab compacted surface mixtures. Field cores taken after approximately four years of service were available for two of the mixtures. Table 1 below shows the mixture information in this study (Recycled binder content is the ratio of the weight of recycled binder to the total binder weight). Letters in the cells indicate the testing conducted at each of the mixture-aging combinations. The mix ID has the specific meaning: the first four-digit numbers indicate binder PG grade, the following letters “S” and “L” mean the nominal maximum aggregate size (NMAS) of 9.5mm and 12.5mm, respectively. The last letter represents the recycled binder content: “V” means no recycled binder, “M” means 14.8-18.9% recycled binder content, “L” means 28.3% recycled binder content.

**TABLE 1 Mixture Types and Aging Levels**

Mixture ID	Virgin Binder Grade	Design Gyration Levels	NMAS (mm)	Total Binder Content (%)	Recycled Binder Content (%)	STA	LTOA		
							5 days 95°C	12 days 95°C	24 hours 135°C
5234LM	PG 52-34	50	12.5	5.3	18.9	AE	ABCD	ABCD	ABCD
5234LL	PG 52-34	50	12.5	5.3	28.3	AE	ABCD	ABCD	ABCD
5834LM	PG 58-34	50	12.5	5.4	18.5	CD	CD	CD	CD
5828SM	PG 58-28	50	9.5	5.9	16.9	ABCD	ABCD	ABCD	ABCD
5828LM	PG 58-28	50	12.5	5.3	18.9	A	D	ABCD	ABCD
5828LL	PG 58-28	75	12.5	5.3	28.3	A	D	ABCD	ABCD
6428SV	PG 64-28	75	9.5	6.4	0	ABCD	ABCD	ABCD	ABCD
6428SM	PG 64-28	75	9.5	6.3	18.5	ABCD	ABCD	ABCD	ABCD
6428LM	PG 64-28	75	12.5	5.8	18.5	ABCD	ABCD	ABCD	ABCD
7034LV	PG 70-34	75	12.5	5.8	0	ABCD	ABCD	ABCD	ABCD
7628SM	PG 76-28	75	9.5	6.1	14.8	ABCD	ABCD	ABCD	ABCD

## **METHODOLOGY**

### **Aging**

In this study, the Asphalt Institute procedure (24 hr. at 135°C on loose mix) and NCHRP recommended 95°C for 5 and 12 days are used on the eleven plant produced mixtures which have already undergone short term aging during production. Loose mix asphalt was spread in steel pans at an approximate depth of 25 mm. The mixtures were stirred and remixed every other day and the pans were rotated around the oven to obtain a consistent aging condition in all mixtures. After aging, the mixtures were cooled and then reheated at 135°C for 2 hours and compacted to achieve final test specimens with air void contents of  $6 \pm 0.5\%$ . Field cores were cored horizontally to obtain small-scale cylindrical specimens ( $\phi 38\text{mm} \times 110\text{mm}$ ) of the surface layer and prepared for the complex modulus tests, the air void of the field cores is between 4.2% and 5.5%.

### **Climatic Aging Index (CAI)**

Recently, a climatic aging index (CAI), based on a simplification of the aging kinetics model, was developed in the NCHRP 09-54 project (12) to determine laboratory aging durations at 95°C for asphalt mixtures that best reflect the time, climate, and pavement depth for a given pavement location in the United States, defined as:

$$t_{oven} = CAI = \sum_{i=1}^N DA \exp(-E_a/RT_i)/24 \quad (1)$$

$$D = \begin{cases} 3.4311 * d^{0.683}, & 6\text{mm} \leq d \leq 35\text{mm} \\ 0.3056, & d \geq 35\text{mm} \end{cases} \quad (2)$$

where  $t_{oven}$  is the required oven aging duration at 95°C to reflect field aging,  $CAI$  is climatic aging index,  $D$  is the depth correction factor,  $A$  is the reaction frequency factor,  $E_a$  is the reaction activation energy,  $R$  is the universal gas constant,  $T_i$  is the pavement temperature obtained from Enhanced Integrated Climatic Model (EICM) at the depth of interest at the hour of interest,  $B$  is the depth dependent fitting parameter, and  $d$  is depth of interest.

### **Testing and Analysis Methods**

To compare the linear viscoelastic properties of asphalt mixtures at different aging levels, complex modulus testing was conducted at 4.4, 21.1, 37.8°C (2.9, 18.0, 30.0°C for field cores) with loading frequencies of 0.1, 0.5, 1, 5, 10, 25 Hz at each temperature, following AASHTO T 342 using an asphalt mixture performance tester (AMPT). The dynamic modulus and phase angle mastercurves of mixtures at different aging levels were constructed using Abatech RHEA® software.

Uniaxial direct tension cyclic testing was conducted following AASHTO TP 107 to evaluate the fatigue behavior of the asphalt mixtures. The simplified viscoelastic continuum damage (S-VECD) approach with the damage characteristic curve (DCC) and the performance

parameter  $D^R$  were used to estimate the ability of the mixtures to resist fatigue cracking (13,14,15).

To evaluate the fracture characteristics of asphalt mixtures, Semi Circular Bending (SCB) testing and Disk Shaped Compact Tension (DCT) tests were conducted. The SCB fracture test (AASHTO TP 124) was performed at an intermediate temperature (25°C). The measured data were analyzed using the IFIT software developed by Illinois Center of Transportation (ICT), to calculate the fracture energy and flexibility index (FI) parameters (16).

The DCT testing (ASTM D 7313) was conducted to compare the thermal cracking behavior of the mixtures with different aging levels. The test temperature for different mixtures is based on the winter-time pavement in-service temperature for the location where mix is being used, which is calculated at 98% reliability +10°C from the LTPPBind database for the nearest weather station to the actual project site. The measured data were analyzed to calculate the fracture energy and the fracture strain tolerance (FST) (17).

### **Cracking Performance Prediction: FlexPAVE™ and IlliTC**

Use of prediction models are essential in predicting the performance of asphalt mixtures during, and at the end of service life. In this study, the FlexPAVE™ (formerly known as the LVECD program) developed by North Carolina State University (NCSU) was used to predict and compare the fatigue performance of the mixtures with different aging levels. The IlliTC thermal cracking prediction system (18) was used for thermal cracking simulations and predictions.

FlexPAVE™ predicts pavement responses and damage evolution (fatigue and rutting) in both spatial distribution and time history modes. One of the outputs of this program is percent damage which is calculated on the basis of cumulative damage model and Miner's rule. In this study, the measured material properties from S-VECD fatigue testing are used in FlexPAVE™ to simulate and predict the fatigue performance of these mixtures with different aging levels based on same cross section (75 mm HMA; 300 mm Granular base) and traffic (daily ESALs: 1000; growth rate: linear at 2.0% per year).

IlliTC thermal cracking prediction system utilizes a two step analysis approach for maintaining practical analysis times for various cases. The system uses a critical cracking condition approach whereby thermo-viscoelastic stress analysis identifies the time period when thermal stresses exceed 80% of mixture tensile strength. These critical conditions are evaluated using finite element analysis with cohesive zone fracture model to simulate quasi-brittle cracking in asphalt concrete. The cohesive zone fracture model in IlliTC uses tensile strength and fracture energy to simulate quasi-brittle and ductile crack propagation. A number of researchers have shown that the cohesive zone fracture approach is well suited for simulation of discrete cracking in asphalt mixtures (19,20).

## **RESULTS AND DISCUSSION**

### **Linear Viscoelastic (LVE) Properties**

Dynamic modulus and phase angle master curves for different aging levels are presented for two example mixtures (5234LM and 5234LL) in Figure 1; each series represents the average of three replicates. As expected, the aged materials show higher stiffness (dynamic modulus) and lower relaxation capability (phase angle), which, in combination, can result in higher

cracking susceptibility. The peak phase angle also decreases and occurs at a lower frequency as materials age. The two higher levels of aging (24 hr. at 135°C and 12 days at 95°C) show statistically similar dynamic modulus and phase angle values. These trends are similar for all mixtures evaluated in this study. There is no significant difference between the dynamic modulus and phase angle of the field cores (approximately 4 years in service) and the 5 days' lab aged mixtures. Based on this preliminary data, the 5 days at 95°C laboratory aging condition appears to simulate approximately four years of field aging for a surface mixture in NH.

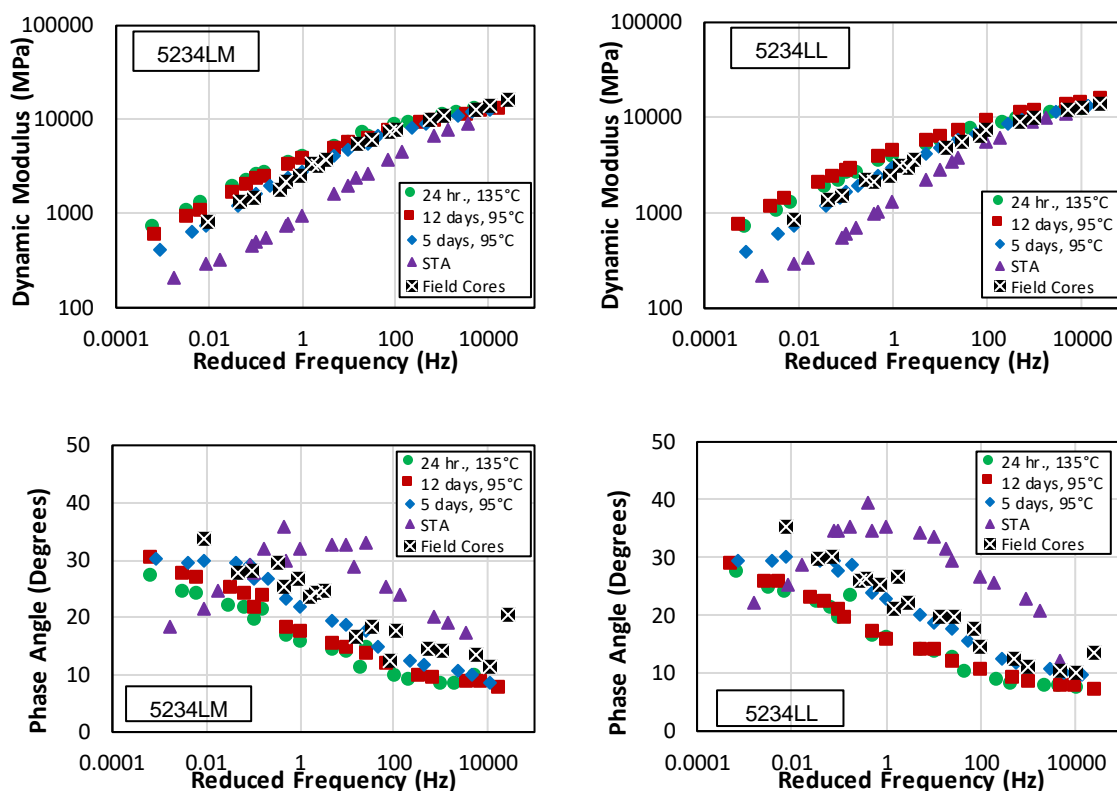


**FIGURE 1 Comparison of Dynamic Modulus and Phase Angle Master Curves for 5234LM Mixture (PG 52-34, 12.5mm, 18.9% RAP), 5234LL Mixture (PG 52-34, 12.5mm, 28.3% RAP) at Different Laboratory Aging Levels with Field Cores**

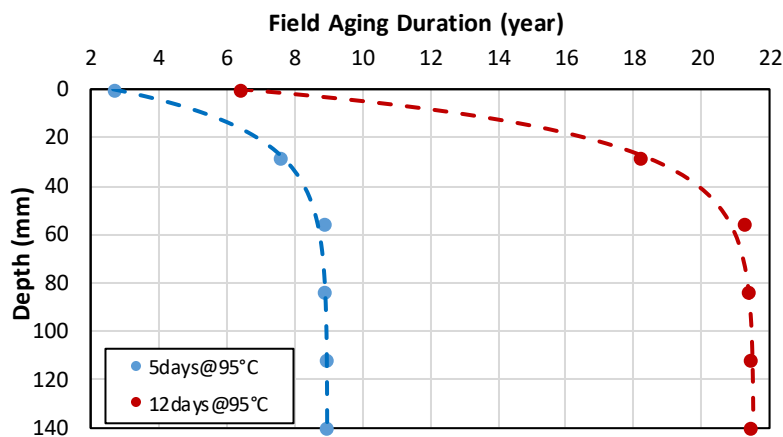
### Climatic Aging Index (CAI) Calculation

Figure 2 below shows the results of the CAI calculation based on the hourly pavement temperatures from the EICM. NCHRP 09-54 suggests that a depth of 20 mm be used to evaluate the bulk behavior of a 37.5 mm thick surface layer. Based on the CAI calculation results, 5 days at 95°C lab aging condition should be equivalent to seven years of aging in the field in NH at a depth of 20 mm. However, the result of the field cores shows that the 5 days at 95°C laboratory aging condition appears to simulate approximately four years of field aging in NH. One possible reason to explain this difference is that CAI calculation from NCHRP 09-54 is developed from the comparison of the binder  $G^*$  value, and the comparison in this study is based on the complex modulus ( $E^*$ ) of the lab aged mixtures and the field cores. Also, the NCHRP 09-54 final report mentioned that the predicted  $G^*$  needs to be calibrated based on



specific project and climate conditions (14).

The complex modulus test results on the field cores correspond to four years of field aging at a depth of 4.3 mm using the 5 days at 95°C lab aging condition. The calculated field aging duration equivalent to the 12 days at 95°C lab aging condition at this depth is 9.6 years. For this study, the 5 days at 95°C laboratory aging condition is considered to simulate four years of field aging in NH, while the 12 days at 95°C laboratory aging condition is expected to simulate 9.6 years of field aging in NH.



**FIGURE 2 Relationship between Field Aging Duration and Pavement Depth Based on CAI Calculation Results (dashed lines show fitted curves to calculated values)**

### Fracture Properties

Figures 3a, 3b, and 3c show the flexibility index (FI) parameter, FI aging ratio (LTOA divided by STA), and the change of the FI aging ratio with field aging duration from the SCB tests, respectively. The average of 3 to 4 replicates for each mixture is shown and the error bars represent one standard deviation interval. Generally, FI and FI aging ratio decrease with increase of aging levels. There is a statistically significant difference in FI between the STA and all three long term aging levels. After 5 days at 95°C (4 years in NH) aging, the FI value of all mixtures except 7034LV is below 7.5. After 12 days at 95°C (9.6 years in NH) aging, the FI value for most of the mixtures is below 5. The FI ratio drops to 20-40% after 5 days at 85°C age conditioning, while 12 days aging at 95°C drops the FI to 5-30% of the STA condition, which indicates that the mixtures lose cracking resistance very quickly with aging, especially within the first several years. The 24 hr. at 135°C condition causes a larger drop in FI aging ratio than the 12 days at 95°C.

The two mixtures without RAP (6428SV and 7034LV) generally have higher FI values at each aging level compared with other mixtures with RAP. The mixtures with the softer binders (5828SM, 5834LM, 5828LM and 5234LM) generally have higher FI values than the mixtures with the stiffer binders (6428SM and 6428LM) when they have comparable RAP content. The 7628SM and 7034LV mixtures, which have the largest difference between PGHT and PGLT, show the most impact from aging on FI values. The FI aging ratio for the other five mixtures is relatively consistent at each aging level (30-40% after 5 days at 95°C; 20-30%

after 12 days at 95°C; 10-17% after 24 hr. at 135°C). However, it is important to note that the FI value for 7034LV mixture after aging is still higher than other mixtures.

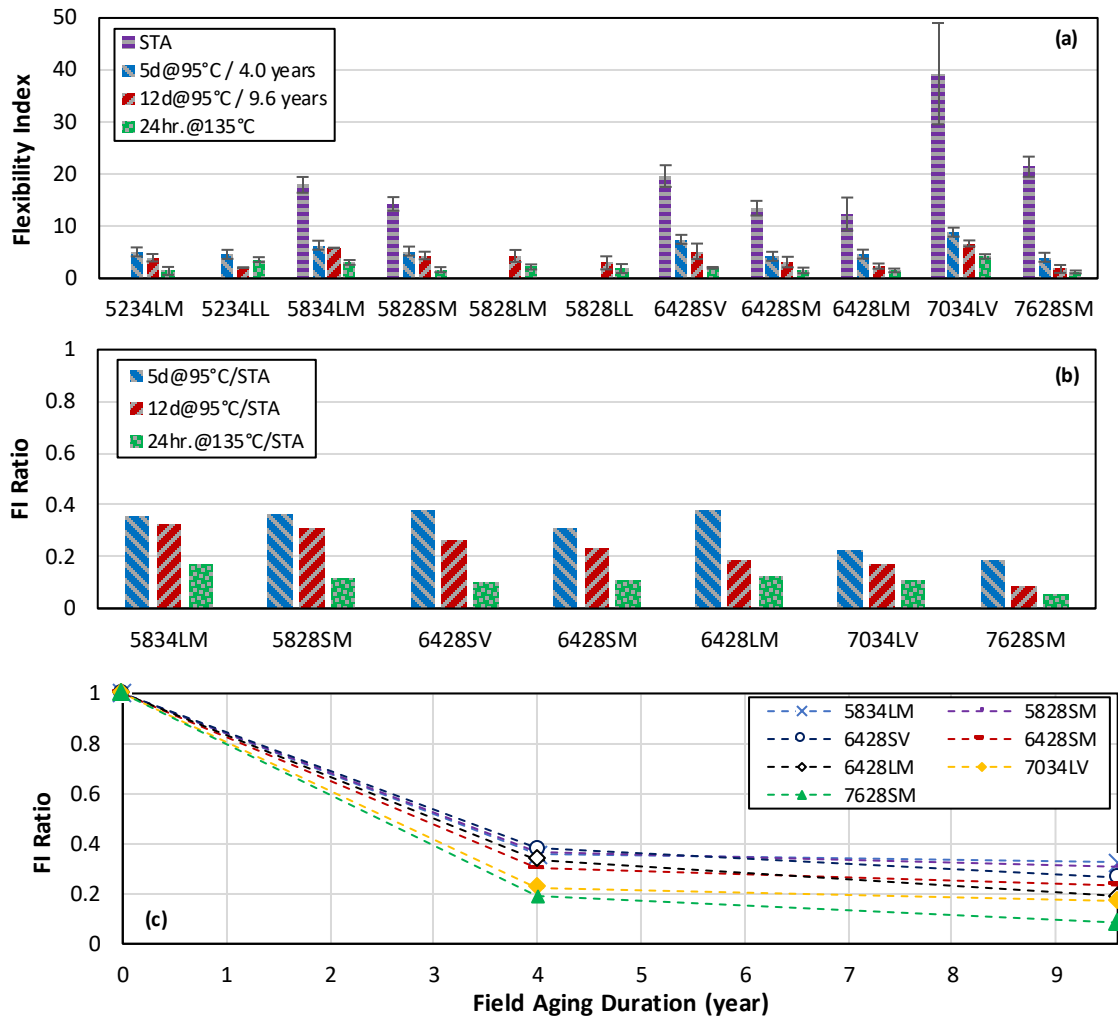


**FIGURE 3 a) Flexibility Index Values; b) Flexibility Index Aging Ratio; c) Change of FI Ratio with Field Aging Duration from SCB Test.**

Figures 4a, 4b, and 4c show the low temperature fracture properties from DCT test in the form of fracture strain tolerance (FST), FST aging ratio (LTOA divided by STA) and the change of the FST aging ratio with field aging duration for all mixtures, respectively. The DCT testing temperature is based on the in-service location, as shown in Figure 4a. Generally, FST and FST aging ratio decrease when aging level increases. There is a statistically significant difference in FST between the STA and the two long term aging levels. After 5 days (4 years) aging, except for the 7034LV mixture, the FST value for all mixtures is below 150. After 12 days (9.6 years) aging, the FST value for most of the mixtures is below 140. The FST ratio drops to 50-95% of the STA condition after 5 days aging condition, while 12 days aging drops the FST to 37-90% of the STA condition. The decrease of FST value is more severe in the early aging stage and the 24hr. at 135°C condition causes a larger drop in FST aging ratio than the 12 days at 95°C.

Similar to the SCB results, the virgin mixtures usually have higher FST values and higher RAP contents result in lower FST values after aging. The 7628SM and 7034LV mixtures have the largest decrease in FST with aging and the FST aging ratio for the other five mixtures is relatively consistent at each aging level (85-95% after 5 days at 95°C; 75-92% after 12 days at 95°C; 70-89% after 24 hr. at 135°C). However, the FST value for the 7034LV mixture after aging is still higher than other mixtures.

As the complex modulus and fracture testing results show, the two higher levels of aging (24 hr. at 135°C and 12days at 95°C) show statistically similar viscoelastic behavior, while mixtures after 24hr. at 135°C condition typically show the worst fracture properties. This may be a result of disrupted polar molecular associations that lead to thermal decomposition of sulfoxides in asphalt binders at temperatures above 100°C (21,22); this leads to significantly different cracking performance results compared to the material aged below 100°C (10).

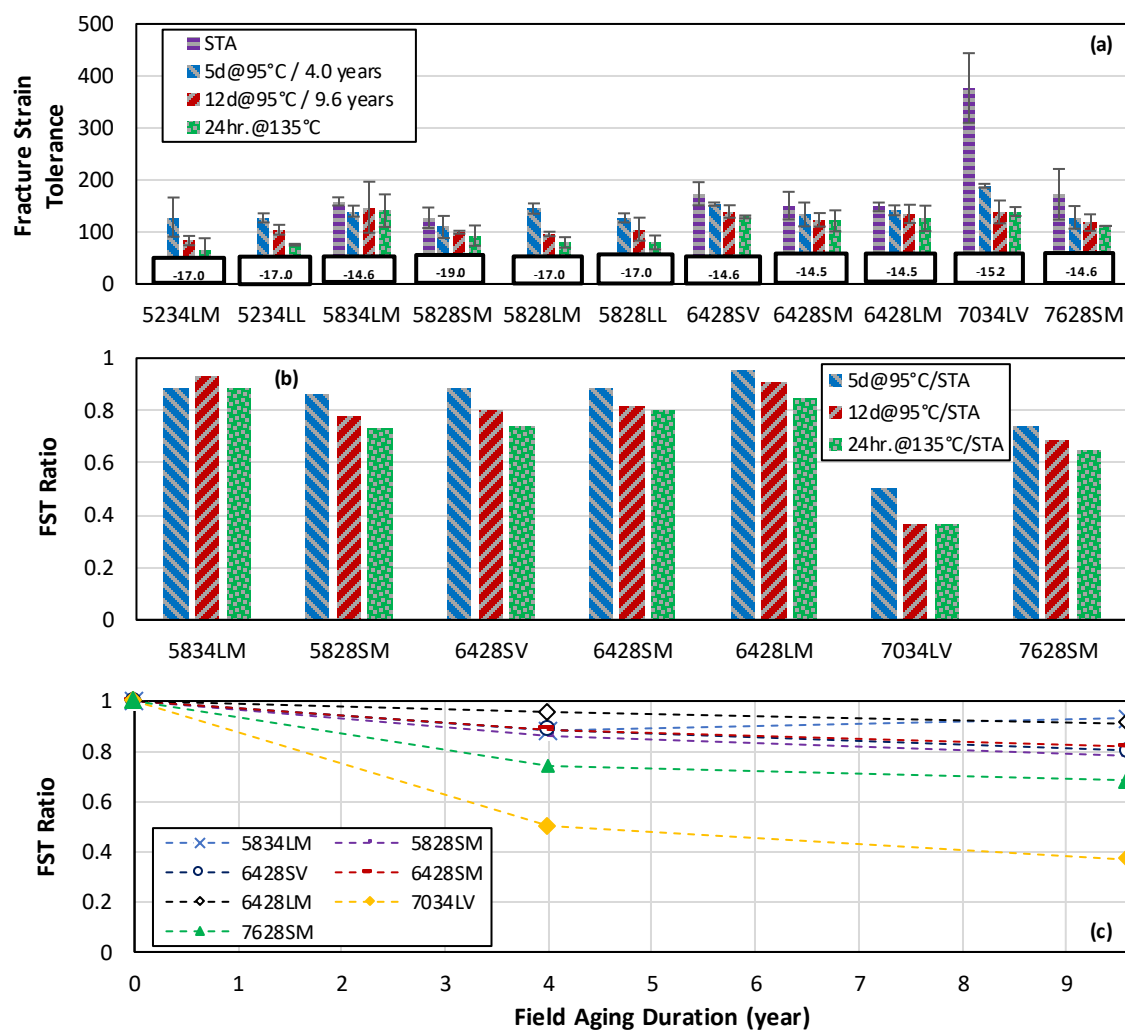


**FIGURE 4 a) Fracture Strain Tolerance Values; b) Fracture Strain Tolerance Aging Ratio; c) Change of FST Ratio with Field Aging Duration from DCT Tests**

## Fatigue Properties

Figures 5a, 5b, and 5c show  $D^R$  values,  $D^R$  aging ratio (LTOA divided by STA) and the change of the  $D^R$  aging ratio with field aging duration for the tested mixtures from S-VECD fatigue testing, respectively. Generally, the higher  $D^R$  value indicates better fatigue behavior. The  $D^R$  values and  $D^R$  aging ratio show a consistent trend with decreasing value with longer aging, which is similar to the SCB and DCT results. Statistical analysis shows that there is no significant difference in  $D^R$  values between the two long term aging levels. One possible explanation is that  $D^R$  value is developed from the simplified viscoelastic continuum damage (S-VECD) model, and related to the pseudo stiffness of the mixtures (15). Since the mixtures after two LTOAs show similar viscoelastic properties (Figure 1), the  $D^R$  value for the mixtures at the two LTOAs also generally show a close trend. Also, the  $D^R$  ratio drops to 65-95% of the STA condition after 5 days at 95°C (4 years) aging condition, while 12 days at 95°C (9.6 years) and 24hr. at 135°C aging drops the  $D^R$  to 35-85% of the STA condition. Similar to the SCB and DCT result, the decrease of  $D^R$  value is more severe in the early aging stage. In Figure 4c, the drop of the  $D^R$  ratio after 5 days (4 years) aging for 6428LM and 7034LV mixtures with the larger NMAS is typically slower than other mixtures with the smaller NMAS.

Similar to the SCB and DCT results, the virgin mixtures and softer base binder grades have higher  $D^R$  value after aging. The  $D^R$  aging ratio for the 7628SM and 7034LV mixtures shows the largest drop with aging as compared to the other mixtures.

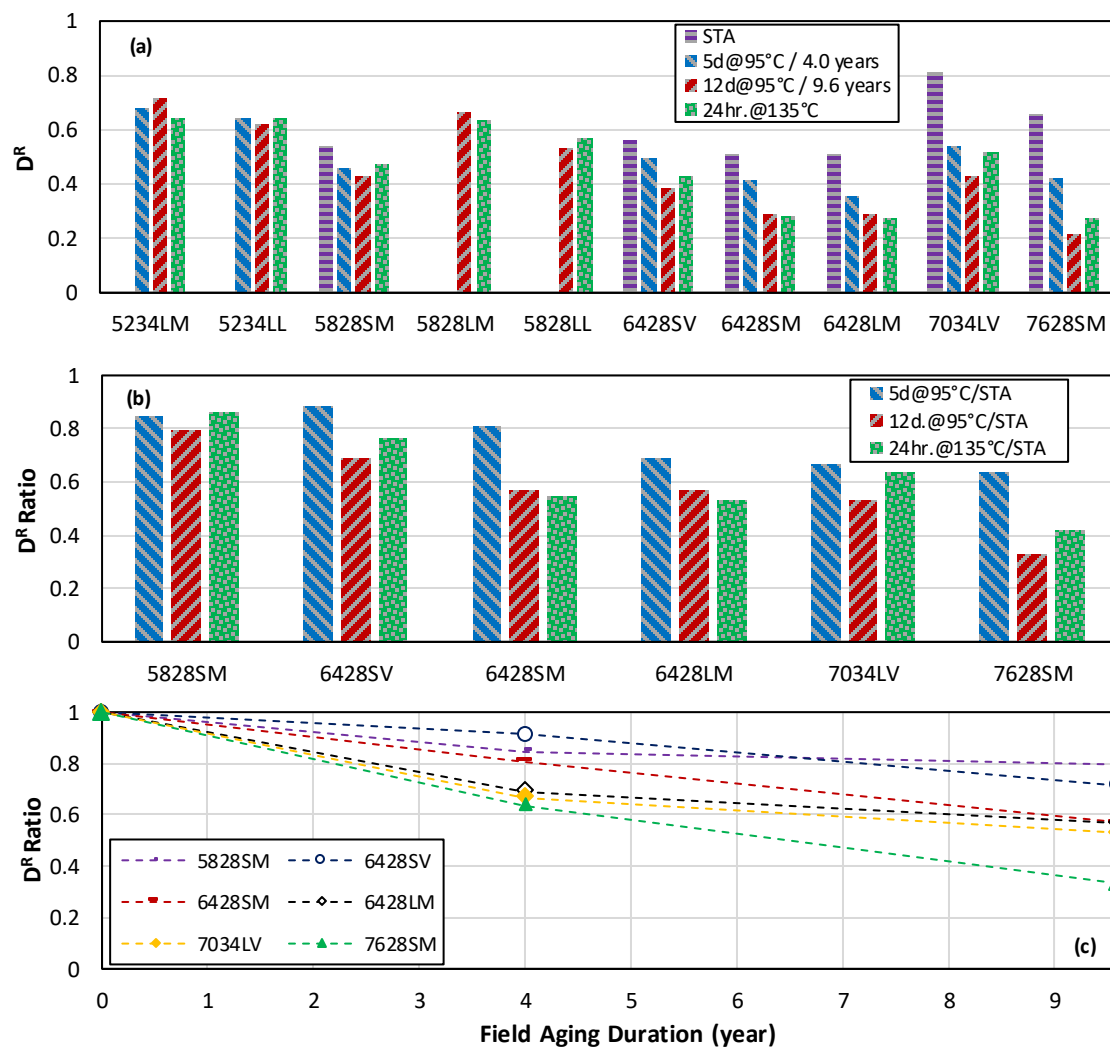


**FIGURE 5 a) D<sup>R</sup> Values; b) D<sup>R</sup> Aging Ratio; and, c) Change of D<sup>R</sup> Ratio with Field Aging Duration from S-VECD Fatigue Tests**

**Thermal Cracking Simulation and Prediction from IlliTC**

Results from IlliTC simulations and prediction of thermal cracking performance of four mixtures (5828SM, 7628SM, 7034LV and 6428SV) with different aging levels are presented in Table 2. The results show that all three PGXX-28 mixtures have potential for thermal cracking after the two long term aging conditions, with the 7628SM and 6428SV being the most susceptible. The 6428SV mixture with softer binder and no RAP content showed lower critical temperature for thermal cracking. For mixtures undergoing only softening, the critical softening temperature is very close to the LTPG. The predicted results support the DCT testing results: with the virgin and softer binder, the mixtures generally show better capability to resist thermal cracking.

**TABLE 2 IlliTC Thermal Cracking Simulation and Prediction**

Mix ID	Aging Levels	Critical Cracking Condition Detected (Thermal stress larger than 80% tensile strength of material)	Percentage of Cracked/Softened (%)	Critical Temperature (Cracking/Softening)	Predicted Thermal Cracking Amount at 5 years (m/500m)
7034LV	STA	0	0	N/A	0
	5d@95°C	0	0	N/A	0
	12d@95°C	3	0	N/A	0
	24hrs.@95°C	3	0	N/A	0
7628SM	STA	0	0	N/A	0
	5d@95°C	3	5% Softened (Damaged)	-28.3	0
	12d@95°C	153	100 Cracked	-12.17	200
	24hrs.@95°C	106	100 Cracked	-12.05	200
6428SV	STA	0	0	N/A	0
	5d@95°C	0	0	N/A	0
	12d@95°C	31	100 Cracked	-17.37	200
	24hrs.@95°C	35	100 Cracked	-17.36	200
5828SM	STA	0	0	0	0
	5d@95°C	2	0	N/A	0
	12d@95°C	7	10% Softened (Damaged)	-27.74	0
	24hrs.@95°C	5	4% Softened (Damaged)	-27.88	0

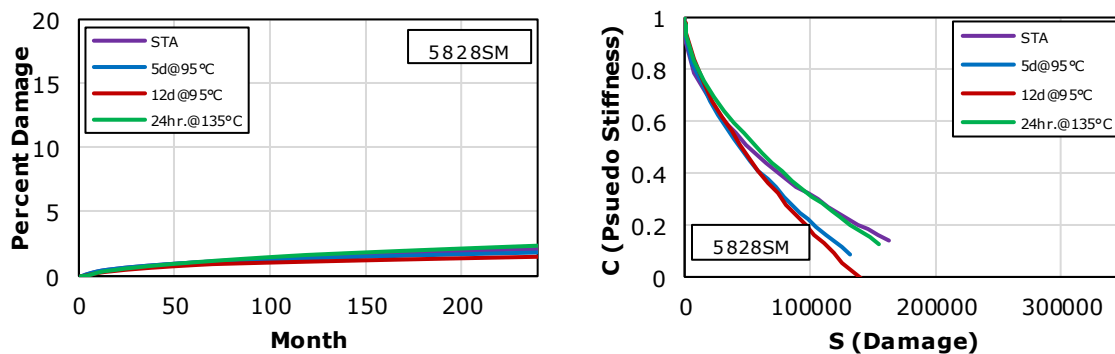
## Fatigue Performance Prediction from FlexPAVE™

Results of the damage characteristic curves (DCC) from the S-VECD fatigue tests and the simulations and predictions of fatigue performance using FlexPAVE™ of the four mixtures (5828SM, 6428SV, 7034LV and 7628SM) are presented in this section. Figure 6 shows the percent damage of the cross section and the DCC curves containing each mixture with different aging levels.

Generally, there is no consistent trend for the predicted percent damage with aging level. For mixture 5828SM, the predicted percent damage for all aging levels are very similar, while the 6428SV mixture shows the fatigue performance becomes better with aging. Both 7034LV and 7628SM mixtures show 24 hr. aging as the worst performance and 5 days aging as the best. These two mixtures typically have higher predicted damage as compared to the others for each aging condition as well. The discrepancy between lab measured fatigue/damage response and prediction of field damage can be attributed to a trade-off between increased stiffness and decreased cracking resistance. Increased stiffness results in lower strains and damage energy dissipation, whereas loss of cracking resistance increases the propensity for fatigue damage.

The DCC curves describe the loss of cracking resistance of asphalt mixtures. The combination of DCC with LVE properties (describing the overall stress-strain response of mixtures) is necessary to evaluate the ability of the mixture to resist fatigue cracking. The mixtures that have DCC curves further up and to the right would be expected to perform better, since they are able to maintain their integrity better during the fatigue tests. Generally, there is also no consistent trend for DCC curves with change of aging levels.

The summary of fatigue analysis presented here is that use of only LVE or damage properties (such as DCC) to compare aging evolution of different mixtures may not be representative of actual fatigue performance of mixtures in the field. In order to capture the fatigue performance, it would be necessary to combine LVE, DCC and pavement structure; the FlexPAVE™ simulation system allows such integration. Some researchers have shown good agreement of the predicted fatigue performance using FlexPAVE™ with measured field fatigue cracking data (15,23). Also, the fatigue performance with aging may be better or worse for each individual mixture depending on the trade-off between increasing stiffness and decreasing fatigue resistance.



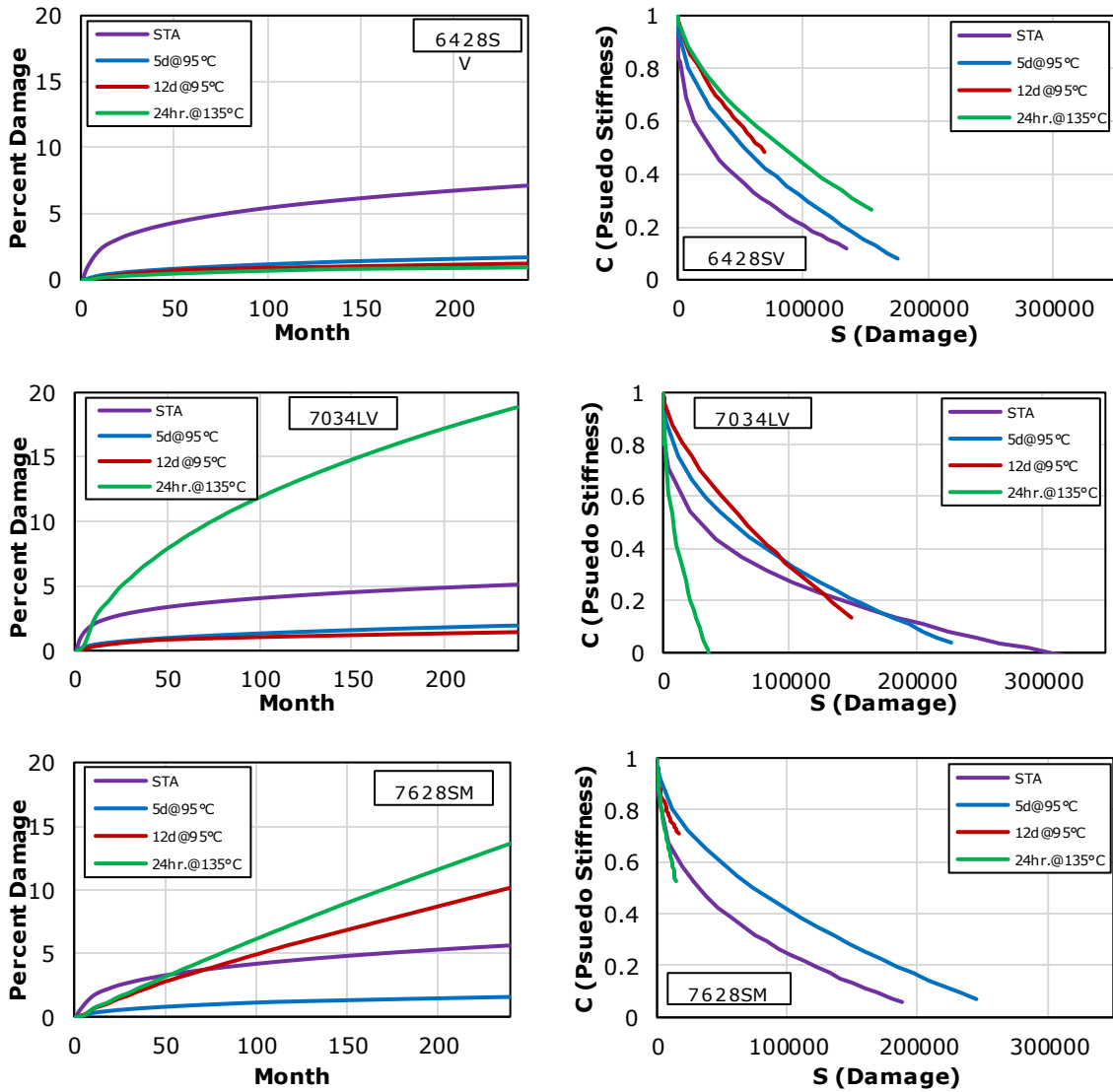


**FIGURE 6 Percent Damage Prediction from FlexPAVE™ and Damage Characteristic Curves from S-VECD Fatigue Tests**

**SUMMARY AND CONCLUSIONS**

The main objective of this study was to investigate the effects of aging on the viscoelastic, fatigue, and fracture properties of asphalt mixtures. This study includes eleven surface course mixtures, evaluated by complex modulus, SCB and DCT fracture, and S-VECD fatigue testing. The CAI developed from NCHRP 09-54 is used to calculate the appropriate field aging duration corresponding with the different laboratory aging protocols based on the New Hampshire climate condition. FlexPAVE™ fatigue cracking and IlliTC thermal cracking performance prediction systems were used to compare aged cracking performance of four mixtures. The following conclusions can be drawn from the results of the testing and analysis:

- The complex modulus, SCB and DCT fracture, and S-VECD fatigue testing, as well as the FlexPAVE™ and IlliTC simulation and prediction programs, can be used to track the change of mixture performance with aging.
- Combining the results of the complex modulus testing with the CAI calculation, 5 days at 95°C laboratory aging condition appears to simulate approximately four years of field aging for the surface mixtures in NH, while 12 days at 95°C laboratory aging simulates 9.6 years of field aging.
- As asphalt materials age, the linear viscoelastic characteristics change with an increase of stiffness and decrease in relaxation capability. The linear viscoelastic properties of mixtures with 24 hr. at 135°C and 12 days at 95°C aging are statistically similar.
- The fracture properties, as measured by SCB and DCT testing, become worse as aging level increases. Mixtures after 24hr. at 135°C condition typically show the worst fracture properties, which can be attributed to the disruption of polar molecular associations and thermal decomposition of sulfoxides for the binders with aging temperatures above 100°C.
- Both the DCT tests result and IlliTC prediction show that the virgin mixtures and those with lower PGLT generally have better capability to resist thermal cracking and have better fatigue properties as measured by the  $D^R$  criterion.
- Based on the  $D^R$  criterion, mixtures are more prone to fatigue cracking with increased aging and fatigue behavior between two long term aging levels is very similar. However, there is no consistent trend in the damage characteristic curves for the mixtures with different aging levels.
- The results of FlexPAVE™ simulation and prediction demonstrate the importance of the combination of the material properties (both LVE and fatigue damage characteristics) with the pavement structure, as well as traffic conditions to predict the fatigue performance of the mixtures.
- The two mixtures with the largest difference between PGHT and PGLT show the most impact from aging based on the fracture and fatigue testing results. However, the virgin mixture still has good fracture and fatigue performance after aging.
- Except for the two mixtures with the largest difference between PGHT and PGLT, the aging ratio of the fracture index (FI and FST) for other mixtures is relatively consistent.

## **FUTURE WORK**

Future work and analysis is planned to investigate the correlation between the viscoelastic properties, fracture, and fatigue cracking characteristics of aged asphalt mixtures and their relationship with the cracking performance of field cored samples and field performance over time. Also, additional mixtures and binders that are extracted and recovered from aged mixtures will be evaluated obtain a wider range of information about the effect of aging on both of mixture and binder properties and develop a database for future analysis.

## **ACKNOWLEDGEMENT**



The authors would like to acknowledge New Hampshire Department of Transportation (NHDOT) for sponsoring this study and the University of New Hampshire Center for Infrastructure Resilience to Climate (UCIRC).

### **AUTHOR CONTRIBUTION**

The authors confirm contribution to the paper as follows: study conception and design: J.E.Sias, E.V. Dave, and R. Zhang; data collection: R. Zhang and R. Rahbar; all authors contributed to analysis and interpretation of results, manuscript preparation, and review.

### **REFERENCES**

1. Bell, C. A., Y. AbWahab, R. E. Cristi, and D. Sognovske. "Selection of Laboratory Aging Procedures for Asphalt-Aggregate Mixtures." Washington, DC: Strategic Highway Research Program, National Research Council, 1994.
2. Oshone, M., Pires, G. M., Carrión, A. J. B., Rahbar-Rastegar, R., Airey, G. D., Daniel, J. S. Bailey, H., Smith, D.(2018) "Simulating plant produced material in the laboratory to replicate rheological and fatigue properties." *Road Materials and Pavement Design*.
3. Harrigan, E. T. *Simulating the Effects of Hot Mix Asphalt Aging for Performance Testing and Pavement Structural Design*. Final Report, National Cooperative Highway Research Program, Research Results Digest 324, National Research Council, Washington, D.C., 2007.
4. Kim, R. Y., Hintz, C., Yousefi Rad, F., Underwood, S., Farrer, M. J., Glaser, R., R., "Long-term Aging of Asphalt Mixtures for Performance Testing and Prediction" Interim Report, NCHRP 09-54, 2013.
5. Elwardany, M. D., F. Yousefi Rad, C. Castorena, and Y. R. Kim. "Evaluation of Asphalt Mixture Laboratory Long-Term Ageing Methods for Performance Testing and Prediction," *Road Materials and Pavement Design*, Vol. 18, No. 1, 2017(b), pp. 28-61.
6. Arega, Z. A., A. Bhasin, and T. De Kesel. "Influence of Extended Aging on the Properties of Asphalt Composites Produced Using Hot and Warm Mix Methods," *Construction and Building Materials*, Vol. 44, 2013, pp. 168-174.
7. Partl, M. N., H. U. Bahia, F. Canestrari, C. De la Roche, H. Di Benedetto, H. Piber, and D. Sybilski. "Advances in Interlaboratory Testing and Evaluation of Bituminous Materials," *The International Union of Laboratories and Experts in Construction Materials, Systems and Structures (RILEM)*, 2013.
8. Reed, J. *Evaluation of the Effects of Aging on Asphalt Rubber Pavements*. Ph.D. Dissertation, Arizona State University, Phoenix, AZ, 2010.
9. Blankenship, P.B., Anderson, M. A., King, G. N., and Hanson, D. I. "A Laboratory and Field 26 Investigation to Develop Test Procedures for Predicting Non-Load Associated Cracking of 27 Airfield HMA Pavements," "Airfield Asphalt pavement technology Program, 2010.
10. Yousefi Rad, F., M. D. Elwardany, C. Castorena, and Y. R. Kim, "Investigation of Proper Long-Term Laboratory Aging Temperature for Performance Testing of Asphalt Concrete," *Construction and Building Materials*, Vol. 147, 2017, pp.

- 616-629.
11. Kim, R. Y., Hintz, C., Yousefi Rad, F., Underwood, S., Farrer, M. J., Glaser, R., R. (2013) *Long-term Aging of Asphalt Mixtures for Performance Testing and Prediction*, Interim Report, NCHRP 09-54.
  12. Kim, R. Y., Castorena, C., Elwardany, M., Yousefi Rad, F., Underwood, S., Gundha, A., Gudipudi, P., Farrer, M. J., Glaser, R., R., 2018 *Long-term Aging of Asphalt Mixtures for Performance Testing and Prediction*, Final Report, NCHRP 09-54.
  13. Rahbar-Rastegar, R., Dave, E. V., and Daniel, J. S., Evaluation of Viscoelastic and Fracture Properties of Asphalt Mixtures with Long-Term Laboratory Conditioning, *Transportation Research Record: Journal of Transportation Research Board*. 2018
  14. Sabouri, M. and Kim Y. R., Development of Failure Criterion for Asphalt Mixtures under Different Modes of Fatigue Loading, *Transportation Research Record: Journal of Transportation Research Board*. 2014.
  15. Wang, Y. and Kim Y. R., Development of a pseudo strain energy-based fatigue failure criterion for asphalt mixtures, *International Journal of Pavement Engineering*. 2017.
  16. Ozer, H., Al-Qadi, I. L., Lambros, J., El-Khatib, A., Singhvi, P., & Doll, B. Development of the fracture-based flexibility index for asphalt concrete cracking potential using modified semi-circle bending test parameters. *Construction and Building Materials*, 115, 390-401. DOI: 10.1016/j.conbuildmat.2016.03.144
  17. Zhu, Y., Dave, E. V., Rahbar-Rastegar, R., Daniel, J. S., and Zofka, A. Comprehensive Evaluation of Low Temperature Cracking Fracture Indices for Asphalt Mixtures, *Road Materials and Pavement Design*. 2017.
  18. Dave, E.V., W.G. Buttlar, S.E. Leon, B. Behnia, and G.H. Paulino. "IlliTC – Low Temperature Cracking Model for Asphalt Pavements," *Road Materials and Pavement Design*, 14(Sup. 2), 2013. pp. 57-78.
  19. Rahbar-Rastegar, R., Dave, E. V., and Daniel, J. S.. "Fatigue and Thermal Cracking Analysis of Asphalt Mixtures Using Continuum-Damage and Cohesive-Zone Models," *Journal of Transportation Engineering*, Part B: Pavements, Vol. 144, Issue 4. 2018.
  20. Baek, J., H. Ozer, H. Wang, and I. Al-Qadi. "Effects of Interface Conditions of Reflective Cracking Development in Hot-Mix Asphalt Overlays," *Road Materials and Pavement Design*, 11(2), pp. 307-334. 2010.
  21. Petersen, J.C. Glaser, R. Asphalt oxidation mechanisms and the role of oxidation products on age hardening revisited, *Road Mater. Pavement Des.* 12 (4) (2011) 795–819.
  22. Glaser, R. Schabron, J. Turner, T. Planche, J.P. Salmans, S. Loveridge, J. Low temperature oxidation kinetics of asphalt binders, *Transp. Res. Rec.* 2370 (2013) 63–68.
  23. 12 (4) (2011) 795–819. Daniel, J. S., Corrigan, M., Jacques, C., Nemat R., Dave, E.V., Congalton, A. Comparison of asphalt mixture specimen fabrication

methods and binder tests for cracking evaluation of field mixtures, *Road Materials and Pavement Design*, 2018. DOI: 10.1080/14680629.2018.1431148

## **Appendix B Paper 2 (Chapter 5)**

### **Development of a Rheology-based Mixture Aging Model to Evaluate the Cracking Performance of Asphalt Material over Time**

Runhua Zhang

University of New Hampshire

W161 Kingsbury Hall, 33 Academic Way, Durham, NH 03824, United States

Tel: 603-285-8739; Email: rz1015@wildcats.unh.edu

Jo E. Sias

University of New Hampshire

W183B Kingsbury Hall, 33 Academic Way, Durham, NH 03824, United States

Tel: 603-285-8739; Email: jo.sias@unh.edu

Eshan V. Dave

University of New Hampshire

W173 Kingsbury Hall, 33 Academic Way, Durham, NH 03824, United States

Tel: 603-285-8739; Email: eshan.dave@unh.edu

## Introduction

Asphalt material undergoes chemical oxidative aging by reacting with atmospheric oxygen. The oxidative reaction of asphalt is an ongoing process throughout pavement service life which takes place at ambient temperatures and pressures. Oxidative aging has a significant impact on the chemical, microstructural, and rheological properties of asphalt material. Oxidation increases the stiffness and brittleness of asphalt binders and mixtures, leading to a high cracking potential. Thus, oxidative aging has been considered to be one of the major distress mechanisms in asphalt pavements. Fundamental modeling of asphalt oxidative aging and the accurate prediction of asphalt mixture properties in terms of pavement service life is of pragmatic importance as more powerful pavement design and performance prediction methods are implemented.

A number of valuable aging models are proposed in the literature. Generally, temperature and pressure dependency of the oxidation reaction rate can be described using the Arrhenius equation [1], as shown in the general form given in **Eq. 1**.

$$k = AP^\alpha \exp\left(\frac{-E_a}{RT}\right) \quad (1)$$

Where,

$k$  is rate of reaction;

$A$  is reaction frequency factor;

$P$  is absolute oxygen pressure;

$E_a$  is reaction activation energy (KJ/mol);

$R$  is universal gas constant;

$T$  is reaction temperature (K).

**Herrington et al. [2]** proposed a kinetics expression, shown in **Eq. 2**, using binder viscosity as an Aging Index Properties (AIP) where the fast reaction rate ( $k_f$ ) and constant reaction rate ( $k_c$ ) can be expressed using **Eq. 3** and **4**, neglecting the pressure dependency term.

$$\log \eta = \log \eta_0 + M(1 - \exp(-k_f t)) + k_c t \quad (2)$$

$$k_f = A_f \left( \exp \frac{-E_{af}}{RT} \right) \quad (3)$$

$$k_c = A_c \left( \exp \frac{-E_{ac}}{RT} \right) \quad (4)$$

Where,

$\eta$  is long-term aged binder viscosity;

$\eta_0$  is short-term aged binder viscosity;

$M$  is fitting parameter related to fast reaction reactive material;

$t$  is reaction time (s);

$k_f$  is rate of fast reaction;

$k_c$  is rate of constant reaction;

$A_f$  is fast reaction frequency factor;

$A_c$  is constant reaction frequency factor;

$E_{af}$  is fast reaction activation energy (KJ/mol);

$E_{ac}$  is constant reaction activation energy (KJ/mol).

Several extensive studies to model the kinetics of asphalt binder oxidative aging using carbonyl area as an AIP have been conducted [3-7]. **Lau et al. [3]** presented a comprehensive study using results from 10 asphalt binders and determined the values of activation energy  $E$  and frequency (pre-exponential) factor  $A$ . **Eq. 5** is the kinetics model developed by Glover and his research team [7]. **Glover et al. [7]** presented an interrelation among kinetics parameters of fast and constant reactions as shown in **Eq. 6 - 8**.

$$CA = CA_0 + M(1 - \exp(-k_f t)) + K_c t \quad (5)$$

$$E_{af} = 0.85E_{ac} - 10.4 \quad (6)$$

$$A_f = 0.52 \exp(0.3328E_{af}) \quad (7)$$

$$A_c = 0.0266 \exp(0.3347E_{ac}) \quad (8)$$

Where,

$CA$  is long-term aged binder carbonyl area;

$CA_0$  is short-term aged binder carbonyl area.

**Glaser et al. [8]** used carbonyl + sulfoxide absorbance peaks as an AIP to fit the oxidation of 12 asphalt binders that originated from a wide variety of sources. The fitting used the same Arrhenius parameters for all 12 binders studied, with only one adjustable parameter, which corresponded to the amount of the fast reaction reactive material (M). **Eq. 9** shows the integral form of the model that was used to fit the isothermal data to determine the adjustable parameters (M). **Eq. 10** shows the form of the model taking into account pressure dependency terms for fast and slow reactions. If the Arrhenius parameters can be applied universally as Glaser et al.'s results suggest, a single aging trial at a single temperature is all that is needed to derive a kinetics model for unmodified binders **[8-9]**.

$$(C + S) = (C + S)_0 + M \left( 1 - \frac{k_c}{k_f} \right) (1 - \exp(-k_f t)) + k_c M t \quad (9)$$

$$(C + S) = (C + S)_0 + M \left( 1 - \frac{k_c * P^n}{k_f * P^m} \right) (1 - \exp(-k_f P^m t)) + k_c M P^n t \quad (10)$$

Where,

$(C+S)$  is long-term aged binder carbonyl + sulfoxide absorbance peaks;

$(C+S)_0$  is short-term aged binder carbonyl + sulfoxide absorbance peaks;

m is the reaction order of fast reaction;

n is the reaction order of constant reaction.

All of the models presented above are based on experimental data obtained by studying the AIPs of asphalt binders aged in thin films at elevated temperatures and/or under pressure. **Elwardany et al. [10]** recommended aging of loose mix in the oven after evaluating different laboratory methods for asphalt mixture to simulate oxidative aging for performance testing. Aging of loose mixture in the oven allows for capturing the physicochemical effects of mineral fillers and aggregate on asphalt binder oxidation rates. Thus, it is assumed to provide better representation of field aging. Based on **Glaser et al.'s [8]** kinetics model framework, **Elwardany et al. [11]** proposed a binder aging model using  $\log G^*$  at 64°C and 10 rad/s frequency as the AIP to track the change of binder properties with aging, as shown in **Eq.11** below:

$$\log G^* = \log G_0^* + M \left( 1 - \frac{k_c}{k_f} \right) (1 - \exp(-k_f t)) + k_c M t \quad (11)$$

Where,

$G^*$  is long-term aged binder shear modulus at 64°C and 10 rad/s (kPa);

$G^*_o$  is short-term aged binder shear modulus at 64°C and 10 rad/s (kPa).

Although significant research efforts have been dedicated to model the kinetics of asphalt binder aging, as discussed above, relatively little attention has been devoted to modeling the aging of asphalt mixtures. The lack of major studies in this area reflects the complexities involved in studying mixture aging. Oxidative reaction rate and mechanism are affected by the physicochemical interaction between the asphalt binder and the aggregate, as well as the mixture variables [12-19]. Also, most aging models as discussed above focus only on the modelling and prediction of the stiffness over time, ignoring the relaxation capability (phase angle) of the asphalt (viscoelastic) material. Researchers have shown that phase angle plays the significant role in the performance of both asphalt binder and mixture.

In order to address the problems mentioned above, a simplified and experimental mixture aging model is developed and validated with nine different mixtures in this study, taking into account mixture variables such as performance grade (PG), RAP and binder content. The mixture Glover-Rowe ( $G-R_m$ ) parameter calculated at the temperature-frequency combination of 20°C-5Hz [20-22] is selected and used as the AIP to modelling the change of mixture properties with aging. The main advantage of using  $G-R_m$  parameter as the AIP to model the aging of asphalt material is that it incorporates both stiffness and relaxation capacity (phase angle) to evaluate the cracking performance of asphalt mixtures. The correlations and comparisons between the  $G-R_m$  parameter with other mixture cracking performance indices measured from the advance fracture and fatigue tests are also evaluated and investigated in the last section of this study.

## Materials

This study includes laboratory testing on nine plant mixed, lab compacted surface mixtures. **Table 1** below shows the detailed mixture information (Recycled binder content is the ratio of the weight of recycled binder to the total binder weight). The mix ID has the specific meaning: the first four-digit numbers indicate binder PG grade, the following letters “S” and “L” indicate the nominal maximum aggregate size (NMAS) of 9.5mm and 12.5mm, respectively. The last letter represents the recycled binder content: “V” means no recycled binder, “M” means 14.8-18.9% recycled binder content, “L” means 28.3% recycled binder content.

**Table 1** Mixture Types and Aging Levels

Mixture ID	Virgin Binder Grade	Design Gyration Levels	NMAS (mm)	Total Binder Content (%)	Recycled Binder Content (%)
5234LM	PG 52-34	50	12.5	5.3	18.9



<b>5234LL</b>	PG 52-34	50	12.5	5.3	28.3
<b>5834LM</b>	PG 58-34	50	12.5	5.4	18.5
<b>5828SM</b>	PG 58-28	50	9.5	5.9	16.9
<b>6428SV</b>	PG 64-28	75	9.5	6.4	0
<b>6428SM</b>	PG 64-28	75	9.5	6.3	18.5
<b>6428LM</b>	PG 64-28	75	12.5	5.8	18.5
<b>7034LV</b>	PG 70-34	75	12.5	5.8	0
<b>7628SM</b>	PG 76-28	75	9.5	6.1	14.8

## Methodology

### Aging Method

Several asphalt mixture laboratory conditioning procedures are used to simulate aging in the field. These procedures can be generally classified based on the state of material during conditioning: compacted specimen and loose mix. In the AASHTO R30 procedure, the loose asphalt mixture is placed in a forced draft oven at  $135 \pm 3^\circ\text{C}$  ( $275 \pm 5^\circ\text{F}$ ) for 4 hr.  $\pm$  5 min to simulate short term aging (STA) during production and placement [23]. For long term aging, short term aged mixtures are compacted using gyratory compactor (following AASHTO T 312) into a specimen that is then conditioned in a forced-draft oven for 5 days at  $85^\circ\text{C}$  to represent five to ten years of aging in the field [24]. However, research [11,25] has shown that this method may not be appropriate to simulate the field aging under all conditions. The AASHTO procedure only includes a single conditioning time and temperature which is considered to match field aging at any location, regardless of the temperature history and climatic region of the pavement of interest. Furthermore, aging on the compacted specimen leads to the development of an aging gradient from the specimen's center to its periphery, which violates the representative volume element requirement for performance testing.

In order to address the problems discussed above, the Asphalt Institute recommends conditioning the loose mix asphalt for 24 hr. at  $135^\circ\text{C}$  to simulate long term aging in the field. Loose mixture aging produces uniform aging and reduces the aging time significantly as compared to compacted specimens [26]. This level of conditioning is expected to simulate 7 to 10 years of aging in the field [27]. However, Yousefi et al. [28] proposed that chemical changes of the binder under higher temperature can lead to significantly different cracking performance results compared to those when the conditioning temperature is below  $95^\circ\text{C}$ . The recent

findings of the National Cooperative Highway Research Program (NCHRP) 09-54 project on long term aging of asphalt mixtures suggests 95°C as an optimal temperature for aging loose mix considering the relationship between binder rheology and chemistry [25]. The recommended aging time varies with the geographical location of the pavement and should be adjusted based on climate conditions and pavement depth.

In this study, the NCHRP 09-54 project recommended 95°C for multiple laboratory conditioning durations (1, 3, 5, 8, 10 and 12 days) is used to condition the nine plant produced mixtures which have already undergone STA during production. **Table 2** below shows the summary of the different laboratory conditioning levels evaluated for each individual mixture.

**Table 2** Summary of the Aging Conditions on Mixtures

Mix ID	STA	1 Day @95°C	3 Days @95°C	5 Days @95°C	8 Days @95°C	10 Days @95°C	12 Days @95°C
5234LM	✓	NA	NA	✓	NA	NA	✓
5234LL	✓	NA	NA	✓	NA	NA	✓
5834LM	✓	✓	NA	✓	✓	NA	✓
5828SM	✓	NA	NA	✓	NA	NA	✓
6428SV	✓	✓	NA	✓	NA	✓	✓
6428SM	✓	NA	✓	✓	NA	NA	✓
6428LM	✓	✓	NA	✓	✓	NA	✓
7034LV	✓	✓	✓	✓	NA	NA	✓
7628SM	✓	✓	✓	✓	NA	NA	✓

NA: Not included in this study

### Climatic Aging Index (CAI)

The climatic aging index (CAI) was also developed from NCHRP 09-54 project [25] to determine laboratory aging durations at 95°C for asphalt mixtures that best reflect the time, climate, and pavement depth for a given pavement location in the United States using Enhanced Integrated Climatic Model (EICM) hourly pavement temperature data. The detailed calculation of CAI is shown below:

$$t_{oven} = CAI = \sum_{i=1}^N DA \exp(-E_a / RT_i) / 24 \quad (12)$$

$$D = \begin{cases} 3.4311 * d^{-0.683}, & 6\text{mm} \leq d \leq 35\text{mm} \\ 0.3056, & d \geq 35\text{mm} \end{cases} \quad (13)$$

Where,

$t_{oven}$  is required oven aging duration (day) at 95°C to reflect field aging (year);

$CAI$  is climatic aging index;

$D$  is depth correction factor;

$A$  is reaction frequency factor;

$E_a$  is reaction activation energy;

$R$  is universal gas constant;

$T_i$  is pavement temperature obtained from Enhanced Integrated Climatic Model (EICM) at the depth of interest, and at the hour of interest (K);

$B$  is depth dependent fitting parameter;

$d$  is depth of interest (mm).

### Testing and Analysis Methods

To measure the linear viscoelastic properties of asphalt mixtures at different aging levels, complex modulus testing was conducted at 4.4, 21.1, 37.8°C with loading frequencies of 0.1, 0.5, 1, 5, 10, 25 Hz at each temperature, following AASHTO T 342 using an asphalt mixture performance tester (AMPT). The dynamic modulus and phase angle mastercurves of mixtures at different aging levels were constructed using Abatech RHEA® software.

The mixture Glover-Rowe ( $G-R_m$ ) parameter can be calculated from the master curves. The Glover-Rowe parameter was initially proposed to assess the cracking resistance of asphalt binders. The basis of this approach was originally proposed by **Glover et al. [29]**. It suggested a correlation between a new DSR function with ductility using a temperature-frequency combination of 15°C and 1 rad/s. **Rowe et al. [30]** rearranged Glover's criterion and using some simplifications, suggested a new expression to evaluate the cracking performance of binders. The Glover-Rowe ( $G-R$ ) parameter captures the complex shear modulus ( $|E^*|$ ) and binder phase angle ( $\delta$ ) at a temperature-frequency combination of 15°C-0.005 rad/s. Later, **Mensching et al. [31]** developed a parameter to evaluate the cracking performance of asphalt mixture in the format of the binder Glover-Rowe parameter, but employing stiffness and phase angle measured on the mixture ( $|E^*|$  and  $\delta$ ), as shown in Eq. 14:

$$G - R_m = \frac{|E^*|(\cos\delta)^2}{\sin\delta} \quad (14)$$

Where,

$|E^*|$  is dynamic modulus (MPa);

$\delta$  is phase angle of the mixture ( $^{\circ}$ ).

In this study, the parameter is calculated at the temperature-frequency combination of 20°C-5Hz, following additional development of the  $G-R_m$  parameter to use a typically measured point to evaluate the cracking performance of asphalt mixtures [20-22].

In addition to the complex modulus test, the advanced fracture tests of asphalt mixtures, including the Semi Circular Bending (SCB) testing and Disk Shaped Compact Tension (DCT) tests, as well as the advanced fatigue test - Uniaxial Direct Tension Cyclic testing which is based on the Simplified Viscoelastic Continuum Damage (S-VECD) concept, are also included in this study. The SCB fracture test (AASHTO TP 124) was performed at an intermediate temperature (25°C). The measured data were analyzed using the IFIT software developed by Illinois Center of Transportation (ICT), to calculate the fracture energy ( $G_f$ ) and flexibility index (FI) parameters (16).

The DCT testing (ASTM D 7313) was conducted to compare the thermal cracking behavior of the mixtures with different aging levels. The test temperature for different mixtures is based on the winter-time pavement in-service temperature for the location where mix is being used, which is calculated at 98% reliability +10°C from the LTPPBind database for the nearest weather station to the actual project site. The measured data were analyzed to calculate the fracture energy ( $G_f$ ) and the fracture strain tolerance (FST) (17).

Uniaxial direct tension cyclic testing was conducted following AASHTO TP 107 to evaluate the fatigue behavior of the asphalt mixtures with different aging conditions. The simplified viscoelastic continuum damage (S-VECD) approach with the damage characteristic curve (DCC) and the performance parameter  $D^R$  were used to estimate the ability of the mixtures to resist fatigue cracking (13,14,15).

The complex modulus test was conducted on the study mixtures with all the aging conditions indicated in **Table 2**, While the fracture testing and the fatigue tests were only conducted on the mixtures with STA, 5 days and 12 days aging conditions.

## **Results and Discussion**

### **CAI Calculation Result**

**Figure 1** below shows the results of the CAI calculation based on the hourly pavement temperatures from the EICM. As shown in **Figure 1**, the corresponding field aging durations decrease with increase of the pavement depth, indicating the aging gradient within the pavement structure. Also, the field aging duration doesn't change significantly below the pavement depth of 80mm because of the restriction of the accessibility for the oxygen.

Previous work [32] has shown that a depth of 4.3 mm can be used as the critical depth to represent and evaluate the bulk behavior of a 37.5 mm thick surface (asphalt) layer in New Hampshire. Therefore, the field aging durations (at 4.3 mm depth) corresponding to the different laboratory conditioning durations are calculated and documented in **Table 3**. **Figure 1 and Table 3** provide a way to correlate the laboratory conditioning methods with the field aging durations based on local climate conditions and pavement depth, which can be used by agencies to select the proper laboratory conditioning time based on the desired equivalent field aging durations to evaluate the change of material performance over the designed pavement service life.

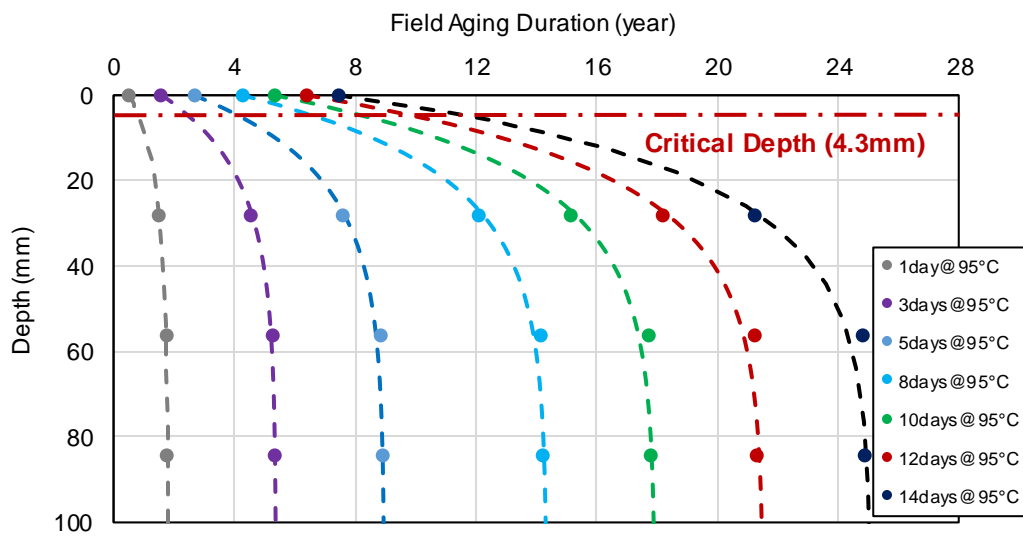


**Fig. 1** Relationship between Field Aging Duration and Pavement Depth Based on CAI Calculation Results (dashed lines show fitted curves to calculated values)

**Table 3** Field Aging Durations Corresponding with Different Laboratory Conditioning Durations

<b>Lab Aging Duration (day@95°C)</b>	1	3	5	8	10	12	14
<b>Field Aging Duration (year)</b>	0.8	2.4	4.0	6.4	8.0	9.6	11.2

### Development of the Mixture Aging Model

In this section, four mixtures (5834LM, 6428SV, 6428LM and 7628SM) are used to develop the mixture aging model.

**Figure 2** below shows the complex modulus and phase angle master curves for one example mixture (7628SM) with multiple aging conditions. The  $G-R_m$  parameter is then calculated from the master curves.

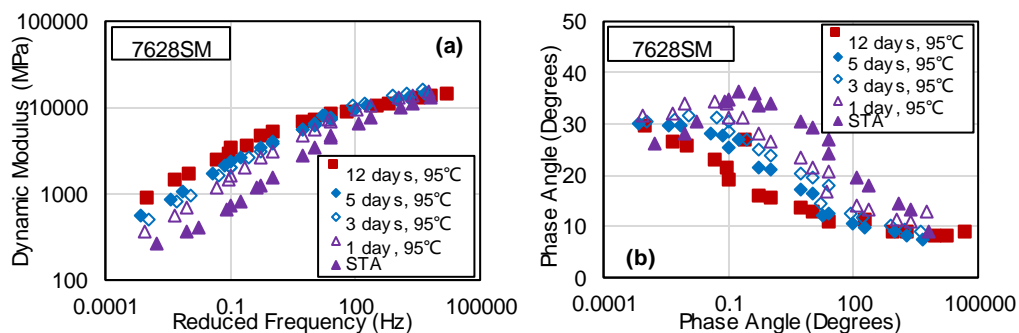


**Fig. 2** Complex Modulus and Phase Angle Mastercurves for Example Mixture (7628SM) with Different Aging Conditions

**Figure 3** shows how the  $G-R_m$  parameter increases with lab aging duration in a semi-logarithmic plot. There are clearly two stages of aging observed: at the early stage from STA (0 days) to approximately 2 days lab aging duration, the  $G-R_m$  parameter increases dramatically compared with the later stage where the rate of increase in  $G-R_m$  parameter is relatively consistent. This general trend has also been observed for asphalt binders [33-37]. All asphalt materials exhibit relatively similar kinetics consisting of an initial fast reaction period, also known as spurt, followed by a slower reaction period that has an approximately constant rate. These two reaction periods are known to be made up of fundamentally different chemical reactions [34]. **Petersen et al. [33]** explains that during the spurt, sulfoxides are the major oxidation product and cause an increase in viscosity. During the slower reaction period, ketones are the major product that cause the increase in viscosity. **Figure 4** depicts the dual oxidative reaction mechanism of asphalt binders proposed by **Petersen et al. [33,35]**.

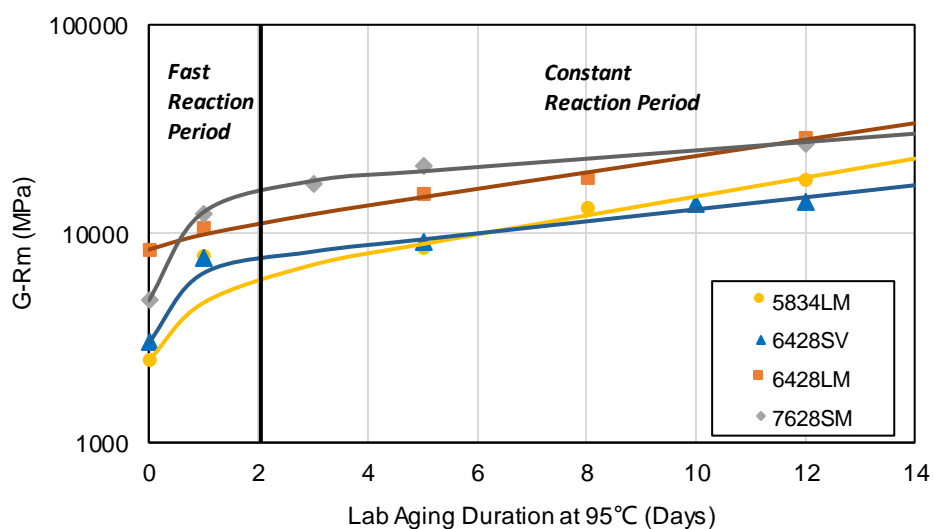


Fig. 3 G-R<sub>m</sub> Parameter for Mixtures with Different Aging Durations

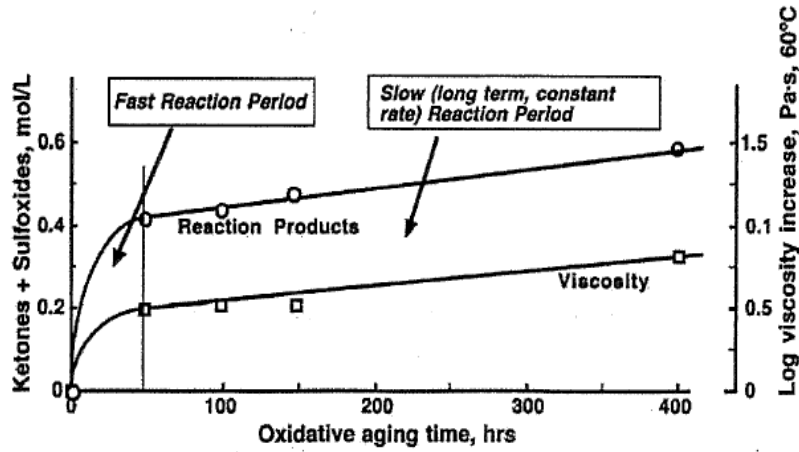


Fig. 4 Dual Oxidation Mechanisms for Asphalt Binder [35]

Therefore, an aging model for asphalt mixtures should also be able to capture the two reaction periods, which can be accomplished using the form shown in Eq. 15:

$$\text{Log}(G - R_m) = \text{Log}(G - R_{m_{STA}}) + M(1 - \exp(-R_s t)) + R_l t \quad (15)$$

Where,

$G - R_{m_{STA}}$  is the G-R<sub>m</sub> value for mixtures after STA;

$M$  is the material-based parameter;

$R_s$  is short-term aging constant (susceptibility);

$R_l$  is long term aging constant (susceptibility).

The parameters  $M$  and  $R_s$  are associated with the fast reaction period, higher  $M$  and  $R_s$  value indicate the high aging rate of asphalt mixtures during the very early stage (short-term) of pavement service life. The long-term aging constant  $R_l$  is calculated from the constant reaction period, indicating the aging rate of asphalt mixtures during the long-term period.

In this model,  $G - R_{m_{STA}}$  can be measured directly on mixtures with STA, the other 3 parameters ( $M$ ,  $R_s$  and  $R_l$ ) need to be determined from analysis of testing data. Using linear regression on the constant-rate data,  $R_l$  value is obtained as the slope of the constant-rate line in the constant reaction period. The  $M$  value can be calculated by Eq.16 below:

$$M = \text{Log}(\text{Intercept}) - \text{Log}(G - R_{m_{STA}}) \quad (16)$$

Where,

*Intercept* is the intercept of the constant-rate line in the constant reaction period with the y-axis;

$G-R_{mSTA}$  is the  $G-R_m$  value for mixtures after STA.

Once the  $M$  and  $R_l$  value are determined from the constant rate period, the only unknown parameter in **Eq. 15** is  $R_s$ . In order to calculate the  $R_s$  parameter, an optimization approach is employed. The objective of the optimization is to minimize the mean square error of model estimates of  $G-R_m$  at all aging conditions. The optimization is done using the Solver function in Excel. In summary, in order to calibrate the three model coefficients  $M$ ,  $R_s$  and  $R_l$ , three aging conditions (at least) are typically needed. One intermediate aging condition associated with one long-term aging condition are needed to calibrate the  $R_l$ , as well as  $M$  from the constant reaction period. The STA is also generally needed to calculate  $G-R_{mSTA}$ ,  $M$  and  $R_s$  value.

The curves in **Figure 3** are fitted by the aging model with calibrated model coefficients  $M$ ,  $R_s$  and  $R_l$  (as shown in **Table 4**, all aging conditions are used for calibration). The  $R^2$  (coefficient of determination, as shown in **Table 4**) shows the quality of the aging model to predict the change of mixture properties over time. Also, the mixture 5834LM, 6428SV and 7628SM are found to have the higher short-term aging susceptibility with the higher model coefficients  $M$  and  $R_s$  compared with mixture 6428LM, while 5834LM and 6428LM show the high log-term aging susceptibility with high value of  $R_l$ .

**Table 4** Summary of the Model Coefficients for Mixtures used for Development of the Model

Mix ID	M	$R_s$	$R_l$	$R^2$
5834LM	0.332	1.20	0.039	0.949
6428SV	0.350	2.03	0.029	0.975
6428LM	0.055	0.90	0.038	0.991
7628SM	0.518	1.50	0.020	0.995

### Validation of the Mixture Aging Model

To further evaluate the mixture aging model, another two mixtures 6428SM and 7034LV are subjected to different aging conditions in laboratory, and the complex modulus tests are conducted on the aged mixtures. The model coefficients were determined using only three aging conditions (STA, 5 days and 12 days), and are shown in **Figure 5**. **Figure 5** below also shows the aging prediction model with all measured points, not just those used to fit the model,



and the corresponding correlation coefficient ( $R^2$ ) value is also calculated. The high  $R^2$  value shows the high quality of mixture aging model to predict the change of G-R<sub>m</sub> parameter for those mixtures.

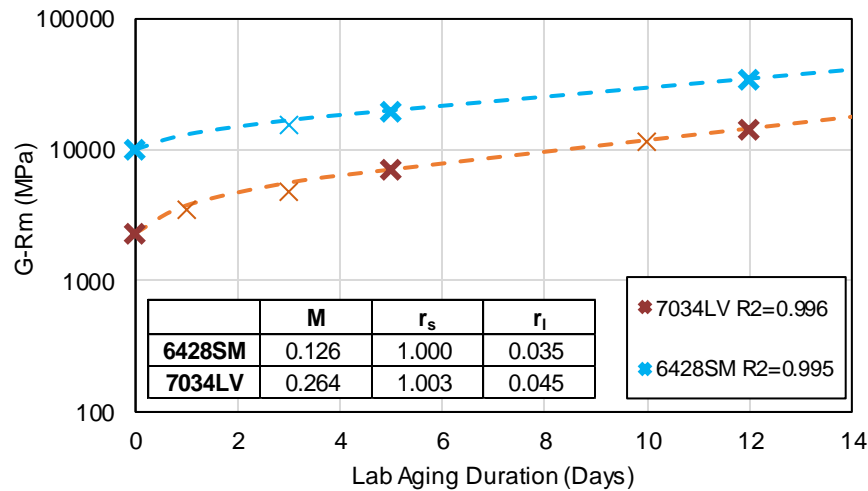


**Fig. 5** Validation of the Mixture Aging Model (bold markers indicate points used to fit the model, non-bold markers indicate validation points)

**Figure 6** below shows the calibration of the mixture aging model (using only three aging conditions: STA, 5 days and 12 days) for all nine mixtures included in this study. **Table 5** shows the summary of the three model coefficients, as well as the corresponding  $R^2$  values. The high  $R^2$  values indicate the high quality of mixture aging model. Comparing the  $R^2$  values of the four mixtures (5834LM, 6428SV, 6428LM and 7628SM, which are used to develop the aging model) in **Table 5** with the corresponding  $R^2$  value in **Table 4** (all aging conditions are included for the calibration), the fitting quality of the aging model doesn't change significantly, indicating that only three aging conditions (STA, one intermediate aging condition and another long-term aging condition) are typically sufficient to calibrate the aging model. And it should be mentioned that the appropriate laboratory conditioning durations (one intermediate and another long-term durations) used to calibrating the aging model can be also selected from **Figure 1** and **Table 3** based on specific project or desired evaluation periods.

From **Table 5**, the mixtures with the lower low temperature performance grade (LTPG) generally have higher model coefficients than other mixtures, indicating these mixtures are more susceptible to aging. Mixtures 6428SV and 7628SM generally have higher short-term aging susceptibility (higher M and  $R_s$  values), however, they do not show high long-term aging susceptibility ( $R_l$ ). **Figure 6** shows the threshold value (19000 MPa) suggested by the NCHRP 09-58 project for long-term oven aging (LTOA) conditions to minimize the material cracking potential.

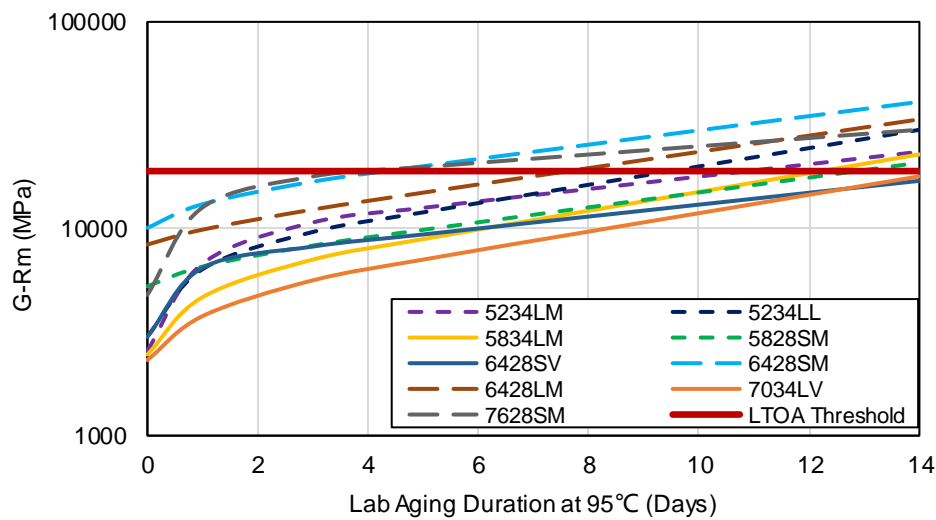


**Fig. 6** Aging Model Calibration for Nine Project Mixtures

**Table 5** Summary of the Model Coefficients for Nine Project Mixtures

Mix ID	M	$r_s$	$r_l$	$R^2$
5234LM	0.541	1.278	0.030	1.000
5234LL	0.378	1.354	0.044	1.000
5834LM	0.306	1.480	0.046	0.947
5828SM	0.093	1.000	0.036	1.000
6428SV	0.351	1.670	0.027	0.973
6428SM	0.126	1.000	0.035	0.995
6428LM	0.079	1.200	0.038	0.990
7034LV	0.264	1.003	0.045	0.996
7628SM	0.559	2.000	0.016	0.990

### Combination of the Aging Model with CAI

As described before, the climatic aging index (CAI) model was developed from the NCHRP 09-54 project to determine laboratory aging durations at 95°C for asphalt mixtures that best reflect the time, climate, and pavement depth for a given pavement location in United States based on the local climate conditions. By employing the CAI model, the field aging durations (at the depth of 4.3 mm) corresponding with the different lab aging conditions can be found in **Figure 1** and **Table 3**. **Figure 7** below shows the mixture aging model with the x-axis replaced by field aging duration from the CAI model.

The number of years for each mixture to reach the threshold value (19000 MPa) is calculated based on **Figure 7** and is listed in **Table 6** with the associated rankings. Based on the rankings, the mixtures can be divided into three categories as highlighted in **Figure 7 and Table 6**: It takes above 10 years for mixture 6428SV, 7034LV and 5834LM to reach the threshold value, while 7.5 to 9.8 years for mixture 5828SM, 5234LM and 5234LL to get to the limit. However, only after 3.4 to 5.5 years, the G-R<sub>m</sub> parameter for mixture 6428SM, 6428LM and 7628SM reaches the threshold value, indicating the high cracking susceptibility of these mixtures. **Figure 7 and Table 6** can also be used for the life cycle analysis (LCA) for specific mixtures and projects.

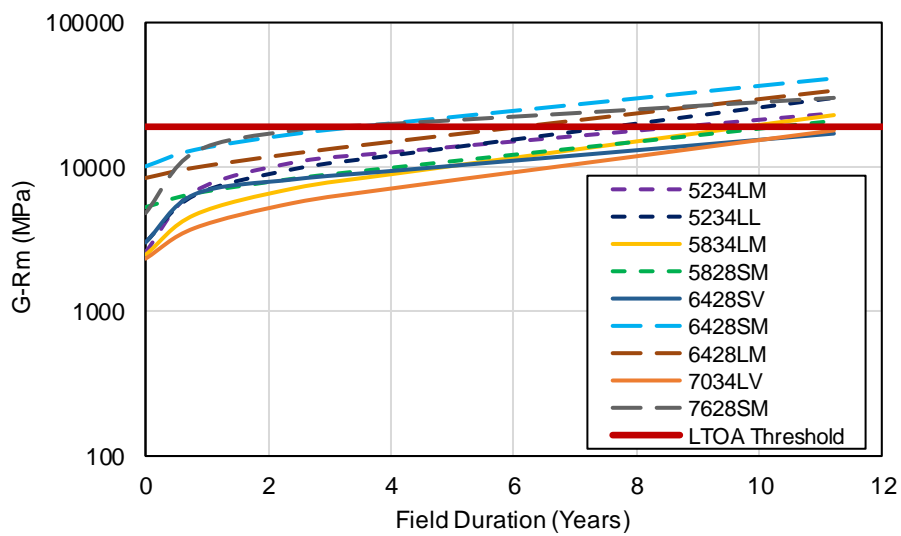


**Fig. 7** Mixture Aging Model (Field Duration)

**Table 6** Ranking of Mixtures Based on the Years to Threshold (background color of cells indicates mixtures with similar aging characteristics)

Mix ID	Years to Threshold	Ranking (Good-Poor)	
6428SV	12	1	Good (>10years)
7034LV	11.8	2	
5834LM	10	3	
5828SM	9.8	4	Moderate (6-10 years)
5234LM	9.2	5	
5234LL	7.5	6	
6428LM	5.5	7	Poor (<6 years)
7628SM	3.5	8	
6428SM	3.4	9	

The mixture aging model combined with CAI model, as described in this section, can be used as an effective, simple, and convenient material selection and pavement design approach that can evaluate and track the change of mixture cracking performance over pavement service life. This can benefit both owner agencies and contractors: owner agencies can have an in-depth understanding of how the cracking and aging susceptibility of individual mixture evolve over time, and obtaining confidence that the pavement can avoid significant cracking damage for a given period of time based on the predicted performance, while the contractors will have knowledge of how the various mixture variables, such as binder performance grade (PG) and RAP, can impact the cracking and aging susceptibility of asphalt mixtures by evaluating the model coefficients, and further adjust their design accordingly.

### **Comparison and Correlation the G-R<sub>m</sub> Parameter with Other Mixture Performance Indices**

Previous work [32,38] has shown how the different cracking performance indices of asphalt mixtures change over time, including the D<sup>R</sup> (average reduction in pseudo stiffness up to failure) value measured from the indirect tension cyclic fatigue test [39], as well as the G<sub>f</sub> (fracture energy), FI (flexibility index) and FST (fracture strain tolerance) measured from the advanced fracture tests [40,41]. All those tests were performed on the (same) nine mixtures, but only 5 days and 12 days aging conditions. In this section, the correlation and comparison between the G-R<sub>m</sub> parameter measured from this study with other performance indices from the previous study are evaluated and investigated based on the study mixtures with the same aging conditions.

The Pearson correlation factor (matrix) is used to investigate the correlation between the different mixture performance indices. The correlation factor shows the strength of linear relationship between each pair of parameters; a correlation factor of 1 indicates a perfect direct linear relationship and a correlation factor of -1 indicates a perfect inverse linear relationship. A value of zero indicates no relationship between two variables. The Pearson correlation factors for the comparison are presented in **Table 7**. Values above an absolute value of 0.7 are shaded green indicating the relatively strong correlation between the two parameters, those between 0.4 and 0.7 are shaded blue showing the moderate correlations, and those below 0.4 (weak correlation) are not shaded with color [42].

As shown in **Table 7** below, G-R<sub>m</sub> parameter and FI generally show moderate to strong correlations with other different mixture performance indices (except for G<sub>f</sub> from SCB; G<sub>f</sub> from SCB does not correlate well with other parameters). G-R<sub>m</sub> shows the strong positive correlation with FI value, while the FI value shows the strong positive correlation with FST value. The fatigue performance index D<sup>R</sup> value only shows the moderate correlations with G-R<sub>m</sub>, FI and G<sub>f</sub> from DCT test.

In summary, the mixture G-R<sub>m</sub> parameter has moderate to strong correlations with many of the mixture parameters, indicating that it has the potential to be used as a simplified index to evaluate and differentiate the performance of asphalt mixtures with different variables in general, while taking aging into account. This is very helpful for agencies to select and design the appropriate mixture, as well as evaluate the performance of asphalt mixtures over the designed service life, while only employing one type of test (complex modulus test) with several aging conditions (three for calibration of the aging model).

**Table 7** Comparisons and Correlations between the G-R<sub>m</sub> Parameter with other Mixture Performance Indices

	<b>G-R<sub>m</sub></b>	<b>G<sub>f</sub> SCB</b>	<b>FI</b>	<b>G<sub>f</sub> DCT</b>	<b>FST</b>	<b>D<sup>R</sup></b>
<b>G-R<sub>m</sub></b>	<b>1.000</b>					
<b>G<sub>f</sub> SCB</b>	-0.141	<b>1.000</b>				
<b>FI</b>	<b>-0.720</b>	0.227	<b>1.000</b>			
<b>G<sub>f</sub> DCT</b>	<b>0.527</b>	0.194	<b>-0.618</b>	<b>1.000</b>		
<b>FST</b>	<b>-0.530</b>	0.301	<b>0.851</b>	-0.172	<b>1.000</b>	
<b>D<sup>R</sup></b>	<b>-0.523</b>	-0.216	<b>0.495</b>	<b>-0.582</b>	0.211	<b>1.000</b>

### Summary and Conclusion

The simplified and experimental mixture aging model developed in this study takes into account mixture variables and mineralogy and is shown to efficiently capture the two aging reaction periods of asphalt materials:

- The three model coefficients (M, R<sub>s</sub> and R<sub>l</sub>) can be used to evaluate and differentiate the aging susceptibility of different asphalt mixtures with various mix variables.
- The mixture aging model combined with Climatic Aging Index (CAI) model can be used as an effective, simple, and convenient material selection and pavement design approach that can evaluate and track the change of cracking performance asphalt mixtures over designed pavement service life.
- To calibrate the model, three aging conditions are sufficient: STA, one intermediate aging condition and another long-term aging condition. The selection of 5 days (intermediate) and 12 days (long-term) at 95°C worked well for the study materials.
- The mixture G-R<sub>m</sub> parameter has the potential to be used as a simplified index to evaluate and differentiate the performance of asphalt mixtures with different variables in general, while taking aging into account.

- Based on the aging model evaluated in this study, the mixtures with the lower low temperature performance grade (LTPG) generally have higher model coefficients than other mixtures, indicating these mixtures are more susceptible to aging. The two virgin mixtures generally show the good cracking performance after each aging condition.

### **Future Work**

Future work and analysis are planned to periodically collect the field performance data for the study mixtures to allow for further development, calibration, and verification of aging model to more accurately evaluate and predict the cracking performance of the pavement.

### **Acknowledgements**

The authors would like to acknowledge New Hampshire Department of Transportation (NH DOT) for sponsoring this study and the University of New Hampshire Center for Infrastructure Resilience to Climate (UCIRC).

### **Conflict of Interest**

The authors declare that they have no conflict of interests.

## Reference

1. Laidler K J (1987) Chemical Kinetics. Third Edition, Harper & Row, New York, pp 42.
2. Herrington PR, Patrick JE, and Ball GF (1994) Oxidation of roading asphalts. Industrial and Engineering Chemistry Research, Vol. 33 (11), pp. 2801-2809.
3. Lau CK, Lunsford KM, Glover CJ, Davison RR, and Bullin JA (1992) Reaction rates and hardening susceptibilities as determined from pressure oxygen vessel aging of asphalts. Transportation Research Record 1342, pp.50-56.
4. Davison RR, Bullin JA, Glover CJ, Chaffin JM, Peterson GD, Lunsford KM, Lin MS, Liu M, and Ferry MA (1994) Verification of an asphalt aging test and development of superior recycling agent and asphalts. <https://static.tti.tamu.edu/tti.tamu.edu/documents/1314-1F.pdf>. Accessed 1 August 2019
5. Liu M, Lunsford KM, Davison RR, Glover CJ, and Bullin JA (1996) The kinetics of carbonyl formation in asphalt. American Institute of Chemical Engineers Journal, Vol. 42 (4), pp. 1069-1076.
6. Domke CH, Davison RR, and Glover CJ (2000) Effect of oxygen pressure on asphalt oxidation kinetics. Industrial and Engineering Chemistry Research, no. 3: pp. 592-598.
7. Glover CJ, Han R, Jin X, Prapaitrakul N, Cui Y, Rose A, Lawrence JJ, Padigala M, Arambula E, Park ES, and Martin AE (2014) Evaluation of binder aging and its influence in aging of hot mix asphalt concrete. <https://static.tti.tamu.edu/tti.tamu.edu/documents/0-6009-1.pdf>. Accessed 1 August 2019
8. Glaser R, Turner TF, Loveridge JL, Salmans SL, and Planche JP (2013) Fundamental properties of asphalts and modified asphalts, Volume III. Quarterly Technical Report, Federal Highway Administration (FHWA), Washington D.C, USA.
9. Glaser R, Turner TF, Loveridge JL, Salmans SL, and Planche JP (2015) Fundamental properties of asphalts and modified asphalt, Volume III. Aging Master Curve (FP 10) and Aging Rate Model (FP 11). Technical White Paper, Western Research Institute, Laramie, Wyoming, USA.
10. Elwardany MD, Yousefi Rad F, Castorena C, Kim YR (2017). Evaluation of asphalt mixture laboratory long-term aging methods for performance testing and prediction. Road Materials and Pavement Design, 18:sup1, pp. 28-61

11. Elwardany, MD, Yousefi Rad F, Castorena C, Kim YR (2018) Climate-, depth-, and time-based laboratory aging procedure for asphalt mixtures. *Journal of the Association of Asphalt Paving Technologists*, 87(0270-2932):pp. 467-512.
12. Moraes R, Bahia HU (2015) Effect of mineral filler on changes in molecular size distribution of asphalt during oxidative ageing. *Road Materials and Pavement Design*, Vol. 16, pp. 55-72.
13. Wu JT, Han WP, Airey G, and Yusoff NIM (2014) The influence of mineral aggregates on bitumen ageing. *International Journal of Pavement Research and Technology*, Vol. 7(2), pp. 115-123.
14. Petersen JC (2009) A review of the fundamentals of asphalt oxidation: chemical, physicochemical, physical property, and durability relationships. *Transportation Research E-Circular (E-C140)*, Transportation Research Board, Washington, D.C.
15. Little DN, Epps JA, and Sebaaly PE (2006) Hydrated lime in hot mix asphalt. National Lime Association. <https://www.lime.org/lime-basics/uses-of-lime/construction/asphalt/>. Accessed 1 August 2019
16. Recasens R, Martínez A, Jiménez F, and Bianchetto H (2005) Effect of filler on the aging potential of asphalt mixtures. *Transportation Research Record: Journal of the Transportation Research Board*, No. 1901, pp. 10-17.
17. Huang SC, Petersen JC, Robertson R, and Branthaver J (2002) Effect of hydrated lime on long-term oxidative aging characteristics of asphalt. *Transportation Research Record: Journal of the Transportation Research Board*, No. 1810, Transportation Research Board of the National Academies, Washington, D.C., pp. 17-24.
18. Jones GM (1997) The effect of hydrated lime on asphalt in bituminous pavements. NLA Meeting, Utah DOT, Utah, USA.
19. Petersen JC, Plancher H, and Harnsberger PM (1987) Lime treatment of asphalt to reduce age hardening and improve flow properties. *Association of Asphalt Paving Technologists*, Vol. 56.
20. Martin AE, Zhou F, Arambula E, Park ES, Chowdhury A, Kaseer F, Carvajal J, Hajj E, Daniel JS, Glover C (2015) The effects of recycling agents on asphalt mixtures with high ras and rap binder ratios. [http://onlinepubs.trb.org/onlinepubs/nchrp/docs/NCHRP09-58\\_PhII\\_DraftInterimReport.pdf](http://onlinepubs.trb.org/onlinepubs/nchrp/docs/NCHRP09-58_PhII_DraftInterimReport.pdf). Accessed 1 August 2019.



21. Pournoman S, Hajj EY, Morian N, Martin AE (2018) impact of recycled materials and recycling agents on asphalt binder oxidative aging predictions. *Transportation Research Record*, 2672(28), 277–289.
22. Oshone M., Sias JE, Dave EV, Epps Martin A, Kaseer F, Rahbar-Rastegar (2019) Exploring master curve parameters to distinguish between mixture variables. *Road Materials and Pavement Design*, DOI: 10.1080/14680629.2019.1633784
23. Bell CA., AbWahab Y, Cristi RE, and Sognovske D (1994) selection of laboratory aging procedures for asphalt-aggregate mixtures, <http://onlinepubs.trb.org/onlinepubs/shrp/SHRP-A-383.pdf> Accessed 1 August 2019.
24. Harrigan ET (2007) simulating the effects of hot mix asphalt aging for performance testing and pavement structural design, <http://www.trb.org/Publications/Blurbs/157804.aspx> Accessed 1 August 2019.
25. Kim RY, Castorena C, Elwardany M, Yousefi Rad F, Underwood S, Gundha A, Gudipudi, P, Farrer MJ, Glaser R (2018) long-term aging of asphalt mixtures for performance testing and prediction, <http://www.trb.org/Publications/Blurbs/176937.aspx> Accessed 1 August 2019.
26. Blankenship PB, Anderson MA, King GN, and Hanson DI. (2010) A laboratory and field investigation to develop test procedures for predicting non-load associated cracking of airfield hma pavements, <https://www.eng.auburn.edu/research/centers/ncat/files/aaptp/Report.Final.06-01.pdf> Accessed 1 August 2019
27. Arega ZA, Bhasin A, and De Kesel T (2013) Influence of extended aging on the properties of asphalt composites produced using hot and warm mix methods, *Construction and Building Materials*, Vol. 44, 2013, pp. 168-174.
28. Yousefi Rad F, Elwardany MD, Castorena C, and Kim YR (2017) investigation of proper long-term laboratory aging temperature for performance testing of asphalt concrete, *Construction and Building Materials*, Vol. 147, 2017, pp. 616-629.
29. Glover CJ, Davison RR, Domke CH, Ruan Y, Juristyarini P, Knorr DB, Jung SH (2005) Development of a new method for assessing asphalt binder durability with field validation. <https://static.tti.tamu.edu/tti.tamu.edu/documents/0-1872-2.pdf> Accessed 1 August 2019
30. Rowe GM (2011) Evaluation of the relationship between asphalt binder properties and non-load related cracking, *Journal of the Association of Asphalt Paving Technologists*, Vol. 80, 649-662.

31. Mensching DJ, Geoffrey MR, and Daniel JS (2017) A mixture-based black space parameter for low-temperature performance of hot mixture asphalt. *Road Materials and Pavement Design*, pp. 404-425.
32. Zhang R, Dave EV, and Daniel JS (2019) Impact of aging on the viscoelastic properties and cracking behaviour of asphalt mixtures. *Transportation Research Record: Journal of Transportation Research Board*. <https://doi.org/10.1177/0361198119846473>
33. Petersen JC, Harnsberger P (1996) Asphalt aging: dual oxidation mechanism and its interrelationships with asphalt composition and oxidative age hardening. *Transportation Research Record: Journal of the Transportation Research Board* 1638, pp. 47-55
34. Petersen JC (1998) A dual, sequential mechanism for the oxidation of petroleum asphalts. *Petroleum Science and Technology*, Vol. 16, No. 9-10, pp. 1023-1059.
35. Petersen JC, Glaser R (2011) Asphalt oxidation mechanisms and the role of oxidation products on age hardening revisited, *Road Mater. Pavement Des.* 12 (4) 795–819.
36. Prapaitrakul N, Han R, Jin X, and Glover CJ (2009) A transport model of asphalt binder oxidation in pavements. *Road Materials and Pavement Design*. 10:sup1, 95-113, DOI: 10.1080/14680629.2009.9690238
37. Han R (2011) Improvement to a transport model of asphalt binder oxidation in pavements: pavement temperature modeling, oxygen diffusivity in asphalt binders and mastics, and pavement air void characterization. <https://pdfs.semanticscholar.org/ebc2/e2d286c31f50f920c04741b5725e84e21d4d.pdf>  
Accessed 1 August 2019
38. Zhang R, Daniel JS, Dave EV (2018) Evaluation of viscoelastic properties and cracking behaviour of asphalt mixtures with laboratory aging, *RILEM252-CMB-Symposium on Chemo Mechanical Characterization of Bituminous Materials*, Springer, pp. 33-38.
39. Wang Y, Kim YR (2017) Development of a pseudo strain energy-based fatigue failure criterion for asphalt mixtures, *International Journal of Pavement Engineering*. 20:10, 1182-1192, DOI: 10.1080/10298436.2017.1394100
40. Ozer H, Al-Qadi IL, Lambros J, El-Khatib A, Singhvi P, and Doll B (2016) Development of the fracture-based flexibility index for asphalt concrete cracking potential using modified semi-circle bending test parameters. *Construction and Building Materials*, 115, 390-401. DOI: 10.1016/j.conbuildmat.2016.03.144

41. Zhu Y, Dave EV, Rahbar-Rastegar R, Daniel JS, and Zofka A (2017) Comprehensive evaluation of low temperature cracking fracture indices for asphalt mixtures, Road Materials and Pavement Design. 18:sup4, 467-490, DOI:[10.1080/14680629.2017.1389085](https://doi.org/10.1080/14680629.2017.1389085)
42. Lane D., 2003. Online Statistics Education: An Interactive Multimedia Course of Study. Rice University, Texas, USA. <http://onlinestatbook.com/> Accessed 1 August 2019

## **Appendix C Paper 3 (Chapter 6)**

### **Correlating Laboratory Conditioning with Field Aging for Asphalt Using Rheological Parameters**

**Runhua Zhang (ORCID ID: 0000-0003-2623-1731)**

University of New Hampshire

W161 Kingsbury Hall, 33 Academic Way, Durham, NH 03824

Tel: 603-285-8739; Email: [rz1015@wildcats.unh.edu](mailto:rz1015@wildcats.unh.edu)

**Jo E. Sias, Ph.D., P.E. (Corresponding Author) (ORCID ID: 0000-0001-5284-0392)**

University of New Hampshire

W183B Kingsbury Hall, 33 Academic Way, Durham, NH 03824

Tel: 603-862-3277; Email: [jo.sias@unh.edu](mailto:jo.sias@unh.edu)

**Eshan V. Dave, Ph.D. (ORCID ID: 0000-0001-9788-2246)**

University of New Hampshire

W173 Kingsbury Hall, 33 Academic Way, Durham, NH 03824

Tel: 603-862-5268; Email: [eshan.dave@unh.edu](mailto:eshan.dave@unh.edu)

Word count: 6470 words text + 4 tables × 250 words (each) = 7470 words

Submission Date: August 1, 2019

## INTRODUCTION

Aging has a significant effect on the performance of asphalt materials and can drastically alter the serviceable life of pavements. Asphalt pavements undergo aging during construction (short term aging, mostly evaporation of lighter weight molecules at the high production temperatures), and over the pavement service life (long term aging due to oxidation and continued loss of lighter weight hydrocarbons) that increases the stiffness and brittleness of the asphalt material and decreases the stress relaxation capability. Consequently, aged asphalt binders and mixtures have increased cracking susceptibility with potentially shorter pavement service lives and lower serviceability of the pavement. Considering the performance prediction asphalt materials with aging and the importance of performance-based design methodologies, there is a need for accelerated laboratory aging methods that can simulate and predict the change of binder and mixture properties over the whole service life. This will help to minimize maintenance and rehabilitation costs due to the different pavement distresses and to increase the confidence level of the pavement designs.

Several laboratory conditioning procedures are used to simulate the aging in the field. These procedures can be generally classified based on the type of material during aging: binders, and asphalt mixtures. In the current Superpave binder specification, the rolling thin film oven (RTFO) aging method (1) is used to simulate the short-term aging (STA) of the pavement in the field for unmodified binders (2). The stirred airflow test procedure is designed to age (short-term) modified binders as well as unmodified binders (3). The pressure aging vessel (PAV) method (4) applied to the asphalt binder obtained from the STA residue is generally used to simulate long-term aging. However, the main drawback of this method is that the corresponding in-service aging time depends on climate and binder kinetics as well as mixture parameters (such as air voids and binder content), thus resulting in variable outcomes (5).

Researchers (6,7,8,9,10) recommend aging the asphalt mixture in the oven to capture the effect of mixture parameters on the asphalt binder oxidation process, such as the air voids, binder content, and the interactions between recycled and virgin binder. AASHTO R30 procedure recommends putting the loose asphalt mixture in a forced draft oven at  $135 \pm 3^{\circ}\text{C}$  ( $275 \pm 5^{\circ}\text{F}$ ) for 4 hr.  $\pm$  5 min to STA (6). For long term aging, STA mixtures are compacted using gyratory compactor (following AASHTO T 312) into a specimen that is then conditioned in a forced-draft oven for 5 days at  $85^{\circ}\text{C}$  to represent five to ten years of aging in the field (7). However, research (11,12,13) has shown that this method may not be appropriate to simulate the field aging under all conditions. The AASHTO procedure only includes a single conditioning time and temperature which is considered to match field aging at any location, regardless of the temperature history and climatic region of the pavement of interest. Furthermore, aging on the compacted specimen leads to the development of an aging gradient from the specimen's center to its periphery, and can result in different aging extents for different specimen geometries. This variability complicates the interpretation of results from different performance testing.

To address the challenges discussed above, the Asphalt Institute recommends conditioning the loose mix asphalt for 24 hours at  $135^{\circ}\text{C}$  to simulate long term aging in the field (14). Loose mixture aging produces uniform aging and reduces the aging time significantly as compared to compacted specimens. This level of conditioning is expected to

simulate 7 to 10 years of aging in the field (8). However, research shows that aging asphalt at temperatures above 100°C may disrupt polar molecular associations, which leads to the thermal decomposition of sulfoxides in asphalt binders (15,16). Yousefi et al. (9) also proposed that these chemical changes of the binder under higher temperature can lead to significantly different cracking performance results compared to the material testing and pavement simulations for aging below 95°C. The recent findings of the National Cooperative Highway Research Program (NCHRP) 09-54 project on long term aging of asphalt mixtures suggests 95°C as an optimal temperature for aging loose mix considering the relationship between binder rheology and chemistry (10).

Apparent gaps still exist between published research and precise description of aging behavior of asphalt materials in the field. One of the biggest concerns of field aging is the aging gradient within the pavement structure due to different factors such as the temperature gradient, oxygen availability and air void distribution (17). Overlooking aging gradient leads to inappropriate characterization of the aging behavior of asphalt mixtures.

The main objective of this study is to correlate the asphalt binder and mixture laboratory conditioning methods with field aging by exploring evolution of rheological parameters of asphalt binders over time, as well as evaluating changes in the aging kinetics with pavement depth. In this study, the rheological indices of binder samples with different aging conditions are measured to evaluate how the properties of asphalt binders change with time. The field aging gradient is evaluated and investigated by testing binder samples extracted and recovered from different layers of field cores. The laboratory aging durations corresponding with the field aging durations of the different layers from field cores are also determined based on New Hampshire climate conditions. This study provides a way to optimize the laboratory conditioning durations and evaluate the performance of asphalt material with respect to pavement life (time) and depth (location) within the pavement structure.

## **MATERIALS**

**Table 1** shows the summary information for binder samples extracted and recovered from the nine mixtures (plant produced) with different aging conditions included in this study (Recycled binder content is the ratio of the weight of recycled binder to the total binder weight). Letters in the cells indicate the testing conducted at each of the mixture-aging combinations. The mix ID is defined as follows: the first four-digit number indicates the original binder PG grade, the following letters indicate the nominal maximum aggregate size (NMAS) of 9.5mm “S” and 12.5mm “L”. The last letter represents the recycled binder content: “V” indicates no recycled binder, “M” indicates 14.8-18.9% recycled binder content, and “L” indicates 28.3% recycled binder content. The field cores (taken after four years in service) from four mixtures (5234LM, 5234LL, 5828LM and 5828LL) were cut into three layers (12.5mm each) and then the binders were extracted and recovered. The binder extraction was performed in accordance with AASHTO T 164, procedure 12, using a centrifuge extractor and toluene solvent. The asphalt binder was recovered based on ASTM D7906-14 using a rotary evaporator. Additionally, seven binder samples (virgin tank samples with RTFO and 20hr. PAV aging) were evaluated in this study. The effect of different conditioning methods (mixture aging levels, and RTFO/ PAV binder aging) on binder properties can be directly compared and evaluated on the virgin binders extracted and recovered from the two virgin mixtures 6428SV and 7034LV.

**TABLE 1 Mixture/Binder Types and Aging Levels**

Mixture ID	Virgin Binder PG	Total Binder Content (%)	Recycled Binder Content (%)	Testing/Analysis (4mm DSR)					
				STA	95°C@5d	95°C@12d	135°C@24hr.	Field Cores	Original Binder (20 hr. PAV)
5234LM	52-34	5.3	18.9	✓	✓	✓	✓	✓	NA
5234LL	52-34	5.3	28.3	✓	✓	✓	✓	✓	NA
5834LM	58-34	5.4	18.5	✓	✓	✓	NA	NA	✓
5828LM	58-28	5.3	18.9	✓	NA	✓	✓	✓	NA
5828LL	58-28	5.3	28.3	✓	NA	✓	✓	✓	NA
6428SV	64-28	6.4	0	✓	✓	✓	NA	NA	✓
6428SM	64-28	6.3	18.5	✓	✓	✓	NA	NA	✓
7034LV	70-34	5.8	0	✓	✓	✓	NA	NA	✓
7628SM	76-28	6.1	14.8	✓	✓	✓	NA	NA	✓

NA: Not included in this study

## METHODOLOGY

### Laboratory Conditioning

The Superpave RTFO+PAV (20hr.) on original binders, the Asphalt Institute procedure (24 hours at 135°C) and NCHRP recommended 95°C for 5 and 12 days on the plant produced mixtures are the laboratory conditioning protocols included in this study. For mixture aging, loose mix asphalt was spread in steel pans at an approximate depth of 25 mm. The mixtures were stirred and remixed every other day and the pans were rotated around the oven to obtain a consistent aging condition in mixtures.

### Testing and Analysis Methods

The rheological properties of asphalt binders were measured using a Dynamic Shear Rheometer (DSR) with a 4 mm plate (18). This test covers a wide range of temperatures (-36°C to 30°C, usually in 3 degrees increments), and frequencies (15 frequencies from 100 rad/sec to 0.2 rad/sec), by using the appropriate strain level at each combination of test temperature and frequency. The isotherm tests are conducted from the coldest to the warmest temperature and from the highest to the lowest frequencies. The complex shear modulus master curve is constructed at 10°C in this study, and fitted using the Christensen-Anderson-Marasteanu model (CAM, as shown in **Equations 1 and 2**) in the Abatech RHEA<sup>®</sup> software.

$$G^*(w) = \frac{G_g}{[1+(w_0/w)^\beta]^{k/\beta}} \quad (1)$$

$$\beta = \log 2 / R \quad (2)$$

Where,

$G^*(w)$ : complex shear modulus at a given frequency (Pa);

$G_g$ : glassy asymptote (modulus) (Pa);

$w$ : frequency (rad/s);

$w_0$ : crossover frequency (rad/s);

$k$ : fitting coefficient;

$R$ : difference between the logarithmic glassy modulus and the logarithmic equilibrium modulus of the binder, simplified as  $\text{Log } |G^*|$  at glassy asymptote minus  $\text{Log } |G^*|$  at the crossover frequency.

Sui et al. (19) developed a method to calculate the slope and magnitude of the shear stress relaxation modulus  $G(t)$  from the relaxation modulus master curve constructed from the 4mm DSR test at 60 seconds and 10°C warmer than the low PG grading temperature, which are correlated with the corresponding  $S(t)$  and  $m$ -values at 60 seconds and 10°C above the true low PG grading temperature from BBR measurements. The  $\Delta T_c$  parameter can be then calculated from the critical temperatures determined by the  $S(t)$  and  $m$ -value.  $\Delta T_c$  is defined as the difference between the temperature at which the  $S(t)$  and  $m$ -value criteria from the BBR testing are met, as shown in **Equation 3**.

$$\Delta T_c = T_{(stiffness)} - T_{(m-slope)} \quad (3)$$

Where,

$T_{(stiffness)}$ : critical low temperature at which  $S(60) = 300$  MPa;

$T_{(m-slope)}$ : critical low temperature at which  $m(60) = 0.300$ .

When the  $\Delta T_c$  value is positive, the binder grade is controlled by the creep stiffness (S-controlled); when the  $\Delta T_c$  value is negative, the binder grade becomes  $m$ -controlled. S-controlled binders typically have better stress relaxation capability and are therefore typically less prone to cracking. Asphalt Institute (20, 21) suggests using  $\Delta T_c = -2.5^\circ\text{C}$  and  $\Delta T_c = -5.0^\circ\text{C}$  as threshold values for crack warning and cracking limit respectively.

The complex modulus master curve from the 4mm DSR test is used to calculate the binder Glover-Rowe parameter. Rowe et al. (21) developed the binder Glover-Rowe parameter to evaluate the cracking susceptibility of asphalt binders, as shown in **Equation 4**. A lower G-R parameter indicates better capability to resist durability cracking. A limiting value of 180 kPa is proposed as a crack warning limit, a second value of 600 kPa is suggested for the development of significant cracking (block cracking). The binder G-R parameter is generally calculated at the temperature and frequency combination of 15°C and 0.005rad/sec.

$$G - R = \frac{|G^*|(\cos\delta)^2}{\sin\delta} \quad (4)$$

Where,



$\delta$ : phase angle of the binder.

### NCHRP 09-54 Binder Oxidation Aging Model

Based on Glaser et al.'s (22) framework, the NCHRP 09-54 project developed an oxidation aging model to predict the change of binder property with aging using  $\log G^*$  at 64°C and 10 rad/s frequency as the AIP (aging index property), as shown in **Equation 5**. The fast and constant reaction rates in **Equation 5** can be calculated using the Arrhenius expressions shown in **Equation 6** and **Equation 7**, respectively. This oxidation aging model is employed in this study to evaluate and simulate the field aging gradient in the laboratory.

$$\log G^* = \log G_0^* + M \left( 1 - \frac{k_c}{k_f} \right) (1 - \exp(-k_f t)) + k_c M t \quad (5)$$

$$k_f = A_f \left( \exp \frac{-E_{af}}{RT} \right) \quad (6)$$

$$k_c = A_c \left( \exp \frac{-E_{ac}}{RT} \right) \quad (7)$$

Where,

$G^*$ : log-term aged binder shear modulus at 64°C and 10 rad/s (kPa);

$G_0^*$ : short-term aged binder shear modulus at 64°C and 10 rad/s (kPa);

$k_f$ : rate of fast reaction;

$k_c$ : rate of constant reaction;

$A_f$ : fast reaction frequency factor;

$A_c$ : constant reaction frequency factor;

$E_{af}$ : fast reaction activation energy (kJ/mol);

$E_{ac}$ : constant reaction activation energy (kJ/mol);

R: universal gas constant, or ideal gas constant (kJ/mol.K);

T: reaction temperature (K);

t: reaction time(s);

M: fitting parameter, material-based constant.

It should be mentioned that this aging model is a simplified temperature-based oxidation aging model. In reality, aging of asphalt material is also affected by the pressure distribution in pavement structure, and more importantly, there is the severe photo aging near the pavement surface due to the ultraviolet light.

## RESULTS AND DISCUSSION

### Change of Rheological Properties with Aging

Complex shear modulus and phase angle mastercurves constructed from the 4 mm DSR testing are presented as the average of three replicates for the extracted and recovered binders from the mixtures, as well as the 20 hr. PAV samples (original without RAP) during production in **Figure 1** (results for two binders are shown as representative examples). Complex modulus increases while phase angle decreases as materials age and the curves become flatter. Both the complex modulus and phase angle values for the different aging levels collapse together at high

frequencies (higher than  $10^5$  Hz at  $10^\circ\text{C}$ ). Generally, the two higher levels of aging (24 hr. at  $135^\circ\text{C}$  and 12 days at  $95^\circ\text{C}$ ) show similar complex modulus and phase angle values. The complex modulus and phase angle of 20 hr. PAV samples typically fall in between STA and 5 days at  $95^\circ\text{C}$  aging level, indicating 20 hr. PAV binder aging condition causes less aging of the asphalt material than 5 days at  $95^\circ\text{C}$  aging on mixtures.

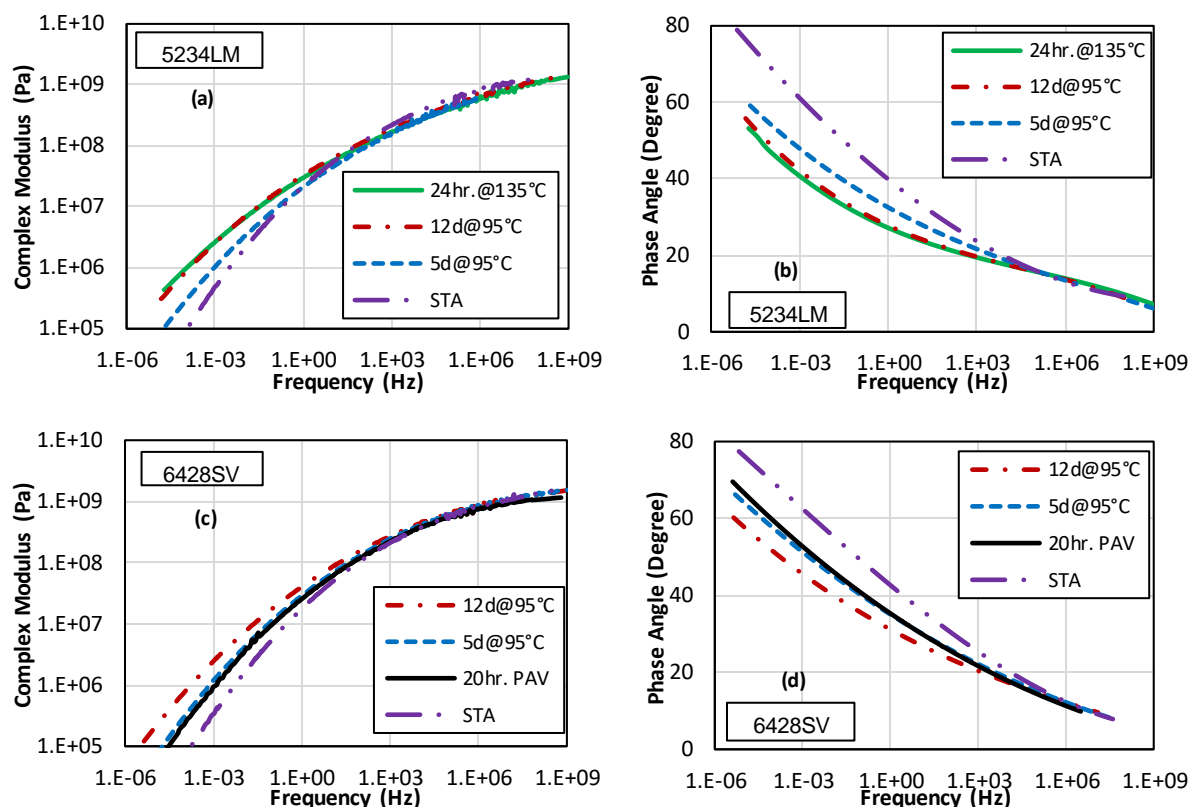


**FIGURE 1 Complex Shear Modulus and Phase Angle Master Curves for Representative Binder Samples with Different Aging Conditions (Reference Temperature:  $10^\circ\text{C}$ )**

**Figure 2** shows the average low temperature performance grade (PGLT), R-value,  $\Delta T_c$  and the binder G-R parameter, as well as the suggested threshold values for the study materials. Error bars show one standard deviation. Generally, PGLT, R-value, and G-R parameter increase with aging, while  $\Delta T_c$  decreases. There is a significant difference in the rheological indices between the STA and the three long-term mixture aging conditions (5 days, 12 days and 24 hours aging). The PGLT, R-value, and G-R parameter for 5834LM, 6428SV, and 7034LV after each aging condition are typically lower than other materials, while the  $\Delta T_c$  value for those binders after aging is higher, indicating better cracking performance compared with other materials. The  $\Delta T_c$  value and G-R parameter for these three binders after aging are typically within the cracking limit, while other binders exceed the cracking limit value after 12 days and 24 hours aging condition (5234LM and 5234LL exceed the cracking limit only after 5 days aging condition). The index values for binders from two virgin mixtures (6428SV and 7034LV) after 20hr. PAV aging are generally between the STA and the 5 days at  $95^\circ\text{C}$  aging condition.

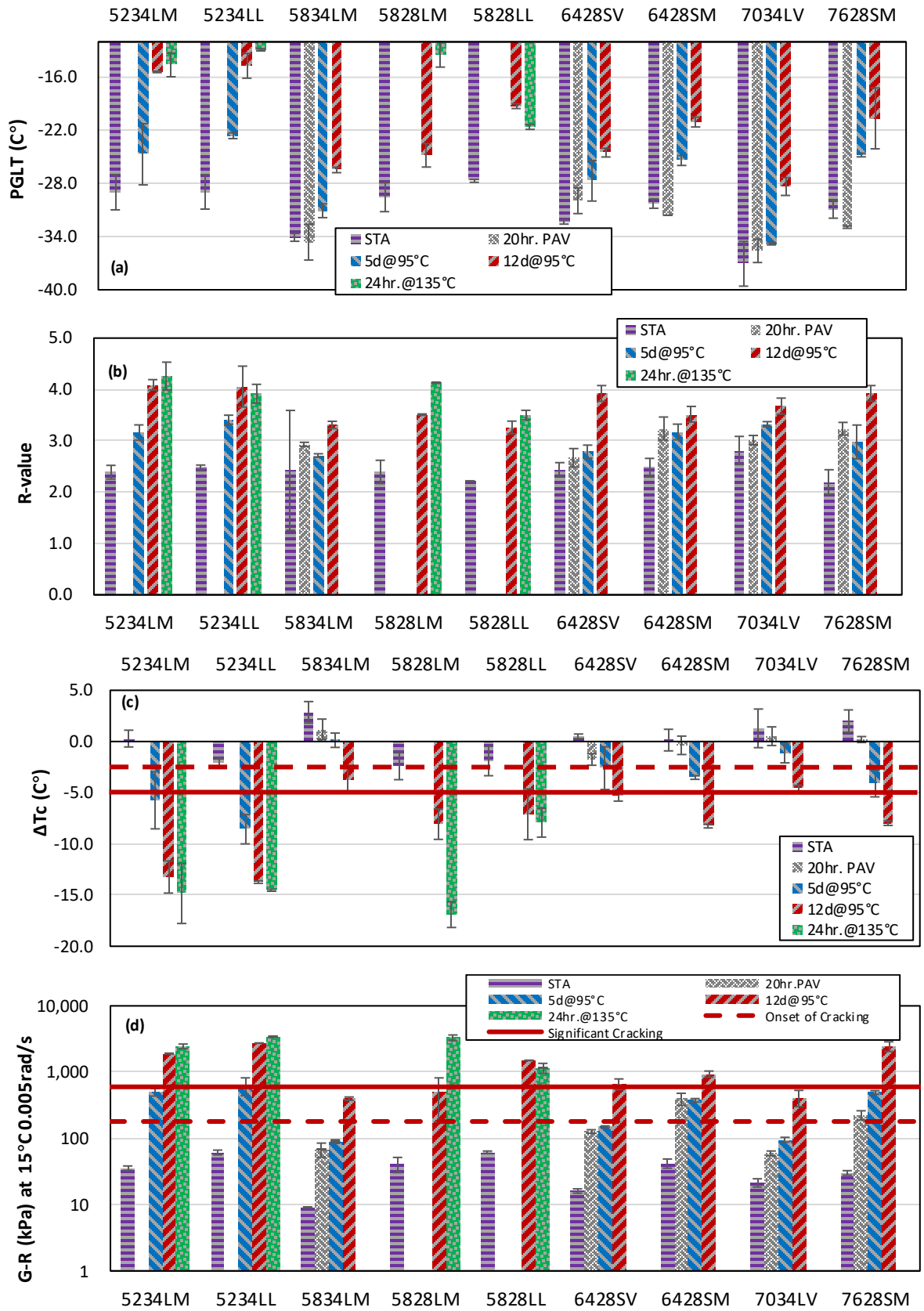


FIGURE 2 Rheological Indices: (a) PGLT; (b) R-value; (c)  $\Delta T_c$ ; (d) G-R Parameter

**Table 2** shows the change of the four rheological indices from STA condition (LTOAs minus STA). A bolded number indicates that the value of the rheological index exceeds the cracking limit value at that condition. The purpose of presenting this table is to evaluate the aging susceptibility of the different binders. As shown in **Figure 2**, the two binders with the softer performance grade (5234LM and 5234LL) and that with the largest difference between PGHT and PGLT (7628SM) generally show good cracking performance for STA. However, these binders have a greater change in the rheological indices with aging, as highlighted in **Table 2**, indicating higher aging susceptibility compared with the other materials. Also, some mixtures (e.g. 6428SV) have a similar change from STA to 5 days, but slower from 5 days to 12 days. From **Figure 2** and **Table 2**, 5234LM, 5234LL and 7628SM clearly show the worst cracking performance even only after 5 days aging condition.

**TABLE 2 Change in Rheological Index Values from STA Condition**

Rheological Indices		5234LM	5234LL	5834LM	5828LM	5828LL	6428SV	6428SM	7034LV	7628SM
PGLT	5d	4.3	6.3	3.0	--	--	4.6	4.9	2.3	6.1
	12d	13.6	14.2	7.6	4.7	8.4	7.8	9.2	8.7	10.3
	24hr	14.4	16.0	--	16.1	6.1	--	--	--	--
	PAV	--	--	-0.5	--	--	2.4	-1.3	1.5	-2.0
R-value	5d	0.8	0.9	0.3	--	--	0.3	0.7	0.5	0.8
	12d	1.7	1.6	0.9	1.1	1.0	1.5	1.0	0.9	1.7
	24hr	1.9	1.4	--	1.7	1.3	--	--	--	--
	PAV	--	--	0.5	--	--	0.2	0.8	0.2	1.0
$\Delta T_c$	5d	<b>-6.0</b>	<b>-6.6</b>	-2.7	--	--	-3.1	-3.7	-2.4	-6.1
	12d	<b>-13.5</b>	<b>-11.7</b>	-6.7	<b>-5.7</b>	<b>-5.2</b>	-5.9	<b>-8.4</b>	-5.8	<b>-10.0</b>
	24hr	<b>-15.1</b>	<b>-12.5</b>	--	<b>-14.5</b>	<b>-6.0</b>	--	--	--	--
	PAV	--	--	-1.2	--	--	-1.8	-0.4	-0.5	-0.2
G-R	5d	465	<b>569</b>	81	--	--	133	333	74	463
	12d	<b>1872</b>	<b>2684</b>	390	457	<b>1441</b>	<b>651</b>	<b>896</b>	394	<b>2428</b>
	24hr	<b>2421</b>	<b>3363</b>	--	<b>3275</b>	<b>1093</b>	--	--	--	--
	PAV	--	--	59	--	--	111	354	38	195

The  $\Delta T_c$  and G-R parameter evaluate the ability of the binder to resist the thermal cracking and durability (block) cracking, respectively. **Figure 3** provides a way to combine these two criteria and evaluate the thermal and durability cracking susceptibility of the binders after different aging conditions together. The two red dashed lines represent the cracking warning values for  $\Delta T_c$  and G-R parameter respectively, while the solid red lines represent the cracking limit values for  $\Delta T_c$  and G-R parameter. The area surrounded by the two dashed lines at the bottom right of the plot, labelled as the safe zone, means that the binders have adequate capability under intermediate and cold temperature to resist cracking. Generally, no cracking problems should be expected when the  $\Delta T_c$  and G-R parameter of the binders fall into this

“safe zone” area. However, if the points fall into the failure zone surrounded by the two solid lines at the top left of the plot, it indicates that the binders have a high susceptibility to both thermal and durability (block) cracking since both  $\Delta T_c$  and G-R parameter values of the binder samples exceed the cracking limit values.

The STA condition binders generally fall into the safe zone, which means that typically no cracking problems are expected. For 5834LM and 7034LV, after 5 days aging, the points are located in the safe zone and even after 12 days aging condition, the  $\Delta T_c$  value and G-R parameter are still within the cracking limits. However, 5234LM, 5234LL, 5828LM, 5828LL, and 7628SM after 12 days and 24 hours aging condition, fall into the failure zone, which means that there may be significant cracking problems based on the  $\Delta T_c$  and G-R criteria.

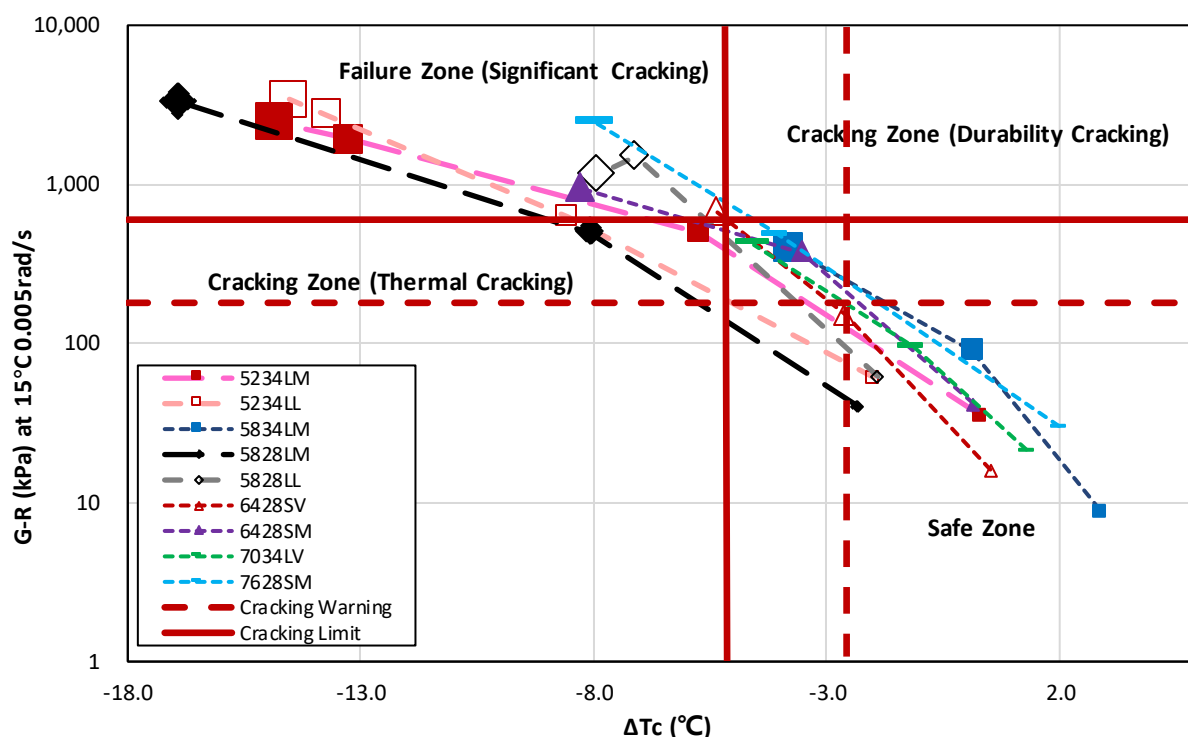


**FIGURE 3 Combination of  $\Delta T_c$  and G-R Criteria (marker size increases with increase of aging conditions; 20 hr. PAV not included)**

### Aging Gradient (Field Cores)

In this section, the DSR test results for the binder samples extracted and recovered from field cores are compared with those recovered from the laboratory aged mixtures. This data is available for four mixtures: 5234LM, 5234LL, 5828LM, and 5828LL.

Complex shear modulus and phase angle mastercurves constructed from the DSR testing are presented as the average of three replicates in **Figure 4** (results for one binder shown as an example). Generally, complex modulus and phase angle of the binder samples extracted from the bottom layer (layer 3) are similar to the STA condition. The complex modulus of the binder samples extracted from the top layer (layer 1) is clearly higher than the STA condition but lower than 5 days aging, while phase angle is lower than STA but higher than 5 days aging.

The complex modulus and phase angle of layer 2 is in between layer 1 and layer 3, illustrating the aging gradient within the pavement structure in the field.

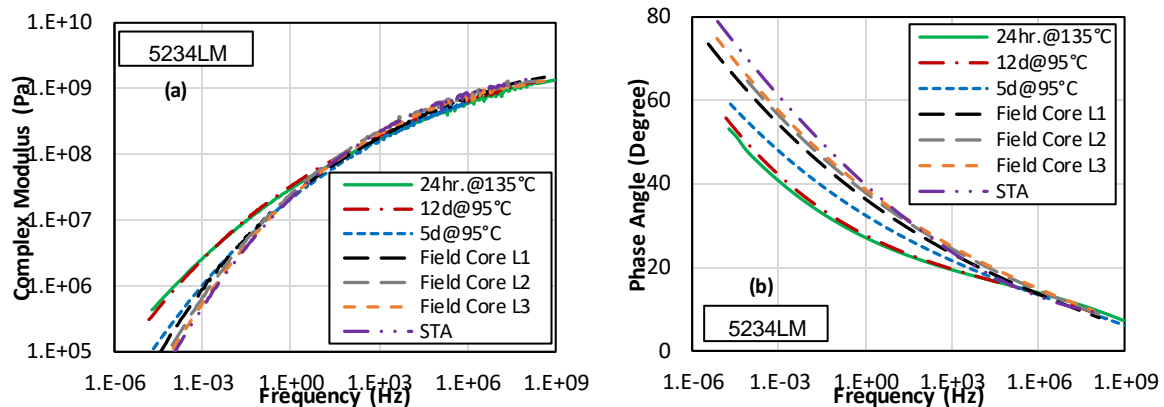


**FIGURE 4 Comparison of the Complex Shear Modulus and Phase Angle Master Curves between the Mixture Aging Conditions with Field Cores (Reference Temperature: 10°C)**

**Figure 5** shows the average PGLT, R-value,  $\Delta T_c$  value and G-R parameter for the binder samples extracted and recovered from the four mixtures and the corresponding field cores, respectively. Error bars show one standard deviation. Generally, the PGLT, R-values,  $\Delta T_c$  values and G-R parameters of the field cores with three layers are in between the STA and 5 days aging condition. With the increase of the pavement depth from layer 1 to layer 3, PGLT, R-value and G-R parameter decrease, while  $\Delta T_c$  value increases, showing the aging gradient within the pavement structure in the field.

The  $\Delta T_c$  value for the layer 1 and layer 2 generally exceeds the cracking warning limit, indicating the thermal cracking potential of the top layers. The G-R parameter for the top layer of 5234LL and 5828LL exceeds the cracking warning limit, indicating durability cracking (non-load associated) potential for the top layer.

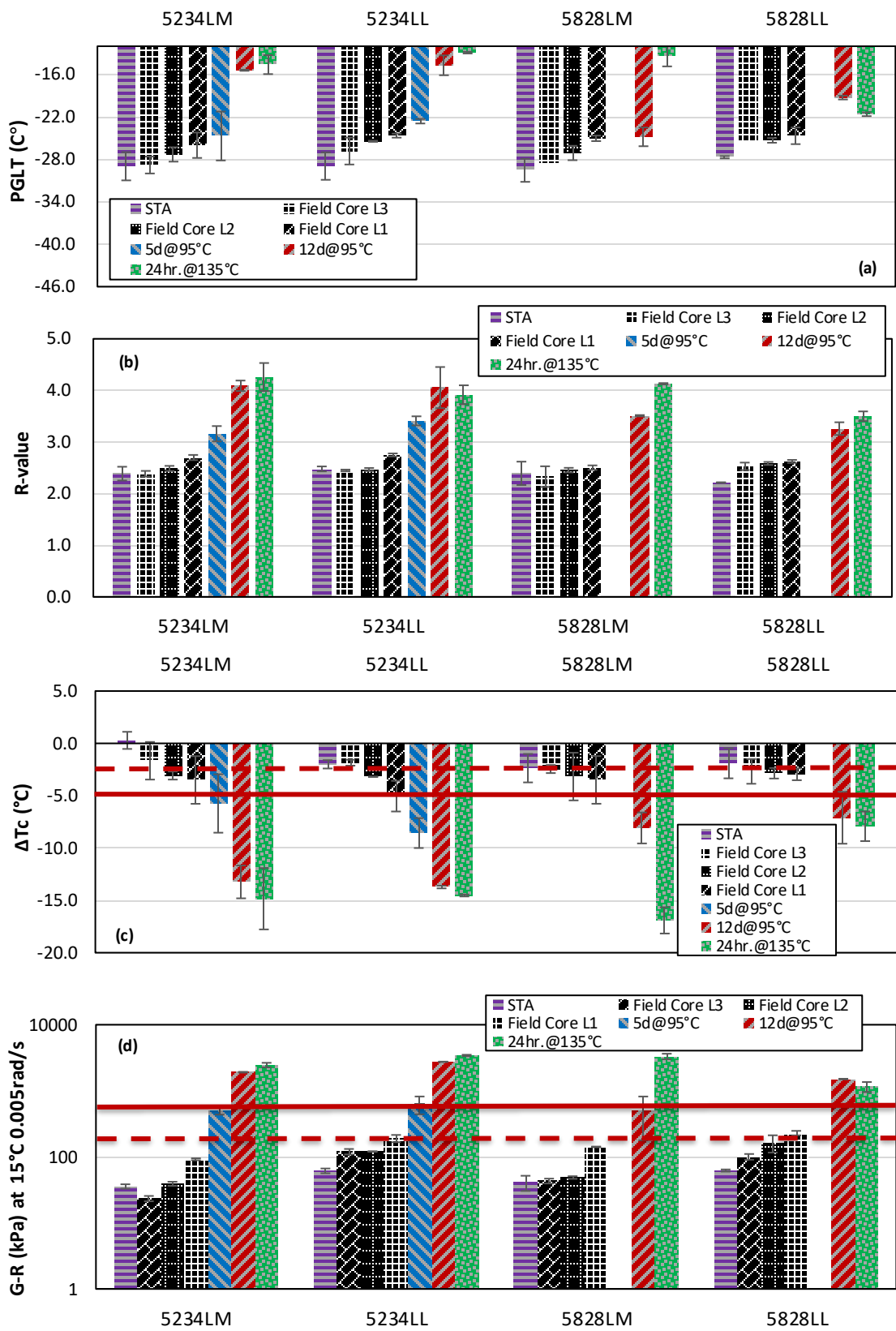


**FIGURE 5 Comparison of the Rheological Indices: (a) PGLT; (b) R-value; (c) ΔTc; (d) G-R Parameter between the Mixture Aging Conditions with Field Cores**

**Figure 6** shows how the binder Glover-Rowe (G-R) parameter changes with pavement depth for the binder samples extracted from the field cores (three layers). The mid-depth location of each layer (6.35mm for layer 1; 19.05mm for layer 2; 31.75mm for layer 3) is selected as the representative depth to reflect the performance of each layer. Error bars show one standard deviation. Previous studies (23,24) have shown that below 50 mm from the surface, asphalt material does not age significantly. Therefore, 60 mm is selected as the representative depth to represent the behaviour of asphalt layers below 50 mm, indicating there is no additional aging experienced for the asphalt material below this depth after STA (during production).

The rate of field aging within the first inch of the pavement is much faster than the layers below it for all four mixtures. Also, the change in G-R from one layer to the next is not the same for all four binders. It is well-known that the different factors, such as temperature gradient, air void distribution, and aging kinetics affect the aging in the field (25). As shown in the legend, the average air void content of those four mixtures (field cores) are not same. The effect of air void on the aging kinetics can be clearly seen on 5828LM. From **Figure 6**, 5828LM shows the largest difference in G-R between layer 1 and layer 2, however, the G-R parameter for 5828LM does not change significantly below layer 2. One reason is that 5828LM has the lowest air void, this restricts the rate of oxidation due to lower oxygen availability, so that the aging of 5828LM is mostly concentrated on the top layer. Then, as observed from the DSR test results, different binders have different aging susceptibility (rate), the aging kinetics is also based on the individual binder sample. Comparing the trend of change in G-R parameter with increase of depth for 5234LM with 5234LL and 5828LM with 5828LL (each pair has the same base (virgin) binder), the presence of different RAP content distinctly shows the impact on how the aging kinetics change with change of pavement depth. The difference in G-R parameters between the three layers observed here reflects the complexity of the aging in field.

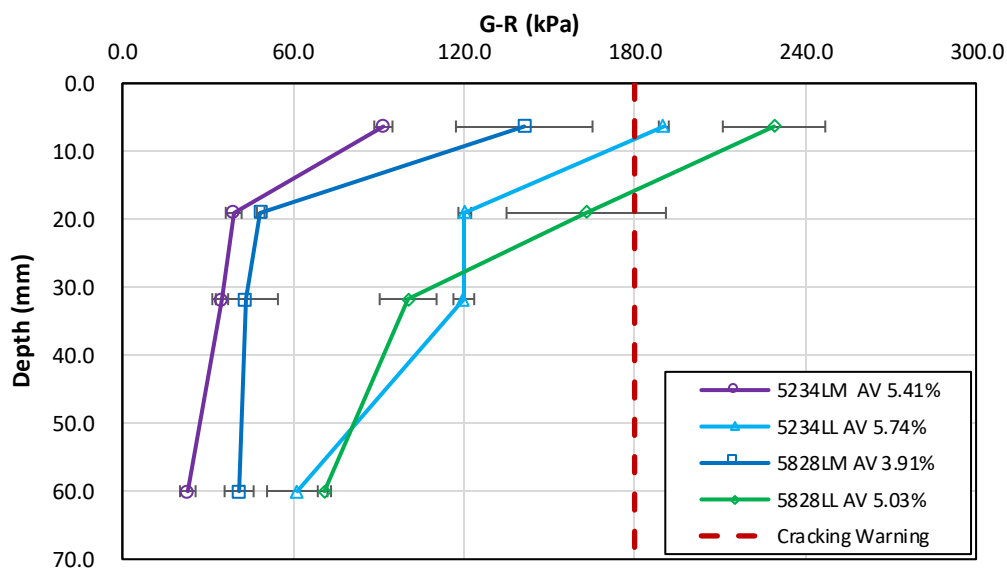


**FIGURE 6 Change of Glover-Rowe (G-R) Parameter with Pavement Depth**



### Quantitative Simulation of Aging Gradient using Laboratory Conditioning Methods

The oxidation aging model developed from the NCHRP 09-54 project is generally used to predict the change of binder property with aging (laboratory aging duration at 95°C), as shown in **Equation 5**. This oxidation aging model is employed in this study to correlate the laboratory conditioning methods with field aging durations, as well as quantitatively simulate and evaluate the aging gradient in the field.

**Table 3** presents the values of the calibrated oxidation aging model parameters in **Equations 5-7**. The universal values of the  $k_f$  and  $k_c$  parameters are obtained from a least mean square error optimization of the data obtained from the calibration binders (the binders extracted and recovered from the laboratory aged mixtures with STA, 5 and 12 days at 95°C aging conditions). After optimizing the  $k_f$  and  $k_c$  parameters, the material-dependent  $M$  values were determined by conducting least square error optimizations for the individual binders. It should be noted that  $M$  accounts for mix-specific aging kinetics; higher  $M$  values indicate greater oxidation susceptibility. By comparing the  $M$  value in **Table 3**, the two binders with the softer performance grade generally show a higher aging rate as compared with other two binders, consistent with the results from the DSR data. Also, comparing the  $M$  value of 5234LM with 5234LL and 5828LM with 5828LL, the higher RAP content results in a lower  $M$  value (slower aging rate).

**TABLE 3 Calibrated Model Coefficients**

Binder ID	$A_f$	$E_{af}$ (kJ/mol)	$A_c$	$E_{ac}$ (kJ/mol)	$R$ (kJ/mol.K)	$T$ (K)	$k_f$	$k_c$	$M$
5234LM	1.2E+13	98.20	3.8E+07	70.01	0.008	368.15	0.41	0.05	0.89
5234LL									0.83
5828LM									0.74
5828LL									0.70

With the calibrated model coefficients above, the laboratory aging durations corresponding with the field aging durations of different layers for the field cores can be back-calculated from **Equation 5**. The calculated results are shown in **Table 4**. The lab aging durations for the same layer vary with the binders, representing the disparate aging kinetics of those binders in the field. The binders with the softer grade clearly show the higher aging rate with the longer laboratory aging durations, as shown in **Table 4**.

Comparing the average laboratory aging durations for those three layers, the aging rate of asphalt material within the first layer is approximately 1.5 times faster than the second layer and 3 times faster than the third layer. With this data, 5 days of mixture aging in the lab appears to simulate around 8 years field aging for the top 12.5 mm layer based on New Hampshire climate condition, while 12 days can simulate approximately 20 years, which typically covers the design service life of the asphalt pavement. The 20 hr. PAV appears to simulate less than 8 years field aging in New Hampshire, indicating that current 20 hr. PAV binder aging method is not adequate to capture the long-term performance in New Hampshire.

**TABLE 4 Laboratory Aging Durations Corresponding with the Field Aging Duration**

Layers (Top to Bottom)	Laboratory Aging Duration (hour)				
	5234LM	5234LL	5828LM	5828LL	Average
Layer 1	62	54	48	46	52
Layer 2	45	30	22	37	33
Layer 3	15	25	12	19	18

The results from the back-calculation of the laboratory aging durations here can be used to correlate the laboratory conditioning methods with the field aging durations (pavement service life), and quantitatively simulate the field aging gradient in the laboratory, providing a way to evaluate the long-term performance of the asphalt binders in the laboratory, and quantitatively estimate and compare the aging kinetics with different binders, as well as with pavement depth. The benefits are:

- The general method described here can be used to more accurately simulate and represent the field aging in the laboratory.
- The correlation between the laboratory conditioning methods with the field aging durations provides agencies a way to select the proper laboratory conditioning time based on the desired equivalent field aging durations to evaluate the change of material performance over the designed pavement service life.
- By calibrating the aging model using DSR data for the binders with different aging conditions, the aging susceptibility (M value) of the binders can be determined, which is helpful in evaluating the long-term performance of the asphalt binders. This, in combination with the material properties in STA condition is useful for agencies to select the appropriate material and design mixtures with confidence that the pavement can avoid significant cracking damage for a given period of time.
- The combination of **Table 4** and **Figure 6** can be used to evaluate cracking potential of the asphalt pavement. Both clearly show how the aging kinetics (rate) of asphalt binders change with change of pavement depth. Also, the results from **Table 4** and **Figure 6** can be used in preservation, maintenance and rehabilitation decisions. Agencies can choose the best time to apply preservation treatments based on the correlation between the laboratory conditioning methods and the field aging durations evaluated in **Table 4**, and determine the appropriate milling depth of asphalt courses based on the results from **Figure 6**.

## SUMMARY AND CONCLUSIONS

The objective of this study is to correlate laboratory conditioning methods with field aging by evaluating how the rheological parameters of asphalt binders evolve over time, as well as how the aging changes with pavement depth. Loose mixtures are aged in the lab (5 and 12 days aging at 95°C, as well as 24 hours at 135°C) and recovered binder rheological properties are compared with those from different layers of field cores. The virgin binder results with 20 hours PAV aging are also included in the analysis. Binder testing is conducted using a dynamic shear rheometer (DSR) with 4mm parallel plate geometry over a wide range of frequencies and

temperatures. Numerous rheological parameters are calculated to evaluate changes with aging: PGLT, R-value, G-R parameter and  $\Delta T_c$ . The field aging gradient is evaluated, the laboratory conditioning durations corresponding with the field aging durations at different depth of pavement are calculated. The following conclusions based on New Hampshire mixtures and climate conditions can be drawn from the results of the testing and analysis:

1. The linear viscoelastic properties of binders with 24 hr. at 135°C and 12 days at 95°C aging are similar.
2. With increase of aging condition, the rheological indices of asphalt binders, PGLT, R-value, and G-R parameter increase, while  $\Delta T_c$  decreases. The two virgin binders show both good thermal and durability cracking performance at each aging condition. The two binders with the softer performance grade (5234LM and 5234LL) and that with the largest difference between PGHT and PGLT (7628SM) show higher aging susceptibility.
3. The binder samples extracted from the field cores illustrate the aging gradient in field, with the top layers (25mm) aged the most. The aging rate of asphalt material within the top 12.5 mm layer is approximately 1.5 times of the middle 12.5 mm layer, and 3 times of the bottom 12.5 mm layer.
4. 5 days at 95°C aging can simulate around 8 years field aging (in New Hampshire) for the top 12.5mm pavement, while 12 days at 95°C aging can simulate approximately 20 years field aging. The 20 hours PAV binder conditioning protocol simulates less than 8 years field aging.

The results from this study benefit highway agencies as follows:

1. The correlation between the laboratory conditioning methods with the field aging durations provides agencies a way to select the proper laboratory conditioning time based on the desired equivalent field aging durations to evaluate the change of material performance over the designed pavement service life.
2. By calibrating the oxidation aging model using DSR data, the aging susceptibility of the binders can be determined. This can be used in combination with the STA properties to select the appropriate material and design mixtures to avoid significant cracking damage for a given period of time.
3. The method included in this study to evaluate the aging gradient within the pavement structure can also be used to detect the thermal, block and top-down fatigue cracking potential of the asphalt material. This will help agencies to determine the best time and ideal milling depth to maintain and rehabilitate their pavements.
4. The general methodology described in this study provides agencies a way to optimize the laboratory conditioning durations and evaluate the performance of asphalt material with respect to pavement life (time), and depth (location) within the pavement structure.

## **FUTURE WORK**

Future work and analysis are planned to continue testing the binder sampled during production and extracted from field cores to further evaluate and correlate the different laboratory aging protocols with actual field aging durations. Other laboratory condition methods in addition to

the methods used in this study will be also evaluated in future. The correlation between the different properties of aged asphalt mixtures and binders, as well as their relationship with the cracking performance of field core samples and field performance should be further investigated. Additional tests that evaluate the binders beyond the linear viscoelastic response (e.g. the Linear Amplitude Sweep (LAS) and Multiple Stress Creep Recovery (MSCR) test), as well as the chemical analytical test (e.g. Fourier Transform Infrared (FTIR) test) are being investigated for inclusion in comprehensive evaluation of the change of asphalt binders' properties with aging. Continued sampling of field cores for study mixtures/binders to better define the aging gradient with depth is also needed. The results from this study will be used in the advanced performance prediction models, such as AASHTOWare Pavement ME and FHWA's FlexPAVE to more precisely simulate and predict the pavement response while taking the aging gradient into account.

### **ACKNOWLEDGEMENT**

The authors would like to acknowledge New Hampshire Department of Transportation (NHDOT) for sponsoring this study and the University of New Hampshire Center for Infrastructure Resilience to Climate (UCIRC).

### **AUTHOR CONTRIBUTION**

The authors confirm contribution to the paper as follows: study conception and design: J.E. Sias, E.V. Dave, and R. Zhang; data collection: R. Zhang; all authors contributed to analysis and interpretation of results, manuscript preparation, and review.

### **REFERENCES**

1. AASHTO T 240. "Standard Method of Test for Effect of Heat and Air on a Moving Film of Asphalt Binder (Rolling Thin-Film Oven Test)". American Association of State Highway and Transportation Officials.
2. Jemison, H. B., R. R. Davison, C. J. Glover, and J. A. Bullin. "Evaluation of Standard Oven Tests for Hot-Mix Plant Aging". Transportation Research Record 1323, TRB, National Research Council, Washington, D.C., 1991, pp. 77–84.
3. Vassiliev, N.Y., R.R. Davison, and C.J. Glover. "Development of a Stirred Airflow Test Procedure for Short-Term Aging of Asphaltic Materials. Bituminous Binders", No. 1810, 2002, pp. 25-32.
4. Cominsky, R.J., Huber, G.A., Kennedy, T.W., Anderson, M. "The Superpave Mix Design Manual for New Construction and Overlays". Strategic Highway Research Program National Research Council. Washington, DC 1994.
5. Glover C.J., Martin, A.E., Chowdhury, A., Han R. "Evaluation of Binder Aging and Its Influence in Aging of Hot Mix Asphalt Concrete: Literature Review and Experimental Design". 2008. Technical Report.

6. Bell, C. A., Y. AbWahab, R. E. Cristi, and D. Sognovske. "Selection of Laboratory Aging Procedures for Asphalt-Aggregate Mixtures." Washington, DC: Strategic Highway Research Program, National Research Council, 1994.
7. Harrigan, E. T. "Simulating the Effects of Hot Mix Asphalt Aging for Performance Testing and Pavement Structural Design". Final Report, National Cooperative Highway Research Program, Research Results Digest 324, National Research Council, Washington, D.C., 2007.
8. Arega, Z. A., A. Bhasin, and T. De Kesel. "Influence of Extended Aging on the Properties of Asphalt Composites Produced Using Hot and Warm Mix Methods," *Construction and Building Materials*, Vol. 44, 2013, pp. 168-174.
9. Yousefi Rad, F., M. D. Elwardany, C. Castorena, and Y. R. Kim, "Investigation of Proper Long-Term Laboratory Aging Temperature for Performance Testing of Asphalt Concrete," *Construction and Building Materials*, Vol. 147, 2017, pp. 616-629.
10. Kim, R. Y., Castorena, C., Elwardany, M., Yousefi Rad, F., Underwood, S., Gundha, A., Gudipudi, P., Farrer, M. J., Glaser, R., R. "Long-term Aging of Asphalt Mixtures for Performance Testing and Prediction", Final Report, NCHRP 09-54. 2018.
11. Kim, R. Y., Hintz, C., Yousefi Rad, F., Underwood, S., Farrer, M. J., Glaser, R., R., "Long-term Aging of Asphalt Mixtures for Performance Testing and Prediction" Interim Report, NCHRP 09-54, 2013.
12. Elwardany, M. D., F. Yousefi Rad, C. Castorena, and Y. R. Kim. "Evaluation of Asphalt Mixture Laboratory Long-Term Ageing Methods for Performance Testing and Prediction," *Road Materials and Pavement Design*, Vol. 18, No. 1, 2017(b), pp. 28-61.
13. Zhang, R., Sias, J. E., Dave, E. V., & Rahbar-Rastegar, R. "Impact of Aging on the Viscoelastic Properties and Cracking Behavior of Asphalt Mixtures". *Transportation Research Record*. 2019. <https://doi.org/10.1177/0361198119846473>
14. Blankenship, P.B., Anderson, M. A., King, G. N., and Hanson, D. I. "A Laboratory and Field 26 Investigation to Develop Test Procedures for Predicting Non-Load Associated Cracking of Airfield HMA Pavements, Airfield Asphalt pavement technology Program, 2010.
15. Petersen, J.C. Glaser, R. "Asphalt oxidation mechanisms and the role of oxidation products on age hardening revisited", *Road Mater. Pavement Des.* 2011. 12 (4) 795–819.

16. Glaser, R. Schabron, J. Turner, T. Planche, J.P. Salmans, S. Loveridge, J. "Low temperature oxidation kinetics of asphalt binders", *Transp. Res. Rec.*2013. 2370 63–68.
17. Yao, Z., Lu, Y., Gong, M., Tang, Z., Xue, J., Zhang, X. "Nanoindentation Characterization of Aging Gradient of Mastic in Asphalt Mixtures". *Construction and Building Materials*. 2019. Volume 214. 187-195
18. Glaser, R.R. Turner, T.F., Loveridge, J.L. Salmans, S.L., Planche, J.P. "Fundamental Properties of Asphalts and Modified Asphalts III Product". 2015. Technical White Paper.
19. Sui, C., Farrar, M. J., Harnsberger, P. M., Tuminello, W. H., & Turner, T. F. "New Low-Temperature Performance-Grading Method: Using 4-mm Parallel Plates on a Dynamic Shear Rheometer". *Transportation Research Record*, 2011, 2207(1), 43–48. <https://doi.org/10.3141/2207-06>
20. Anderson, M., G. King, D. Hanson, and P. Blankenship, "Evaluation of the Relationship Between Asphalt Binder Properties and Non-Load Related Cracking" *Journal of the Association of Asphalt Paving Technologists*, Vol. 80, 2011, pp. 615-661
21. Rowe, G. M. Prepared Discussion for the AAPT paper by Anderson et al.: "Evaluation of the Relationship between Asphalt Binder Properties and Non-Load Related Cracking", *Journal of the Association of Asphalt Paving Technologists*, Vol. 80, 2011, pp. 649-662.
22. Glaser, R., T. F. Turner, J. L. Loveridge, S. L. Salmans, and J. P. Planche. "Fundamental Properties of Asphalts and Modified Asphalts", Volume III. Quarterly Technical Report, Federal Highway Administration (FHWA) Contract No. DTFH61-07-D-00005, October 2013.
23. Luo, X., Gu, F., & Lytton, R. L. (2015). "Prediction of Field Aging Gradient in Asphalt Pavements". *Transportation Research Record*, 2507(1), 19–28. <https://doi.org/10.3141/2507-03>
24. Koohi, Y., Lawrence, Y.J., Luo, R., Lytton, R.L. "Complex Stiffness Gradient Estimation of Field-Aged Asphalt Concrete Layers Using the Direct Tension Test". 2012, [https://doi.org/10.1061/\(ASCE\)MT.1943-5533.0000466](https://doi.org/10.1061/(ASCE)MT.1943-5533.0000466)
25. Woo, W. J., Chowdhury, A., and Glover, C. J. "Field aging of unmodified asphalt binder in three texas long-term performance pavements." *Transportation Research Record* 2051, Transportation Research Board, Washington, DC, 2008, 15–22.

## **Appendix D Paper 4 (Chapter 7)**

### **Development of New Performance Indices to Evaluate the Fatigue Properties of Asphalt Binders with Aging**

Runhua Zhang<sup>a\*</sup>; Jo E. Sias<sup>b</sup>; Eshan V. Dave<sup>c</sup>

\*Civil and Environmental Engineering, University of New Hampshire

Durham, NH 03824, United States

Tel: 603-285-8739; Email: rz1015@wildcats@unh.edu

Word count: 6,900 words

## 1. Introduction

Fatigue Cracking is a major concern for asphalt pavements since it affects ride quality and allows water to infiltrate from the surface to underlying base and soil layers, decreasing the serviceability of the pavement, elevating the chance of road accidents and requiring considerable amount of public funds on more frequent maintenance or rehabilitation. Fatigue cracking is generally caused by repetitive stresses and strains induced from traffic loading and environmental factors, appearing in the form of longitudinal and eventual alligator cracking on the surface of the pavement (Ayazi et al., 2017; Behbahani et al., 2017; Ziari et al., 2014&2018). Fatigue behavior of asphalt mixtures is typically affected by many factors such as loading, environmental conditions, pavement structure, mixture characteristics, binder and aggregate characteristics. It is reported that among the mixture components, binder plays the most important role in fatigue behavior of asphalt mixtures (Bahia et al., 2001; Anderson et al., 2001; Ameri et al., 2016; Ziari et al., 2017). Hence, it is important to find a valid test method and the corresponding parameters to efficiently and effectively capture the fatigue properties of asphalt binders.

Significant research efforts have been dedicated to find a method for evaluating the fatigue properties of asphalt binders in recent decades. The  $G^*\sin\delta$  fatigue index was initially developed as a fatigue criterion during the SHRP program. However, it has received considerable criticism as it does not account for the repeated traffic and does not capture the damage accumulation generated in the binder (Anderson et al., 2001; Zhou et al., 2012). During the National Cooperative Highway Research Program (NCHRP) 9–10 Project, the time sweep test performed using a Dynamic Shear Rheometer (DSR) was introduced to better evaluate the fatigue properties of asphalt binder. But the main drawback of this method is its long testing time (Anderson et al., 2001; Bonnetti et al., 2002; Martono et al., 2007). To address this issue, additional investigations into a more time efficient asphalt binder fatigue test method led to the Linear Amplitude Sweep (LAS) test (Planche et al., 2001) introduced by Bahia et al. (2010). The test analysis is based on Viscoelastic Continuum Damage (VECD) principles, which have been successfully used for characterizing fatigue properties of asphalt mixtures by many researchers (Daniel et al., 2002&2004; Sabouri et al., 2015; Wang et al., 2017; Zhang et al., 2019). Studies (Zhou et al., 2012; Clopotel et al., 2012) have also shown that the LAS test can be used as an effective test method to evaluate the binder fatigue properties and has been shown to correlate fairly well with the Long-Term Pavement Performance (LTPP) field fatigue cracking data (Hintz et al., 2011).

Although the LAS test has been positively received for evaluation of the fatigue properties of asphalt binders, researchers recently have found some challenges with using the current performance parameters measured from the LAS test to investigate the effect of asphalt modifiers on binder fatigue behavior (Sabouri et al., 2018) and the aging effect on binder's



long-term performance (Tabatabaee et al., 2014; Zhou et al., 2017). Using the current performance parameters, Sabouri et al. (2018) reported that all the (SBS) modified binders show better fatigue performance than the neat binders at lower strain levels, while the trend is reversed at the higher strain levels. Studies from Teymourpour et al. (2014) and Zhou et al. (2017) have shown that the fatigue properties of asphalt binders is significantly improved with increase of the binder aging condition (even after severe 40 and 60 hours PAV aging), which is contradictory with expectations. With these raised challenges for the current parameters as discussed above, the primary objective of this study is to explore and develop the new performance parameters to better understand and evaluate the fatigue properties of asphalt binders by incorporating the aging effects.

## **2. Methodology**

### ***2.1 Laboratory Conditioning Method***

The accelerated laboratory conditioning (aging) method is of great importance to simulate the aging of asphalt materials in the field (Hveem et al., 1963; Vassiliev et al., 2002; Cominsky et al., 1994; Glover et al., 2008; Bell et al., 1994; Harrigan et al., 2007; Kim et al., 2018; Elwardany et al., 2017; Blankenship et al., 2010; Zhang et al., 2019). The recent findings of the NCHRP 09-54 project recommends conditioning the loose mix asphalt at 95°C as an optimal temperature considering the relationship between binder rheology and chemistry to simulate long term aging in the field (Kim et al., 2018). Also, as compared to aging of the compacted specimens (Harrigan et al., 2007), loose mixture aging produces uniform aging and reduces the aging time significantly (Blankenship et al., 2010; Elwardany et al., 2017; Kim et al., 2018). Because of these advantages, the NCHRP recommended 95°C for 5 (intermediate aging level) and 12 days (long-term aging level) were selected in this study and used on five plant produced mixtures which have already undergone short-term aging during production. Previous work (Zhang et al., 2019) has shown that 5 days at 95°C laboratory aging condition simulates approximately four years of field aging for the surface mixtures in the region where mixtures have been procured, while 12 days at 95°C laboratory aging simulates approximately 10 years of field aging.

### ***2.2 Laboratory Performance Tests***

#### ***2.2.1 Frequency and Temperature Sweep test***

The frequency and temperature sweep testing using a Dynamic Shear Rheometer (DSR) with a 4 mm plate was conducted in this study to measure the rheological characteristics of the asphalt binders (Glaser et al., 2015). This test covers a wide range of temperatures (-36°C to 30°C, usually in 3 degrees increments), and frequencies (15 frequencies from 100 rad/sec to

0.2 rad/sec), by using the appropriate strain level at each combination of test temperature and frequency. The isotherm tests are conducted from the coldest to the warmest temperature and from the highest to the lowest frequencies. The complex shear modulus and phase angle master curve are then constructed, and the binder Glover-Rowe (Rowe et al., 2011) parameter is calculated as shown in **Eq. 1**.

$$G - R = \frac{G^*(\cos\delta)^2}{\sin\delta} \quad (1)$$

Where  $G^*$  is the complex shear modulus at 15°C, 0.005rad/sec;  $\delta$  is the value of phase angle at 15°C, 0.005rad/sec. A lower G-R parameter indicates better capability to resist durability cracking. A limiting value of 180kPa is proposed for the onset of cracking, a second value of 600kPa is suggested for the development of significant cracking (block cracking) (Rowe et al., 2011).

Sui et al. (Sui et al., 2011) developed a method to calculate the critical temperatures determined by the S(t) and m-value that are generally measured from the BBR measurements directly from the 4 mm DSR test. Using this method, the  $\Delta T_c$  parameter can be then calculated from difference between the two critical temperatures, as shown in **Eq. 2**.

$$\Delta T_c = T(S) - T(m) \quad (2)$$

Where,

T(S): critical low temperature at which creep stiffness at 60 seconds,  $S(60) = 300$  MPa;

T(m): critical low temperature at which slope of creep stiffness curve at 60 seconds,  $m(60) = 0.300$ .

Asphalt Institute (Rowe et al., 2011; Anderson et al., 2011) suggests using  $\Delta T_c = -2.5^\circ\text{C}$  and  $\Delta T_c = -5.0^\circ\text{C}$  as threshold values for crack warning and cracking limit respectively.

### 2.2.2 Linear Amplitude Sweep (LAS) test

The LAS test evaluates the ability of asphalt binder to resist fatigue damage. This test is an oscillatory strain sweep test that generates damage to the binder by applying linearly increasing load amplitudes. The LAS test consists of two steps: first, a frequency sweep is performed in order to get information about undamaged material properties and evaluate the rheological characteristics of the binder. Second, the damage characteristics of the binder are measured employing a linear amplitude strain sweep test. In this study, frequency sweeps were conducted

at a strain amplitude of 0.1% with a range of frequencies from 0.2 to 30 Hz according to AASHTO TP101. The amplitude sweep test was done at a constant frequency of 10 Hz. The testing protocol consisted of applying a linearly increasing strain from zero to 30% over 3100 cycles of loading. All tests were conducted using a DSR device with an 8 mm diameter parallel plate and a 2 mm gap. Three replicates were run for each binder. The integrity ( $C(t)$ ) and damage accumulation ( $D(t)$ ) curve (fatigue law, also referred to as damage characteristic curve (DCC)) of the binder sample during the test is calculated by **Eq. 3-5**. The relationship between  $C(t)$  and  $D(t)$  can be fit to the power law, as **Eq. 5** shown.

$$C(t) = \frac{G^* \sin \delta(t)}{G^* \sin \delta_{initial}} \quad (3)$$

$$D(t) = \sum_{i=1}^N [\pi \gamma_0^2 (C_{i-1} - C_i)]^{\frac{\alpha}{1+\alpha}} (t_i - t_{i-1})^{\frac{1}{1+\alpha}} \quad (4)$$

$$C_{(t)} = C_0 - C_1 (D)^{C_2} \quad (5)$$

where  $G^*$  is the complex modulus;  $\delta$  is the phase angle;  $\gamma_0$  is the applied strain;  $\alpha$  is calculated from the frequency sweep test;  $t$  is test time. **Fig. 1** below shows the typical C-D plot determined from the LAS test.

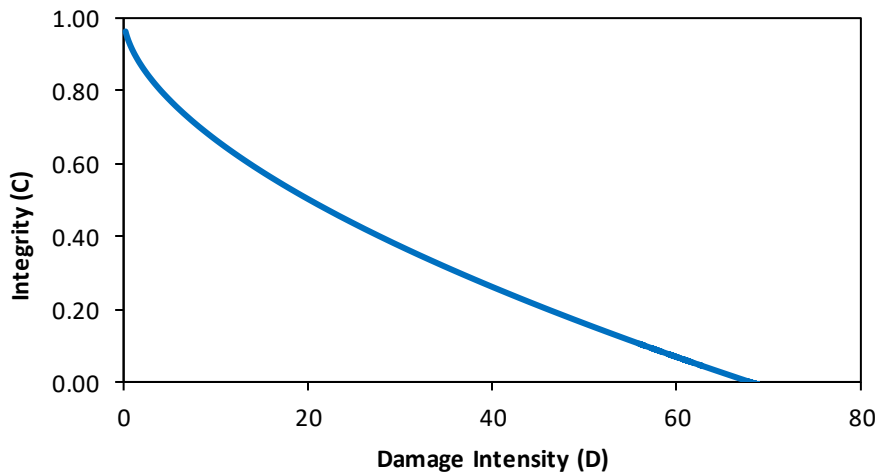


**Figure 1 Typical Damage Characteristic Curve (DCC) from LAS Test**

The number of cycles to failure is calculated using **Eq. 6-9**. The failure definition in LAS test in the current AASHTO TP101 is defined as 35% reduction in the initial modulus (Hintz et al., 2011).

$$N_f = A(r_{max})^B \quad (6)$$

$$A = \frac{f(D_f)^k}{k(\pi I_D C_1 C_2)^\alpha} \quad (7)$$

$$B = 2\alpha \quad (8)$$

$$D_f = 0.35 \left( \frac{C_0}{C_1} \right)^{\left( \frac{1}{C_2} \right)} \quad (9)$$

where  $A$  and  $B$  are VECD model coefficients that depend on the material characteristics,  $r_{max}$  is the applied strain,  $D_f$  is defined as damage at failure, which corresponds to a 35% reduction in  $G \cdot \sin \delta$ ;  $f$  is loading frequency (10Hz). With the measured  $A$  and  $B$  parameters from the LAS test,  $N_f$  vs. strain curve can be calculated following Eq. 6, and plotted in **Fig. 2**. Generally, “ $A$ ” parameter represents the material’s ability to keep its integrity during loading cycles and accumulated damage. This parameter is directly related to the storage modulus. In other words, as the storage modulus decreases through loading cycles, the  $A$  parameter decreases, which indicates the decreasing ability of the binder to maintain its integrity. The sensitivity of the asphalt binder to strain level is described by the  $B$  parameter. Higher absolute values of  $B$  indicate that the fatigue life decreases at a higher rate (steeper (negative) slope of the  $N_f$ -strain curve as shown in **Fig.2**) when strain level increases. In general, more fatigue resistant binders tend to have higher  $A$  values and lower absolute  $B$  values (Ameri et al., 2011).

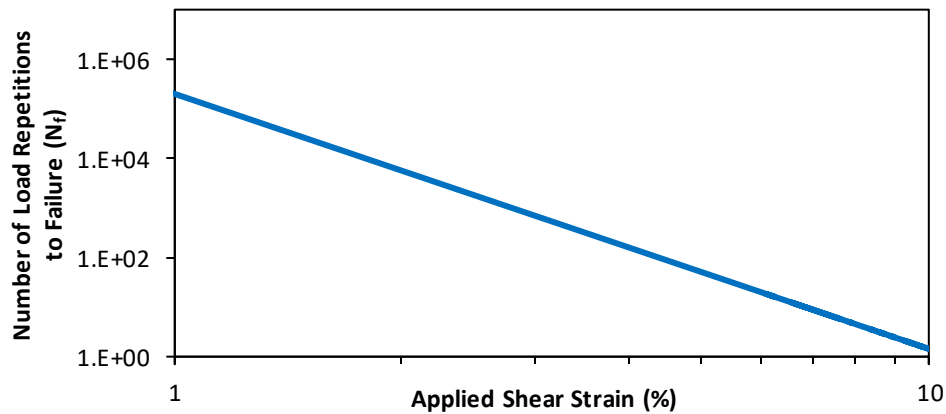


**Figure 2 Typical Fatigue Characterization ( $N_f$ -strain) Plot from LAS Test**

### 2.2.3 Direct Tension Cyclic Fatigue Test

The uniaxial fatigue test was performed in accordance with AASHTO TP 107 in a direct cyclic tension mode on the asphalt mixtures in this study, and the analysis is conducted using the Simplified Viscoelastic Continuum Damage (S-VECD) approach. The test is conducted on 130×100 mm specimens (110×38 mm for field cores) that are preconditioned with respect to binder performance grade at temperature equal to  $(\frac{PGHT-PGLT}{2} - 3^{\circ}C)$ . The test is conducted on four replicates each at a different strain level under cyclic tension and constant crosshead testing mode. The performance parameter  $D^R$  (average reduction in pseudo stiffness per loading cycle) and  $S_{app}$  (the accumulated damage when  $C$  (pseudo stiffness) is equal to  $1-D^R$ ) are used to estimate the ability of the mixtures to resist fatigue cracking (Sabouri et al., 2015; Wang et al., 2017).

### 2.3 Material

Table 1 below shows the summary information for the study mixtures (plant produced) and the corresponding binders extracted and recovered from these mixtures with different aging conditions (Recycled binder content is the ratio of the weight of recycled binder to the total binder weight). The mix ID is defined as follows: the first four-digit number indicates the original binder PG grade, the following letters indicate the nominal maximum aggregate size (NMAS) of 9.5mm “S” and 12.5mm “L”. The last letter represents the recycled binder content: “V” indicates no recycled binder, “M” indicates 14.8-18.9% recycled binder content, and “L” indicates 28.3% recycled binder content. The binders in mixture 7034LV and 7628SM are modified binders (styrene–butadiene–styrene (SBS) with aromatic oil (3%) for 7034LV and polyphosphoric acid (PPA) for 7628SM).

Field cores for two mixtures (5234LM FC and 5828LL FC; taken after four years in service) are also available in this study. They were cut into three layers (12.5mm each, as shown in **Fig.3**) and then the binders are extracted and recovered. The binder extraction is performed in accordance with AASHTO T 164, procedure 12, using a centrifuge extractor and toluene solvent. The asphalt binder is recovered based on ASTM D7906-14 using a rotary evaporator.

**Table 1 Mixture Types and Aging Levels**

Mixture ID	Virgin Binder Type	Total Binder Content (%)	Recycled Binder Content (%)	Testing/Analysis			
				STA	95°C@5days	95°C@12days	Field Cores (4 years)
5834LM	PG 58-34	5.4	18.5	✓	✓	✓	NA
6428SV	PG 64-28	6.4	0	✓	✓	✓	NA
6428SM	PG 64-28	6.3	18.5	✓	✓	✓	NA
7034LV	PG 70-34 (SBS Modified /Aromatic Oil)	5.8	0	✓	✓	✓	NA
7628SM	PG 76-28 (PPA Modified)	6.1	14.8	✓	✓	✓	NA
5234LM FC	PG 52-34	5.3	18.9	NA	NA	NA	✓
5828LL FC	PG 58-28	5.3	28.3	NA	NA	NA	✓



**Figure 3 Schematic of Cutting of the Field Cores (surface layer) for Binder Extraction and Recovery**

### 3. Result and Discussion

#### 3.1 Current Parameters from LAS Test

The A and B parameters, as well as the  $N_f$ -strain plot are the outputs of the LAS test that are currently used to evaluate the fatigue properties of asphalt binders. Fig. 4 below shows the result of the calculated A and B parameters for the five binders with various aging conditions, as well as the binder samples from the different layers in the field cores. Generally, binder 6428SM and binder 7628SM consistently show degradation of fatigue properties (both A and

B parameter decrease) as aging conditions increase. However, there is no consistent trend observed for change of A parameter with increase of conditioning levels for binder 5834LM and binder 6428SV, while 7034LV consistently increases with aging.

For the two binders extracted and recovered from the field cores, there is no clear trend observed for change of A parameter with increase of pavement depth (from L1 – L3). For binder 5828LL FC, the fatigue resistance in terms of A parameter decreases with increase of pavement depth. This observation is contradictory with common expectation of the aging gradient in the field.

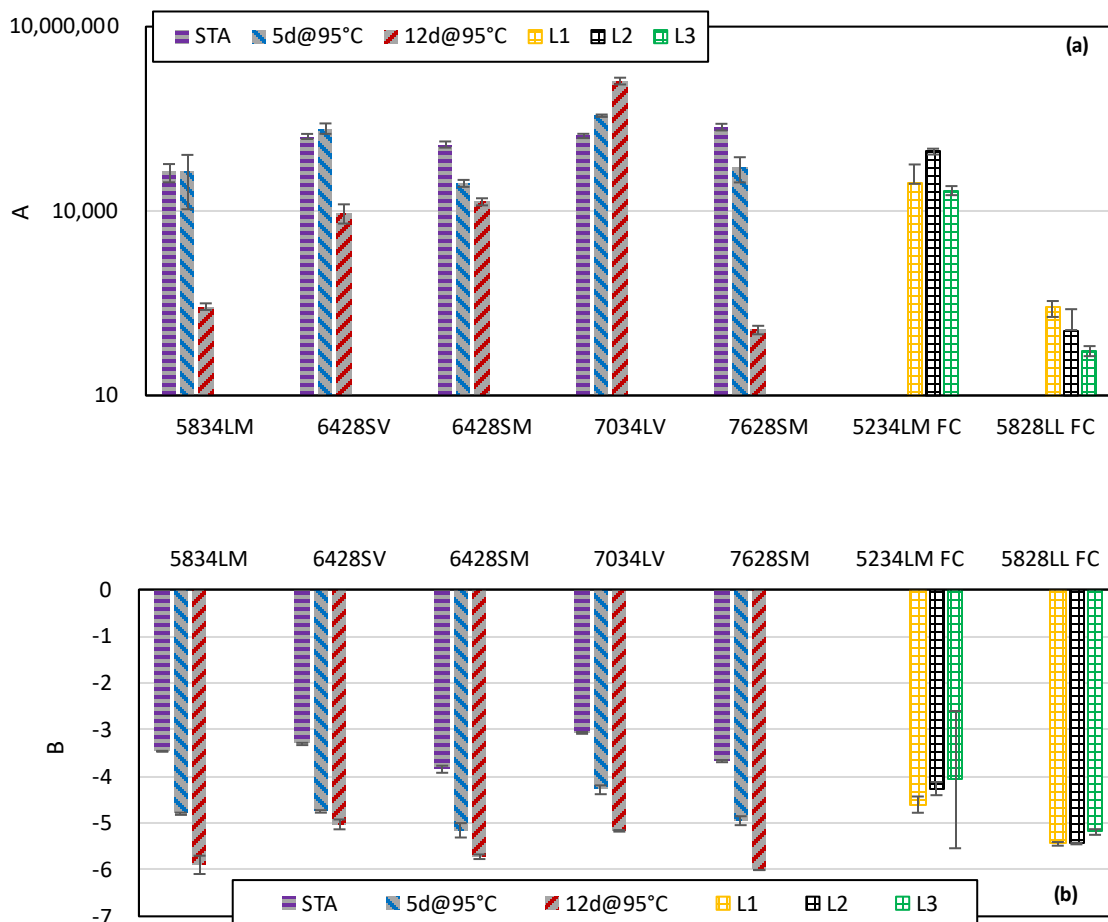


**Figure 4 Current a) A Value; b) B Value Calculated from LAS Test**

**Fig. 5** below shows examples of two  $N_f$ -strain plots (using binder 5834LM and 6428SV as examples). Binder 5834LM generally shows a lower  $N_f$  value after 12 days aging condition, while there is no clear trend for change of  $N_f$  value with increase of strain levels after STA and 5 days aging. Binder 6428SV shows higher  $N_f$  values after 5 and 12 days aging in the small strain range (lower than 0.5%). However, in the higher strain range (over 1.1%), STA shows the highest  $N_f$  value. Similar results have also been observed for binder 7628SM and field cores

(5234LM FC and 5828LL FC), this is due to the inconsistent trend for A parameter with increase of aging condition and pavement depth.

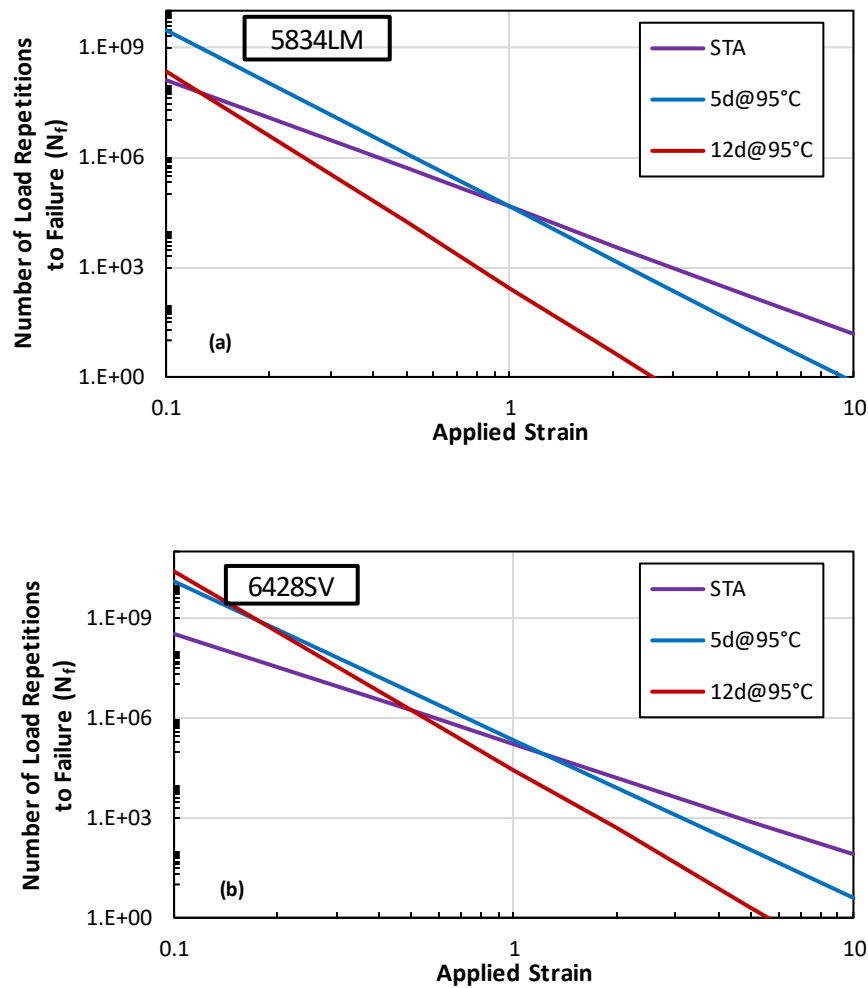


**Figure 5 Fatigue Characterization ( $N_f$ -Strain) Plots from LAS Test for a)5834LM; b)6428SV**

### 3.2 Development of New LAS Parameters.

As shown in **Fig. 4** and **Fig. 5**, there is no consistent trend observed with the current parameters with change of aging conditions and pavement depth. This can be explained by how the A parameter is calculated from the LAS test. As shown in **Eq. 6**, the A value is a function of  $\alpha$  and  $D_f$ ;  $\alpha$  is calculated from the frequency sweep test while the failure point  $D_f$  is defined as the 35% reduction in the initial modulus. This is a default value that may not effectively capture the failure point different binder types (especially with different aging levels and with different modifiers).



In order to define an appropriate failure point of the binder sample during the test, the stress-strain curve during the LAS fatigue test is plotted and shown in **Fig.6a**. There is a peak point that shows the maximum stress on the stress-strain curve, indicating that damage has initiated and material capacity is greatly diminished. Using the peak stress point identified from the stress-strain curve as a reasonable definition of failure, the  $D_f$  and  $C$  values for different binders at this point can be calculated, as illustrated in **Fig.6b**. The new parameters that incorporate this defined failure point can then be developed.

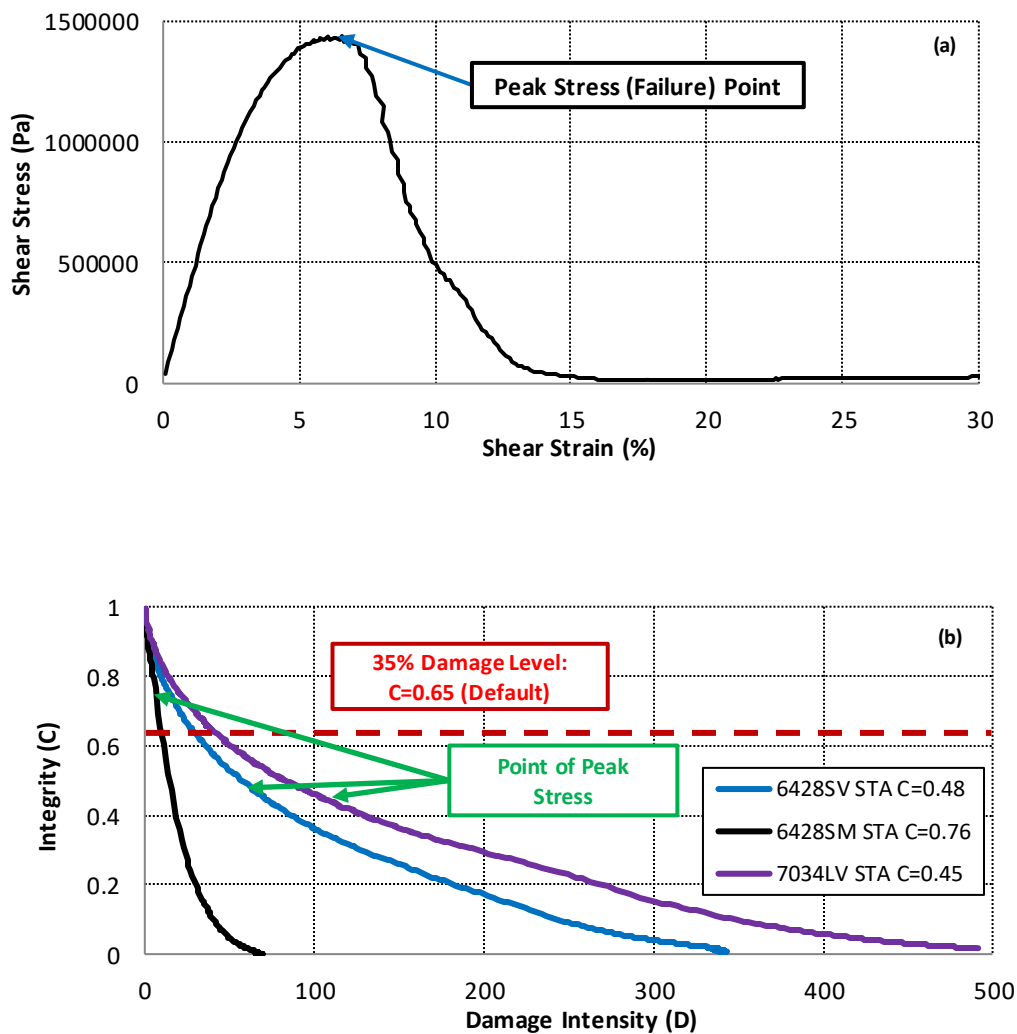


**Figure 6 a) Typical Stress-Strain Plot from LAS Test; b) Illustration of the Default Failure Points as Compared to Points where Peak Stress Occurs**

### 3.2.1 Average Reduction in Integrity up to Failure ( $I^R$ )

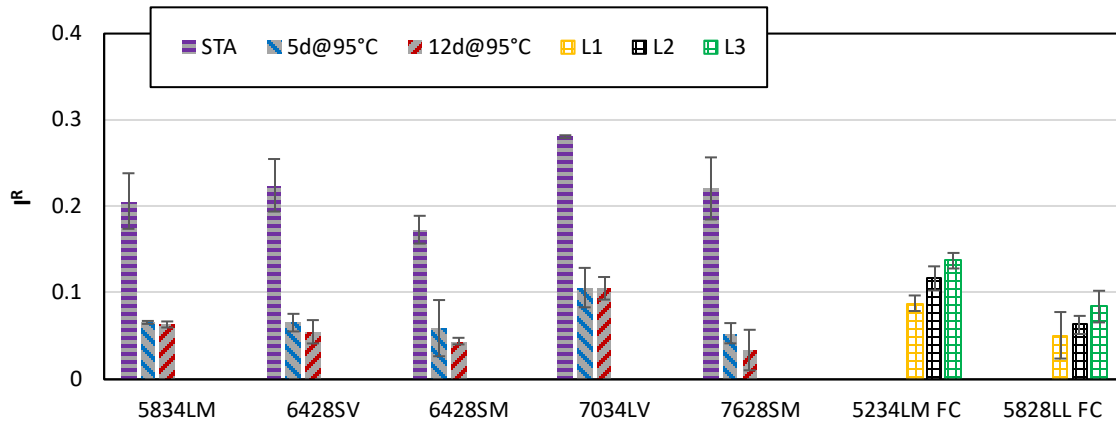
Wang et al. (2017) developed an index  $D^R$  (average reduction in pseudo stiffness up to failure) which is based on the S-VECD theory to evaluate the fatigue properties of asphalt mixtures. Zhang et al. (2019) found that this parameter consistently decreases as material age, showing the degradation of the fatigue resistance of mixtures over time. In this study, the same concept used to determine  $D^R$  is used to develop the new parameter  $I^R$ , Average Reduction in Integrity up to Failure, to evaluate the fatigue properties of different asphalt binders with various aging conditions. The calculation of  $I^R$  is shown as Eq. 10 below:

$$I^R = \frac{\int_0^{N_f} (1-C) dN}{N_f} \quad (10)$$

Where  $N_f$  is the number of load cycles to failure (defined as peak stress) point from the LAS test and  $C$  is pseudo stiffness that is calculated by Eq.3. A higher  $I^R$  value is preferred, indicating the material has better capability to resist fatigue cracking.

**Fig. 7** below shows the  $I^R$  values measured from the study binder samples with different aging conditions. Error bars show one standard deviation. Generally, the  $I^R$  value decreases with increase in aging. There is a significant difference in the  $I^R$  value between STA and long-term aging conditions. The two virgin binders 6428SV and 7034LV (SBS modified), and binder 5834LM generally show higher  $I^R$  values after each aging condition as compared to other binders. Binder 7628SM (PPA modified) initially has a high  $I^R$  value after STA, however, it clearly shows the lowest  $I^R$  values after two long-term aging conditions (5 days and 12 days).

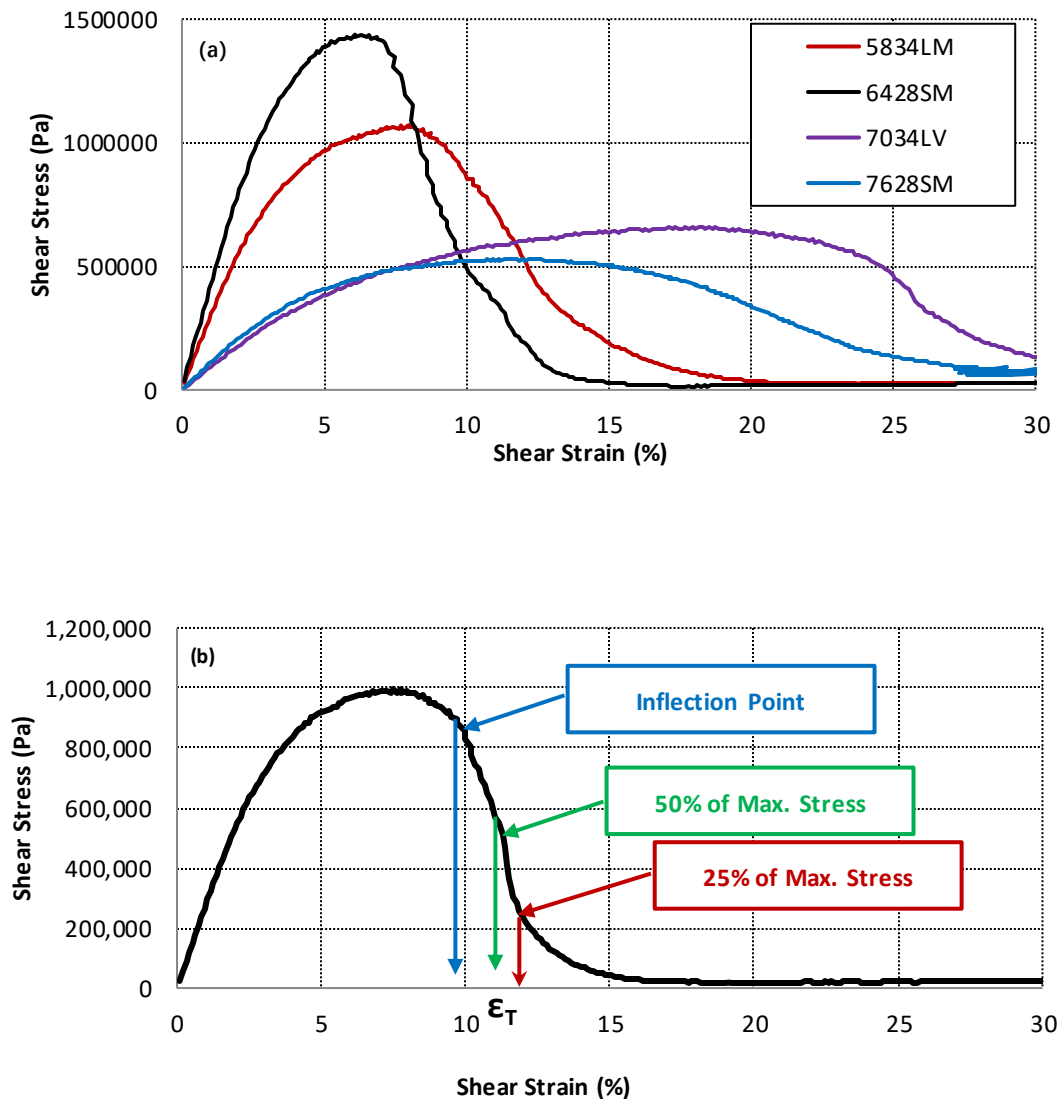
For the binder samples extracted and recovered from the field cores, binder 5234LM FC with the softer grade binder and lower RAP content clearly shows a higher  $I^R$  value at each layer as compared to the binder 5828LL FC.  $I^R$  value of each layer significantly increases with increase of pavement depth (from L1 to L3), illustrating the aging gradient within the pavement structure in the field. The  $I^R$  value of bottom layer for both binders are typically around 1.5 to 2 times of the top layer, indicating the top-down cracking potential of the asphalt pavements.



**Figure 7 Average Reduction in Integrity to Failure from LAS Test**

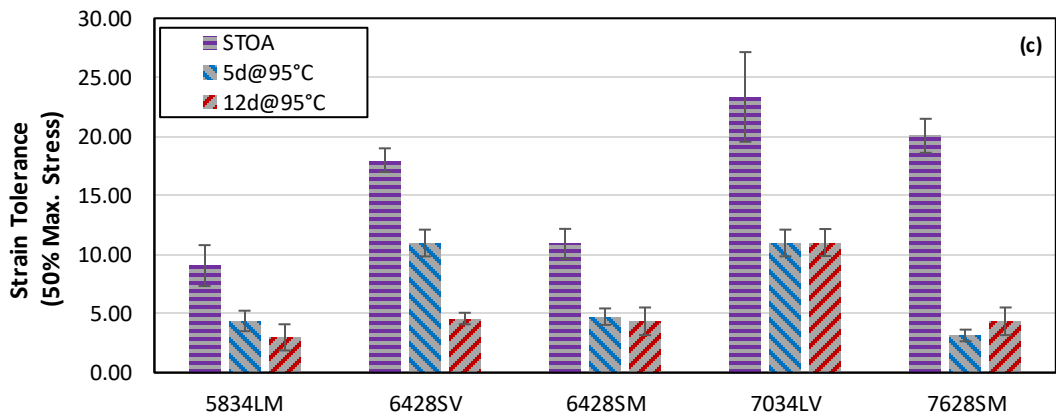
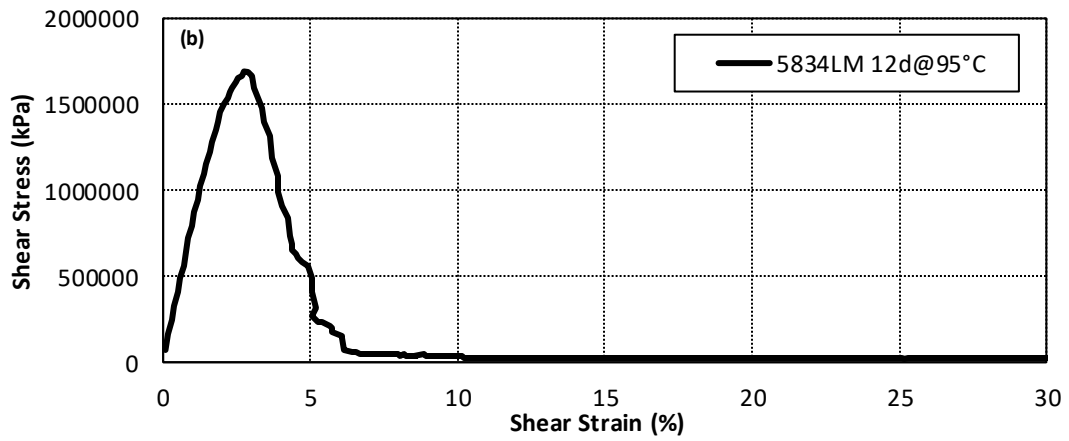
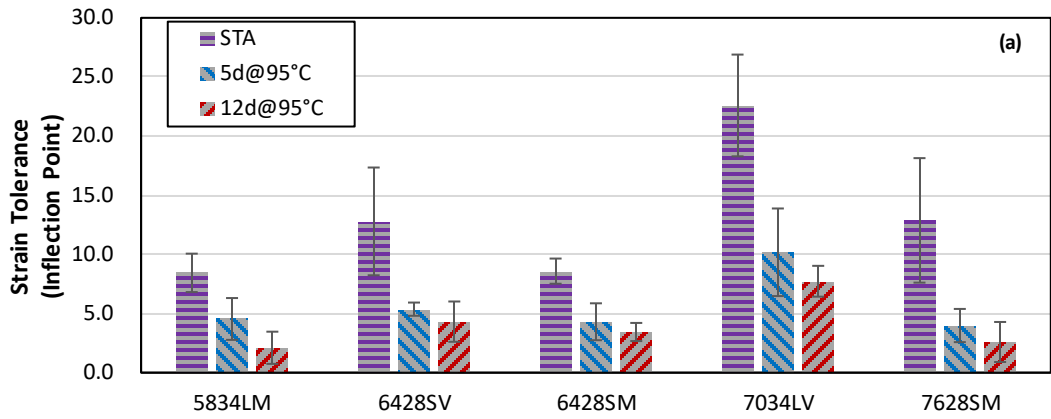
### 3.2.2 Stain Tolerance up to Failure ( $\epsilon_T$ )

The  $I^R$  parameter ignores the post-peak part of the stress-strain curve where the binder sample still has some load carrying capability (as shown in **Fig. 8a**). Also, the modified binders (7034LV and 7628SM) generally show longer and flatter post-peak curves as compared to other binders. The longer and flatter curve can be attributed to the benefits of adding the polymer modifiers into binder samples, where the applied force/stress is trying to break down the cross-linked structure within the modified binder samples after the peak stress point as observed from **Fig. 8a**. To capture this important post-peak behavior of the binder samples during the LAS test, the Stain Tolerance ( $\epsilon_T$ ) parameter is developed. First, an “end” point for the data to be included in the analysis needs to be defined. Different points on the post-peak part of the stress-strain curve have been examined including the inflection point (the point with the lowest negative slope on the stress-strain curve where the shear stress significantly drops), 50% of the maximum stress point and the 25% of the maximum stress point, as indicated in **Fig. 8b**. Stain Tolerance ( $\epsilon_T$ ) is then defined as the strain level corresponding with the selected “end” points.



**Figure 8 a) Typical Stress-Strain Curves for Different Binders; b) Illustration of the End Points**

The effect of aging and modifier can be effectively measured using the inflection point, as shown in **Fig.9a**. However, for the severely aged binder, this point is generally difficult to identify on the stress-strain curve as indicated in **Fig. 9b**, and the variability of the calculated  $\epsilon_T$  parameter between the replicates for each binder is relatively high (shown by error bars in **Fig. 9a**). The point of 50% of the maximum stress can also capture the aging and modifier effects with lower variability than the inflection point (**Fig. 9c**). However, as indicated in **Fig. 9d**, it may not be able to fully capture the effect of modifiers on the post-peak behavior (sample still has certain stress capability with the smooth and flat stress-strain curve after the 50% of the maximum stress point remaining, as shown in **Fig. 9d**).



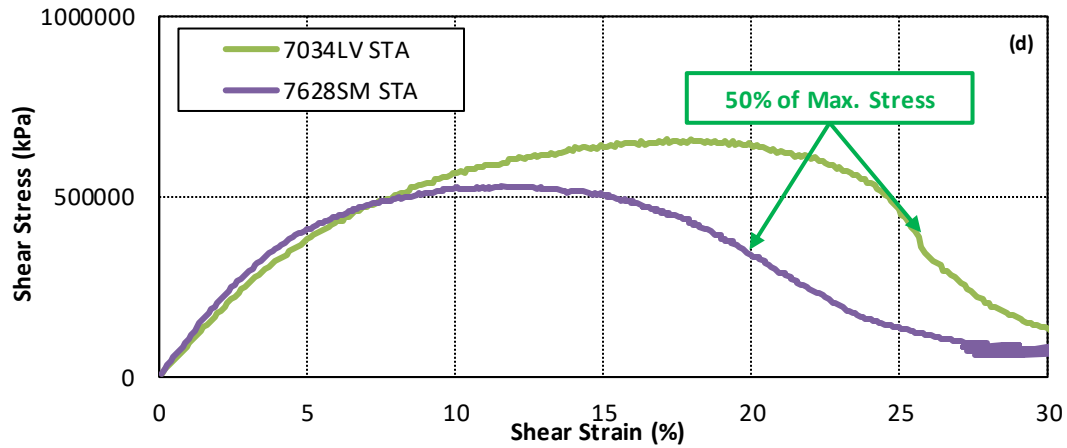


**Figure 9 Examination of a) & b) Inflection Point and;  
c) & d) 50% Max. Stress Point**

The point of 25% of the maximum stress was selected as the end point for calculation of the strain tolerance parameter in this study, the result is shown in **Fig. 10**. The advantages of selecting 25% as the end point are:

- (1) It is easier to identify and the result (calculated strain tolerance) shows lower variability as compared to the inflection point.
- (2) It can fully capture the effect of modifiers on post-peak behavior of binder samples as compared with other two examined points (inflection and 50% max. stress point).
- (3) It can automatically trim the data where the stress is close to 0 at end of the stress-strain curve (the long “tails” of 5834LM and 6428SM as shown in **Fig. 8a**), and the data for some binder samples where the stress-strain curve fluctuates near the end of the test caused by the debonding of the binder samples (**Fig.9b and 9d**), improving the reliability and accuracy of the analysis results.

As shown in **Fig. 10**, the strain tolerance  $\epsilon_T$  generally decreases with increase in aging. There is a significant difference in the  $\epsilon_T$  values between the STA and the two long-term aging conditions. Similar to trends observed from the  $I^R$  parameter, two virgin binders 6428SV and 7034LV (SBS modified) generally show a higher strain tolerance value after each aging condition as compared to other binders. Binder 7628SM (PPA modified) initially has a high  $\epsilon_T$  value with STA (comparable with 7034LV), however,  $\epsilon_T$  value for this binder dramatically decreases after two long-term aging conditions.

For the binder samples extracted from the field cores, binder 5234LM FC with the softer grade binder and lower RAP content typically shows a higher  $\epsilon_T$  value at each layer as compared to the binder 5828LL FC. The  $\epsilon_T$  value of each layer significantly increases with increase of pavement depth (from L1 to L3), showing the aging gradient in the field. The  $\epsilon_T$  value of bottom layer for both binders are typically around 2 to 3 times of the top layer, indicating the possibility of top-down cracking for asphalt pavements in the field.

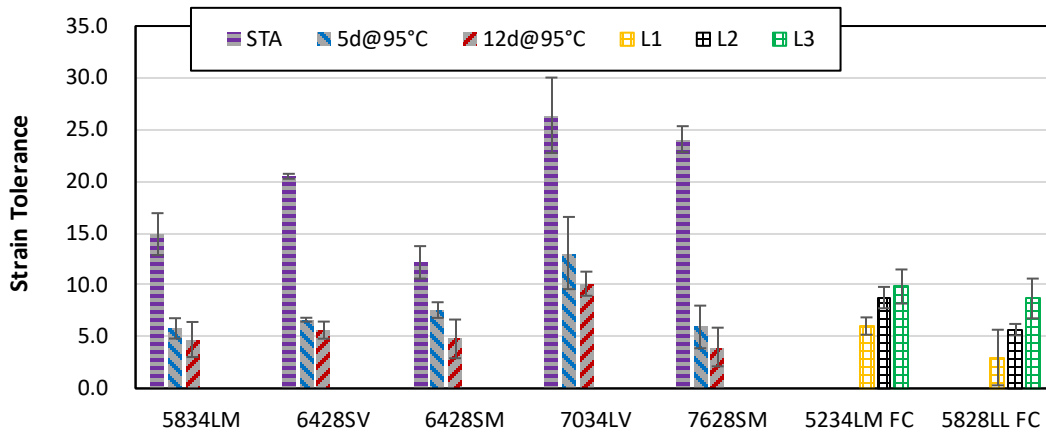


**Figure 10 Strain Tolerance from LAS Test**

### 3.2.3 Strain Energy Tolerance ( $E_f$ )

The concept of energy has been widely used in pavement engineering since it combines the load and displacement (stress and strain) history of the samples during the tests. The Superpave binder grading system used ( $G^* \times \sin \delta$ ) to limit the amount of energy dissipated per loading cycle to minimize the development of the fatigue cracking of asphalt pavement. Researchers (Mohammad et al., 2012; Ozer et al., 2016; Zhu et al., 2017) have proposed the so-called fracture energy measured from the Semi Circular Bending (SCB) and the Disk Shaped Compact Tension (DCT) tests to evaluate the ability of asphalt mixtures to resist cracking. Sabouri et al. (2015) and Wang et al. (2017) also developed the energy based parameters  $G^R$  (the rate of averaged reduction in pseudo strain energy) and  $D^R$  (average reduction in pseudo stiffness up to failure) to evaluate the initiation of fatigue cracking using S-VECD theory. Therefore, an energy-based index for asphalt binders was developed in this work to evaluate their fatigue properties. As shown in **Fig. 11**, the area under the stress-strain curve to the end point (25% of max. stress) is defined as the Strain Energy Tolerance ( $E_f$ ).

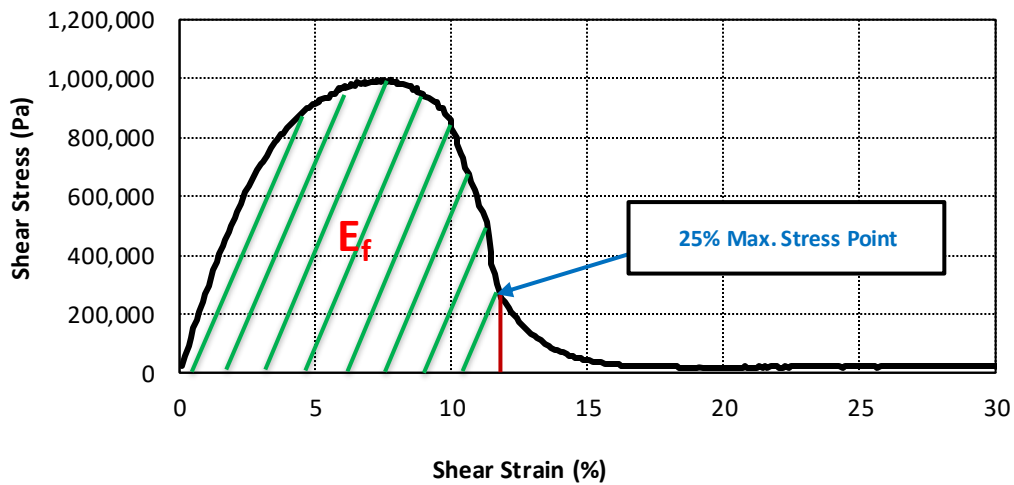


**Figure 11 Illustration of the Calculation of  $E_f$**

**Fig. 12** below shows the values of Strain Energy Tolerance ( $E_f$ ) measured from the study binder samples. Error bars show one standard deviation. Generally,  $E_f$  value decreases with increase in aging. There is a significant difference in  $E_f$  values between STA and the long-term aging conditions. Binder 7034LV (SBS modified) generally has a higher  $E_f$  value after each aging condition as compared to other binders. Binders 6428SM and 7628SM (PPA modified) generally have lower  $E_f$  value after two long-term aging conditions.

For the binder samples extracted from the field cores, binder 5234LM FC with the softer grade binder and lower RAP content typically shows higher  $E_f$  values at each layer as compared to the binder 5828LL FC. The  $E_f$  value of each layer typically increases with increase of pavement depth (from L1 to L3), showing the aging gradient in the field.

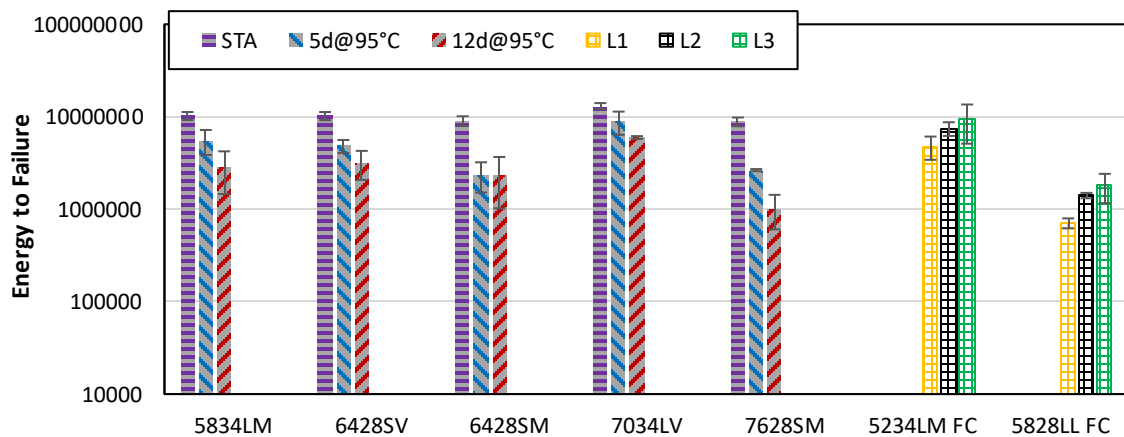


**Figure 12 Energy to Failure from LAS Test**



### 3.3 Mixture Fatigue Index vs. Binder Fatigue Parameter

**Fig. 13** shows the mixture  $D^R$  and  $S_{app}$  values measured from the DTCF fatigue test. Generally, higher  $D^R$  and  $S_{app}$  values indicate better fatigue behavior. The  $D^R$  values show a consistent trend with decreasing values at longer aging conditions, while there is no consistent trend for change of  $S_{app}$  parameter with aging. Mixtures 5834LM, 6428SV and 7034LV generally shows better fatigue properties, while 7628SM shows good performance at the STA condition but the worst performance after the long-term aging.

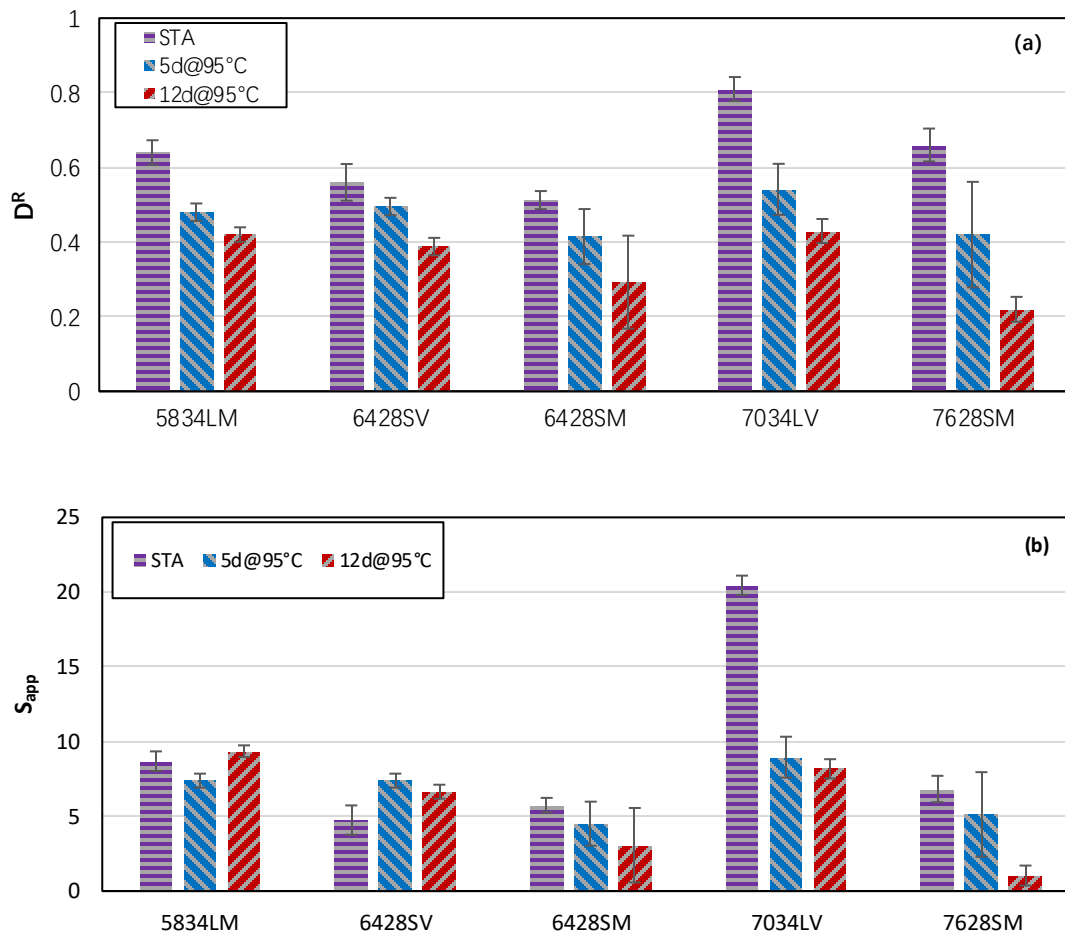


**Figure 13 a)  $D^R$  and; b)  $S_{app}$  Values for Different Mixtures with Various Aging Conditions**

Since the  $S_{app}$  parameter does not show a consistent trend with aging for all mixtures in this study, the comparison and correlation between the binder and mixture fatigue properties will focus on comparing the binder fatigue parameters with the mixture  $D^R$  index.

**Fig. 14a, 14b and 14c** below show good correlations between the measured binder fatigue parameters and the mixture  $D^R$  values, as the high  $R^2$  values indicate. The good correlations

observed here can be attributed to 1) The developed fatigue parameters can effectively capture the failure point of each individual binder sample during the test; 2) The tested binder samples are extracted and recovered from the corresponding mixtures with different aging conditions; 3) Test temperatures for both binder LAS test and mixture DTCF test are the same; and 4) Both  $I^R$  and  $D^R$  values are measured and calculated based on the VECD theory.

**Fig. 14** also reinforces the results observed by researchers (Bahia et al., 2001; Anderson et al., 2001; Ameri et al., 2016; Ziari et al., 2017) that binder plays a significant role in fatigue behavior of asphalt mixtures. The strong correlations between the binder fatigue parameters and mixture  $D^R$  values also indicate that the developed binder fatigue parameters have the potential to be used to evaluate and estimate the fatigue properties of asphalt mixtures, including the effect of aging.

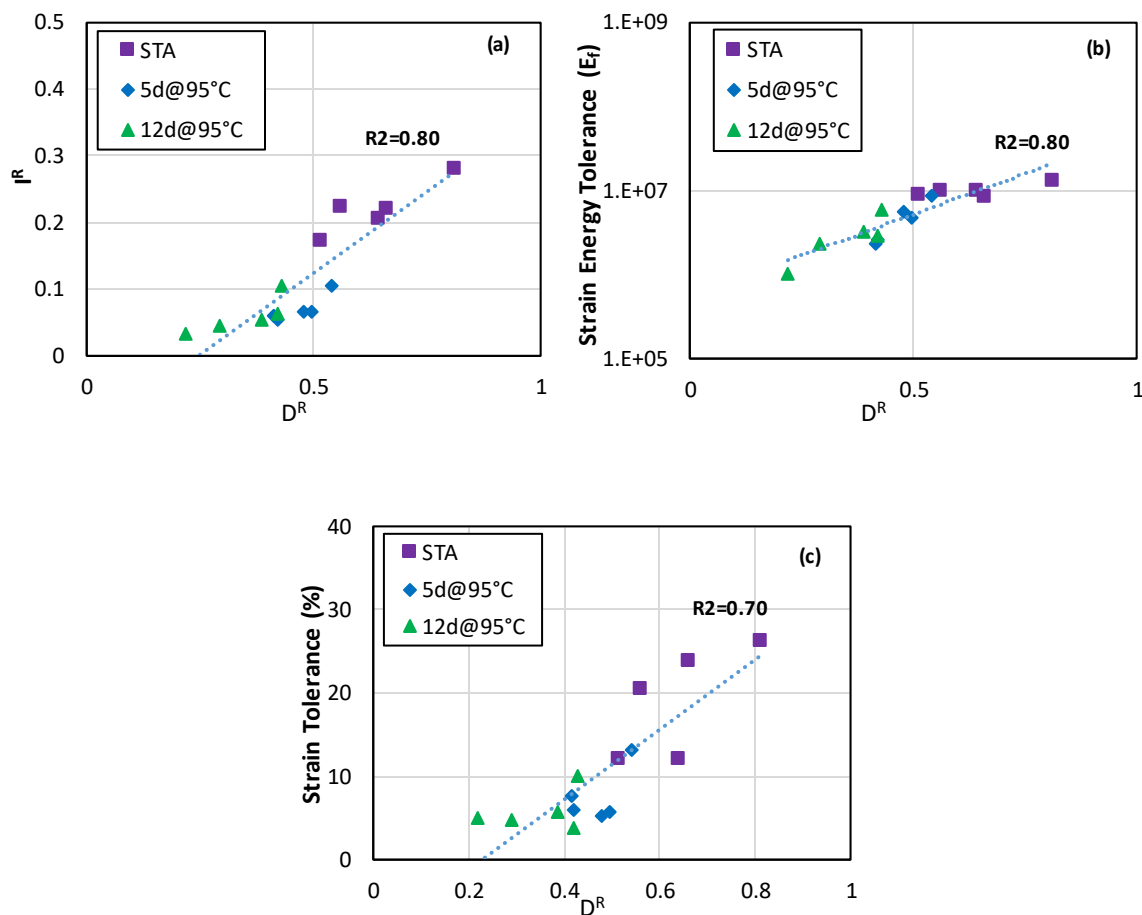
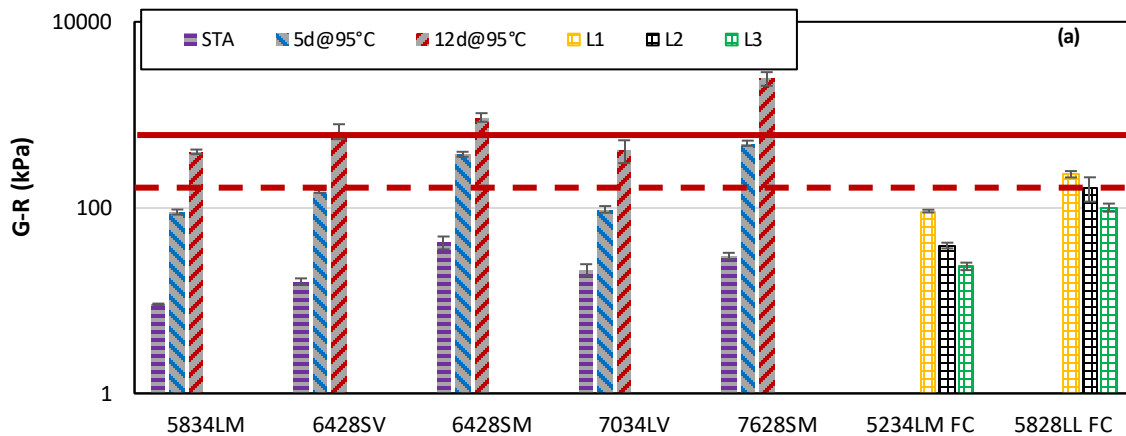


**Figure 14 Binder Fatigue Parameters vs. Mixture Fatigue Index**

### 3.4 Environmental vs. Fatigue Cracking

**Fig. 15** shows the average binder G-R parameter and  $\Delta T_c$  value for the study materials, as well as the suggested threshold values. Error bars show one standard deviation. Generally, with aging, G-R parameter increases, while  $\Delta T_c$  decreases. There is a significant difference in the two indices between the STA and the other two long-term aging conditions. The G-R parameter for 5834LM, 6424SV, and 7034LV after each aging condition is typically lower than other materials, while the  $\Delta T_c$  value for those binders after aging is higher, indicating better cracking performance compared with other materials. The  $\Delta T_c$  value and G-R parameter for these three binders after aging are typically within the cracking limit ( $>-5.0^\circ\text{C}$  for  $\Delta T_c$ ,  $<600\text{kPa}$  for G-R parameter), while other binders exceed the cracking limit value after 12 days aging condition. Also, binder 7628SM generally shows good cracking performance for STA. However, this binder clearly shows the worst cracking performance after 5 days and 12 days aging condition.

For the binder samples extracted from the field cores, G-R parameter generally increases while  $\Delta T_c$  value decreases with increase of pavement depth (from L1 to L3), showing the aging gradient in the field. Binder 5234LM FC with the softer grade binder and lower RAP content typically shows lower G-R and higher  $\Delta T_c$  values at each layer as compared to the binder 5828LL FC, indicating the better cracking performance.



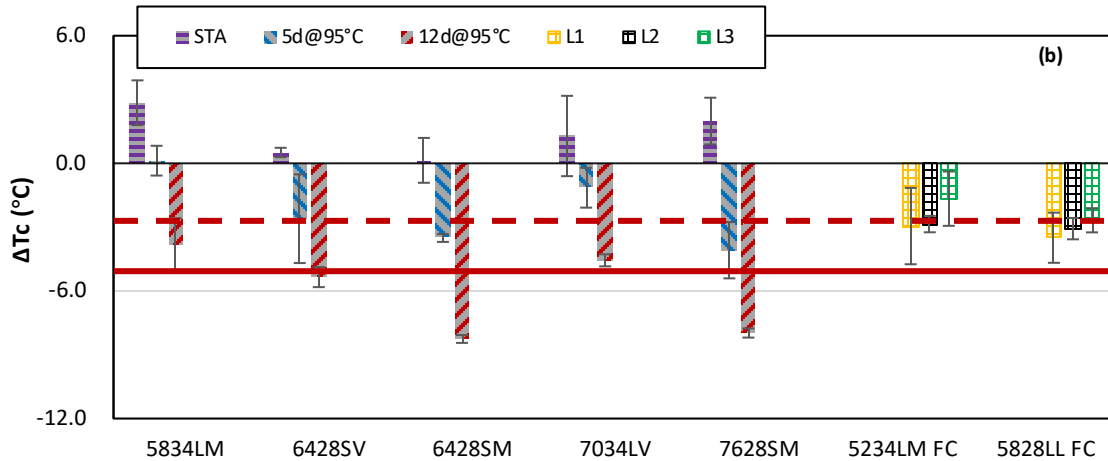


**Figure 15 Binder a) Glover-Rowe; and b)  $\Delta T_c$  Parameter from 4mm DSR Test**

As discussed above, the binder G-R and  $\Delta T_c$  parameter measured from the 4mm DSR test are generally used to evaluate the binder property to resist durability/thermal cracking problem (non-load associated). The fatigue indices ( $E_f$ ;  $\epsilon_T$ ;  $I^R$ ) developed from this study are measured from LAS test where the binder samples are subjected to repeated loading until the cracking/failure point. So, the combination of binder G-R and  $\Delta T_c$  parameter with the fatigue parameters can be very useful and effective for agencies and researchers to select the appropriate binders and design the mixtures with proper cracking performance in general. **Fig. 16** below shows an example of the combination of binder G-R parameter with fatigue parameter  $E_f$  in a single plot. As the materials age, G-R increases and  $E_f$  parameter decreases substantially, while G-R decreases and  $E_f$  parameter increases significantly with increase of pavement depth. Binder 7034LV clearly shows the good capability to resist both environmental and fatigue cracking, while binder 7628SM shows the worse cracking performance after 5 days and 12 days aging. In addition, binder 5828LL FC from each layer generally shows the good ability to resist durability cracking problem (G-R parameter still within the significant limit value), but it generally shows the poor fatigue cracking resistance with the lower  $E_f$  value as compared to other binders.

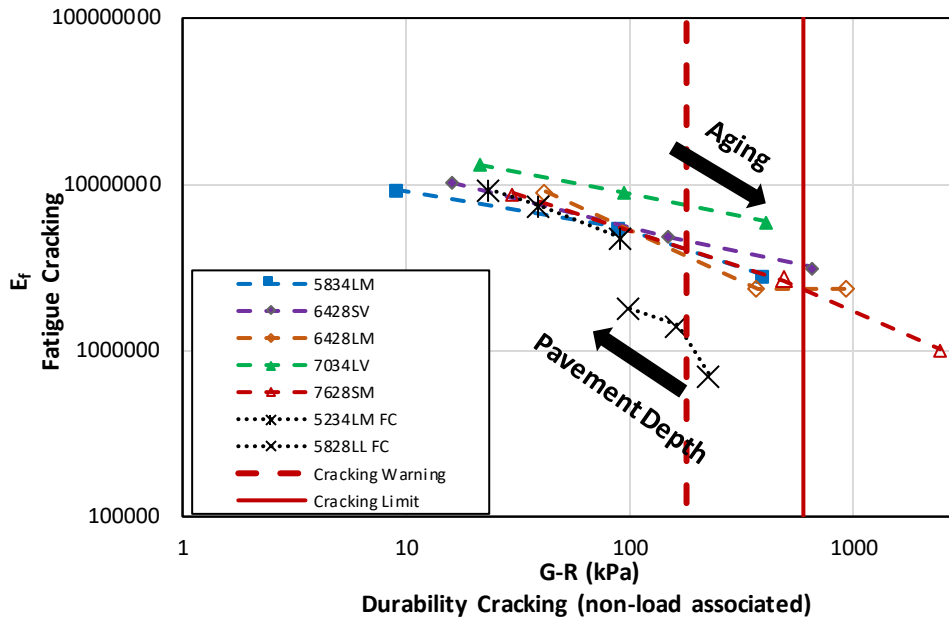


**Figure 16 Combination of binder G-R Parameter from 4mm DSR with Energy to Failure from LAS Test**

#### 4. Summary and Conclusions

The main objective of this study is to explore new performance indices to evaluate the fatigue properties of asphalt binders while also considering the effects of aging. Five mixtures were subjected to three different conditioning levels (short term aging during production, loose mix for 5 and 12 days at 95°C in laboratory), and the corresponding binders were extracted and recovered. Direct Tension Cyclic Fatigue (DTCF) tests were performed on the mixtures to characterize the mixture fatigue performance using the simplified viscoelastic continuum damage (S-VECD) analysis approach. Frequency and temperature sweep tests using a Dynamic Shear Rheometer (DSR) with a 4 mm diameter plate and the Linear Amplitude Sweep (LAS) test were conducted on the recovered binders to evaluate the binder rheological and fatigue properties. Three new performance indices are developed from the LAS test and these were used to track the changes in binder fatigue capacity with aging: Strain Tolerance ( $\epsilon_T$ ), Strain Energy Tolerance ( $E_f$ ), and Average Reduction in Integrity to Failure ( $I^R$ ). The following conclusions can be drawn from the results of the testing and analysis:

- Compared with the traditional A and B parameters determined from the LAS test, the new parameters show a consistent decrease in the fatigue properties of the binder samples with aging.

- The three new parameters can effectively capture the failure point of the binder samples during LAS test, the  $\epsilon_T$  and  $E_f$  can also be used to evaluate the post-peak behavior after damage is initiated.
- The new parameters show good correlation with mixture fatigue performance index  $D^R$  value measured from the DTCF test, indicating the new parameters have the potential to be used for evaluating the fatigue properties of asphalt mixtures while also taking aging into account.
- The new parameters together with the binder rheological parameters (e.g. G-R and  $\Delta T_c$ ) can be used to evaluate environmental and fatigue cracking properties of asphalt materials at the same time.
- The new parameters proposed in this study can not only be used to evaluate the aging gradient within the pavement structure, but they are also applicable for detecting the top-down cracking potential of asphalt pavements.

## 5. Future Work

Future work and analysis are planned to continue testing on mixtures and extracted and recovered binder samples. Specifically, more binders/mixtures with different types of modifiers should be included to comprehensively evaluate how the modifiers impact the different fatigue parameters developed from this study. In addition, multiscale modelling associated with the micromechanics analysis should be conducted to further investigate the links between the newly developed binder fatigue properties with mixture fatigue properties. Such approach can allow for mechanistic inclusion of the mix volumetrics and aggregate properties in upscaling of binder fatigue properties to mixture fatigue properties. At present, it is planned to continuously obtain field cores as well as pavement performance data over time for the study materials. Through these continued efforts, the correlation between the different properties of aged asphalt mixtures and binders, as well as their relationship with the field core test results and field cracking performance will be further investigated.

## 6. References

Anderson D., Hir Y., Marasteanu M., Planche J.-P., Martin D., Gauthier G. (2001). Evaluation of fatigue criteria for asphalt binders, *Transp. Res. Rec.: J. Transp. Res. Board* 48–56.

Anderson, M., G. King, D. Hanson, and P. Blankenship, (2011). Evaluation of the Relationship 2 Between Asphalt Binder Properties and Non-Load Related Cracking” Journal of the Association of Asphalt Paving Technologists, Vol. 80, pp. 615-661

Ayazi M.J., Moniri A., Barghabany P. (2017). Moisture susceptibility of warm mixed reclaimed asphalt pavement containing Sasobit and Zycotherm additives, *Pet.Sci. Technol.* 35 890–895.

Ameri M., Nowbakht S., Molayem M., Mirabimoghaddam M.H. (2016). A study on fatigue modeling of hot mix asphalt mixtures based on the viscoelastic continuum damage properties of asphalt binder, *Constr. Build. Mater.* 106 243–252.

Bahia H.U., Hanson D., Zeng M., Zhai H., Khatri M., Anderson R. (2001). NCHRP Report 459: Characterization of modified asphalt binders in superpave mix design, Transportation Research Board.

Behbahani H., Ayazi M.J., Moniri A., (2017). Laboratory investigation of rutting performance of warm mix asphalt containing high content of reclaimed asphalt pavement, *Pet. Sci. Technol.* 35 1556–1561.

Bell, C. A., Y. AbWahab, R. E. Cristi, and D. (1994). Sognovske. Selection of Laboratory Aging Procedures for Asphalt-Aggregate Mixtures. Washington, DC: Strategic Highway Research Program, National Research Council.

Blankenship, P.B., Anderson, M. A., King, G. N., and Hanson, D. I. (2010). A Laboratory and Field Investigation to Develop Test Procedures for Predicting Non-Load Associated Cracking of Airfield HMA Pavements, Airfield Asphalt pavement technology Program.

Bonnetti K., Nam K., Bahia H. (2002). Measuring and defining fatigue behavior of asphalt binders, *Transp. Res. Rec.: J. Transp. Res. Board* 33–43.

Clopotel C., Velasquez R., Bahia H., Pérez-Jiménez F., MiróR., Botella R. (2012). Relationship between binder and mixture damage resistance at intermediate and low temperatures, *Transp. Res. Rec.: J. Transp. Res. Board* 39–47.

Cominsky, R.J., Huber, G.A., Kennedy, T.W., Anderson, M. (1994). The Superpave Mix Design Manual for New Construction and Overlays. Strategic Highway Research Program National Research Council. Washington, DC.

Daniel J.S., Bisirri W., Kim Y.R. (2004). Fatigue evaluation of asphalt mixtures using dissipated energy and viscoelastic continuum damage approaches, *J. Assoc. Asphalt Paving Technol.* 73 557–583.

Daniel J.S., Kim Y.R. (2002). Development of a simplified fatigue test and analysis procedure using a viscoelastic continuum damage model, *J. Assoc. Asphalt Paving Technol.* 71 619–650.

Elwardany, M. D., F. Yousefi Rad, C. Castorena, and Y. R. Kim. (2017). Evaluation of Asphalt Mixture Laboratory Long-Term Ageing Methods for Performance Testing and Prediction, *Road Materials and Pavement Design*, Vol. 18, No. 1, pp. 28-61.

Glaser, R.R. Turner, T.F., Loveridge, J.L. Salmans, S.L., Planche, J.P. (2015). Fundamental Properties of Asphalts and Modified Asphalts III Product. Technical White Paper.

Glover C.J., Martin, A.E., Chowdhury, A., Han R. (2008). Evaluation of Binder Aging and Its Influence in Aging of Hot Mix Asphalt Concrete: Literature Review and Experimental Design. Technical Report.

Harrigan, E. T. (2007). Simulating the Effects of Hot Mix Asphalt Aging for Performance Testing and Pavement Structural Design. Final Report, National Cooperative Highway Research Program, Research Results Digest 324, National Research Council, Washington, D.C.

Hintz C., Velasquez R., Johnson C., Bahia H. (2011). Modification and validation of linear amplitude sweep test for binder fatigue specification, *Transp. Res. Rec.: J. Transp. Res. Board* 2207 99–106.

Hveem, F.N., Zube, E. and Kog, J.S. (1963). Proposed New Tests and Specifications for Paving Grade Asphalt. *Journal of Association of Asphalt Paving Technologists*, 32: 271–327.

Johnson C., (2010) Evaluation of Accelerated Procedures for Fatigue Characterization of Asphalt Binders, ph.D, Wisconsin.

Kim, R. Y., Castorena, C., Elwardany, M., Yousefi Rad, F., Underwood, S., Gundha, A., Gudipudi, P., Farrer, M. J., Glaser, R., R., (2018) Long-term Aging of Asphalt Mixtures for Performance Testing and Prediction, Final Report, NCHRP 09-54.

Ozer, H., Al-Qadi, I. L., Lambros, J., El-Khatib, A., Singhvi, P., & Doll, B. (2016). Development of the fracture-based flexibility index for asphalt concrete cracking potential



using modified semi-circle bending test parameters. *Construction and Building Materials*, 115, 390-401. DOI: 10.1016/j.conbuildmat.

Planche J.-P., Anderson D., Gauthier G., Hir Y. Le, Martin D., (2004). Evaluation of fatigue properties of bituminous binders, *Mater. Struct.* 37 356–359.

Rowe, G. M. (2011). Evaluation of the Relationship between Asphalt Binder Properties and Non-Load Related Cracking, *Journal of the Association of Asphalt Paving Technologists*,

Sabouri M., Bennert T., Daniel J.S., Kim Y.R. (2015). Fatigue and rutting evaluation of laboratory-produced asphalt mixtures containing reclaimed asphalt pavement, *Transp. Res. Rec.: J. Transp. Res. Board* 32–44.

Sabouri M., Mirzaiyan D., Moniri A. (2018). Effectiveness of Linear Amplitude Sweep (LAS) asphalt binder test in predicting asphalt mixtures fatigue performance, *Construction and Building Materials*, Volume 171, Pages 281-2

Sui, C., Farrar, M. J., Harnsberger, P. M., Tuminello, W. H., & Turner, T. F. (2011). New Low-Temperature Performance-Grading Method: Using 4-mm Parallel Plates on a Dynamic Shear Rheometer. *Transportation Research Record*, 2207(1), 43–48.

<https://doi.org/10.3141/2207-06>

Tabatabaee, H.A., Bahia, H., (2014). Establishing Use of Asphalt Binder Cracking Tests for Prevention of Pavement Cracking." Accepted for Presentation and Publication in the *Journal of the Association of Asphalt Pavement Technologists*, Vol. 83

Martono W., Bahia H.U., D'angelo J. (2007). Effect of testing geometry on measuring fatigue of asphalt binders and mastics, *J. Mater. Civil Eng.* 19 746–752.

Mohammad L.N., Kim M., Elseifi M. (2012) Characterization of Asphalt Mixture's Fracture Resistance Using the Semi-Circular Bending (SCB) Test. In: Scarpas A., Kringos N., Al-Qadi I., A. L. (eds) 7th RILEM International Conference on Cracking in Pavements. RILEM Bookseries, vol 4. Springer, Dordrecht

Vassiliev, N.Y., R.R. Davison, and C.J. Glover. (2002). Development of a Stirred Airflow Test Procedure for Short-Term Aging of Asphaltic Materials. *Bituminous Binders*, No. 1810, pp. 25-32.

Wang, Y. and Kim Y. R., (2017). Development of a pseudo strain energy-based fatigue failure criterion for asphalt mixtures, *International Journal of Pavement Engineering*.

Zhang, R., Sias, J. E., Dave, E. V., & Rahbar-Rastegar, R. (2019). Impact of Aging on the Viscoelastic Properties and Cracking Behavior of Asphalt Mixtures. *Transportation Research Record*. <https://doi.org/10.1177/0361198119846473>

Zhou, F., Karki, P., & Im, S. (2017). Development of a Simple Fatigue Cracking Test for Asphalt Binders. *Transportation Research Record*, 2632(1), 79–87.  
<https://doi.org/10.3141/2632-09>

Zhou F., Mogawer W., Li H., Andriescu A., Copeland A. (2012). Evaluation of Fatigue Tests for Characterizing Asphalt Binders, *J. Mater. Civ. Eng.* 25 610–617.

Ziari H., Babagoli R., Ameri M., Akbari A., (2014). Evaluation of fatigue behavior of hot mix asphalt mixtures prepared by bentonite modified bitumen, *Constr. Build. Mater.* 68 685–691.

Ziari H., Amini A., Goli A., Mirzaeiyan D. (2018). Predicting rutting performance of carbon nano tube (CNT) asphalt binders using regression models and neural networks, *Constr. Build. Mater.* 160 415–426.

Ziari H., Moniri A., Imaninasab R., Nakhaei M. (2017). Effect of copper slag on performance of warm mix asphalt, *Int. J. Pavement Eng.* 1–7.

Zhu, Y., Dave, E. V., Rahbar-Rastegar, R., Daniel, J. S., and Zofka, (2017). A. Comprehensive Evaluation of Low Temperature Cracking Fracture Indices for Asphalt Mixtures, *Road Materials and Pavement Design*.

## **Appendix E Paper 5 (Chapter 8)**

### **Comparison and Correlation of Asphalt Binder and Mixture Cracking Parameters Incorporating the Aging Effect**

Runhua Zhang

University of New Hampshire

W161 Kingsbury Hall, 33 Academic Way, Durham, NH 03824, United States

Tel: 603-285-8739; Email: [rz1015@wildcats.unh.edu](mailto:rz1015@wildcats.unh.edu)

Jo E. Sias

University of New Hampshire

W183B Kingsbury Hall, 33 Academic Way, Durham, NH 03824, United States

Tel: 603-285-8739; Email: [jo.sias@unh.edu](mailto:jo.sias@unh.edu)

Eshan V. Dave

University of New Hampshire

W173 Kingsbury Hall, 33 Academic Way, Durham, NH 03824, United States

Tel: 603-285-8739; Email: [eshan.dave@unh.edu](mailto:eshan.dave@unh.edu)

## 1. Introduction

Cracking – both environmental and load related - is one of the primary distresses for asphalt pavements. Cracking affects ride quality and allows water to penetrate from the surface to underlying soil layers, decreasing the life of the pavement and requiring more frequent maintenance or rehabilitation application. In order to efficiently and effectively evaluate and control the cracking performance of asphalt pavement, there are significant research efforts in recent decades that have been dedicated to developing different laboratory characterization tests and the corresponding performance parameters to evaluate the cracking susceptibility of asphalt materials. These tests can be generally divided into two categories: those that evaluate the cracking properties of asphalt mixtures and those that evaluate the cracking properties of asphalt binders.

Various methods have been developed to characterize the cracking properties of asphalt binders. These tests can be generally divided into two categories: rheological measurement (within the Linear Viscoelastic (LVE) range of materials' response) and damage characterization (out of the LVE range). Rheological measurement includes the typical Frequency and Temperature Sweep test using Dynamic Shear Rheometer (DSR) and Bending Beam Rheometer (BBR) test, while Linear Amplitude Sweep (LAS) test, Asphalt Binder Cracking Device (ABCD) test and Single-Edge Notch Bending (SENB) or Double-Edge Notch Bending (DENB) test are the typical damage characterization methods. The binder DSR test characterizes the fundamental rheological properties of asphalt binder, and the measured rheological indices (e.g. R-value, crossover frequency and binder Glover-Rowe parameter) have been proved to correlate well with the cracking performance of asphalt pavements [1-3]. The traditional BBR measurement, and the recently developed ABCD, SENB and DENB tests are typically performed to evaluate the low temperature properties of asphalt binder, aimed to control the thermal cracking susceptibility of asphalt pavement [4-11]. The LAS test, which is based on Viscoelastic Continuum Damage (VECD) theory, is typically used to evaluate fatigue properties of asphalt binders under the repeated loading condition [12,13]. Recent study conducted by Zhang [14] have shown that the performance parameters measured from LAS test can effectively represent the asphalt mixture's fatigue performance.

Besides the binder cracking tests, many mixture tests have also been proposed and widely accepted for evaluation of the cracking properties of asphalt mixtures. These tests can also be generally divided into two categories: rheological measurement and damage characterization. Rheological measurement includes the Complex Modulus ( $E^*$ ) test, while Semi-circular Bending (SCB, also well-known as I-FIT) and Ideal Cracking Test (CT-Index) test, Disk-shaped Compact Tension (DCT) test and Direct Tension Cyclic Fatigue (DTCF) test are the typical damage characterization methods for asphalt mixtures. The rheological indices (e.g. R-value, crossover frequency and mixture Glover-Rowe parameter) measured from the mixture

Complex Modulus ( $E^*$ ) test have also been correlated with the field cracking performance of asphalt pavement [15,16]. The SCB test and the recently developed CT-Index test have been shown to effectively evaluate the cracking resistance of the asphalt mixtures in general [15,17,18]. Currently, they are being widely evaluated by states for implementation within mixture design and quality assurance (QA) process. The Disk-shaped Compact Tension (DCT) test was originally developed by Wagoner [19]. Recent research [15,20,21] have shown that the performance indices measured from the DCT test can be used as the effective parameters to evaluate low temperature cracking performance of asphalt mixtures. For characterization of the fatigue behavior of asphalt mixtures, the traditional Flexural Beam Fatigue test, and the newer Direct Tension Cyclic Fatigue (DTCF) test which is developed based on the Simplified Viscoelastic Continuum Damage (S-VECD) theory are widely accepted and used by researchers and agencies [15,22,23].

These different tests and their corresponding performance parameters described above provide researchers a valuable way to evaluate the cracking susceptibility for both asphalt binders and mixtures, however, there is still a question of how the mixture properties change with changes in binder characteristics and how the binder and mixture testing methods may differentially evaluate expected performance of asphalt materials with respect to cracking. Also, the relationship between binder cracking performance and mixture cracking behavior is still not completely understood. Several preliminary studies have recently been conducted to explore this relationship. Safaei et al. [24] compared the fatigue properties of asphalt binders and mixtures by conducting the LAS and DTCF test associated with the S-VECD analysis, and the results showed that there is a good agreement between two tests. Sabouri et al. [25] performed the binder DSR and LAS tests, as well as the mixture Four-point Bending Beam (FBB) fatigue test on the study binders and mixtures, and the results showed that a strong correlation exists between LAS and FBB rankings while the Superpave binder fatigue index ( $G^*\sin\delta$ ) does not show a strong correlation with either LAS or FBB tests. In terms of thermal cracking, Moon et al. [26] measured the thermal stresses calculated from binder BBR measurement and mixture creep data collected from indirect tensile test (IDT), and demonstrated that there is a significant difference between the results. A study by Reinke et al. [27] showed only a moderate correlation of  $\Delta T_c$  measured from the field cores with the field thermal cracking ( $R^2 \approx 0.6$ ) performance, while a strong correlation of  $\Delta T_c$  with fatigue only or to total cracking (including thermal cracking) with a  $R^2 > 0.9$ . Based on the Pearson (linear) correlation analysis, Reyhaneh et al. [28] found that there is good correlation was observed between binder and mixture stiffness-based parameters, but there was generally low correlation observed between binder and mixture cracking parameters.

Although these preliminary research efforts have been dedicated to exploring and investigating the relationship between binder cracking properties and mixture cracking behaviors, these studies are conducted based on the limited testing and analysis methods to evaluate the specific cracking behavior (e.g. fatigue or thermal) of asphalt material. In addition, relatively little attention has been devoted to evaluate this relationship while also incorporate the aging effect which has been proved to significantly impact the cracking performance for both binders and mixtures. With the current research gap listed above, the primary objective of this study is to comprehensively compare and correlate the asphalt mixture and binder cracking properties by conducting the different advanced performance tests (e.g. binder DSR and LAS; mixture Complex Modulus, SCB and DCT, DCFT) and employing the various statistical methods (e.g. Pearson, Kendall and Hoeffding's D analysis, frequency (density) curve) in this study, while also consider the aging effect by conditioning the material in the laboratory following different procedures to simulate the different field aging periods.

## **2. Methodology**

### **2.1 Laboratory Conditioning Methods**

The accelerated laboratory conditioning method is of great importance to simulate and predict the change of binder and mixture properties over the pavement service life, which will help to minimize maintenance and rehabilitation cost due to the different pavement distress and to increase the confidence level of the design of pavement. In this study, the Asphalt Institute procedure (24 hours at 135°C) [29] and NCHRP recommended 95°C for 5 and 12 days [30] on the plant produced mixtures (already subjected to the short-term aging during production) are included as the laboratory conditioning methods to simulate the aging in field. Previous work [15] has shown that 5 days at 95°C laboratory aging condition simulates approximately four years of field aging while 12 days at 95°C laboratory aging simulates approximately 10 years of field aging for the environment where these surface course mixtures are commonly used.

### **2.2 Binder Testing Methods and Parameters**

#### **2.2.1 4mm Dynamic Shear Rheometer (DSR)**

The rheological properties of asphalt binders are measured by conducting the complex shear modulus test on a Dynamic Shear Rheometer (DSR) with a 4 mm plate [31]. This test covers a wide range of temperatures (-36°C to 30°C, usually in 3 degrees increments), and frequencies (15 frequencies from 0.2 rad/sec to 100 rad/sec), by using the appropriate strain level at each combination of test temperature and frequency. The isotherm tests are conducted from the coldest to the warmest temperature and from the highest to the lowest frequencies. The complex shear modulus master curve is constructed and various rheological parameters are further calculated including: (1) Glover-Rowe (G-R) parameter (indicated in **Eq. 1**); (2) critical

temperatures determined by creep stiffness ( $T_c(S)$ ) and the relaxation rate ( $T_c(m)$ ); (3) critical temperature difference ( $\Delta T_c$ , shown in **Eq.2**); (4) performance grade low temperature (PGLT); (5) R-value (known as the difference between the logarithmic glassy modulus and the logarithmic equilibrium modulus of the binder) [32,33].

$$G - R = \frac{|G^*|(\cos\delta)^2}{\sin\delta} \quad (1)$$

$$\Delta T_c = T_{(stiffness)} - T_{(m-slope)} \quad (2)$$

Where,

$G^*$ : complex shear modulus;

$\delta$ : phase angle;

$T_{(stiffness)}$ : critical low temperature at which  $S(60) = 300$  MPa;

$T_{(m-slope)}$ : critical low temperature at which  $m(60) = 0.300$ .

A lower G-R parameter indicates better capability to resist durability cracking. A limiting value of 180 kPa is proposed as a crack warning limit, a second value of 600 kPa is suggested for the development of significant cracking (block cracking) [1]. For  $\Delta T_c$  parameter, a positive value indicates that the binder grade is controlled by the creep stiffness (S-controlled); when the  $\Delta T_c$  value is negative, the binder grade becomes m-controlled. S-controlled binders typically have better stress relaxation capability and are therefore typically less prone to cracking. Asphalt Institute [2] suggests using  $\Delta T_c = -2.5^\circ\text{C}$  and  $\Delta T_c = -5.0^\circ\text{C}$  as preliminary threshold values for crack warning and cracking limit respectively.

The transition temperatures (glassy transition temperature ( $T_g$ ); viscoelastic (crossover) transition temperature ( $T_t$ ); and the intermediate region temperature range ( $\Delta T_{IR}$ )) can also be measured from the 4mm DSR test [34,35]. These three temperatures are typically calculated from the storage and loss modulus master curves in the temperature domain with a frequency of 10 rad/s or 1.59 Hz (as shown in **Fig. 1**). Glass transition temperature ( $T_g$ ) is the temperature where the loss modulus starts to drop near the glassy transition region, while viscoelastic transition temperature ( $T_t$ ) is the temperature where loss modulus is equal to storage modulus in between of the intermediate and terminal region. The Intermediate Region Temperature ( $\Delta T_{IR}$ ) is the difference between the viscoelastic temperature and the glassy transition temperature, indicating the “length” of the intermediate “transition” region.

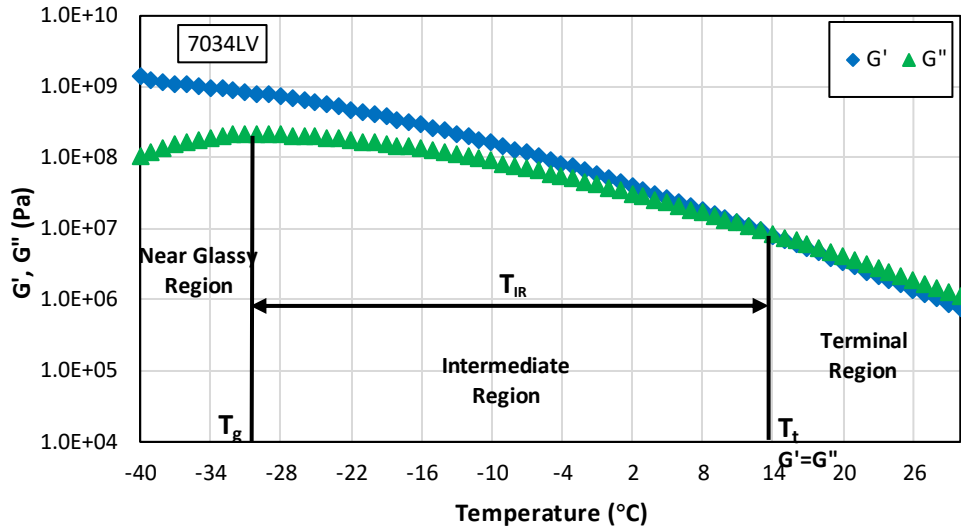


**Figure 1  $T_g$ ,  $T_t$  and  $T_{IR}$  in  $G'$  and  $G''$  Master Curve (Temperature Domain)**

### 2.2.2 Linear Amplitude Sweep (LAS) Test

The LAS test evaluates the ability of asphalt binder to resist fatigue damage. This test is an oscillatory strain sweep test that generates damage to the binder by applying linearly increasing load amplitudes. In this study, frequency sweeps are conducted at a strain amplitude of 0.1% with a range of frequencies from 0.2 to 30 Hz according to AASHTO TP101. Amplitude sweep test is done at a constant frequency of 10 Hz. The testing protocol consisted of applying a linearly increasing strain from zero to 30% over 3100 cycles of loading. All tests are conducted using DSR device with an 8mm diameter parallel plate and a 2mm gap. The new performance indices (Strain Tolerance ( $\epsilon_T$ ); Strain Tolerance Energy ( $E_f$ ); Average Reduction in Integrity up to Failure ( $I^R$ )) developed from the previous study [14] are used to evaluate the binder fatigue performance. The strain tolerance ( $\epsilon_T$ ; strain level corresponding with the 25% maximum stress point) and strain tolerance energy ( $E_f$ ; area under the stress-strain curve up to the 25% maximum stress point) are calculated from the stress-strain curve generated during the LAS test (as indicated in **Fig. 2**), while the average reduction in integrity up to failure ( $I^R$ ) is calculated based on the VECD theory (as shown in **Eq.3**).

$$I^R = \frac{\int_0^{N_f} (1-C) dN}{N_f} \quad (3)$$

Where  $N_f$  is the number of load cycles to failure (defined as peak stress) point from the LAS test and  $C$  is pseudo stiffness. A higher  $I^R$  value is preferred, indicating the material has better capability to resist fatigue cracking.



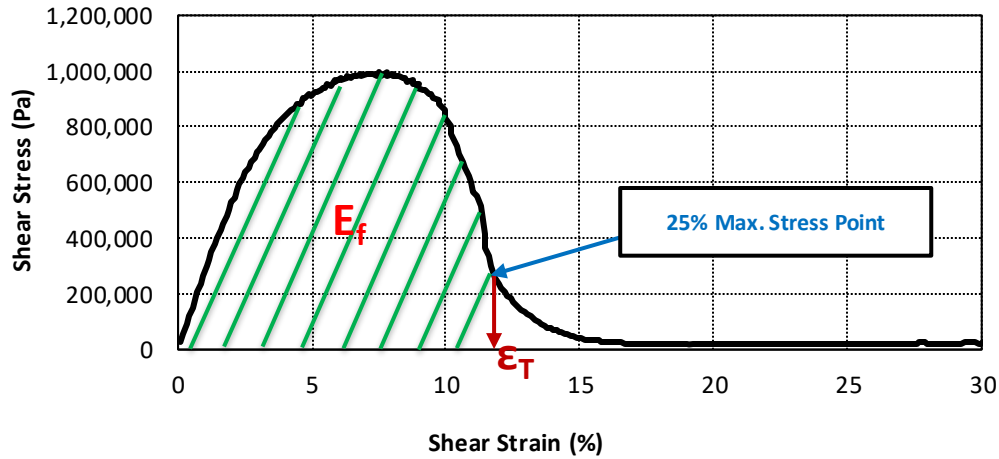


**Figure 2 Illustration of Strain Tolerance ( $\epsilon_T$ ) and Strain Tolerance Energy ( $E_f$ )**

## 2.3 Mixture Testing Methods and Parameters

### 2.3.1 Complex Modulus Test

The complex modulus test is performed in accordance with AASHTO T342 standard using an Asphalt Mixture Performance Tester (AMPT) machine on 150×100 mm cylindrical specimens. The test is conducted on three replicate specimens at different temperatures (4.4, 21.1 and 37.8°C) and loading frequencies (25, 10, 5, 1, 0.5, 0.1 Hz) to characterize the linear viscoelastic properties of the asphalt mixtures: dynamic modulus  $|E^*|$  and phase angle ( $\delta$ ). The dynamic modulus and phase angle mastercurves of mixtures at different aging levels are then constructed using Abatech RHEA® software.

A generalized sigmoidal equation with five parameters is generally used to fit the  $|E^*|$  master curves:

$$\log|E^*| = \delta + \frac{\alpha}{1 + e^{\beta + \gamma \log(\omega)}} \quad (4)$$

where  $|E^*|$  is dynamic modulus,  $\omega$  is frequency, and  $\delta$ ,  $\alpha$ ,  $\beta$ , and  $\gamma$  are the fit coefficients that describe the shape of the dynamic modulus master curve that have been used to evaluate cracking performance and aging effect [36,37]. The  $\alpha$  and  $\delta$  parameters are related to the glassy modulus (upper asymptote) and the equilibrium modulus (lower asymptote) of the master curve, respectively. The  $\gamma$  value controls the width of relaxation spectra, and the frequency of the inflection point can be calculated from  $10^{-\beta/\gamma}$ , which describes the elastic-viscous transition exhibited as a result of a shift between behavior dominated by the aggregate structure and the binder. These shape parameters from dynamic modulus master curves are described and illustrated in **Fig. 3**. Generally,  $\gamma$  increases when aging level increases, while  $-\beta/\gamma$  decreases as aging level increases, which means the asphalt mixtures will become more elastic as the elastic-

viscous transition point moves to a lower frequency, resulting in a flatter dynamic modulus curve.

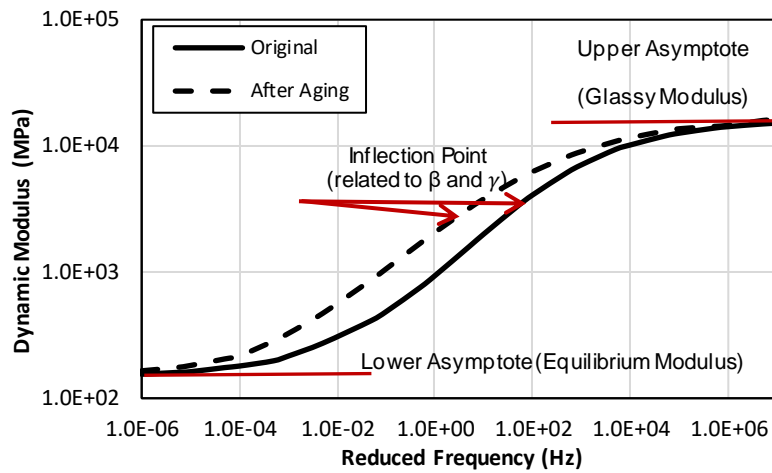


**Figure 3 Shape Parameters from Dynamic Modulus Master Curve**

A generalized Lorentzian model (Eq. 5) with three parameters is used to fit the  $\delta$  master curves:

$$\delta = \frac{a \cdot b^2}{[(\log(\omega) - c)^2 + b^2]} \quad (5)$$

where  $\delta$  is phase angle (degree),  $\omega$  is frequency (Hz), and a, b, and c are the fit coefficients as follows: “a” shows the peak value of phase angle, b controls the slope of the curve, and c is related to the horizontal position of the peak point (the frequency of the peak point can be calculated from  $10^c$ ). The “a” and c values typically decrease as aging level increases, moving the curve to the bottom left of the plot. The shape parameters from phase angle master curves are also described and illustrated in Fig. 4.

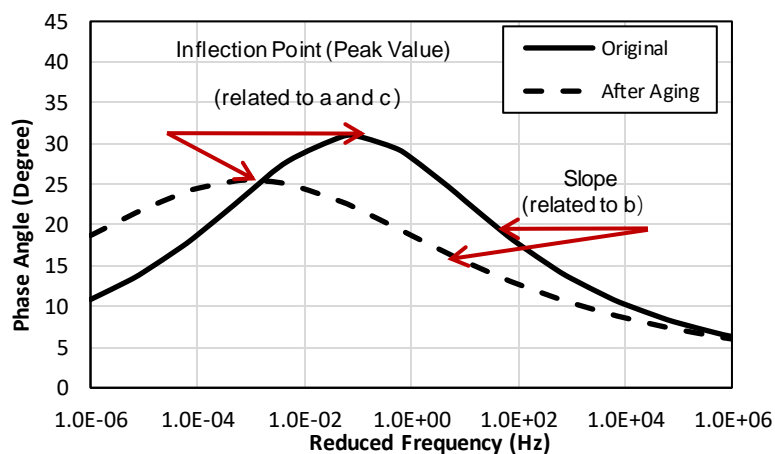


**Figure 4 Shape Parameters from Phase Angle Master Curve**

The mixture Glover-Rowe (G-R<sub>m</sub>) parameter can also be calculated from the master curves to assess the cracking resistance of asphalt mixtures, as indicated in **Eq. 6** [16]. A threshold value of 19000 MPa [38,39] is suggested to minimize the material cracking potential.

$$G - R_m = \frac{|E^*|(\cos\delta)^2}{\sin\delta} \quad (6)$$

where  $|E^*|$  is dynamic modulus and  $\delta$  is phase angle of the mixture. In this study, the parameter is calculated at the temperature-frequency combination of 20°C-5Hz, following additional development of the G-R<sub>m</sub> parameter to use a typically measured point to evaluate the cracking performance of asphalt mixtures in the NCHRP 09-58 project [38,39].

### 2.3.2 Direct Tension Cyclic Fatigue Test (DTCF)

The uniaxial fatigue test is performed in accordance with AASHTO TP 107 to evaluate the fatigue performance of asphalt mixtures. The test is conducted on 130×100 mm specimens that are preconditioned with respect to binder performance grade at temperature equal to  $(\frac{PGHT - PGLT}{2} - 3^\circ C)$ . The test is conducted on four replicates each at a different strain level under cyclic tension and constant crosshead testing mode. The performance parameter  $D^R$  (average reduction in integrity up to failure) and  $S_{app}$  (the accumulated damage when  $C$  (pseudo stiffness) is equal to  $1 - D^R$ ) calculated from the simplified viscoelastic continuum damage (S-VECD) approach are used as the output to estimate the ability of the mixtures to resist fatigue cracking [40].

### 2.3.3 Semi Circular Bending (SCB) Test

The Semi-Circular Bending test is performed to determine the intermediate temperature fracture properties of asphalt mixtures in accordance with AASHTO TP 124 standard. The test is conducted in monotonic loading conditions, using a line-load displacement rate of 50mm/min at 25°C for 3 replicates. Fracture energy ( $G_f$ ), defined as the amount of energy required to create unit fracture surface, and the Illinois Flexibility Index (FI), which normalizes the fracture energy by the post peak slope at the inflection point, are calculated for evaluation of the fracture properties of different mixtures with various aging conditions [17]. An FI value greater than or equal to 8 has been found to be an adequate threshold for distinguishing good performing from poor performing mixtures [41].

In addition to the fracture energy ( $G_f$ ) and flexibility index (FI), Nemati et al. [42] develop the rate-dependent cracking index (RDCI) to better discriminate the asphalt mixtures with various mix variables. The calculation of RDCI is shown below:

$$RDCI = \frac{\int_{t_{peak}}^{t_{0.1 peak}} W_C dt}{P_{t_{peak}} \times \text{ligament area}} \times C \quad (7)$$

where RDCI is the rate-dependent cracking index,  $\int_{t_{peak}}^{t_{0.1 peak}} W_C dt$  is the post-peak area under the cumulative work versus time curve,  $P_{t_{peak}}$  is the instantaneous power at peak force,  $C$  is the unit correction factor set to 0.01 to lower the order of magnitude of the RDCI and for simplicity of plotting and ligament area is the specimen thickness times the ligament length.

### 2.3.4 Disk Shaped Compact Tension (DCT) Test

The disk-shaped compact tension (DCT) test is performed in accordance with the ASTM D7313 standard testing method on three replicates. The test is conducted in monotonic loading conditions and measures the low temperature fracture properties of the asphalt mixtures. The test temperature for different mixtures is based on the winter-time pavement in-service temperature for the location where mix is being used, which is calculated at 98% reliability +10°C from the LTPPBind database for the nearest weather station to the actual project site. The two index parameters that are used to analyze the DCT test results are the Fracture Energy ( $G_f$ ) and the Fracture Strain Tolerance (FST), as indicated in **Eq. 8 and 9** [43]. The threshold value of 400 J/m<sup>2</sup> for  $G_f$  has been proposed as the primary limit value to control the thermal cracking problem of the asphalt mixtures [44].

$$S_f = \frac{2P(2W+a)}{t(w-a)^2} \quad (8)$$

$$FST = \frac{G_f}{S_f} \quad (9)$$

$S_f$  : Fracture strength

$P$ : Maximum load sustained by specimen

$w$  and  $a$  : M are indicated in

$t$ : Specimen thickness

## 3. Materials

### 3.1 Asphalt Mixtures

This study includes laboratory testing on nine plant mixed, lab compacted surface mixtures. **Table 1** below shows the mixture information (Recycled binder content is the ratio of the weight of recycled binder to the total binder weight). The aging conditions were described above. Letters in the cells indicate the testing conducted at each of the mixture-aging combinations. The mix ID has the specific meaning: the first four-digit numbers indicate binder PG grade, the following letters “S” and “L” mean the nominal maximum aggregate size (NMAS) of 9.5mm and 12.5mm, respectively. The last letter represents the recycled binder

content: “V” means no recycled binder, “M” means 14.8-18.9% recycled binder content, “L” means 28.3% recycled binder content.

**Table 1 Mixtures Properties and Information**

Mixture ID	Virgin Binder Grade	Design Gyration Level	NMAAS (mm)	Total Binder Content (%)	Recycled Binder Content (%)	STA	LTOA		
							5 days 95°C	12 days 95°C	24 hours 135°C
5234LM	PG 52-34	50	12.5	5.3	18.9	A	ABCD	ABCD	ABCD
5234LL	PG 52-34	50	12.5	5.3	28.3	A	ABCD	ABCD	ABCD
5834LM	PG 58-34	50	12.5	5.4	18.5	CD	CD	CD	CD
5828LM	PG 58-28	50	12.5	5.3	18.9	A	D	ABCD	ABCD
5828LL	PG 58-28	75	12.5	5.3	28.3	A	D	ABCD	ABCD
6428SV	PG 64-28	75	9.5	6.4	0	ABCD	ABCD	ABCD	ABCD
6428SM	PG 64-28	75	9.5	6.3	18.5	ABCD	ABCD	ABCD	ABCD
7034LV	PG 70-34	75	12.5	5.8	0	ABCD	ABCD	ABCD	ABCD
7628SM	PG 76-28	75	9.5	6.1	14.8	ABCD	ABCD	ABCD	ABCD

**A: Complex Modulus Testing; B: DTCT Fatigue Testing; C: SCB Testing; D: DCT Testing.**

### 3.2 Asphalt Binders

Table 2 below shows the summary information for binder samples extracted and recovered from the nine study mixtures with different aging conditions. The binder extraction is performed in accordance with AASHTO T 164, procedure 12, using a centrifuge extractor and toluene solvent in order to determine the asphalt binder content. The asphalt binder is recovered based on ASTM D7906-14 using a rotary evaporator.

**Table 10 Summary Information for Binders**

Mixture ID	Virgin Binder PG	Total Binder Content (%)	Recycled Binder Content (%)	STA	LTOA		
					5 days 95°C	12 days 95°C	24 hours 135°C
5234LM	52-34	5.3	18.9	A	A	A	A
5234LL	52-34	5.3	28.3	A	A	A	A
5834LM	58-34	5.4	18.5	AB	AB	AB	NA
5828LM	58-28	5.3	18.9	A	NA	A	A
5828LL	58-28	5.3	28.3	A	NA	A	A
6428SV	64-28	6.4	0	AB	AB	AB	NA
6428SM	64-28	6.3	18.5	AB	AB	AB	NA
7034LV	70-34	5.8	0	AB	AB	AB	NA

7628SM	76-28	6.1	14.8	AB	AB	AB	NA
--------	-------	-----	------	----	----	----	----

**A: 4mm DSR; B: LAS.**

#### 4. Comparisons and Correlations

In this section, the correlations and comparisons between (1) different binder parameters (including the rheological indices, transition temperatures, as well the fatigue parameters); (2) different mixture parameters (including the cracking parameters and the shape parameters); (3) mixture and binder parameters are evaluated using the statistical analysis. The statistical methods employed in this study include the Pearson correlation coefficient, Kendall rank correlation coefficient, different fitting (linear and non-linear) functions provide by Excel and the Hoeffding's D correlation analysis.

- Kendall rank correlation coefficient, commonly referred to as Kendall's  $\tau$  coefficient, is a statistic used to measure the ordinal association between two measured quantities. It is a measure of rank correlation: the similarity of the orderings of the data when ranked by each of the quantities. Values of Kendall coefficient range from -1 to +1, with larger absolute values indicating a stronger relationship [45].
- Pearson correlation coefficient is a measure of the linear correlation between two variables or quantities. It has a value between +1 and -1, where 1 is total positive linear correlation, 0 is no linear correlation, and -1 is total negative linear correlation [46].
- The different fitting functions (e.g. exponential, logarithmic, polynomial and power functions) provided by Excel are used to evaluate the linear, more importantly the non-linear correlations.
- Hoeffding's D correlation is employed in this study to specifically investigate and evaluate the non-monotonic relationship between the different parameters in addition to the three methods described above which are primarily used to evaluate the monotonic correlations. It has values between -0.5 to 1, with larger values indicating a stronger relationship between the variables. The sign of Hoeffding coefficient has no interpretation. Generally, if two variables have a very low Pearson coefficient value and a very high value of Hoeffding's D coefficient, it indicates a strong non-monotonic relationship exists between the two variables [47].

In addition to exploring the correlations and comparisons between the different parameters, the distribution of the data points for each parameter with aging is also evaluated in this section by employing the statistical frequency (density) curve.

#### 4.1 Comparison of Binder Parameters

The Kendall rank correlation coefficient (matrix) and Pearson correlation factor (matrix) are used to first investigate the linear correlations between the binder indices determined from the different tests and disparate conditioning levels with respect to their rankings and values respectively. The Kendall correlation coefficients for the comparisons are shown in **Table 3**, while Pearson correlation factors are presented in **Table 4**. Values above an absolute value of 0.7 are shaded green indicating a relatively strong correlation between the two parameters, those between 0.4 and 0.7 are shaded blue showing moderate correlations, and those below 0.4 (weak correlation) are not shaded with color [46].

As shown in **Table 3 and Table 4**, Kendall rank correlation coefficients for the pairs of parameters typically show the similar trend with the Pearson correlation factors, except for  $T_g$  value shows the moderate relationship with  $\Delta T_{IR}$  and  $\epsilon_T$  value, and R value shows the moderate correlation with PGLT, while there are no obvious relationships between these pairs in terms of ranking the binders with various aging conditions. Generally, these binder parameters evaluated in this study including the rheological parameters (PGLT,  $\Delta T_c$ , R-value and G-R parameter), transitions temperatures ( $T_G$ ,  $T_t$  and  $\Delta T_{IR}$  parameter) and the fatigue indices ( $\epsilon_T$ ,  $E_f$ ,  $I^R$ ) all correlate well with each other in context of the various aging conditions.

Binder rheological parameter PGLT,  $\Delta T_c$  and G-R parameter typically show the overall moderate to strong correlations with the three binder transition temperatures. Binder R-value shows the highest Pearson correlation coefficient (0.92) with  $\Delta T_{IR}$  parameter due to the similarity in calculation of these two parameters: R-value is the difference between the logarithmic glassy modulus and the logarithmic equilibrium modulus (calculated from the complex shear modulus master curve in frequency domain), while  $\Delta T_{IR}$  parameter is the difference between the viscoelastic (equilibrium) temperature and the glassy transition temperature (calculated from the complex shear modulus master curve in temperature domain). Among these three transition temperatures,  $T_t$  and  $\Delta T_{IR}$  typically show the strong correlations with all the rheological parameters in terms of both rankings and values. These good correlations between the binder rheological parameter and binder transition temperatures observed here indicate the relationships between asphalt binder's fundamental thermo-rheological properties.

Three binder fatigue parameters also show the good correlations with other binder parameters with respect to their rankings and values. The value of the fatigue parameters typically shows the strong correlations with binder PGLT,  $\Delta T_c$ ,  $T_t$  and  $\Delta T_{IR}$  parameters, while the moderate correlations with binder  $T_g$ , R-value and G-R parameters.

Overall, all the binder parameters evaluated in this study generally correlate well with each other by incorporating the aging effect. This observation indicates their potential interchangeability to evaluate the cracking properties of asphalt binders.

**Table 3. Kendall Correlations between the Different Binder Parameters**

	PGLT	$\Delta T_c$	R	G-R	$T_G$	$T_t$	$\Delta T_{IR}$	$\epsilon_T$	$E_f$	$I^R$
PGLT	1.00									
$\Delta T_c$	-0.79	1.00								
R	0.39	-0.50	1.00							
G-R	0.84	-0.82	0.52	1.00						
$T_G$	0.62	-0.43	0.19	0.49	1.00					
$T_t$	0.71	-0.94	0.72	0.92	0.45	1.00				
$\Delta T_{IR}$	0.58	-0.85	0.77	0.79	0.35	0.87	1.00			
$\epsilon_T$	-0.68	0.64	-0.50	-0.66	-0.33	-0.66	-0.60	1.00		
$E_f$	-0.79	0.68	-0.48	-0.73	-0.56	-0.70	-0.60	0.70	1.00	
$I^R$	-0.75	0.71	-0.54	-0.77	-0.45	-0.73	-0.64	0.85	0.81	1.00

**Table 4. Pearson Correlations between the Different Binder Parameters**

	PGLT	$\Delta T_c$	R	G-R	$T_G$	$T_t$	$\Delta T_{IR}$	$\epsilon_T$	$E_f$	$I^R$
PGLT	1.00									
$\Delta T_c$	-0.92	1.00								
R	0.56	-0.63	1.00							
G-R	0.90	-0.84	0.62	1.00						
$T_G$	0.80	-0.64	0.35	0.69	1.00					
$T_t$	0.91	-0.97	0.87	0.82	0.69	1.00				
$\Delta T_{IR}$	0.81	-0.93	0.92	0.79	0.51	0.96	1.00			
$\epsilon_T$	-0.77	0.75	-0.63	-0.51	-0.40	-0.79	-0.76	1.00		
$E_f$	-0.93	0.86	-0.68	-0.66	-0.66	-0.90	-0.83	0.89	1.00	
$I^R$	-0.80	0.81	-0.70	-0.56	-0.50	-0.85	-0.80	0.96	0.93	1.00

Based on the preliminary observations from **Table 3 and 4** where there are the strong linear correlations exist between the pairs of different parameters, **Figure 5** further investigates these pairs of parameter by employing the different (linear and non-linear) fitting functions (e.g. linear, exponential, logarithmic, polynomial and power functions) provided by Excel software. The comparisons and correlations of the parameters with the overall  $R^2$  value larger than 0.7 are shown and discussed below. The  $R^2$  value of each individual aging condition is also calculated and shown in the legends, aiming to investigate the comparisons between different parameters after each individual conditioning level, and further compare with the overall correlations while including all the aging conditions.

**Figure 5a, 5b** and **5c** show the overall strong relationships between the binder thermo-rheological parameters. As shown in the figure legends, the  $R^2$  values of each individual aging condition are also fairly high. This indicates that these parameters generally correlate well with each other despite of the aging conditioning levels applied, which can be due to the fact that they are all calculated from the complex modulus and phase angle master curves (in both temperature and frequency domain) of asphalt binders.

**Figure 5a** shows the overall strong correlation between binder  $\Delta T_c$  and G-R parameter with a  $R^2$  value of 0.85 (using a logarithmic fitting function). As asphalt mixtures aged,  $\Delta T_c$  value



decreases while G-R value increases, resulting in the point moving towards to the bottom-right of the plot. This good correlation between G-R and  $\Delta T_c$  has also been found by many studies [1-3]. As shown in **Figure 5a**, most of the binder samples exceed the significant cracking limit values for both  $\Delta T_c$  and G-R parameter after 12 days and 24 hours aging conditions.

**Figure 5b** shows the good correlation between  $\Delta T_c$  and  $\Delta T_{IR}$  parameter with an overall  $R^2$  value of 0.87 (using a linear fitting function). With increase of aging condition,  $\Delta T_c$  value decreases while  $\Delta T_{IR}$  value increases, resulting in the point moving towards to the bottom-right of the plot. Based on this preliminary analysis, binders with  $\Delta T_{IR}$  greater than  $60^\circ\text{C}$  (corresponding with  $\Delta T_c = -5.0^\circ\text{C}$ ) should be avoided because of the poor relaxation and cracking resistance performance. **Figure 5c** shows the overall good correlation between binder R-value and  $\Delta T_{IR}$  with a  $R^2$  value of 0.85 (using a linear fitting function). With increase of aging condition, R-value increases while  $\Delta T_{IR}$  value increases, moving the points towards to the top-right of the plot.

**Figure 5d**, **5e** and **5f** show the overall good relationships between the binder thermo-rheological parameters measured from 4mm DSR test with the fatigue indices measured from the LAS test. **Figure 5d** and **5e** show the strong correlations between binder G-R and  $I^R$  parameter, and G-R and  $E_f$  parameter with the overall  $R^2$  value of 0.78 and 0.77 respectively (using an exponential fitting function for both). As asphalt aged, G-R value increases while  $I^R$  and  $E_f$  parameter decrease. There is also a good correlation observed between  $\Delta T_c$  and  $I^R$  with a  $R^2$  value of 0.76 (using a logarithmic fitting function) in **Figure 5f**. These three figures can be used to evaluate both environmental and fatigue properties of asphalt binders together by incorporating the aging effect.

However, comparing the  $R^2$  values for each individual aging condition in **Figure 5d**, **5e** and **5f**, the  $R^2$  value for STA is typical very low, while it increases with increase of aging conditions with the 12 days aging conditioning level has the highest  $R^2$  value. The poor correlations between the parameters after STA and the improved correlations after the long-term conditions can be attributed to: (1) these three figures compare the different binder parameters measured from the different tests, representing the different behavior for asphalt material, which could result in the low  $R^2$  value for STA; (2) after aging especially the long-term aging conditions, binders' general cracking properties would probably be more dominated by the linear viscoelasticity because of the improved stiffness (less stress/strain generated within the material body) and the significant drop of the damage/failure tolerance beyond the LVE range [2,20,27], which causes the improved correlations after long-term aging conditions. Another more intuitive reason which can be observed from **Figure 5** is that for the binders with STA condition, there are relatively larger difference for the measured parameters between the different binders as compared to binders after long-term aging conditions (more scattered points for STA). The result discussed here indicates that for the binders with short-term

conditioning levels, the thermo-rheological parameters cannot capture the fatigue behavior of asphalt binders and vice versa. However, for the aged material, especially after long-term conditions, one single test associated with the corresponding parameters could be employed and used to estimate the overall cracking properties of asphalt binders in general.

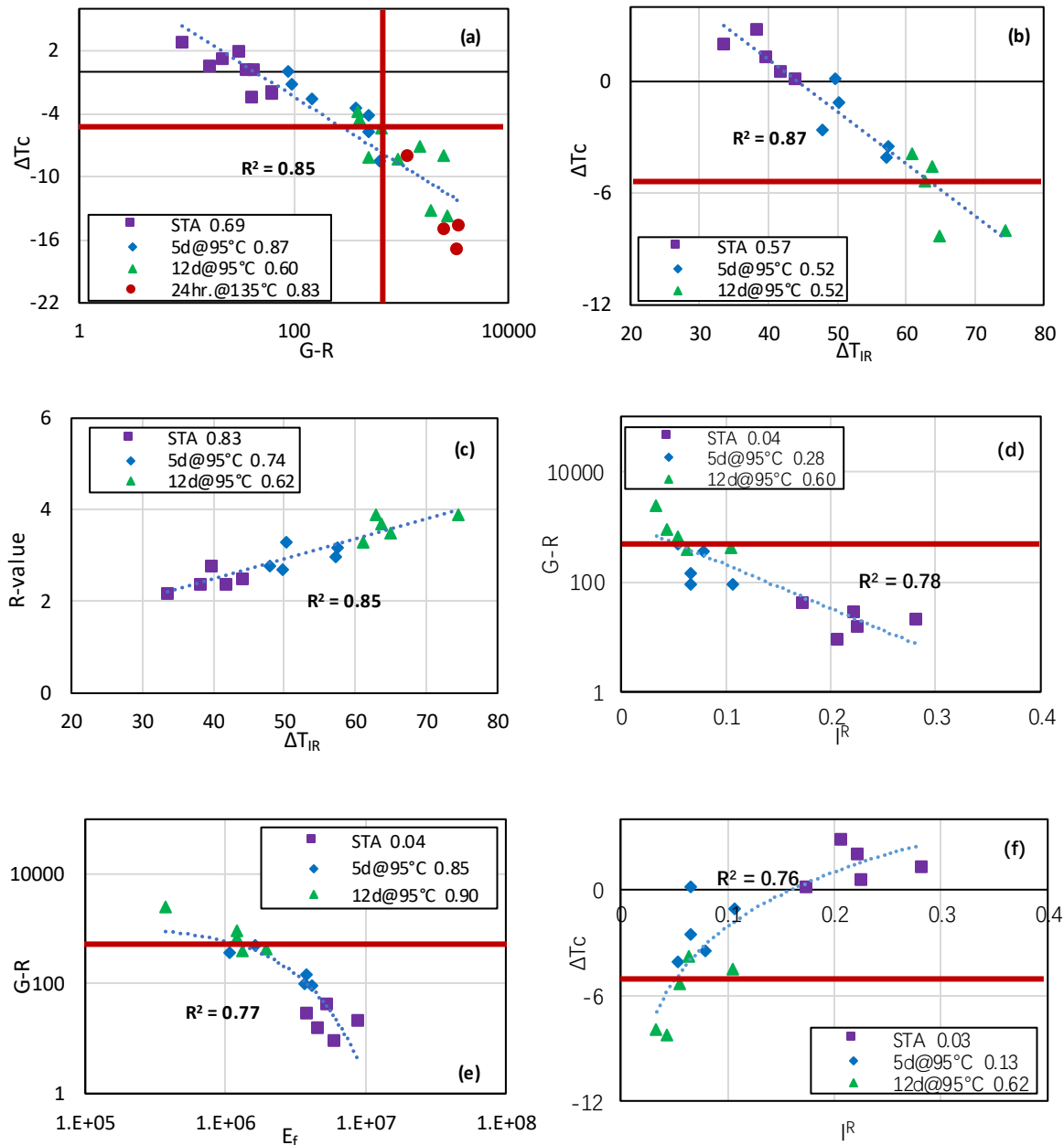


**Figure 5 Strong Correlations between a)  $\Delta T_c$  and G-R; b)  $\Delta T_c$  and  $\Delta T_{IR}$ ; c) R-value and  $\Delta T_{IR}$ ; d) G-R and  $I^R$ ; e) G-R and  $E_f$ ; and f)  $\Delta T_c$  and  $I^R$**

Hoeffding's D correlation analysis is applied on the pair of binder R-value and  $T_g$  parameter, since there is no linear relationship exists (with a Pearson coefficient of 0.35) as shown in **Table 4**. The calculated Hoeffding's D correlation coefficient is -0.03, indicating that there is no strong non-monotonic relationship between the two parameters.

The frequency (density) curve is of great importance for statistical analysis of the distribution of a data set, showing the probability at any given data point. The distribution of the binder cracking parameters including the binder thermo-rheological indices ( $\Delta T_c$ ; R-value, G-R and  $\Delta T_{IR}$ ) and three fatigue parameters ( $E_f$ ,  $\epsilon_T$  and  $I^R$ ) with three aging conditions (STA, 5 and 12 days@95°C) is evaluated by employing the frequency (density) curve. **Figure 6** below shows the frequency curves (standardized normal distribution) for the selected binder parameters. The frequency value is shown on y-axis, while the percentiles on the normalized x-axis represents the scale of each data set (e.g. 0% means the minimum value, while 100% represents the maximum value for the selected data set).

As shown in **Figure 6**, the mean value of R parameter is very close to the median point (highlighted in the figure), showing that the data points for this parameter are evenly distributed with change of aging conditions. Parameter  $\Delta T_c$  and three fatigue parameters generally show the “left-bias” distribution, with the mean value of each data set is smaller than the median point, indicating that these parameters generally decrease dramatically from STA to the intermediate aging condition (5 days), and then gradually drop from the intermediate aging to the long-term aging conditions (12 days) (can also be clearly seen in **Figure 5d** and **5f**). This left-bias distribution results in majority of the data points are located in the small value range, as illustrated by the frequency curves in **Figure 6**. Since binder G-R parameter and  $\Delta T_{IR}$  typically increase with increase of aging conditions, these two parameters typically show the opposite “bias” distribution as compared to the parameters discussed above, with the mean value is higher than the median point within the data set.

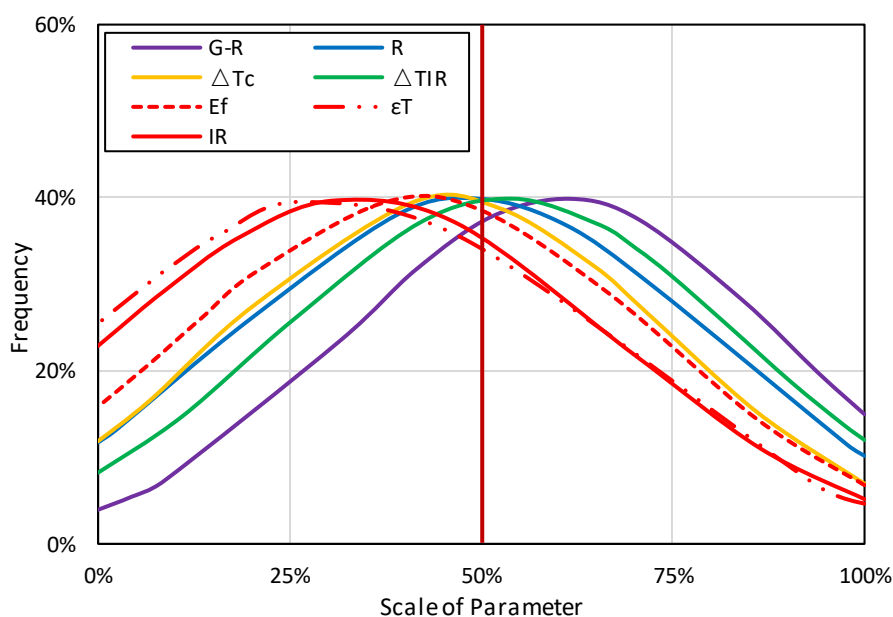


**Figure 6 Frequency (Density) Curve for Different Binder Parameters**

## 4.2 Comparison of Mixture Parameters

The Kendall rank correlation coefficient (matrix) and Pearson correlation factor (matrix) are also used to first investigate the linear correlations between the different mixture indices measured from the various performance tests and conditioning levels with respect to their rankings and values respectively. The Kendall correlation coefficients for the comparisons are shown in **Table 5**, while Pearson correlation factors are presented in **Table 6**.

As shown in **Table 5 and Table 6** Kendall rank correlation coefficients for the pairs of parameters typically show the similar trend with the Pearson correlation factors, except for  $D^R$  value shows the moderate relationship with FI and RDCI value, Sapp value shows the moderate relationship with  $c$  parameter, G-Rm value and the value of fracture indices, while there is no obvious relationship observed between these pairs of parameters in terms of ranking the mixtures with various aging conditions. Generally, the mixture rheological parameters including the master curve shape parameters and the mixture G-Rm parameter show the overall moderate to strong correlations (for both rankings and values; mostly strong correlations between the values, as indicated in **Table 6**) with each other in context of aging effect. The fracture indices also correlate well with each other, except for  $G_f$  measured from SCB. There is no obvious correlation observed between the two fatigue parameters.

Comparing the parameters measured from the different behaviors (rheology, fatigue and fracture) of asphalt mixture with various aging conditions, rheological parameter  $-\beta/\gamma$  and  $c$ , and mixture G-Rm typically show the strong correlations with fracture indices FI and RDCI, while the moderate correlations with  $G_f$  from DCT and FST. One potential reason is that  $-\beta/\gamma$ ,  $c$  and mixture G-Rm parameter, as well as FI and RDCI are all calculated from the ambient temperature as compared to  $G_f$  from DCT and FST which are measured at the low temperature environment. As indicated in **Table 6**, fracture indices FI and RDCI also show the good (moderate to strong; mostly strong) correlations with all the mixture rheological parameters.

There is no strong relationship observed between fatigue parameters with any other mixture indices. One possible reason is that the two fatigue parameters are measured from the DTCF fatigue test associated with the S-VECD analysis to characterize the damage accumulation with gradually increase of cyclic loading, while other two types of parameter are measured either within the small strain range (rheological parameters) or a simple destructive test with the monotonic loading condition (fracture parameters). Another potential reason is that most of the rheological and fracture parameters included and evaluated in **Table 5 and 6** are primarily developed and used to evaluate the relaxation capability or flexibility of the asphalt mixtures for resistance of cracking, while mixtures' fatigue properties rely not only on the relaxation capability but also the overall stiffness of asphalt material [15,32].

As described in the previous section, three binder fatigue parameters generally show the improved correlations with other binder parameters as compared to the mixture fatigue parameters discussed here. This could be attributed to the less variability of the binder test as compared to the mixture tests in general. In addition, extracted binders represent fully blended conditions between virgin and recycled binders, which could explain the better correlations observed between the binder parameters.

Overall, the mixture G-Rm, FI parameter have moderate to strong correlations with many of the mixture cracking parameters while incorporating the aging effect. The shape parameters ( $-\beta/\gamma$  and  $c$ ) also show the good correlations (mostly strong correlations for both rankings and values) with mixture cracking parameters, indicating the probability of using these two important shape parameters to evaluate the cracking performance of asphalt mixtures with different mix variables and aging levels.

**Table 5. Kendall Correlations between the Different Mixture Indices**

	$\gamma$	$-\beta/\gamma$	a	b	c	G-Rm	D <sup>R</sup>	Sapp	G <sub>r</sub> SCB	FI	RDCI	G <sub>r</sub> DCT	FST
$\gamma$	1.00												
$-\beta/\gamma$	-0.80	1.00											
a	-0.59	0.61	1.00										
b	0.65	-0.63	-0.49	1.00									
c	-0.70	0.80	0.52	-0.65	1.00								
G-Rm	0.62	-0.77	-0.61	0.52	-0.77	1.00							
D <sup>R</sup>	-0.13	0.21	0.30	-0.09	0.22	-0.41	1.00						
Sapp	-0.14	0.22	0.07	-0.21	0.24	-0.27	0.12	1.00					
G <sub>r</sub> SCB	-0.21	0.19	0.12	-0.26	0.19	-0.09	-0.18	0.08	1.00				
FI	-0.59	0.71	0.55	-0.53	0.70	-0.73	0.31	0.25	0.20	1.00			
RDCI	-0.63	0.73	0.52	-0.61	0.80	-0.75	0.29	0.27	0.21	0.85	1.00		
G <sub>r</sub> DCT	-0.54	0.51	0.30	-0.46	0.52	-0.39	-0.12	0.13	0.31	0.46	0.48	1.00	
FST	-0.51	0.59	0.36	-0.54	0.58	-0.46	-0.02	0.20	0.13	0.57	0.58	0.71	1.00

**Table 6. Pearson Correlations between the Different Mixture Indices**

	$\gamma$	$-\beta/\gamma$	a	b	c	G-Rm	D <sup>R</sup>	Sapp	G <sub>r</sub> SCB	FI	RDCI	G <sub>r</sub> DCT	FST
$\gamma$	1.00												
$-\beta/\gamma$	-0.90	1.00											
a	-0.84	0.71	1.00										
b	0.87	-0.80	-0.73	1.00									
c	-0.92	0.89	0.78	-0.87	1.00								
G-Rm	0.81	-0.86	-0.80	0.70	-0.89	1.00							
D <sup>R</sup>	-0.29	0.24	0.46	-0.16	0.34	-0.52	1.00						
Sapp	-0.35	0.38	0.23	-0.34	0.41	-0.44	0.30	1.00					
G <sub>r</sub> SCB	-0.28	0.28	0.15	-0.38	0.26	-0.14	-0.22	0.21	1.00				
FI	-0.82	0.69	0.70	-0.70	0.82	-0.72	0.49	0.54	0.23	1.00			
RDCI	-0.86	0.73	0.73	-0.74	0.86	-0.76	0.48	0.55	0.24	0.99	1.00		
G <sub>r</sub> DCT	-0.64	0.62	0.36	-0.58	0.66	-0.50	0.07	0.54	0.42	0.80	0.81	1.00	
FST	-0.67	0.60	0.43	-0.56	0.69	-0.53	0.21	0.62	0.30	0.85	0.84	0.96	1.00

Based on the preliminary observations from **Table 5 and 6**, where there are the strong linear correlations exist between the pairs of different parameters, **Figure 7** further investigates these

pairs by employing the different (linear and non-linear) fitting functions (e.g. linear, exponential, logarithmic, polynomial and power functions) provided by Excel software. The comparisons and correlations of the parameters with the  $R^2$  value larger than 0.7 are shown and further discussed below (the  $R^2$  values of each individual aging condition is also calculated and shown in the legend).

**Figure 7a and 7b** indicate the overall strong correlations between the mixture rheological parameters. As shown in the figure legends, the  $R^2$  values of each individual aging condition are also fairly high, which can be due to the reason that they are all calculated from the complex modulus and phase angle master curves of asphalt mixtures.

**Figure 7a** shows the overall strong correlation between the inflection point parameters from complex modulus master curve  $-\beta/\gamma$  and phase angle master curve  $c$  with a  $R^2$  value of 0.91 (using a polynomial fitting function). With increase of aging condition, both  $-\beta/\gamma$  and  $c$  value drops significantly, indicating the increase of the stiffness and decrease of relaxation capability of asphalt material over time. **Figure 7b** shows the overall good correlation between  $G-Rm$  and  $-\beta/\gamma$  with the  $R^2=0.78$  (using a polynomial fitting function). Based on this preliminary analysis, mixture with  $-\beta/\gamma$  lower than -2.5 (corresponding with  $G-Rm = 19000MPa$ ) should be avoided because of its poor cracking resistance performance.

**Figure 7c and 7d** indicate the general good correlations between the mixture rheological parameters and the fracture indices. As shown in the figure legends, the  $R^2$  values of each individual aging condition are also fairly high except for the 24 hours@135°C conditioning level. This can be attributed to the effect of conditioning the asphalt material at the temperature above 100 ° C, which disrupts the polar molecular associations and leads to thermal decomposition of sulfoxides in asphalt binders, resulting in the significantly different fracture properties as compared to the material aged below 100°C [2,27].

**Figure 7c** shows the overall strong correlation between mixture  $G-Rm$  and FI parameter with a  $R^2$  value of 0.77 (using a power fitting function). It should be mentioned that this  $R^2$  value is calculated without including the point with the distinctive (high) FI value as highlighted in **Figure 7c**, due to its substantial impact on the overall fitting as well-established in statistical practices. As shown in **Figure 7c**, as asphalt mixtures aged,  $G-Rm$  value increases while FI value decreases, resulting in the point moving towards to the top-left of the plot. This good correlation between  $G-Rm$  and FI has also been found by NCHRP 09-58 project [38,39]. **Figure 7d** shows the overall good correlation between FI and  $c$  with a  $R^2$  value of 0.86 (using a polynomial fitting function; exclusion of the point with distinctive FI value). Based on this preliminary analysis, mixture with  $c$  lower than -1.8 (corresponding with FI = 8) should be avoided because of its poor cracking resistance performance. The good relationships between

the two shape parameters and the mixture cracking indices observed from **Figure 7b** and **7d** indicate the potential ability of using these shape parameters to evaluate and estimate the mixture cracking performance.

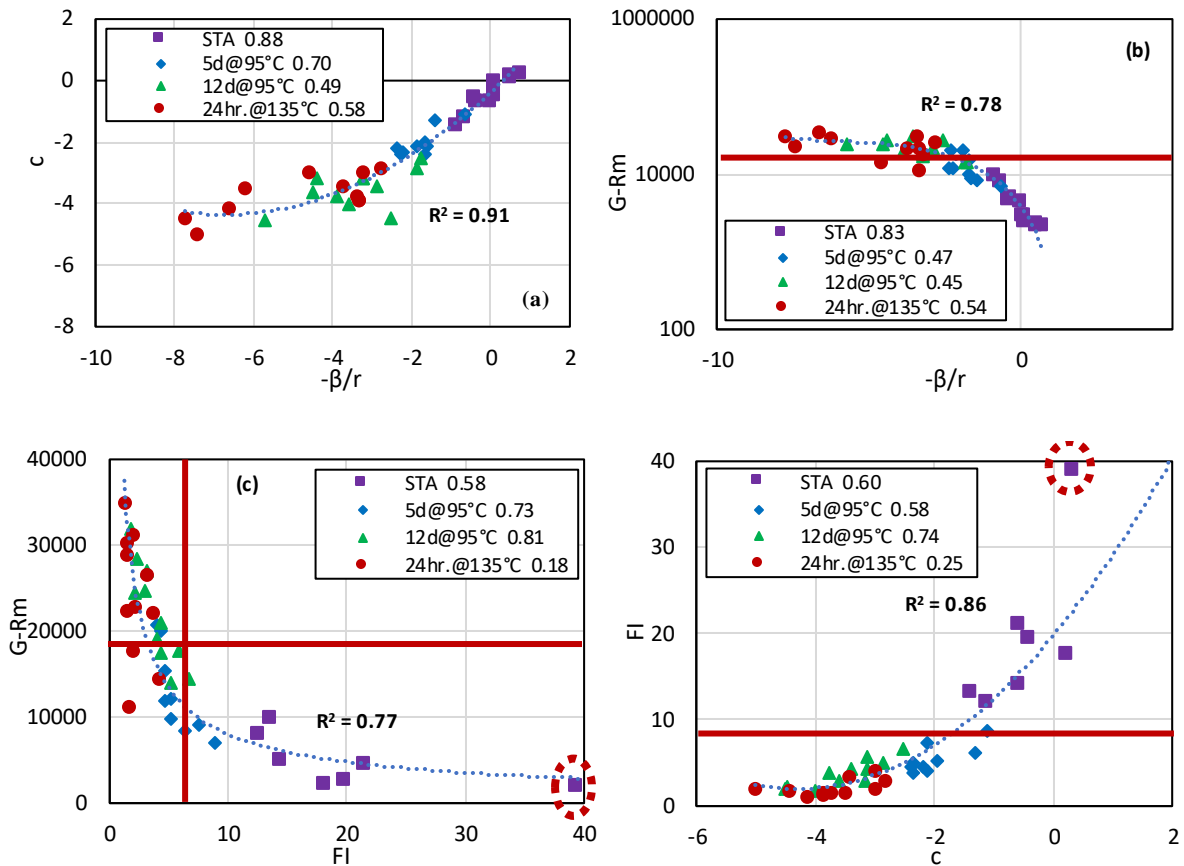


**Figure 7 Strong Correlations between a)  $c$  and  $-\beta/\gamma$ ; b)  $G-Rm$  and  $-\beta/\gamma$ ; c)  $G-Rm$  and  $FI$ ; and d)  $FI$  and  $c$**

**Table 7** below shows the result of the Hoeffding's D correlation analysis. As mentioned before, if a pair of two variables have very low Pearson coefficient value and a very high value of Hoeffding's D coefficient, it indicates a non-monotonic relationship exists between the two variables. Thus, the Hoeffding's D correlation coefficient is only calculated for the pair of parameters that showed the low Pearson coefficient ( $< 0.4$ , weak linear correlation) as highlighted in **Table 7**. As shown in **Table 7**, the values of Hoeffding's D correlation coefficient are generally very low (close to 0), indicating that there are no non-monotonic relationships between the parameters.

**Table 7. Hoeffding Correlations between the Different Mixture Indices**

	$\gamma$	$-\beta/\gamma$	a	b	c	G-Rm	D <sup>R</sup>	Sapp	G <sub>r</sub> SCB	FI	RDCI	G <sub>r</sub> DCT	FST
$\gamma$	1.00												
$-\beta/\gamma$	L	1.00											
a	L	L	1.00										
b	L	L	L	1.00									
c	L	L	L	L	1.00								
G-Rm	L	L	L	L	L	1.00							
D <sup>R</sup>	0.02	0.05	L	0.02	0.06	L	1.00						
Sapp	0.01	0.01	-0.01	0.02	L	L	-0.01	1.00					
G <sub>r</sub> SCB	0.02	0.02	0.01	0.03	0.01	0.00	0.01	L	1.00				
FI	L	L	L	L	L	L	L	L	0.01	1.00			
RDCI	L	L	L	L	L	L	-0.01	L	0.01	L	1.00		
G <sub>r</sub> DCT	L	L	0.06	L	L	L	0.02	L	L	L	L	1.00	
FST	L	L	L	L	L	L	0.00	L	-0.01	L	L	L	1.00

*L: Linear Relationship*

The distribution of the mixture parameters including the mixture cracking indices (G-Rm, FI, RDCI, G<sub>r</sub>DCT, FST, D<sup>R</sup> and Sapp) and two important shape parameters ( $-\beta/\gamma$  and c) with three aging conditions (STA, 5 and 12 days@95°C) is evaluated by employing the frequency curve. **Figure 8** below shows the frequency curves (standardized normal distribution) for the selected mixture parameters. The frequency value is shown on y-axis, while the percentiles on the normalized x-axis represents the scale of each data set (e.g. 0% means the minimum value, while 100% represents the maximum value within the selected data set).

As shown in **Figure 8**, the mean values of  $-\beta/\gamma$  and c parameters are very close to the median point, indicating that the data points for these two parameters are evenly distributed with increase of aging conditions. Interestingly, all the fracture indices and fatigue parameter generally show the “left-bias” distribution with the mean value of each data set is far away from the median point (the four fracture indices show the relatively more severe “bias” distribution). The “left-bias” distribution indicates that these parameters generally decrease dramatically from STA to the intermediate aging condition (5 days), and then gradually drop from the intermediate aging to the long-term aging conditions (12 days) (can be also clearly seen in **Figure 7c** and **7d**), which has also been observed by other studies [15,32]. Due to this general trend, most of the data points are locating in the low value range, as indicated in **Figure 8**. Specially, the most severe “bias” distribution of the FI value illustrates that the FI parameter couldn’t be able to differentiate the disparate mixtures with various mix variables after the severely (long-term) aging conditioning [15,32]. Since mixture G-Rm parameter typically increases with increase of aging conditions as compared to other parameters described above, it shows the opposite “bias” distribution with the average value is much higher than the median value within the data set.

**Figure 9** shows the severe “left-bias” distribution using the mixture FI parameter as an example. As shown in **Figure 9**, change of FI parameter from STA to 5 days aging is generally much



higher than change from 5 days to 12 days condition, resulting in the ununiform distribution of the frequency curve. After the 5 days and 12 days conditioning levels, the FI values are relatively close.

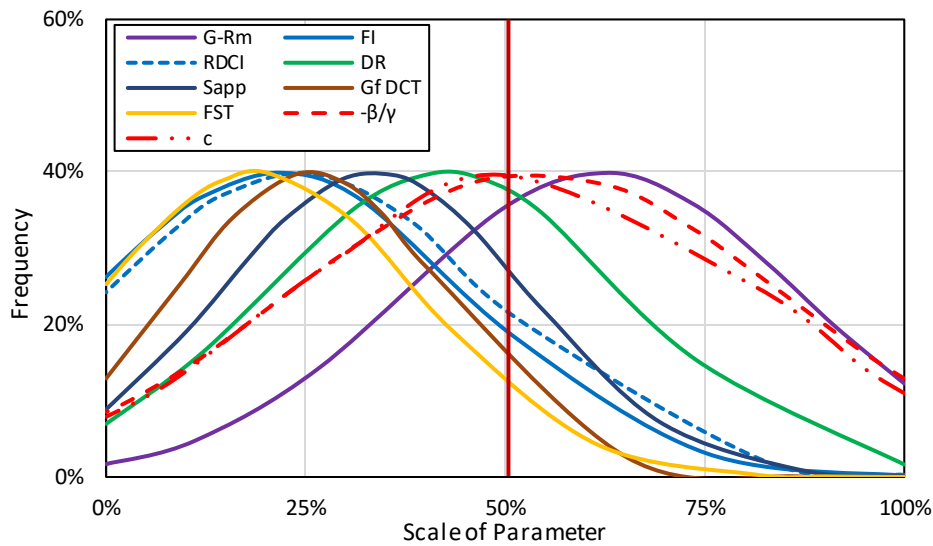


**Figure 8 Frequency (Density) Curve for Different Mixture Parameters**

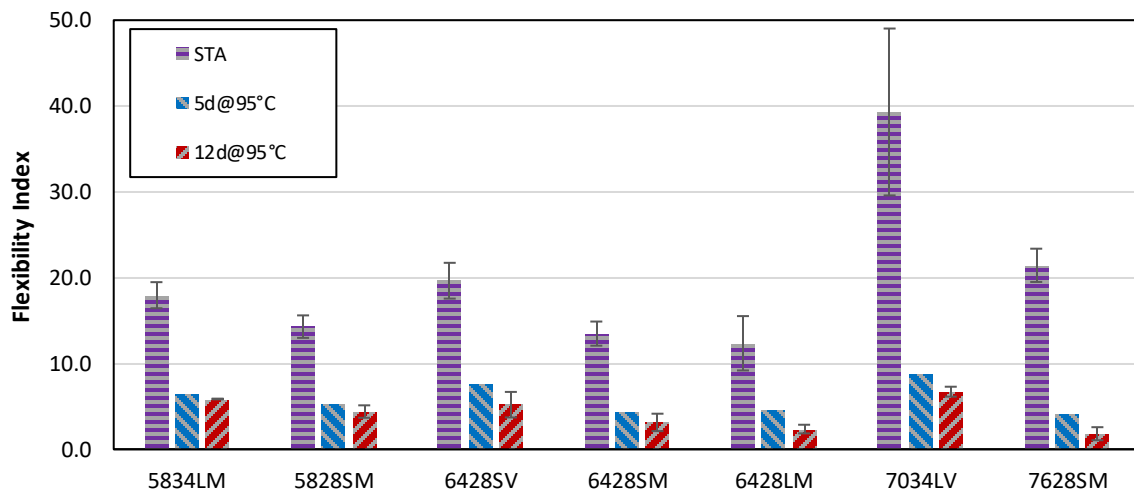


**Figure 9 Change of Flexibility Index (FI) with Increase of Aging Conditions**

### 4.3 Comparison of Mixture and Binder Parameters

The Kendall rank correlation coefficient (matrix) and Pearson correlation factor (matrix) are also used to first investigate the linear correlations between the binder performance indices and mixture parameters with respect to their rankings and values respectively. The Kendall correlation coefficients for the comparisons are shown in **Table 8**, while Pearson correlation factors are presented in **Table 9**.

As shown in **Table 8 and Table 9**, Kendall rank correlation coefficients for the pairs of parameters typically show the similar trend with the Pearson correlation factors, except for  $T_g$  value shows the moderate relationship with  $G_f$  from DCT and  $\gamma$  value,  $G_f$  from DCT value shows the moderate correlation with  $\Delta T_c$ , and Sapp value shows the moderate correlations with the binder parameters PGLT,  $\Delta T_c$ , G-R and three binder fatigue indices ( $E_f$ ,  $\epsilon_T$  and IR), while there are no obvious relationships between these pairs in terms of ranking of the mixtures with various aging conditions.

In context of aging effect, there are generally moderate to strong correlations between the mixture rheological indices and all the binder parameters with the G-Rm and inflection point parameters  $-\beta/\gamma$  and  $c$  typically show the higher correlation coefficients for both rankings and values as compared to others. The two transition temperature  $T_t$  and  $\Delta T_{IR}$  and the three binder fatigue indices generally show the strong correlations with all the mixture rheological indices in terms of their values as indicated in **Table 9**.

Comparing the mixture fracture parameters with binder indices measured from various aging conditions, there are also moderate to strong correlations between each pair of them (except for  $G_f$  from SCB), and three binder fatigue parameters generally show the strong correlations with the mixture fracture indices for both rankings and values. None of the binder rheological indices show the strong correlations with the mixture fatigue performance indices, however, three binder fatigue parameters typically show the strong correlations with  $D^R$  parameter and the moderate correlations with Sapp parameter, indicating that the binder rheological parameters could not capture the fatigue behavior of asphalt mixtures but the binder fatigue parameters have the potential to be used for evaluation of mixtures fatigue properties. The good relationships observed between the binder and mixture fatigue parameters are due to (1) both LAS and DTFC tests are developed based on the VECD theory; (2) test temperature for both tests are same; and (3) binder samples are extracted and recovered from the corresponding mixtures with certain aging conditions.

Overall, considering the effect of aging, mixture rheological and fracture parameters (except for  $G_f$  from SCB) generally show the moderate to strong correlations with all the binder indices, while mixture fatigue parameters only correlate well with the binder fatigue parameters. Mixture G-Rm parameter, two inflection point parameters  $-\beta/\gamma$  and  $c$  generally show the moderate to strong correlations with all the binder parameters. Binder fatigue parameters typically show the strong correlations with the mixture parameters except for  $G_f$  from SCB.

**Table 8. Kendall Correlations between Mixture and Binder Parameters**

	$\gamma$	$-\beta/\gamma$	a	b	c	G-Rm	D <sup>R</sup>	Sapp	G <sub>f</sub> SCB	FI	RDCI	G <sub>f</sub> DCT	FST
PGLT	0.63	-0.67	-0.46	0.56	-0.66	0.61	-0.04	-0.28	-0.24	-0.66	-0.70	-0.71	-0.76
$\Delta T_c$	-0.68	0.69	0.51	-0.69	0.70	-0.60	-0.03	0.15	0.33	0.70	0.74	0.69	0.74
R	0.44	-0.44	-0.53	0.52	-0.51	0.45	-0.22	-0.09	-0.04	-0.42	-0.46	-0.26	-0.34
G-R	0.69	-0.71	-0.54	0.64	-0.72	0.66	-0.05	-0.23	-0.20	-0.67	-0.72	-0.62	-0.70
T <sub>G</sub>	0.33	-0.50	-0.20	0.25	-0.47	0.58	-0.46	-0.49	0.43	-0.47	-0.49	-0.33	-0.54
T <sub>t</sub>	0.77	-0.75	-0.64	0.73	-0.83	0.75	-0.78	-0.07	0.18	-0.75	-0.81	-0.50	-0.68
$\Delta T_{IR}$	0.68	-0.66	-0.70	0.71	-0.73	0.66	-0.78	0.00	0.12	-0.70	-0.75	-0.45	-0.66
$\epsilon_f$	-0.73	0.75	0.45	-0.57	0.75	-0.68	0.77	0.09	0.09	0.75	0.73	0.73	0.60
E <sub>f</sub>	-0.66	0.83	0.56	-0.50	0.75	-0.83	0.78	0.15	-0.14	0.83	0.81	0.62	0.71
I <sup>R</sup>	-0.70	0.79	0.45	-0.54	0.75	-0.75	0.78	0.13	-0.03	0.87	0.81	0.62	0.71

**Table 9. Pearson Correlations between Mixture and Binder Parameters**

	$\gamma$	$-\beta/\gamma$	a	b	c	G-Rm	D <sup>R</sup>	Sapp	G <sub>f</sub> SCB	FI	RDCI	G <sub>f</sub> DCT	FST
PGLT	0.75	-0.76	-0.59	0.75	-0.80	0.73	-0.01	-0.51	-0.38	-0.71	-0.75	-0.80	-0.75
$\Delta T_c$	-0.80	0.82	0.62	-0.87	0.87	-0.76	-0.08	0.41	0.49	0.68	0.72	0.74	0.69
R	0.65	-0.54	-0.75	0.71	-0.71	0.66	-0.42	-0.19	-0.09	-0.53	-0.56	-0.28	-0.32
G-R	0.61	-0.65	-0.51	0.67	-0.69	0.63	0.05	-0.42	-0.32	-0.49	-0.53	-0.60	-0.55
T <sub>G</sub>	0.45	-0.60	-0.29	0.39	-0.67	0.73	-0.68	-0.63	0.55	-0.52	-0.56	-0.54	-0.54
T <sub>t</sub>	0.85	-0.91	-0.75	0.81	-0.97	0.94	-0.93	-0.39	0.28	-0.80	-0.84	-0.60	-0.58
$\Delta T_{IR}$	0.81	-0.87	-0.76	0.77	-0.91	0.90	-0.89	-0.29	0.17	-0.74	-0.78	-0.50	-0.50
$\epsilon_f$	-0.85	0.84	0.71	-0.73	0.84	-0.74	0.87	0.44	0.05	0.93	0.92	0.74	0.74
E <sub>f</sub>	-0.87	0.91	0.72	-0.70	0.93	-0.89	0.91	0.47	-0.15	0.88	0.91	0.75	0.72
I <sup>R</sup>	-0.89	0.87	0.75	-0.75	0.88	-0.78	0.89	0.43	-0.10	0.94	0.95	0.73	0.71

Based on the preliminary observations from **Table 8 and 9**, where there are the strong linear correlations exist between the pairs of different parameters, **Figure 10-12** further investigate these pairs of parameter by employing the different (linear and non-linear) fitting functions (e.g. linear, exponential, logarithmic, polynomial and power functions) provided by Excel software. The comparisons and correlations of the parameters with the R<sup>2</sup> value larger than 0.7 are shown and discussed below (the R<sup>2</sup> value of each individual aging condition is also calculated and shown in the legend).

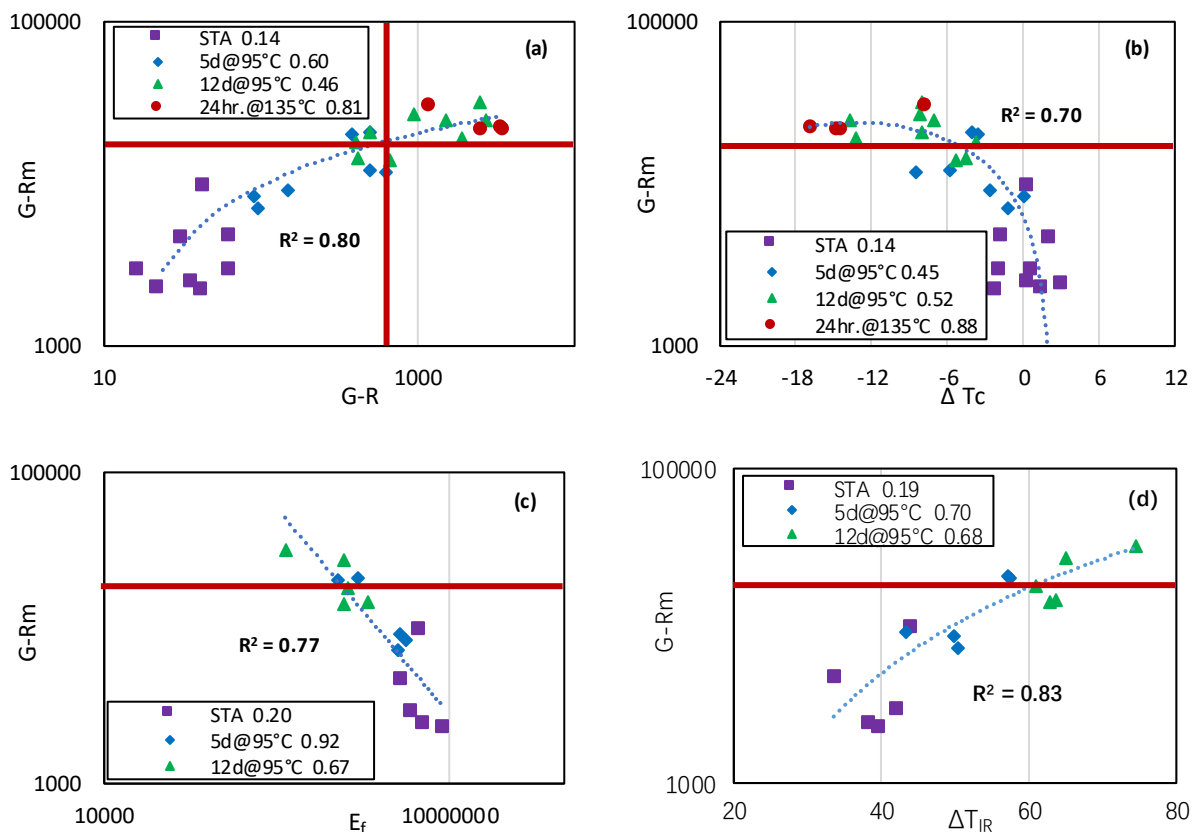
**Figure 10** shows the overall good relationships between the mixture rheological parameters and binder indices. As shown in the figure legends, the R<sup>2</sup> values of each individual aging condition are also fairly high except for the STA level. This observation indicates that for the new produced mixtures, the binder rheological parameters may not capture the mixtures' viscoelastic behaviors with other mixture variables also play the significant roles. However, with increase of the aging conditions, the mixture rheological properties tend to be more dominated by the binders' behaviors, as supported by the improved R<sup>2</sup> values for the long-term aging levels in **Figure 10**.

Generally, **Figure 10a-10d** indicate the overall strong correlations between the mixture G-Rm parameter with the different binder parameters (including the thermo-rheological and fatigue parameters). **Figure 10a** shows the strong correlation between mixture G-Rm and binder G-R

parameter with a  $R^2$  value of 0.80 (using a logarithmic fitting function), while **Figure 10b** shows the good correlation between mixture G-Rm and binder  $\Delta T_c$  parameter with a  $R^2$  value of 0.70 (using a polynomial fitting function). After 12 days aging, most of the mixtures/binders exceed the significant cracking limit, and after 24 hours aging, all mixtures and binders exceed the limit. One interesting observation from **Figure 10a and 10b** is that if the binders exceeds the (binder) cracking limit value, most of mixtures contained these binders will also exceed the (mixture) cracking limit. This observation together with the good correlations between the mixture parameters and binder indices as observed from **Table 8 and 9** and shown in **Figure 10** indicate that binder plays a significant role in the cracking performance of asphalt mixtures.

**Figure 10c and 10d** shows the overall good correlations between G-Rm and  $E_f$  parameter, and G-Rm and  $\Delta T_{IR}$  parameter with the  $R^2$  value of 0.77 and 0.83 respectively (using the power and polynomial fitting function). As shown in **Figure 10d**, binders with  $\Delta T_{IR}$  greater than  $60^\circ\text{C}$  (corresponding with G-Rm = 19000MPa) should be avoided because of poor cracking performance, which is consistent with the conclusion observed from the previous section (binder evaluation).

**Figure 10e and 10f** show the overall good relationships between the mixture shape parameters with the different binder parameters. These strong correlations indicate again that the two inflection point parameters can not only be used to evaluate the cracking performance of asphalt mixtures, but also the cracking properties of the corresponding asphalt binders.



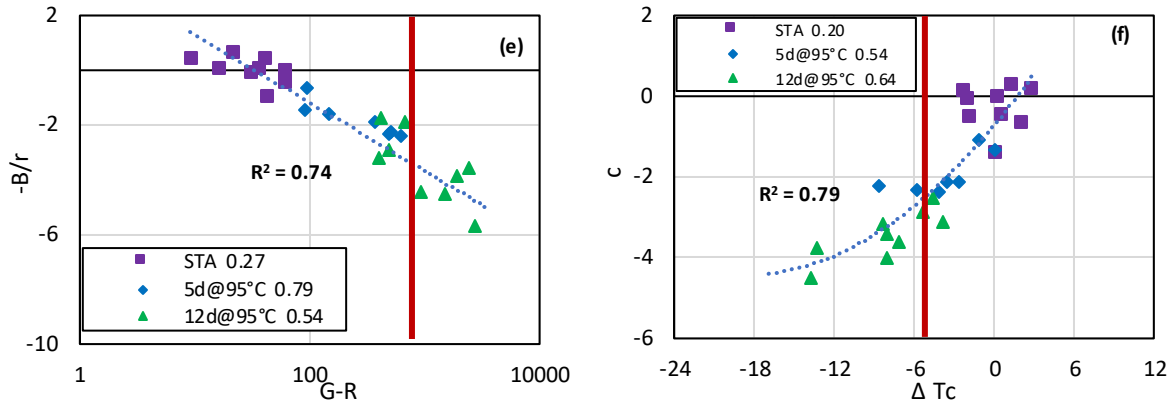
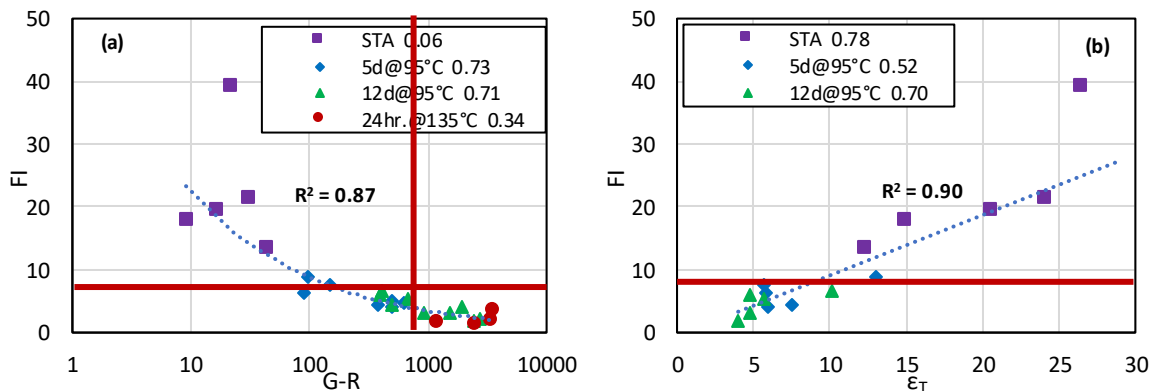


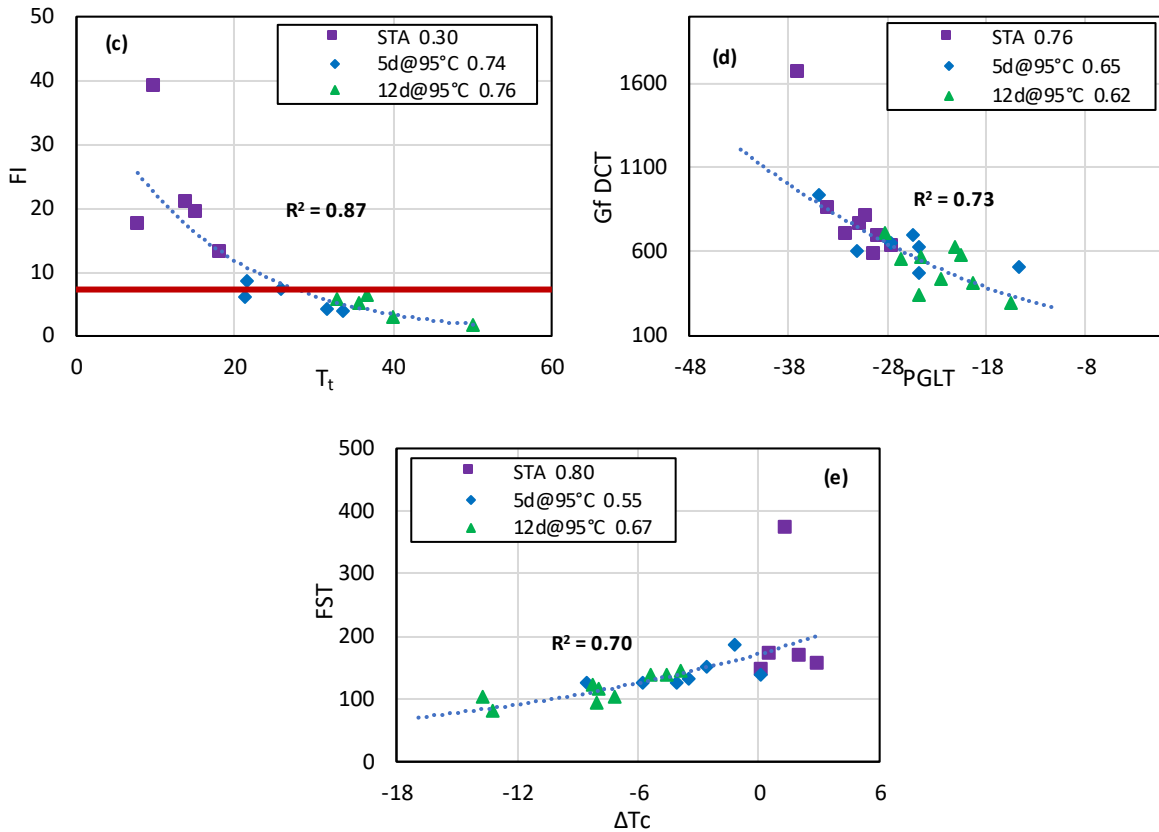
**Figure 10** Correlations between a) G-Rm and G-R; b) G-Rm and  $\Delta T_c$ ; c) G-Rm and  $E_f$ ; d) G-Rm and  $\Delta T_{IR}$ ; and e)  $-\beta/\gamma$  and G-R; f)  $c$  and  $\Delta T_c$

**Figure 11** shows the general good relationships between the mixture fracture parameters with the different binder parameters. Also, the  $R^2$  values of each individual aging condition are shown in the figure legends.

**Figure 11a, 11b and 11c** show the overall good correlations between FI and G-R parameter ( $R^2=0.86$ ; power fitting), FI and  $\epsilon_T$  parameter ( $R^2=0.90$ ; polynomial fitting), and FI with  $T_f$  parameter ( $R^2=0.87$ ; exponential fitting) respectively (the point with distinctive high FI value is not included). As shown in **Figure 11a**, if the binders exceed the cracking limit value of G-R, the mixtures will fail by the FI limit. Among these three comparisons, FI shows the strongest overall correlation, as well as the high  $R^2$  values for each individual aging condition with  $\epsilon_T$  parameter due to the reason that both tests (SCB and binder LAS) are conducted at the ambient temperature to measure the behavior of asphalt material beyond the linear viscoelastic range (LVE) response range.

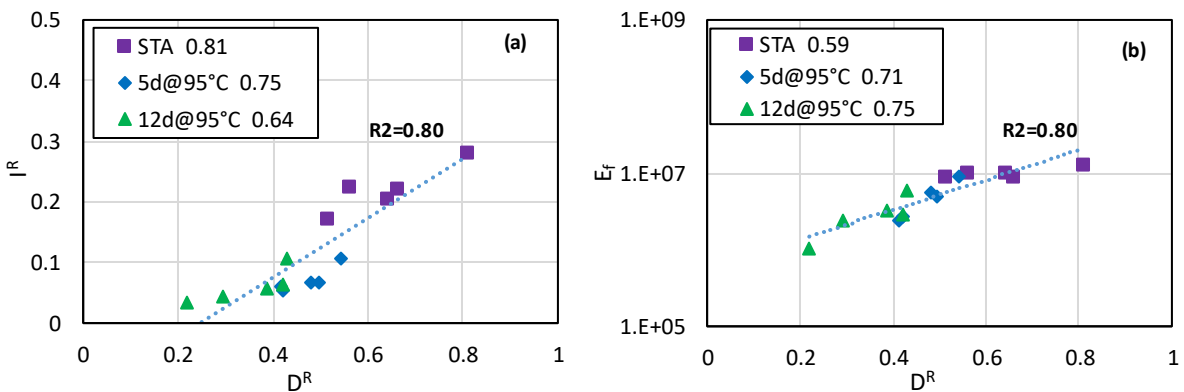
**Figure 11d and Figure 11e** show not only the overall good correlations but also the high  $R^2$  values for each individual aging condition between the  $G_f$  measured from DCT and binder PGLT parameter, FST and binder  $\Delta T_c$  parameter. These observations indicate that binders' low temperature properties are of great importance for determining the mixtures' low temperature fracture performance.





**Figure 11 Correlations between a) FI and G-R; b) FI and  $\epsilon_T$ ; c) FI and  $T_t$ ; d)  $G_f$  (DCT) and PGLT; e) FST and  $\Delta T_c$**

**Figure 12a-12c** show the good correlations between the binder fatigue indices with the mixture fatigue parameter  $D^R$  with the high overall  $R^2$  value and the  $R^2$  values for each individual aging condition. These good correlations indicate that the binder fatigue parameters have the potential to be used to evaluate and estimate the fatigue properties of asphalt mixtures while incorporating the aging effect. These good relationships also reinforce the results observed by researchers [53-56] that binder plays a significant role in fatigue behavior of asphalt mixtures. Interestingly, the fundamental thermal parameter  $\Delta T_{IR}$  also shows the overall good relationship with mixture  $D^R$  value ( $R^2=0.80$ , linear fitting), as observed from **Figure 12d**.



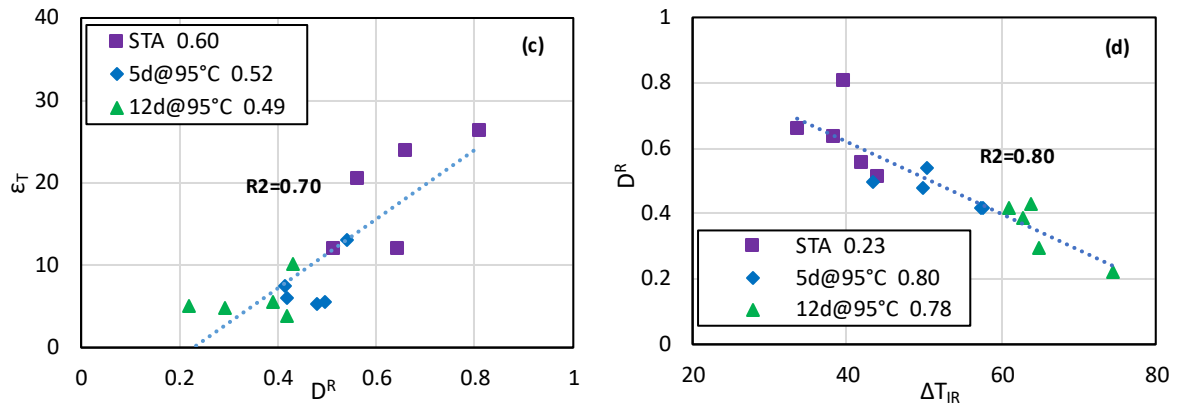


**Figure 12 Correlations between a)  $I^R$  and  $D^R$ ; b)  $E_f$  and  $D^R$ ; c)  $\epsilon_T$  and  $D^R$ ; d)  $D^R$  and  $\Delta T_{IR}$**

**Table 10** below shows the result of the Hoeffding's D correlation analysis conducting on the pairs of parameters that showed the low Pearson coefficient ( $< 0.4$ , weak linear correlation; as shown in **Table 9**) and highlighted in **Table 10**. The values of Hoeffding's D correlation coefficient are generally very low (close to 0), indicating that there are no non-monotonic relationships between the parameters.

**Table 10. Hoeffding Correlations between Mixture and Binder Parameters**

	$\gamma$	$-\beta/\gamma$	a	b	c	G-Rm	$D^R$	Sapp	$G_r$ SCB	FI	RDCI	$G_r$ DCT	FST
PGLT	L	L	L	L	L	L	0.02	L	0.02	L	L	L	L
$\Delta T_c$	L	L	L	L	L	L	0.03	L	L	L	L	L	L
R	L	L	L	L	L	L	L	0.00	-0.04	L	L	0.02	0.05
G-R	L	L	L	L	L	L	0.01	L	0.01	L	L	L	L
$T_G$	L	L	-0.03	0.00	L	L	L	L	L	L	L	L	L
$T_t$	L	L	L	L	L	L	L	-0.06	-0.04	L	L	L	L
$\Delta T_{IR}$	L	L	L	L	L	L	L	-0.07	-0.05	L	L	L	L
$\epsilon_f$	L	L	L	L	L	L	L	L	-0.05	L	L	L	L
$E_f$	L	L	L	L	L	L	L	L	-0.03	L	L	L	L
$I^R$	L	L	L	L	L	L	L	L	-0.03	L	L	L	L

*L: Linear Relationship*

In general, the overall good correlations between binder and mixture cracking parameters while including the aging effect observed from this section indicate that binders play an important role in the cracking (both fatigue and environmental; especially the long-term) performance of asphalt mixtures. The fairly good correlations between the binder and mixture parameters evaluated in this study are building upon the aging of the mixtures on the loose state which provides the uniform aging of asphalt material, and the binder samples are extracted and recovered from the corresponding mixtures with certain aging conditions.

## 5. Summary and Conclusions

The main objective of this research is to compare different binder and mixture parameters that are used to evaluate cracking susceptibility of asphalt mixtures and binders also including the aging effect. Nine plant produced mixtures were subjected to various conditioning protocols (5 and 12 days aging at 95°C, and 24 hours at 135°C on loose mixtures), and the corresponding binders were extracted and recovered from those mixtures. Mixture performance were measured from Complex Modulus ( $E^*$ ), Simplified Viscoelastic Continuum Damage (S-VECD) approach, Semi Circular Bending (SCB) and Disk-shaped Compact Tension (DCT) fracture tests. Mixture parameters evaluated include mixture Glover-Rowe parameter (G-R<sub>m</sub>), fracture energy ( $G_f$ ), flexibility index (FI), fracture strain tolerance (FST) and the average reduction in pseudo stiffness up to failure ( $D^R$ ), as well as the shape parameters from the complex modulus and phase angle master curves. Binder tests were conducted on the dynamic shear rheometer (DSR) by using the 4mm plate to measure thermo-rheological behavior of asphalt binders, and the Linear Amplitude Sweep (LAS) test to measure the fatigue performance of the asphalt binders. Binder parameters evaluated include binder Glover-Rowe (G-R) parameter, critical temperatures determined by creep stiffness ( $T_c(S)$ ) and the relaxation rate ( $T_c(m)$ ), and the difference between those two ( $\Delta T_c$ ), performance grade low temperature (PGLT), binder R-value, transition temperatures (glassy transition temperature ( $T_g$ ); visco-elastic (crossover) transition temperature ( $T_i$ ); and the intermediate region temperature range ( $\Delta T_{IR}$ )), strain tolerance ( $\epsilon_T$ ), strain tolerance energy ( $E_f$ ) and average reduction in integrity to failure ( $I^R$ ). The following conclusions can be drawn from the results of testing and analysis:

1. All the binder parameters evaluated in this study including the thermo-rheological parameters and fatigue indices, generally correlate well with each other in context of aging conditions, indicating their potential interchangeability to evaluate the cracking properties of asphalt binders.
2. Comparing the different mixture parameters, mixture G-R<sub>m</sub> and FI parameter generally show the moderate to strong correlations with many of the mixture cracking parameters, indicating that they have the potential to be used as a simplified index to evaluate and differentiate the performance of asphalt mixtures with different variables in general, while also taking aging into account. The shape parameters ( $-\beta/\gamma$  and  $c$ ) also have the potential to be used to correlate with mixture cracking performance.
3. Comparing the binder parameters with mixture indices, mixture rheological and fracture parameters (except for  $G_f$  from SCB) generally show the moderate to strong correlations with all the binder indices while incorporating the aging effect.
4. None of the binder rheological indices correlate well with the mixture fatigue performance indices, however, binder fatigue parameters typically show the strong correlations with mixture fatigue performance indices, indicating that the binder



rheological parameters cannot capture the fatigue behavior of asphalt mixtures but the binder fatigue parameters have the potential to be used for evaluation of mixtures' fatigue properties.

5. Overall, the mixture G-Rm parameter has moderate to strong correlations with many of the mixture and binder parameters indicating that it has the potential to be used as a simplified index to evaluate and differentiate the cracking properties of asphalt material in general.
6. Based on the preliminary analysis, mixtures with  $-\beta/\gamma$  lower than -2.5 and c lower than -1.8, and binders with  $\Delta T_{IR}$  greater than 60°C should be avoided because of their poor cracking resistance performance.
7. Most of the mixture and binder cracking parameters dramatically change in their values with increase of aging condition from STA to intermediate aging condition, and then gradually change from intermediate aging to the long-term aging condition. These changes match up with the trends observed for change of binder chemical composite with aging, indicating the fundamental relationships between the asphalt chemistry and its physical and engineering properties.

## 6. Future Work

Future work and analysis are planned to continue testing on field cores and collecting the pavement performance data. The correlation between the different properties of aged asphalt mixtures and binders, as well as their relationship with the cracking performance of field core samples and field performance will be further investigated.

## 7. References

1. Ozer, H., Al-Qadi, I. L., Lambros, J., El-Khatib, A., Singhvi, P., & Doll, B. Development of the fracture-based flexibility index for asphalt concrete cracking potential using modified semi-circle bending test parameters. *Construction and Building Materials*, 115, 390-401. DOI: 10.1016/j.conbuildmat.2016.03.144
2. Zhang, R., Sias, J. E., Dave, E. V., & Rahbar-Rastegar, R. (2019). Impact of Aging on the Viscoelastic Properties and Cracking Behavior of Asphalt Mixtures. *Transportation Research Record*, 2673(6), 406–415. <https://doi.org/10.1177/0361198119846473>
3. Zhou F., Lm S., Sun L., S T. (2017). Development of an IDEAL cracking test for asphalt mix design and QC/QA. *Road Materials and Pavement Design*, Volume 18, 405-427.
4. Wagoner, M. P., W. G. Buttlar, and G. H. Paulino. Development of a Single-Edge Notched Beam Test for the Study of Asphalt Concrete Fracture. *Geotechnical Special Publication No. 130: Advances in Pavement Engineering, Proc., Sessions of the GeoFrontiers 2005 Congress, Austin, Tex., 2005*

5. Schokker A. (2019) Disc Shaped Compact Tension (DCT) Specifications Development for Asphalt Pavement. Technical Report, MN/RC 2019-24.
6. Dave, E.V., W.G. Buttlar, S.E. Leon, B. Behnia, and G.H. Paulino. "IlliTC – Low Temperature Cracking Model for Asphalt Pavements," Road Materials and Pavement Design, 14(Sup. 2), 2013. pp. 57-78.
7. Sabouri, M. and Kim Y. R., Development of Failure Criterion for Asphalt Mixtures under Different Modes of Fatigue Loading, Transportation Research Record: Journal of Transportation Research Board. 2014.
8. Etheridge R.A., Wang Y.D., Kim S.S., Kim Y.R. Evaluation of Fatigue Cracking Resistance of Asphalt Mixtures Using Apparent Damage Capacity. Journal of Materials in Civil Engineering, Volume 31. 2019.
9. Mensching DJ, Geoffrey MR, and Daniel JS (2017) A mixture-based black space parameter for low-temperature performance of hot mixture asphalt. Road Materials and Pavement Design, pp. 404-425.
10. Velasquez R, Tabatabaee H, Bahia H. Low temperature cracking characterization of asphalt binders by means of the single-edge notch bending (SENB) test. Asphalt Paving Technology-Proceedings Association of Asphalt Technologists. 2011;80:583.
11. Marasteanu M, Zofka A, Turos M, Li X, Velasquez R, Li X, et al. Investigation of low temperature cracking in asphalt pavements national pooled fund study 776. 2007.
12. Andriescu A, Hesp SA, Youtcheff JS. Essential and plastic works of ductile fracture in asphalt binders. Transportation Research Record. 2004;1875(1):1-7.
13. Dongre R, Sharma M, Anderson D. Development of fracture criterion for asphalt mixes at low temperatures. Transportation Research Record. 1989;1228:94-105.
14. Zofka A, Marasteanu M. Development of double edge notched tension (DENT) test for asphalt binders. Journal of Testing and Evaluation. 2006;35(3):259-65.
15. Hou Y, Wang L, Yue P, Sun W. Fracture failure in crack interaction of asphalt binder by using a phase field approach. Materials and Structures. 2015;48(9):2997-3008.
16. Kim S-S, Wysong Z, Kovach J. Low-temperature thermal cracking of asphalt binder by asphalt binder cracking device. Transportation Research Record: Journal of the Transportation Research Board. 2006(1962):28-35.
17. Kim S-S. Direct measurement of asphalt binder thermal cracking. Journal of Materials in Civil Engineering. 2005;17(6):632-9.

18. C. Johnson, Evaluation of Accelerated Procedures for Fatigue Characterization of Asphalt Binders, ph.D, Wisconsin, 2010.
19. C. Hintz, R. Velasquez, C. Johnson, H. Bahia, Modification and validation of linear amplitude sweep test for binder fatigue specification, *Transp. Res. Rec.: J. Transp. Res. Board* 2207 (2011) 99–106.
20. Runhua Zhang, Jo E. Sias, Eshan V. Dave (2020). Development of New Performance Indices to Evaluate the Fatigue Performance of Asphalt Binders with Aging. *Journal of Road Materials and Pavement Design*.
21. Anderson, M., G. King, D. Hanson, and P. Blankenship, "Evaluation of the Relationship 2 Between Asphalt Binder Properties and Non-Load Related Cracking" *Journal of the Association of Asphalt Paving Technologists*, Vol. 80, 2011, pp. 615-661
22. Rowe, G. M. Prepared Discussion for the AAPT paper by Anderson et al.: "Evaluation of the Relationship between Asphalt Binder Properties and Non-Load Related Cracking", *Journal of the Association of Asphalt Paving Technologists*, Vol. 80, 2011, pp. 649-662.
23. Glaser, R., T. F. Turner, J. L. Loveridge, S. L. Salmans, and J. P. Planche. "Fundamental Properties of Asphalts and Modified Asphalts", Volume III. Quarterly Technical Report, Federal Highway Administration (FHWA) Contract No. DTFH61-07-D-00005, October 2013.
24. Blankenship, P.B., Anderson, M. A., King, G. N., and Hanson, D. I. "A Laboratory and Field 26 Investigation to Develop Test Procedures for Predicting Non-Load Associated Cracking of Airfield HMA Pavements, Airfield Asphalt pavement technology Program, 2010.
25. Kim, R. Y., Castorena, C., Elwardany, M., Yousefi Rad, F., Underwood, S., Gundha, A., Gudipudi, P., Farrer, M. J., Glaser, R., R. "Long-term Aging of Asphalt Mixtures for Performance Testing and Prediction", Final Report, NCHRP 09-54. 2018.
26. Glaser, R., T. F. Turner, J. L. Loveridge, S. L. Salmans, and J. P. Planche. "Fundamental Properties of Asphalts and Modified Asphalts", Volume III. Quarterly Technical Report, Federal Highway Administration (FHWA) Contract No. DTFH61-07-D-00005, October 2013.
27. Sias, J.E., Dave, E.V., Zhang, R., Rahbar-Rastegar, R. 2019. Incorporating Impact of Aging on Cracking Performance of Mixtures during Design. Technical Report, NHDOT 269620. New Hampshire Department of Transportation.
28. Sui, C., Farrar, M. J., Harnsberger, P. M., Tuminello, W. H., & Turner, T. F. "New Low-Temperature Performance-Grading Method: Using 4-mm Parallel Plates on a Dynamic

- Shear Rheometer". *Transportation Research Record*, 2011, 2207(1), 43–48.  
<https://doi.org/10.3141/2207-06>
29. Elwardany, MD., Planche, JP., Adams, JJ. Determination of Binder Glass Transition and Crossover Temperatures using 4-mm Plates on a Dynamic Shear Rheometer. *Transportation Research Record*. <https://doi.org/10.1177/0361198119849571> (2019)
  30. Turner, TF., and Branthaver, JF. DSC Studies of Asphalt and Asphalt Components, *Asphalt Science and Technology*, Usmani, A. M., Ed. Marcel Dekker Inc., New York.7 (1997), pp. 59–101.
  31. Oshone, M., Sias, J.E., Dave, E.V., Epps Martin, A., Kaseer, F., Rahbar-Rastegar, R. 2019. Exploring Master Curve Parameters to Distinguish between Mixture Variables. *Road Materials and Pavement Design*, DOI: 10.1080/14680629.2019.1633784.
  32. Rowe, G., G. Baumgardner, and M. Sharrock. 2016. Functional forms for master curve analysis of bituminous materials. 7th international RILEM symposium ATCBM09 on advanced testing and characterization of bituminous materials, vol. 1, 81-91.
  33. Martin, A.E., Zhou, f., Arambula, E., Park, E.S., Chowdhury, A., Kaseer, F., Carvajal, J., Hajj, E., Daniel, J.S., Glover, C. 2015. The effects of recycling agents on asphalt mixtures with high RAS and RAP binder ratios. Available at: [http://onlinepubs.trb.org/onlinepubs/nchrp/docs/NCHRP09\\_58\\_PhII\\_DraftInterimReport.pdf](http://onlinepubs.trb.org/onlinepubs/nchrp/docs/NCHRP09_58_PhII_DraftInterimReport.pdf) (Accessed 1 December 2018)
  34. Martin, A.E., Kaseer, F., Arambula, E., Bajaj, A., Daniel, J.S., Hajj, E., Morian N., Ogbo, C. 2018. Component Materials Selection Guidelines and Evaluation Tools for Binder Blends and Mixtures with High Recycled Materials Content and Recycling Agents. *Transportation Research Record*, 2672(28), 277–289. .
  35. Wang, Y. and Kim Y. R., Development of a pseudo strain energy-based fatigue failure criterion for asphalt mixtures, *International Journal of Pavement Engineering*. 2017.
  36. Al-Qadi, I. L., S. Wu, D. L. Lippert, H. Ozer, M. K. Barry, and F. R. Safi. 2017. Impact of high recycled mixed on HMA overlay crack development rate. *Road Materials and Pavement Design*, Vol. 18, No. sup4, pp. 311–327.
  37. Nemati, R., Haslett, K., Dave, E.V., Sias, J.E. (2019).Development of a rate-dependent cumulative work and instantaneous power-based asphalt cracking performance index,*Road Materials and Pavement Design*,20:sup1,S315-S331,DOI:10.1080/14680629.2019.1586753

38. Zhu, Y., Dave, E. V., Rahbar-Rastegar, R., Daniel, J. S., and Zofka, A. (2017). Comprehensive Evaluation of Low Temperature Cracking Fracture Indices for Asphalt Mixtures, Road Materials and Pavement Design.
39. Deusen, D.V. DCT. 2015. Low Temperature Fracture Testing Pilot Project. Technical Report, MN/RC 2015-20. Minnesota Department of Transportation.
40. Lane D., 2003. Online Statistics Education: An Interactive Multimedia Course of Study. Rice University, Texas, USA. <http://onlinestatbook.com/> last accessed 2019/08/21.
41. Agresti, A. (2010). Analysis of Ordinal Categorical Data (Second ed.). New York: John Wiley & Sons. ISBN 978-0-470-08289-8.
42. Hollander and Wolfe, Non-parametric statistical methods (Section 8.7), 1999. Wiley.
43. Petersen JC, Harnsberger P (1996) Asphalt aging: dual oxidation mechanism and its interrelationships with asphalt composition and oxidative age hardening. Transportation Research Record: Journal of the Transportation Research Board 1638, pp. 47-55
44. Petersen JC (1998) A dual, sequential mechanism for the oxidation of petroleum asphalts. Petroleum Science and Technology, Vol. 16, No. 9-10, pp. 1023-1059.
45. Petersen JC, Glaser R (2011) Asphalt oxidation mechanisms and the role of oxidation products on age hardening revisited, Road Mater. Pavement Des. 12 (4) 795–819.
46. Prapaitrakul N, Han R, Jin X, and Glover CJ (2009) A transport model of asphalt binder oxidation in pavements. Road Materials and Pavement Design. 10:sup1, 95-113, DOI: 10.1080/14680629.2009.9690238
47. Han R (2011) Improvement to a transport model of asphalt binder oxidation in pavements: pavement temperature modeling, oxygen diffusivity in asphalt binders and mastics, and pavement air void characterization.  
<https://pdfs.semanticscholar.org/ebc2/e2d286c31f50f920c04741b5725e84e21d4d.pdf>  
Accessed 1 August 2019